INVESTIGATING THE ROLE OF SARCO-ENDOPLASMIC RETICULUM Ca^{2+}-ATPase (SERCA) IN AIRWAY DEVELOPMENT

Nicholas Lansdale

A thesis submitted in accordance with the requirements of the University of Liverpool for the Degree of Doctor in Philosophy

Department of Women's and Children's Health
Institute of Translational Medicine
University of Liverpool

July 2013

Abstract

Background: Disorders of lung development cause death and disability in the young and old: novel insights into developmental regulators can aid therapeutic strategies. The Ca^{2+}ATPase SERCA, already implicated in asthma and cystic fibrosis, appears to play a key role in lung development. SERCA inhibition with cyclopiazonic acid (CPA) *in vitro*, reduces both airway branching and peristalsis reversibly and dose dependently, whilst also halting myogenesis. It is unclear however, whether changes in branching are mediated via SERCA dependent contractility, or whether SERCA is a direct regulator of airway branching.

Aims: (i) to further explore the CPA-induced embryonic lung phenotype by assaying gene expression and cell proliferation; and (ii) to determine effects of genetic perturbation of SERCA function *in vivo* on airway branching morphogenesis, in the absence of contractility (using a *Drosophila* model).

Methods: Embryonic mouse (E11.5) lung explants were cultured +/- CPA at an air/fluid interface. Standard techniques were used to rear *Drosophila* and SERCA expression manipulated using conditional, heat-sensitive mutants and RNAi targeted to the trachea. Positively labelled, loss-of-function 'flip-out' RNAi and mutant clones were produced using heat-shock induced FLP-recombinase. Gene expression was assayed using real-time RT-PCR and SERCA function assessed using calcium dyes and genetic indicators. Embryonic and larval fly airways were imaged using fluorescent proteins and immunostaining, with live or fixed-sample confocal microscopy. Immunofluorescent staining was used to assess protein expression and cell proliferation.

Results: SERCA inhibition with CPA significantly up or down regulated mRNA levels of key genes involved in lung branching morphogenesis, myogenesis and angiogenesis in vitro. CPA treatment also reduced cell proliferation dose-dependently in the lung epithelium and mesenchyme. In the fly embryo, neither conditional SERCA mutants nor targeted RNAi significantly affected tracheal morphology. However, residual SERCA mRNA and protein function was evident at this stage of development. Tracheal maturation, in the form of gas filling was significantly impaired though, in embryos expressing a conditional SERCA mutation. In larvae, development of the dorsal air sac primordium (ASP) was

severely disrupted by targeted SERCA RNAi and this phenotype could be reproduced when sufficient numbers of loss-of–function clones were present. SERCA inhibition reduced the number of mitotic cells in the ASP and correspondingly, SERCA deficient clones comprised fewer cells than control counterparts: SERCA regulation of airway cell proliferation was therefore evident across species. Fewer SERCA deficient cells reached the tip of the ASP during morphogenesis compared to controls, whereas a greater proportion remained in the stalk, findings that indicate a cell-autonomous defect in cell migration. Changes in morphology were independent of changes in expression of the key ASP signalling pathways MAP kinase and Notch. Expression of the ASP tip-cell marker escargot was expanded in SERCA deficient larvae, with a number of positive cells being abnormally present in the stalk. This finding could be explained by a failure of these cells to migrate to the tip, alternatively by changes in cell fate. Given key roles of tip cells in morphogenetic signalling, escargot may play a role in SERCA inhibition-induced dysmorphogenesis.

Conclusions: SERCA has an essential, conserved role in airway branching morphogenesis across species: this role appears independent of contractility. SERCA regulates cell migration and proliferation processes in the airway, findings that may have wider relevance, e.g. in proliferative disease, metastasis and tissue regeneration. Given evidence in plants and fungi of Ca^{2+} cycling regulating budding, findings here may indicate a role for SERCA as a generic regulator of iterative branching across biology, with clear implications for further research.

Table of Contents

List of Tables

List of Figures

Acknowledgements

Whilst it is not possible for me to list in entirety all those who have contributed to and influenced this thesis, I attempt to catalogue those who have played particularly important roles. Edwin Jesudason and Daimark Bennett have provided exemplary supervision at all stages: not only have they been a source of inspiration, advice and thoughtful critique, but they also supplied invaluable encouragement through times of difficulty and occasional despair. I would like to thank other members of the laboratory, including Gwen Connell, Angela Midgley, Anita Lucaci, Neville Cobbe and Dave Spiller for their training and stewardship, particularly in the early days when I felt like a 'square peg in a round hole'. I was lucky enough to carry out some of this work at the University of Stockholm; I would like to thank Christos Samakovlis and Vasilios Tsarouhas for their hospitality, time and expert advice.

Others who have provided great inspiration to my career and whom I have been lucky enough to call mentors are: Alan Gregg, my biology teacher at Stockport Grammar who fostered my initial interest in life sciences; Jenny Walker, former Consultant Paediatric Surgeon at Sheffield who first introduced me to the speciality; and Sean Marven, another Paediatric Surgeon who taught and encouraged me with boundless enthusiasm.

I would like to thank my charitable funders, the Royal College of Surgeons of England and the Wellcome Trust: their generous Fellowship awards afforded me the true privilege of pursuing research into something of great interest.

I am indebted to family and friends who have provided the support required for me to achieve what I have done: this thesis is a further example of what otherwise would not have been possible without them. Finally, I would like to dedicate this thesis to my loving, supportive and endlessly tolerant wife Ruth and our son Thomas.

July 2013

Author's Declaration

I declare that, except where explicit reference is made to the contribution of others, this thesis is the result of my own work. Specifically, MG Connell performed counting of mitotic nuclei in Chapter 3.3.1 and V Tsarouhas performed measurements of tracheal diameter in Chapter 6.5.2. The material contained in this thesis has not been presented, nor is currently being presented, either wholly or in part for any other degree of qualification.

This research was carried out at the Institute of Child Health, Royal Liverpool Children's Hospital (Alder Hey) and the School of Biological Sciences, University of Liverpool.

Signature…….

Printed name……..

List of Abbreviations

AEL	After embryo laying
AP	Airway peristalsis
ASM	Airway smooth muscle
ASP	Dorsal air sac primordium
Bnl	Branchless
BPD	Bronchopulmonary dysplasia
Btl	Breathless
CDH	Congenital diaphragmatic hernia
CFTR	Cystic fibrosis transmembrane regulator
COPD	Chronic obstructive pulmonary disease
CPA	Cyclopiazonic acid
EGF	Epidermal growth factor
esg	Escargot
FETO	Fetal endoscopic tracheal occlusion
FGF	Fibroblast growth factor
FRET	Fluorescence resonance energy transfer
FRT	FLP recombination target
GECI	Genetically encoded Ca^{2+} indicator
GFP	Green fluorescent protein
IQR	Inter-quartile range
MAP	Ras/Mitogen-activated protein
MARCM	Mosaic analysis with a repressible cell marker
RNAi	RNA interference
RFP	red fluorescent protein
SD	Standard deviation
SEM	Standard error of mean
SERCA	Sarco-Endoplasmic Reticulum Calcium ATPase
SHH	Sonic hedgehog
SPRY	Sprouty
UAS	Upstream activating sequence
VEGF	Vascular endothelial growth factor
YFP	Yellow fluorescent protein

Chapter 1

INTRODUCTION

1.1 Disorders of lung development result in a spectrum of disease

Defects in prenatal development frequently manifest in the newborn infant as congenital disorders: there is now increased recognition that adult diseases also have origins in fetal life (Gluckman, Hanson, Cooper, & Thornburg, 2008; Hales & Barker, 1992). Defects in lung organogenesis present in the young and old, both as structural lung anomalies and inadequate respiratory function. The burden of such disease is considerable, both in terms of acute mortality and long-term morbidity. Understanding normal pulmonary development is therefore paramount to discovery of novel therapeutics for these frequently devastating disorders.

1.1.1 Pulmonary hypoplasia

Pulmonary hypoplasia encompasses a range of conditions characterised by impaired lung development. Initially defined by inadequate alveolar formation, the term is also used to describe inadequacies of pre-alveolar lung development and / or inadequate pulmonary vascularisation (Askenazi & Perlman, 1979; Kitagawa, Hislop, Boyden, & Reid, 1971; Reale & Esterly, 1973; Wigglesworth, Desai, & Guerrini, 1981). Historically these diagnostic features were obtained at autopsy, but advances such as magnetic resonance imaging now allow determination of lung size prenatally: given that measuring lung volume may not accurately predict pulmonary function, care must be taken when trying to use such techniques prognostically (A. Lee, Kratochwil, St√°mpften, Deutinger, & Bernaschek, 1996). Pulmonary hypoplasia may be an isolated lesion, as primary pulmonary hypoplasia, or more frequently, occur in conjunction with other congenital abnormalities (Page & Stocker, 1982; Swischuk, Richardson, Nichols, & Ingman, 1979). Lung hypoplasia can be associated with an array of birth defects, affecting many systems. Two key examples are discussed below.

The Bochdalek-type of congenital diaphragmatic hernia (CDH) is a birth defect comprising a posterolateral diaphragmatic defect, intrathoracic herniation of abdominal viscera, and varying degrees of pulmonary hypoplasia (Figure 1.1) (Bochdalek, 1848). With an incidence of approximately 1:2500 live births in population-based studies, it is as common as cystic fibrosis (J. Colvin, Bower, Dickinson, & Sokol, 2005; Gallot et al., 2007). Despite advances in treatment,

such as improved ventilation strategies and novel surgical approaches, true mortality rates, taking into account factors such as stillbirths, may be as high as 40% (Lansdale, Alam, Losty, & Jesudason, 2010; Stege, Fenton, & Jaffray, 2003; Wung, Sahni, Moffitt, Lipsitz, & Stolar, 1995). Much of this acute mortality is due to effects of pulmonary hypoplasia and persistent pulmonary hypertension. Long-term pulmonary morbidity is also common. Survivors display impaired respiratory function, sometimes requiring repeat hospital admission and oxygen therapy in the longer term (Muratore et al., 2001). Given these high rates of mortality and morbidity are refractory to existing interventions, research into new approaches for treating CDH is required.

The aetiology of isolated CDH and lung hypoplasia is still largely unknown. It was thought that pulmonary manifestations of CDH were due to compression of the developing lung by herniated viscera: discovery that lung abnormalities precede herniation fostered understanding of CDH as a global embryopathy (Jesudason, Connell, Fernig, Lloyd, & Losty, 2000; Keijzer, Liu, Deimling, Tibboel, & Post, 2000). A small proportion of CDH is syndromal, often with known genetic determinants e.g. isochromosome 12p (tetrasomy 12p; Pallister-Killian syndrome) (Pallister et al., 1977). However, given the implication of a range of disparate genetic candidates (e.g. *COUP-TFII* and *Fog2*), epigenetic factors (e.g. retinoic acid) and environmental influences (e.g. maternal alcohol intake) in the aetiology of CDH, attempts to correct single aberrant developmental pathways with novel molecular or gene based therapies, seem unlikely to be successful (Ackerman et al., 2005; Andersen, 1941; Felix et al., 2008; You et al., 2005). Development of therapies to tackle the most problematic part of CDH, that is pulmonary hypoplasia and pulmonary hypertension, has therefore been the focus of most work in this area. One notable example of such work is fetal endoscopic tracheal occlusion (FETO): conceived after observations of pulmonary hyperplasia in cases of laryngeal atresia, experiments to occlude the trachea in fetal lambs demonstrated improvements in lung growth (DiFiore et al., 1994; Hedrick et al., 1994; Wilson, Difiore, & Peters, 1993). Pioneering work led to translation of this technique; modern approaches to this therapy involve minimally invasive, endoscopic insertion of a balloon into the fetal trachea and subsequent removal prior to birth (Figure 1.1) (Deprest, Gratacos, & Nicolaides, 2004; Harrison et al., 1998). Despite initial clinical trials failing to demonstrate

convincing benefits, a recent randomised controlled trial suggested that when FETO is used in the most severely affected cases, survival rates improve (Harrison et al., 2003; Ruano et al., 2011). Controversy persists over whether or not current methods to select supposedly high-risk cases for FETO are sufficiently accurate in their prognostication of postnatal outcome (Ba'ath, Jesudason, & Losty, 2007).

This text box is where the unabridged thesis included the following third party copyrighted material:

http://www.chop.edu/img/fetal-diagnosis-and-treatment/congenital-diaphragmatic-hernia-img.html

Jani J et al. (2005). Percutaneous fetal endoscopic tracheal occlusion (FETO) for severe left-sided congenital diaphragmatic hernia. Clinical Obstetrics and Gynecology, 48(4), 910-922.

Figure 1.1 Congenital diaphragmatic hernia (CDH)

Panel A. Schematic diagram of an infant with CDH: a diaphragmatic defect, herniation of abdominal viscera into the thorax and pulmonary hypoplasia are demonstrated. (Illustration adapted from Children's Hospital of Philadelphia website www.chop.edu/img/fetal-diagnosis-and-treatment/congenital-diaphragmatic-hernia-img.html).

Panel B. Schematic diagram of fetal endoscopic tracheal occlusion (FETO): insertion and inflation of a balloon in the fetal trachea using an endoscope passed through the mother's abdominal wall into the fetal mouth. (Illustration adapted from Jani *et al*. Percutaneous fetal endoscopic tracheal occlusion (FETO) for severe left-sided congenital diaphragmatic hernia. *Clinical Obstetrics and Gynecology.* 2005; 48: 910-22) (Jani et al., 2005).

The first association of oligohydramnios and pulmonary hypoplasia was observed in 1946 by Potter, when abnormalities in the lungs of fetuses with bilateral renal agenesis were reported (Potter, 1946). The importance of adequate volumes of amniotic fluid for pulmonary development is further demonstrated by lung maldevelopment in a range of obstructive uropathies e.g. posterior urethral valves and also in cases of prolonged amniotic fluid leakage (e.g. prolonged preterm rupture of amniotic membranes) (I. T. Thomas & Smith, 1974). The exact physiological role of amniotic fluid in pulmonary development is not fully understood, but a combination of mechanical and biochemical effects are likely (Adzick, Harrison, Glick, Villa, & Finkbeiner, 1984; Moessinger, Harding, Adamson, Singh, & Kiu, 1990). Despite recent advances in neonatal intensive care, the clinical outcome of infants born with oligohydramnios-related pulmonary hypoplasia is frequently poor; contemporary mortality rates range from 30-40% (Everest, Jacobs, Davis, Begg, & Rogerson, 2008; Kemper & Mueller-Wiefel, 2007; Mehler et al., 2011). In an attempt to relieve antenatal urinary obstruction and restore amniotic fluid volume necessary for pulmonary development, novel fetal surgical techniques were pioneered in animal models and successfully translated into humans: fetuses with oligohydramnios and dilated urinary system indicating bladder outlet obstruction (e.g. posterior urethral valves), can undergo a procedure whereby a catheter is inserted between the fetal bladder and amniotic cavity, via the mother's abdominal wall, so called vesicoamniotic shunting (Harrison, Golbus, & Filly, 1982; Harrison, Nakayama, Noall, & De Lorimier, 1982). In selected, severely afflicted cases, there are indications this technique may improve perinatal survival: firm conclusions are precluded by a lack of high quality evidence and results of randomised controlled trials are awaited (Clark et al., 2003).

These two contrasting aetiological examples illustrate how different prenatal events result in similar pulmonary hypoplasia, with consequent profound effects on infant health and survival. They also exemplify how inter-related biomechanical and biochemical factors regulate pulmonary organogenesis, factors that have been targeted in the development of novel therapeutics.

1.1.2 Lung disease in the premature infant

Prematurity is the most common cause of respiratory failure in the newborn. Respiratory distress syndrome (RDS, also known as hyaline membrane disease) affects approximately 1% of all infants and is the leading cause of death in those born prematurely (Rodriguez, Martin, & Fanaroff, 2002). Its incidence is inversely proportional to gestation: infants born prior to 29 weeks gestation have a 60% chance of developing RDS, whilst the risk for those born around term approaches zero (Robertson et al., 1992). Given that premature birth is common and may be increasing in incidence, RDS is a major global public health problem: not only does it account for significant infant mortality, but RDS also predisposes to bronchopulmonary dysplasia (BPD), a form of chronic lung disease (Northway Jr, Rosan, & Porter, 1967). BPD occurs in around 20% of very low birth weight infants (<1500 g) and is responsible for significant long-term pulmonary morbidity, including obstructive symptoms such as wheeze, a susceptibility to infection, long-term oxygen dependency and reduced pulmonary function, manifest for example, as impaired exercise tolerance (Baraldi & Filippone, 2007; Lemons et al., 2001). RDS therefore results in both significant acute mortality and chronic morbidity, placing a high burden on the child, family and healthcare provider.

Recognition that RDS involved distinct defects in pulmonary development began with early observations at autopsy of 'hyaline membranes' in lungs of infants who died shortly after birth, but not in stillborns (Hochheim, 1903). In the 1920s, von Neergaard investigated surface tension in isolated lungs, eventually postulating the existence of a substance in the lung that reduces this tension, allowing airways to open (v. Neergaard, 1929). Further work in the 1950s led to the discovery by Avery and Mead that hyaline membrane disease of the newborn was due to surfactant deficiency (Avery & Mead, 1959; Clements, 1957; Macklin, 1954; Pattle, 1955). Experiments of surfactant replacement in animal models demonstrated its benefit in prematurity and led to the first human study in 1980: 10 premature infants were given modified bovine surfactant, resulting in significant improvements to clinical and radiological parameters (Enhorning & Robertson, 1972; Fujiwara et al., 1980) Subsequently, a host of trials have investigated multiple natural and synthetic surfactants and have confirmed their benefit in reducing mortality and morbidity: surfactant therapy has

revolutionised the care of premature infants, resulting in up to 50% decrease in neonatal mortality and pulmonary air leaks when reviewed at meta-analysis and significantly reducing the burden of chronic morbidity (Soll, 2000a, 2000b). RDS is an elegant example of how increased understanding of pulmonary development transformed medical care and ensured survival and future health for generations of infants.

1.1.3 Developmental origins of lung disease in later life

For certain diseases, the role of an individual's genetic predisposition has long been apparent. In contrast, many common adult lung diseases were thought to arise due to environmental factors e.g. tobacco smoking, industrial pollutants or infectious organisms. However, the importance of genetic contributions for these multifactorial adult lung diseases is being studied more closely. Genetic variations can now be associated with adult outcomes, such as particular lung diseases or overall lung function. Unsurprisingly, a number of these associations occur where the relevant genes play key roles in lung development. Therefore, two particularly common, chronic respiratory diseases are now discussed in the context of potential developmental origins.

Chronic obstructive pulmonary disease (COPD) incorporates emphysema and chronic bronchitis and is known as a disease of ageing tobacco smokers. Emphysema is the abnormal, permanent enlargement of air-spaces distal to terminal bronchioles, accompanied by destruction of their walls and without obvious fibrosis: chronic bronchitis is defined clinically, as the presence of a chronic productive cough, not attributable to other lung disease, present for an extended period of time, e.g. greater than half the time for two successive years (British Thoracic Society and others, 1997; Snider, 1989). Although the pathogenesis of COPD is somewhat complex and can vary between patients, the principal common factor is airway obstruction, which is largely irreversible; this obstruction causes impairment of lung function, disability and death. COPD has been described as a global epidemic and in 2004 was the fourth leading cause of death worldwide, accounting for 5% of all deaths: by 2030, COPD mortality is predicted to exceed that from HIV and TB (World Health Organization, 2008). Interestingly, only around 20% of smokers develop emphysema and non-smokers can, albeit rarely, also develop COPD, indicating variable genetic susceptibility

to this disease (Sethi & Rochester, 2000). Knockout studies have implicated a number of genes in the developmental origin of COPD, e.g. (i) *Smad3* null mutant mice display early onset emphysema which is also accelerated by smoke exposure; and (ii) targeted knockdown of CCAAT/enhancer binding protein α (C/EBPα), results in a COPD-like phenotype of chronic bronchial inflammation, excess mucous production and emphysema (H. Chen et al., 2005; Didon, Roos, Elmberger, Gonzalez, & Nord, 2010; Farkas et al., 2011). Further review of these genetic candidates demonstrates roles in early pulmonary development *and* their dysregulation in COPD. *Smad3* is a key effector in the TGF-ß signalling pathway; null-mutants display impaired alveolarisation and failure of extracellular matrix organisation in the lung, as well as increased metalloproteinase (MMP) activity, indicating that correct matrix assembly may protect against proteolytic degradation of alveoli seen in emphysema: polymorphisms in other TGF-ß pathway and MMP genes are found in COPD sufferers, further implicating these mechanisms in its pathogenesis (H. Chen et al., 2005; Hersh et al., 2006; Joos et al., 2002). C/EBPs are a group of transcription factors known to regulate gene expression in the lung; they are essential for normal early lung development, with C/EBPα loss of function resulting in pulmonary immaturity and surfactant deficiency in newborn mice, a phenotype similar to that of BPD: activity of these factors is impaired in COPD sufferers when compared to healthy smokers (Cassel & Nord, 2003; Didon, Qvarfordt, Andersson, Nord, & Riise, 2005; Martis et al., 2006). Collectively, these studies demonstrate that factors responsible for early lung development are implicated in the pathogenesis of COPD.

Asthma is another chronic respiratory disorder that has been characterised as a global epidemic: it is estimated that 300 million people suffer from asthma worldwide (Masoli, Fabian, Holt, & Beasley, 2004). Asthma afflicts both children and adults, usually presenting with wheeze, cough, difficulty breathing and chest tightness (Douglas et al., 2008). Sufferers frequently depend on long-term drug therapies, often have restricted exercise capacity and may require recurrent hospital admissions: asthma causes 250,000 deaths each year globally (Masoli et al., 2004). It is characterised by obstruction of the conducting airways, smooth muscle hyper-responsiveness and chronic mucosal inflammation, with oedema and excess mucous production (Stephen T. Holgate, 2008). Remodelling of the airway wall occurs as an injury response and includes

ASM hypertrophy, hyperplasia and ectopic spreading (Bousquet et al., 1992). In addition, several pieces of evidence indicate that airway remodelling may play a role in early development and this could be an essential precursor to the onset of asthma: (i) infants who later develop asthma, but are asymptomatic at point of investigation, already display airway inflammation and remodelling; (ii) asthmatics may continue to express developmental genes abnormally; (iii) molecular regulation is similar for both airway epithelial differentiation during ontogenesis and remodelling/repair; and (iv) the epithelial–mesenchymal trophic units active in asthma remodelling and repair, share signalling with lung development; this is supported by upregulation of morphogens such as EGFR and persistence of high TGFβ levels, despite effective anti-inflammatory treatment (Baldwin & Roche, 2002; Bousquet, Yssel, & Vignola, 2000; Dizier et al., 2000; S. T. Holgate et al., 2001; Kasper & Fehrenbach, 2000; Nakao, 2001; Puddicombe et al., 2000; Warner, Marguet, Rao, Roche, & Pohunek, 1998). A large, prospective cohort study recently demonstrated that children who go on to develop asthma by age 7, have lung function deficits and increased bronchial responsiveness in the neonatal period, strongly indicating fetal and early-life origins for the disease (Bisgaard, Jensen, & Bonnelykke, 2012). Further support for an underlying, non-immune basis for asthma, is provided by a number of trials that have demonstrated prolonged treatment with inhaled corticosteroids in children of asthmatic and atopic parents, does not influence the natural history of the subsequent asthmatic phenotype: if airway inflammation was the sole initiator of asthma, it would be expected that its prevention during disease onset should alter disease outcome (Bisgaard, Hermansen, Loland, Halkjaer, & Buchvald, 2006; Guilbert et al., 2006; Murray, Woodcock, Langley, Morris, & Custovic, 2006). In summary, there is a significant body of evidence to suggest that the pathogenesis of asthma involves a pre-programmed, developmental component and this may be independent of more traditional, immunological mechanisms (inflammation and allergy), also known to be extremely important in the disease process. Shifting the paradigm of asthma pathogenesis away from one solely based on inflammation has allowed the development of novel therapeutics, targeting areas such as growth factor signalling (e.g. EGF) and airway smooth muscle dysfunction (bronchial thermoplasty) (Cox, Miller, Mitzner, & Leff, 2004; Ingram & Bonner, 2006; Jesudason, 2009).

1.2 Normal Lung Development

Having discussed the importance of lung disease to human health, and the developmental origins for such problems, we should next review the principal components of lung organogenesis.

1.2.1 Developmental anatomy, embryology and histology

Lung development starts at 4-5 weeks gestation in humans and continues until around seven years of age with alveolarisation: key stages in this process are illustrated in Figure 1.2 and summarised below [reviewed in (Cardoso & Lu, 2006; Warburton et al., 2010)]. The respiratory tract arises from primitive foregut endoderm, which also contributes alimentary structures e.g. the oesophagus and stomach: initial pulmonary development must therefore begin with establishment of respiratory cell fate. Following this, epithelial tubes undergo iterative branching events, forming the 'tree-like' structure of the airways; later they undergo alveolarisation, the process whereby most of the gas exchange epithelial surfaces are formed: in humans, this branched system of airways is divided into three lobes on the right and two on the left (Figure 1.2). Foregut endoderm differentiates into numerous types of epithelial cells, which line the inner surface of the lung and trachea: pulmonary mesenchyme, derived from the lateral plate mesoderm, is also essential; it gives rise to numerous components of the lung, including airway smooth muscle, connective tissue, tracheal cartilage and pleural mesothelium. In addition to airway branching morphogenesis and alveolarisation, development of a pulmonary vasculature is integral to the lung's structure and function: occurring through a combination of angiogenesis (migration of blood vessels from the aortic arches and left atrium) and vasculogenesis (blood vessels develop *de novo* in the pulmonary mesenchyme, near epithelial end-buds), a rudimentary capillary network forms and later connects to larger vessels, giving rise to the lung vasculature.

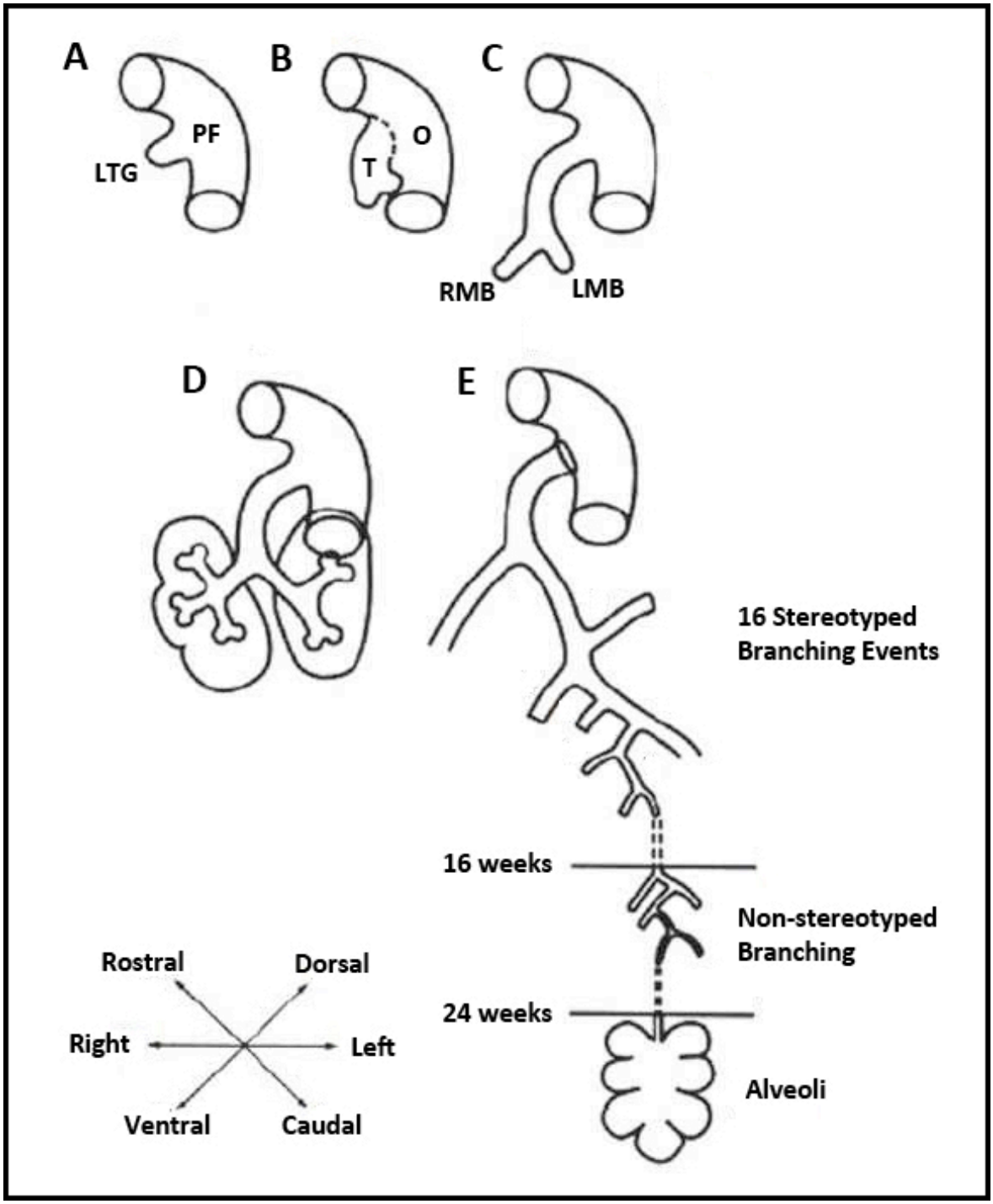

Figure 1.2 Stages of Pulmonary Organogenesis

Schematic diagram illustrating the key elements of lung development. A: The lung first emerges from the ventral surface of the primitive foregut (PF) as the laryngotracheal groove (LTG) at 4-6 weeks of human gestation. B: The primitive trachea (T) separates dorsoventrally from the primitive oesophagus (O). C: Progenitor cells in the distal trachea give rise to the left and right main bronchi (LMB and RMB). D: The lobar bronchi branch from the two primary bronchi at around 7 weeks gestation. E: There are 16 highly stereotyped airway branches that form by 16 weeks gestation. Between 16 and 24 weeks, further branching is not stereotyped. The process of alveolar formation starts at around 20 weeks gestation and continues until around 7 years of age. (Illustration adapted from Warburton *et al.* Lung organogenesis. *Curr Top Dev Biol.* 2010; 90: 73-158)

Histologically, pulmonary development is often divided into four stages: (i) *pseudoglandular* (5-17 weeks gestation): epithelial tubes lined with cuboidal epithelium undergo branching and resemble an exocrine gland: at this stage the tubes are fluid filled and do not function as a respiratory organ; (ii) *canalicular* (16-25 weeks): increases in length and diameter of the respiratory tree are accompanied by vasculogenesis and angiogenesis; there is a great increase in capillary number; terminal bronchioles divide into respiratory bronchioles and alveolar ducts; airway epithelial cells differentiate into squamous cells distally and cuboidal cells proximally; (iii) *terminal saccular* (24 weeks to late fetal period): the pulmonary interstitium become much thinner; alveolar epithelial cells clearly differentiate into squamous type I pneumocytes (for gas exchange) and secretory type II pneumocytes (for surfactant production); capillary growth in mesenchyme surrounding the saccules, forms a network of closely aligned, thin walled air spaces and blood vessels for gas exchange: later in this stage the lung can function sufficiently to sustain life e.g. infants born prematurely; and (iv) *alveolar* (late fetal period to around 7 years of age): in this period, alveoli, alveolar ducts and terminal saccules all expand in number and hence increase the lung's capacity for gas exchange.

1.2.2 Biochemical regulation of pulmonary morphogenesis

Partly driven by a search for novel therapeutic targets, a great deal of endeavour has been devoted to understanding the molecular basis of lung development; this has revolutionised our understanding of the genetic and epigenetic pathways required to build such a complex structure and vast array of differentiated cell types. Reviewing the biochemical regulation of lung organogenesis in its entirety is beyond the scope of this thesis: here, an overview of key aspects is given and further, more detailed discussion of selected candidates provided in Chapter 3.

Pioneering experiments in the 1960s demonstrated that transplanted pulmonary mesenchyme was capable of inducing ectopic branches of the trachea; this led to the concept of epithelial-mesenchymal signalling (crosstalk), now known to be fundamental to lung development (Alescio & Cassini, 1962). It is this signalling that directs morphogenetic patterning, e.g. branch position; dictates cell differentiation and stimulates cell growth and migration in the developing lung

(Shannon & Hyatt, 2004). These epithelial-mesenchymal interactions are mediated by a host of diffusible factors, tightly controlled in their spatial and temporal expression. For the purpose of this overview, biochemical factors involved in such processes are grouped into: (i) transcription factors; (ii) peptide growth factors; and (iii) other biochemical factors, as per a recent comprehensive review (Warburton et al., 2010). Examples of key lung transcription factors include, the zinc finger Gli and GATA families, homeodomain transcription factors (e.g. Nkx2.1 and Hox family) and the forkhead box family (e.g. Foxa1&2 and HFH4&8): spatial and temporal changes in the activity or expression level of such transcription factors, differentially activates target gene expression through specific binding to promoter regions (Costa, Kalinichenko, & Lim, 2001). Peptide growth factors are critical effectors of lung development; their closely regulated expression controls cell growth, migration and differentiation in the branching lung buds, developing mesenchyme and vasculature: key examples include, fibroblast growth factors (FGFs), sonic hedgehog (Shh), Wnt Genes and ß-Catenin, bone morphogenetic proteins (BMPs) and other transforming growth factor (TGF) family members, epidermal growth factors (EGFs) and vascular endothelial growth factors (VEGFs) [reviewed in (Cardoso & Lu, 2006; Warburton et al., 2010)]. These factors may mediate both autocrine and paracrine signals, serving to directly affect cellular processes, but also control each other's spatio-temporal expression patterns. Further discussion of individual growth factors and their regulation is provided in Chapter 3. Examples of other biochemical factors involved in lung development include: (i) retinoic acid signalling, which is critical for primary lung bud initiation, airway maturation and alveolarisation; and (ii) extracellular matrix components (ECMs, e.g. laminins), which mediate cell-cell and cell-ECM interaction: ECMs provide structural support, appear to modulate cell proliferation and differentiation, and define barriers and reservoirs for growth factors (Cardoso et al., 1995; Dickman, Thaller, & Smith, 1997; Hilfer, 1996; Lwebuga-Mukasa, 1991; McGowan et al., 2000).

1.2.3 Biomechanical regulation of pulmonary morphogenesis

Evidence for mechanical factors playing fundamental roles in pulmonary development derives from naturally occurring birth defects and *in utero* animal studies: (i) abolishing fetal breathing movements by transection of the phrenic

nerve induces pulmonary hypoplasia; (ii) loss of lung liquid e.g. from fetal tracheostomy results in similar impairments in lung development; (iii) intrathoracic pressure effects e.g. from a mass or surgically created fetal diaphragmatic hernia, impairs lung development; and (iv) fetal laryngeal or tracheal occlusion (either congenital or iatrogenic e.g. FETO) results in pulmonary overgrowth and distension, as discussed above (Fewell, Hislop, Kitterman, & Johnson, 1983; Miller, Hooper, & Harding, 1993; Starrett & de Lorimier, 1975; Wilson et al., 1993). These observations confirm that careful regulation of prenatal airway and intrathoracic mechanics, including maintenance of lung liquid homeostasis, is critical to normal lung development.

A further area of interest in prenatal pulmonary mechanics is airway peristalsis (AP); this spontaneous, phasic contractility of prenatal airway smooth muscle (ASM), is conserved from birds to mammals: increasing in frequency through gestation, AP propels lung liquid to the distal airways, causing cycles of stretch and relaxation at the growing, terminal end buds (Figure 1.3) (Schittny, Miserocchi, & Sparrow, 2000). AP waves have been shown to arise from a right-sided pulmonary pacemaker and appear coupled to lung growth (increases or decreases in AP frequency result in parallel changes in growth and *vice versa*); they are underpinned by spontaneous, propagating intracellular Ca^{2+} waves that depend on Ca^{2+} stores and gap junctions (N. C. Featherstone et al., 2005; Jesudason et al., 2005). Quite why the developing fetus expends significant energy on AP, and also why ASM has been evolutionarily conserved, despite its role in asthma, remains unclear, but it has been hypothesised that both have key roles in normal lung development; there is also evidence to suggest ASM dysfunction in disease states, such as experimentally induced pulmonary hypoplasia (N. C. Featherstone et al., 2006; Jesudason, 2009). Continued investigation into ASM and AP is seen as a priority and may yield novel therapeutic targets with which to both rescue inadequate prenatal lung growth and treat common respiratory disorders, e.g. it has been hypothesised that bronchial thermoplasty, already used to treat refractory asthma, may mediate its effects via ablation of pulmonary pacemaker cells, rather than by reducing ASM mass as previously suggested (Cox et al., 2004; Jesudason, 2009).

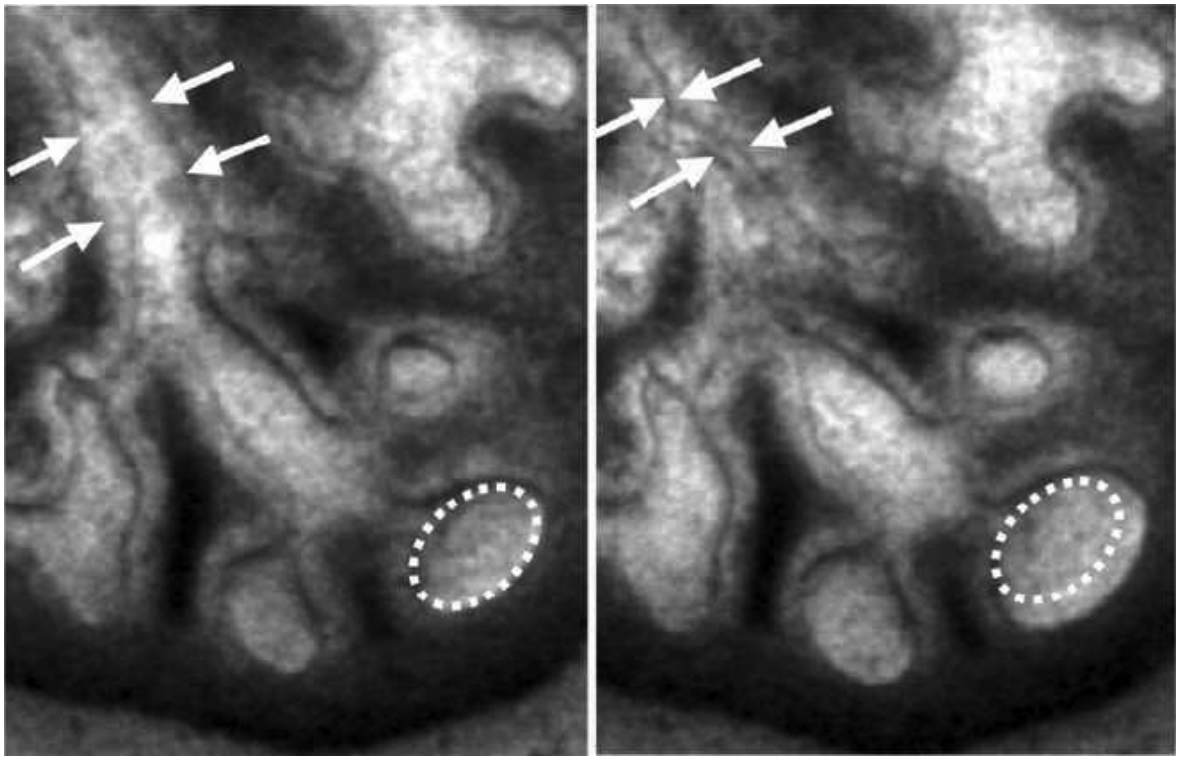

Figure 1.3 Waves of airway peristalsis (AP) in the developing lung occlude the airway proximally and distend it distally

Sequential photomicrographs of cultured embryonic lung: arrows demonstrate the proximal airways that are open in the left panel but occluded by contraction in the right. Effects of AP on the distal airway are shown in a terminal lung bud, which increases in size with contraction (the ovoid outline is the same size in both images). These effects are repeated with each wave of AP. (Illustration courtesy of E.C. Jesudason)

1.2.4 Pulmonary progenitor and stem cells

The regeneration of damaged tissues involves cellular mechanisms that include compensatory hyperplasia, dedifferentiation of mature cells to produce stem cells and the activation of resident adult stem cells (Stocum, 2008). Attempts to exploit stem cells for exogenous application, in order to repair diseased human tissues, has been at the forefront of modern medical research for many years. Successes such as the transplantation of a human stem cell derived main bronchus have provided hope that such approaches could ultimately provide solutions to other more complex and refractory lung disease (Macchiarini et al., 2008). Mammalian lung contains distinct, regional pools of lineage-restricted progenitor cells; these have been shown to display some of the properties inherent to stem cells and are capable of giving rise to specific lung structures through differentiation into at least one other cell type; these progenitors have been found in both epithelial and mesenchymal niches (Lama et al., 2007; Rawlins & Hogan, 2006). It has been thought that regional progenitors rather than multipotent stem cells are responsible for endogenous regeneration capacity. However, Kajstura *et al* isolated a population of c-kit positive cells from adult human lung, which appeared to differentiate into multiple cell types (both endodermal and mesodermal) *in vitro* and when they were grafted into cryo-injured murine lung *in-vivo* (Kajstura et al., 2011). Other groups have yet to replicate these findings and they have been the source of some controversy (Stripp, Hogan, & Thannickal, 2011).

Although trials of cell based therapies for the lung are underway (including the infusion of mesenchymal stem cells to treat COPD, BPD, and asthma), animal studies indicate any benefits are largely due to paracrine or immunomodulatory roles in the lung: lung regeneration may not be the best way to describe these trials (Kotton, 2012; Weiss et al., 2011). The application of endogenous lung progenitors or pluripotent cells (e.g. embryonic stem (ES) or induced pluripotent stem (iPS) cells) for 'true regeneration' continues to be explored though and organ recellularisation may be an alternative approach: recellualrised lungs have already been implanted briefly in rodents (Ott et al., 2010; Petersen et al., 2010). The pitfalls for clinical translation however, are widely described and further understanding of the stem cell biology has been called for (Kotton, 2012; Weiss et al., 2011). Finally, patient-specific or disease-specific iPS cells from

humans with lung diseases and the subsequent correction of their disease-causing gene mutations via zinc finger nuclease–mediated gene repair is an alluring idea (Kotton, 2012; Urnov, Rebar, Holmes, Zhang, & Gregory, 2010). iPS cells generated from patients with α1-antitrypsin deficiency have undergone gene correction *in vitro* using this technology and have subsequently been transplanted into rodent livers: an obvious potential application for this technique could be the correction of the ΔF508 CFTR mutation in the lungs of cystic fibrosis sufferers (Kotton, 2012; Weiss et al., 2011; Yusa et al., 2011).

In this section, the normal development of the lung has been described and some biochemical, biomechanical and stem/progenitor cell factors briefly discussed with regard to their roles in regulating development and tissue regeneration or repair. The burden of pulmonary disease described earlier mandates that further research into such factors is required. In this thesis, the role of an intracellular Ca^{2+} ATPase pump, SERCA, is investigated in this very context.

1.3 Sarco-Endoplasmic Reticulum Calcium ATPase (SERCA)

Given the diverse yet fundamental roles that Ca^{2+} signalling plays in almost every aspect of biology, close spatio-temporal regulation of Ca^{2+} is paramount to normal cellular function (Berridge, Lipp, & Bootman, 2000). This depends upon an array of intra and extra-cellular proteins, ranging from sensor/adaptor proteins e.g. calmodulin, to membrane spanning channels e.g. IP_3R and ATPase pumps e.g. PMCA. One key effector of intracellular Ca^{2+} homeostasis is the Ca^{2+} ATPase pump, SERCA; this protein will now be considered in some detail and the rationale for this thesis explained.

1.3.1 SERCA genetics

Vertebrates have evolved three SERCA paralogues (*ATP2A 1-3*) and each may have numerous mRNAs (from alternative splicing): *ATP2A 1-3* therefore encode the SERCA1a/b, SERCA2a/b and SERCA3a-e protein isoforms, each showing 76 - 84% amino acid sequence identity with each other in humans (Wuytack, Raeymaekers, & Missiaen, 2002). SERCA is found specifically in membranes of the endoplasmic reticulum (ER) or in specialised ER-derived sub-compartments, such as the sarcoplasmic reticulum (SR) in muscle: tissue expression of different SERCA isoforms varies significantly though, with SERCA1, the most specialised form, being largely confined to fast-twitch skeletal muscle; SERCA2a is restricted to cardiac and slow-twitch skeletal muscle, whereas SERCA2b is expressed fairly ubiquitously; finally, SERCA3 isoforms are expressed in a diverse but limited range of non-muscle tissues and appear to co-express with SERCA2b (Anger et al., 1993; Brandl, Green, Korczak, & MacLennan, 1986; Lytton & MacLennan, 1988; MacLennan, Brandl, Korczak, & Green, 1985). Despite these disparate expression patterns, the biochemical functions of individual SERCA isoforms are thought to be largely the same, as supported by conservation of key functional residues (e.g. Ca^{2+} and ATP binding sites) and effects of their mutagenesis (Lytton, Westlin, Burk, Shull, & MacLennan, 1992).

1.3.2 SERCA protein structure

SERCA is a P-type ATPase: first discovered in 1957 by Skou, P-type ATPases are defined by their function as catalysts for self-phosphorylation of a conserved

aspartate residue within their cytoplasmic domain; they most frequently transport cations but are also known to move phospholipids (Skou, 1957). SERCA's structure consists of four distinct domains, defined by the folding of a single polypeptide chain; these include the 10 alpha-helical transmembrane (M) domain and three cytosolic domains, the actuator (A), the phosphorylation (P) and the nucleotide-binding (N) domains (Figure 1.4); links between the A and M, as well as N and P domains are thought to be flexible, permitting conformational change upon ATP and Ca^{2+} binding (Toyoshima, Nakasako, Nomura, & Ogawa, 2000; Toyoshima & Nomura, 2002). SERCA has two Ca^{2+} binding sites within the M domain and these alternate between two states: (i) a high Ca^{2+} affinity state when they face the cytosol (known as E1); and (ii) a low Ca^{2+} affinity state when they face the lumen of the membrane (E2). An accepted model for SERCA mediated Ca^{2+} transport based on crystal structures involves the following series of events (Figure 1.4): SERCA in an E1 state binds two cytosolic Ca^{2+} ions and ATP; phosphorylation and ATP hydrolysis then produce a high energy phospho-intermediate and bound Ca^{2+} is occluded; transformation to a low energy state results in significant conformational change to E2, whereby the Ca^{2+} binding sites move to face the lumen and have low affinity; the cycle is completed by release of Ca^{2+} into the lumen and return to E1 (Toyoshima et al., 2000; Toyoshima & Nomura, 2002; Wuytack et al., 2002).

This text box is where the unabridged thesis included the following third party copyrighted material:

Toyoshima C. (2005). Cover picture: Cartoon of the reaction cycle of SERCA Ca2+-ATPase, based on crystal structures of its four principal conformations: during a complete cycle, two cytoplasmic Ca2+ ions are extruded into the lumen of the sarcoplasmic reticulum in exchange for two protons, at the expense of hydrolysis of a single molecule of ATP. The Journal of General Physiology, 126(1), cover.

Figure 1.4 Schematic diagram of the reaction cycle of SERCA

During the cycle, two Ca^{2+} ions are moved from the cytoplasm into the lumen of the endoplasmic reticulum (ER) or ER variant; there is exchange for two protons and hydrolysis of a single molecule of ATP. The four domains of SERCA's structure are labelled: the transmembrane (M), the actuator (A), the phosphorylation (P) and the nucleotide-binding (N). Conformational changes in SERCA's structure are also highlighted. (Illustration adapted from Toyoshima C. *J Gen Physiol 2005; 126(1): cover image*)

1.3.3 SERCA function

The principal function of SERCA is to pump Ca^{2+} ions from the cytoplasm to the lumen of the ER and other specialised compartments, such as the SR and Golgi: SERCA is therefore responsible for both returning cytosolic free Ca^{2+} concentration back to its resting level following cell activation and also maintaining high concentrations of Ca^{2+} in organellar lumens, therefore creating Ca^{2+} gradients across the cell, environments which are critical for a number of cellular functions.

Reviewing the results of SERCA knockout in mice provides further insight into its important roles in normal cellular physiology. SERCA1-null mutants are initially viable but die soon after birth from respiratory failure; this is presumed to be due to a lack of SERCA1 in muscles of the diaphragm and chest wall (where it would normally be expressed in abundance) and consequent impaired muscular function (Pan et al., 2003). SERCA2-null mutants are non-viable, indicating that SERCA2 plays a fundamental role in the functioning of numerous cell types, rather than one confined to muscle physiology: further evidence of a more general, 'house-keeping' type role for SERCA is provided by the ubiquitous nature of SERCA2b expression and strong phylogenetic conservation of SERCA's amino acid sequence (Periasamy et al., 1999; Wuytack et al., 2002). Interestingly, SERCA3 deficient mice do not display an apparently abnormal phenotype: in contrast to SERCA2, SERCA3 therefore does not appear to play key roles during embryogenesis, nor serve an essential housekeeping function (Lynne H. Liu et al., 1997). Possible explanations for this apparently diminished role in Ca^{2+} homeostasis may incorporate SERCA3's reduced affinity for Ca^{2+} and altered pH dependence when compared to other isoforms: an alternative explanation may include functional redundancy between isoforms, for which there is some evidence e.g. SERCA1a has been shown to functionally substitute SERCA2a in the hearts of transgenic mice (Ji, Loukianov, Loukianova, Jones, & Periasamy, 1999; Lytton et al., 1992).

1.3.4 SERCA in human disease

Mutations in SERCA paralogues have been implicated in a number of human diseases and SERCA manipulation has also been explored for a host of therapeutic goals. Brody's disease is characterised by exercise-induced,

progressive impairment of skeletal muscle relaxation, causing cramps, stiffness and muscle pain; it is most frequently due to autosomal recessive inheritance of a mutation in *ATP2A 1* (SERCA1) and consequent reduction in Ca^{2+} uptake into the SR of skeletal muscle cells (Brody, 1969; Odermatt et al., 1996). Darier disease is an autosomal dominant condition due to a mutation in *ATP2A 2* (SERCA2); almost exclusively limited to the skin, it is characterised by defects in keratinocyte adhesion and aberrant epidermal keratinisation: quite why this mutation appears to solely manifest in the skin (with the exception of occasional neuropsychiatric involvement) is unclear, but the affected cell type is somewhat in-keeping with high rates of squamous cell carcinoma seen in SERCA2 deficient mice (L. H. Liu, Boivin, Prasad, Periasamy, & Shull, 2001; Sakuntabhai et al., 1999). Interestingly, patients with Darier disease do not display defects in cardiac function, indicating that one copy of *ATP2A 2* is sufficient to maintain SERCA2a function in cardiac myocytes (where it is known to play essential roles in cardiac physiology), a similar picture to that seen in mice heterozygous for a SERCA2 mutation (Tavadia, Tait, McDonagh, & Munro, 2001). SERCA3 is expressed in pancreatic ß-cells and mutations in *ATP2A 3* have been found in humans with type II diabetes; furthermore, SERCA3 expression is reduced in a murine model of diabetes and Ca^{2+} signalling is perturbed in SERCA3 deficient ß-cells (Arredouani et al., 2002; Levy, Zhu, & Dunbar, 1998; Varadi et al., 1999). Collectively, these observations of naturally occurring SERCA mutations indicate a broad role for this protein in human physiology, ranging from excitation contraction coupling in muscle, to cell adhesion and intracellular signalling.

There has been a great deal of interest in the role of SERCA dysfunction in human heart failure: SERCA mRNA and protein levels are decreased in end-stage heart failure and are closely related to the degree of SR Ca^{2+} uptake and measures of myocardial function, as demonstrated by the analysis of tissue from patients undergoing cardiac transplant (Arai, Alpert, Maclennan, Barton, & Periasamy, 1993; Hasenfuss et al., 1994; Mercadier et al., 1990). It is postulated that these findings may explain abnormalities in Ca^{2+} handling and myocardial relaxation seen in cardiac failure, by a mechanism of reduced SERCA dependent Ca^{2+} uptake to the SR. Given these reproducible findings, investigators have explored the use of gene therapy to restore SERCA expression levels *in-vitro* and *in-vivo* with the aim of rescuing myocardial function in animal models of heart

failure: results of these efforts are promising, with adenoviral delivered gene transfer resulting in improvements in SERCA protein levels, SR Ca^{2+} uptake, myocardial function and animal survival (del Monte et al., 1999; del Monte et al., 2001; Miyamoto et al., 2000). These discoveries have now been translated into humans and there are at least two clinical trials of SERCA2 gene therapy ongoing: preliminary reports have demonstrated the safety of this intervention and suggest efficacy; results of larger, long-term studies are eagerly awaited (Jaski et al., 2009; Jessup et al., 2011).

SERCA's role in proliferative disease has also been investigated: *in-vitro* data in prostate cancer cell lines shows SERCA inhibition with RNAi or thapsigargin inhibits growth and prevents growth factor stimulation of cell proliferation; furthermore, SERCA is upregulated during stimulated cell proliferation and reciprocally downregulated when proliferation is reduced (Crepin et al., 2007; Humez et al., 2004; Legrand et al., 2001). Given the potential for clinical translation of these findings, investigators have explored the application of anti-SERCA agents for use as cytotoxic therapies in proliferative diseases; one of the most notable examples is the use of thapsigargin-derived drugs. Thapsigargin is a natural product originally discovered in the 1970s by Rasmussen *et al* from the umbelliferous plant *Thapsia garganica*, based on its ability to liberate histamine from mast cells of the skin: thapsigargin is a potent and selective inhibitor of SERCA function through its strong binding to the protein (Rasmussen, Broogger Christensen, & Sandberg, 1978; Sagara & Inesi, 1991; Thastrup, Cullen, Drobak, Hanley, & Dawson, 1990). Exposing cancer cell lines (e.g. prostate or liver) to thapsigargin results in their apoptosis; the mechanism of this cytotoxicity is widely regarded to be due to thapsigargin's dose-dependent ability to elevate intracellular Ca^{2+} sufficiently to activate programmed cell death (Furuya, Lundmo, Short, Gill, & Isaacs, 1994; Kaneko & Tsukamoto, 1994). Thapsigargin's cytotoxic action, whilst apparently effective at inducing cell death in cancer, is not cell-specific and would therefore likely result in considerable side-effects if used systemically in humans: thapsigargin's effects have been exploited clinically by specifically targeting it to cancer cells e.g. by coupling to a peptide carrier through chemical modification, to produce a prodrug that is activated only at deposits of tumour cells (Denmeade et al., 2003). A thapsigargin prodrug, G-202 has been produced to target prostate specific membrane antigen (PSMA),

a type II membrane carboxypeptidase which is over-expressed in prostate cancer cells and the neovasculature of most other solid tumours: G-202 is currently being evaluated in a clinical trial of patients with advanced solid tumours (trial protocol available at http://clinicaltrials.gov/ct2/show/NCT01056029 (Ghantous, Gali-Muhtasib, Vuorela, Saliba, & Darwiche, 2010). This translation of basic science to clinical medicine provides a further example of how discoveries of SERCA's roles in cell biology can be applied to the treatment of common and frequently debilitating medical problems. Further discussion of SERCA's apparent roles in pulmonary health and disease will now be considered and form the basis for this thesis.

1.4 SERCA and the Lung

SERCA has been implicated in diseases of the lung including asthma and cystic fibrosis; this, combined with recent evidence suggesting an essential role for SERCA in normal pulmonary development, indicates that further investigation into SERCA's role in the lung is warranted.

1.4.1 SERCA deficiency in the pathogenesis of asthma

Abnormal Ca^{2+} handling has been proposed to underpin airway hyper-responsiveness in asthma, since Ca^{2+} is a key regulator of ASM contractility (Parameswaran, Janssen, & O'Byrne, 2002; Triggle, 1983). Ca^{2+} reuptake into the SR is critical for ASM function; given that SERCA is a key regulator of Ca^{2+} reuptake, it is likely that SERCA activity is essential for ASM functions: this inter-relationship of ASM function and SERCA derived SR Ca^{2+} reuptake, as well as pro-inflammatory cytokine mediated repression of SERCA in ASM has led to SERCA being explored as a novel asthma target (Hirota, Helli, & Janssen, 2007; Sathish et al., 2009). Mahn *et al* demonstrated that SERCA2 mRNA and protein expression is reduced in ASM of patients with asthma; this reduction correlates with disease severity and is associated with corresponding changes in Ca^{2+} homeostasis, such as attenuation in response of intracellular Ca^{2+} to thapsigargin stimulation (Mahn et al., 2009). Interestingly, ASM taken from asthmatics, or healthy subjects then subjected to siRNA mediated SERCA knockdown, displayed increased cell proliferation, cell-spreading and cytokine secretion, effects similar to those known to underpin the asthmatic ASM phenotype. The authors conclude that an underlying SERCA2 deficiency in ASM may induce these cellular effects that contribute to ASM remodelling, a mechanism central to the pathogenesis of asthma: restoration of SERCA2 function is hence proposed as a novel therapeutic target in asthma.

1.4.2 SERCA as a treatment target in cystic fibrosis

Cystic fibrosis, a relatively common (incidence 1:2500 live births), lethal autosomal recessive disease, is most frequently caused by a mutation of the cystic fibrosis transmembrane regulator (CFTR) gene, known as ΔF508, which prevents it functioning as a cAMP-dependent Cl^- ion channel. This mutation results in a CFTR protein that is retained in the ER; retention is dependent upon

chaperone proteins, many of which require high Ca^{2+} concentrations for optimal activity (S. H. Cheng et al., 1990). Given *in vitro* evidence that mutant ΔF508-CFTR protein can function as a Cl^- ion channel if permitted to reach the cell surface, a landmark study aimed to create conditions that would enable CFTR protein to exit the ER, by depleting ER Ca^{2+} stores and hence inhibit the action of chaperone proteins retaining the CFTR (Dalemans et al., 1991; Egan et al., 2002; Rubenstein, Egan, & Zeitlin, 1997). In order to deplete ER Ca^{2+}, the SERCA inhibitor thapsigargin was administered to CFTR cell lines and also *in vivo* to ΔF508 mutant mice via aerosol: thapsigargin treatment released ER-retained ΔF508-CFTR to the plasma membrane, where it functioned effectively as a Cl^- channel; furthermore, it reversed the nasal epithelial potential difference defect observed in the CF mouse model (Egan et al., 2002). In view of the potential implications of these data for CF pharmacotherapeutics, a host of studies have investigated the use SERCA pump inhibitors (thapsigargin, curcumin and cyclopiazonic acid) with the aim of correcting the CF phenotype: although a number report highly promising results, with significant improvements in CFTR Cl^- channel function *in vitro* and *in vivo*, others have failed to reproduce these findings and controversy persists (Berger et al., 2005; Dragomir, Bj√∂rstad, Hjelte, & Roomans, 2004; Egan et al., 2004; Grubb et al., 2006; Loo, Bartlett, & Clarke, 2004; Norez, Antigny, Becq, & Vandebrouck, 2006; Seng et al., 2004). More recently, work has been carried out to optimise drug delivery and nanoparticles have been used to deliver curcumin to CF mice orally, resulting in a partial correction of CF defects: SERCA continues to be explored as a therapeutic target in CF (Cartiera et al., 2009).

1.4.3 Evidence for a fundamental role for SERCA in lung development

Initial observations of SERCA's role in prenatal lung development occurred during investigation of AP and the propagating ASM Ca^{2+} waves that underpin it (N. Featherstone et al., 2005; N. C. Featherstone et al., 2005). As discussed above, AP waves arise from a right-sided pulmonary pacemaker and appear coupled to lung growth (Jesudason et al., 2005). To determine the origin of these Ca^{2+} waves specific pharmacological blockers were used to test the role of intracellular Ca^{2+} stores, extracellular Ca^{2+} entry and gap-junction connectivity (N. C. Featherstone et al., 2005). Cyclopiazonic acid (CPA), a specific SERCA

inhibitor was used on cultured and contracting lung explants to determine if Ca^{2+} stores were required for the AP waves and underlying Ca^{2+} transients (Seidler, Jona, Vegh, & Martonosi, 1989). CPA induced several key effects that might be expected from its mode of action: (i) ASM Ca^{2+} transients were abolished; (ii) baseline intracellular Ca^{2+} concentration was increased; (iii) AP was replaced with tonic ASM contraction (Figure 1.5). However, an unexpected finding was that branching morphogenesis was halted (Figure 1.6) (N. Featherstone et al., 2005; N. C. Featherstone et al., 2005). Importantly, these effects were reversible, with branching resuming when CPA was removed, thus indicating that effects on pulmonary growth were not simply due to toxicity e.g. death of the explanted tissue (N. Featherstone et al., 2006). Further investigation revealed decreases in lung branching and AP frequency were dependent on CPA dose, with higher doses abolishing both (Lansdale, Connell, Featherstone, Midgley, & Jesudason, 2010).

CPA's effects indicate a fundamental role for SERCA in pulmonary organogenesis. Given that: (i) branching morphogenesis and AP have been shown to be coupled *in vitro*, and (ii) SERCA mediated Ca^{2+} reuptake into the SR is critical for smooth muscle function (discussed above), it was necessary to determine if CPA-induced abolition of ASM contractility was required for abrogation of branching. To test this, we sought a model of airway branching morphogenesis that occurs in the absence of ASM and in which genetic, rather than pharmacological inactivation of SERCA can be used. This led us to the *Drosophila* model discussed later.

In addition to questions related to SERCA and the interplay of airway branching and ASM function, further consideration of the CPA-induced lung explant phenotype yields a number of other questions that require wider investigation: e.g. (i) what are the cellular mechanisms that underpin the witnessed changes in airway branching and peristalsis? (ii) are these changes reproducible *in vivo*? (iii) could off-target effects of CPA (outside of SERCA inhibition) be responsible for these changes in development, or can they be reproduced by genetic SERCA inhibition? These questions will be considered in detail by this thesis and are further discussed below.

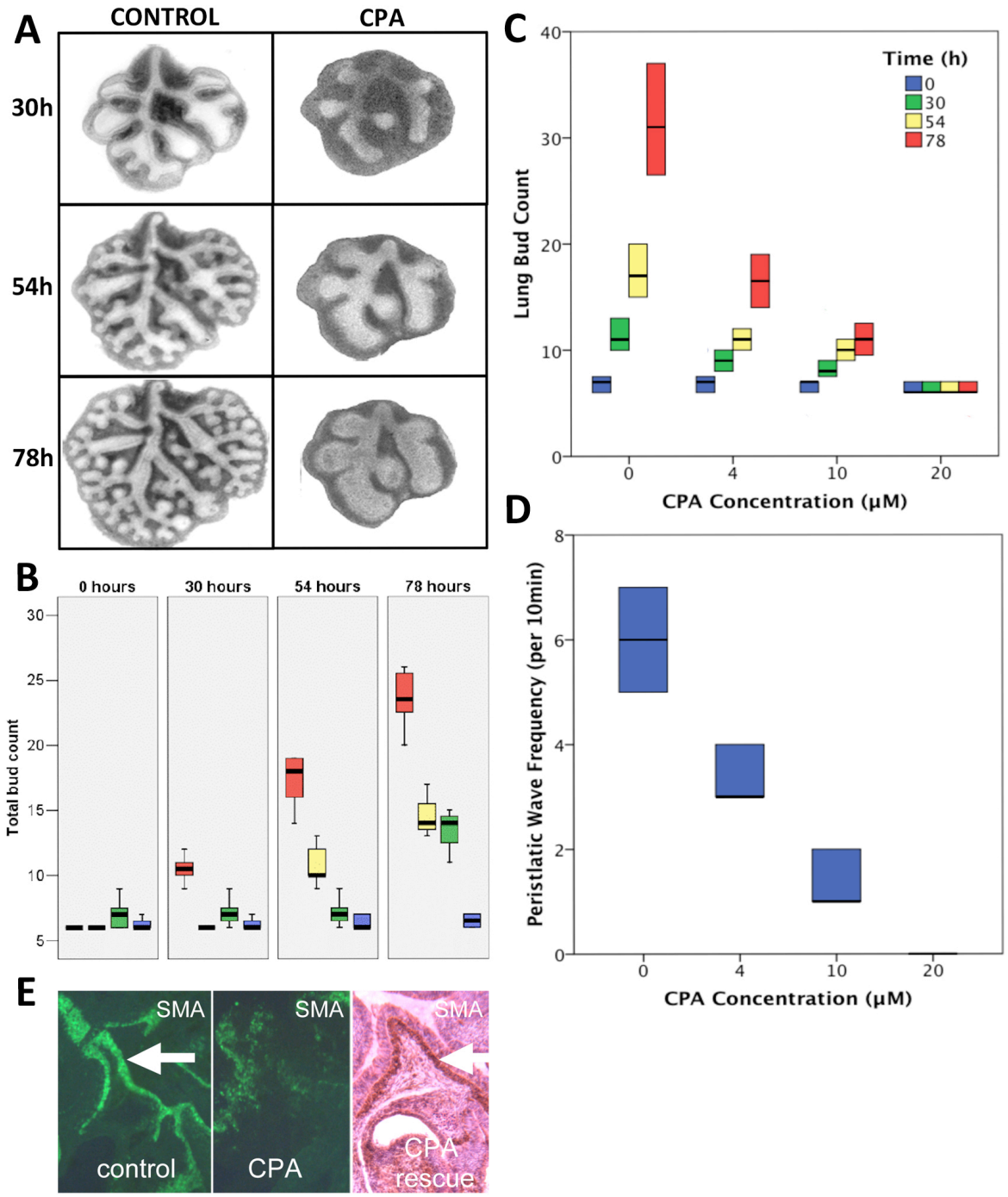

Figure 1.5 SERCA blockade with cyclopiazonic acid (CPA) reduces both airway branching and peristalsis reversibly and dose dependently, whilst reversibly halting Smooth Muscle Actin (SMA) expression

Panel A: photomicrographs of E13 rat lung explants cultured +/- 20 µM CPA (time in culture indicated in hours). Panel B: lung bud number vs. time (medians, IQR & range); normal lung (red) branches throughout; CPA treatment for all 78 hours (blue) abolishes branching; removal from CPA at 30 hours (yellow) and 54 hours (green) restarts branching within 24 hours. Panel C: lung bud number (median & IQR) vs. CPA concentration at 0, 30, 54 & 78 hours (n=>25 in all groups). Panel D: number of peristaltic waves in 10min (median & IQR) vs. CPA concentration (n=>10 in all groups). Difference between CPA concentration groups statistically significant ($p<0.05$). Panel E: SMA immunohistochemistry labelling (green) of proximal ASM in control lung (arrowed, left) with a paucity of SMA in CPA-treated lung (middle) and return of SMA (brown, arrowed) in lung rescued from CPA >24 hours previously (right). (All data and photomicrograph images courtesy of N.C. Featherstone, M.G. Connell and E.C. Jesudason)

1.5 Animal models of lung development

Data presented above indicate that further exploration of SERCA's role in lung development is warranted and could yield novel insights into those translational opportunities that have already been explored for SERCA in pulmonary disease. Given this potential importance, it seems prudent to review different experimental techniques that could be exploited in order to achieve this aim. To determine the roles of SERCA in airway development, animal models are required and their various strengths and weaknesses are briefly reviewed below.

1.5.1 Vertebrate models

The rich history of developmental analysis in the mouse has made it the model of choice for studying mammalian development and it remains the principal model with which to study the airway: in the past two decades or so, transgenic mice have permitted dramatically improved understanding of the cellular processes underlying lung development, homeostasis, and repair (discussed above) (Cardoso & Lu, 2006; Warburton et al., 2010). Mice have clear advantages as a model organism, including the close homology of lung development between mammalian species and the ever-increasing availability of mutants. Notable examples of murine data advancing the field include, Alescio and Cassini's early work on epithelial-mesenchymal cross-talk (discussed above), Metzger *et al's* painstakingly detailed cataloguing of the three-dimensional branching patterns and lineage of the mouse bronchial tree, and discoveries of FGF-10's key chemotactic role in inducing epithelial lung branching (Alescio & Cassini, 1962; Bellusci, Grindley, Emoto, Itoh, & Hogan, 1997; Metzger, Klein, Martin, & Krasnow, 2008; Park, Miranda, Lebeche, Hashimoto, & Cardoso, 1998). Murine work may involve the assessment of lung tissue (e.g. gross morphology, histology or molecular cell biology) from animals post mortem or after *in vitro* culture of explants. Gene expression can be manipulated in these systems with an array of techniques, broadly divisible into: (i) *in vitro* agents e.g. pharmacological inhibitors or RNA interference (RNAi); and (ii) *in vivo* means e.g. chemical mutagenesis, site-directed gene knock-out or conditional, lung-specific transgenesis (such as the Cre-LoxP system) (Paddison et al., 2004; Sauer & Henderson, 1988; K. R. Thomas & Capecchi, 1987). Creating novel transgenic and mutant mice can be challenging, due to relatively long generation times, difficulties in conditional mutant generation to circumvent lethality and also

issues such as genetic redundancy and developmental plasticity. For phenotypic assessment, an array of imaging techniques have been developed for use in live and fixed tissues, including different forms of microscopy (e.g. light, fluorescent and confocal), magnetic resonance imaging and bioluminescence. Live imaging of the developing mouse embryo is largely reserved to *ex utero* culture systems: *in utero* imaging of embryogenesis has been described with ultrasound backscatter microscopy or optical coherence tomography, but detailed imaging of the lung has not been reported (Syed, Larin, Dickinson, & Larina, 2011; Turnbull, Bloomfield, Baldwin, Foster, & Joyner, 1995).

Chick and quail embryos have also been used as a system with which to study pulmonary development; key advantages of these models include cost, availability, rate of development (which can be mainpulated with changes in temperature), ease of manipulation (including ability to perform microsurgery on the living organism and transgenesis) and advanced imaging capabilities. Important discoveries have been made in the chick embryo, including the existence of embryonic germ layers, the neural crest giving rise to the peripheral nervous system and the development of left right asymmetry [reviewed in (Stern, 2005)]. Novel whole organism (*in ovo*) live imaging techniques have been devised in avian embryos and promise a great deal; one such exciting potential use may be live imaging of AP in the developing lung *in ovo*, although practicalities of this, such as minimising artefact from the nearby beating heart have yet to be determined (Kulesa, Bailey, Cooper, & Fraser, 2010).

In this thesis, an established embryonic lung explant culture model is exploited that has been successfully used in the past to study both branching morphogenesis and AP in the developing lung.

1.5.2 Drosophila

Drosophila melanogaster is a classical model organism: used by geneticists and developmental biologists since the early 20th century, research in the fruit fly has channelled modern biology. A number of properties lend *Drosophila* to this role, for example: (i) they generate prolifically, are cheap to maintain, easily transportable and simple to culture; (ii) they are highly relevant to biomedical research, given that an estimated 75% of 1378 human disease loci detected at

genome wide association studies have fly counterparts; (iii) vast libraries of experimental resources e.g. transgenic fly lines, are held at large collaborative laboratories and are available to researchers relatively cheaply; and (iv) *Drosophila* offer an unparalleled, powerful genetic tool kit to researchers. Examples of these tools include, the bipartite *GAL4/UAS* system that permits inducible overexpression of genes, site-specific recombination and mosaic analysis systems e.g. mosaic analysis with a repressible cell marker (MARCM), and an almost genome wide library of inducible *in vivo* RNA interference (RNAi) lines for gene silencing: many of these tools will be discussed prior to their use later in this thesis (Brand & Perrimon, 1993; Dietzl et al., 2007; Lasko, 2002; T. Lee & Luo, 1999).

1.5.3 Development of the Drosophila respiratory organ

Looking at respiratory organogenesis, the fly offers a comparatively simple, highly stereotyped, branched tracheal system to study, but one that remains directly homologous to mammalian lung development, owing to conservation of key genetic pathways through evolution. It is a network of tubes that fulfils respiratory demands of the fly by allowing air to enter through specialised openings, called spiracles and then be transported through the network to blind-ended capillaries that facilitate gas exchange with target tissues. For effective function, it is critical that (i) tracheal branches find their way to all tissues in the fly; and (ii) trachea have the correct dimensions for optimal gas flow. The complex genetic regulation of these events has largely been discovered and provides a fascinating insight into the similar regulation of mammalian lung development. Classically, the tracheal system of *Drosophila* embryos has been used as a model with which to explore these pathways and it is this that will now be discussed in some detail. Less well studied and more variable in nature, *Drosophila* larvae also have a branched network of respiratory tubes and related appendages; these will be reviewed when investigated in Chapter 7.

Embryonic tracheal morphogenesis occurs through a series of iterative branching events that result in an elaborate network of single-cell thick epithelial tubes with cuticular lining: originating from 10 pairs of metameric tracheal sacs, comprising around 80 cells each, the network is built without further cell division by orientated cell migration, changes in cell shape, selective growth of

the apical cell membrane and intracellular lumen formation (Figure 1.6) (Manning & Krasnow, 1993; Samakovlis, Hacohen et al., 1996; A. Uv, Cantera, & Samakovlis, 2003). The 20 tracheal sacs form by invagination of planar ectodermal cells in the embryo, a process brought about by expression of the transcription factor *trachealess* and its interaction with its cofactor *tango*. The first branching event occurs when this sac develops six stereotyped primary branches (Figure 1.6B), events that are induced by a member of the fibroblast growth factor family, Branchless (Bnl): *bnl* is 'turned-on' in patches of mesenchyme around each sac and promotes branch migration towards its source through activation of Breathless (Btl), the receptor tyrosine kinase expressed in the tracheal epithelium (Klambt, Glazer, & Shilo, 1992; Sutherland, Samakovlis, & Krasnow, 1996). The dynamic, differential expression of *bnl* controls the patterning of branch outgrowth. *bnl* expression is therefore a key factor in determining tracheal system structure: misexpression of *bnl* in novel locations induces ectopic branch formation (Sutherland et al., 1996). The intracellular protein Downstream-of-FGF-receptor, encoded for by *dof* (*stumps*) is specifically required for FGF signal transduction; in *stumps* mutants, tracheal cells fail to move out from the epithelial sacs and only rudimentary tracheal branches form (Imam, Sutherland, Huang, & Krasnow, 1999). Primary branch growth entails three major cellular events: extension of actin filaments (filipodia) towards the source of Bnl; movement of the nucleus and cell body in the same direction; and enlargement of the apical cell surfaces to accommodate the growing lumen (A. Uv et al., 2003). Early patterning genes induce the specific, regional identities of the primary branches shown in Figure 1.6B: (i) cells exposed to Decapentaplegic (Dpp) signalling maintain expression of two early tracheal transcription factors, Knirps (Kni) and Knirps-related (Knrl) and will migrate either dorsally to populate the dorsal branch (DB) or ventrally to populate the lateral trunk branches (LTa & LTp/GB); (ii) activation of EGF by Rhomboid (Rho) in a central subset of tracheal cells is required for development of the dorsal trunk (DT) and visceral branch (VB); and (iii) the differentiation between DT and VB cells is mediated by Wingless (Wg) signalling which induces DT cell fates (Chihara & Hayashi, 2000; Llimargas, 2000; Llimargas & Casanova, 1999; Wappner, Gabay, & Shilo, 1997). Given that EGF and Wg promote the transcription factor Spalt, which is repressed by Kni and Knrl, a clear system of regional specification of primary branch migration is apparent (C. K. Chen et al., 1998).

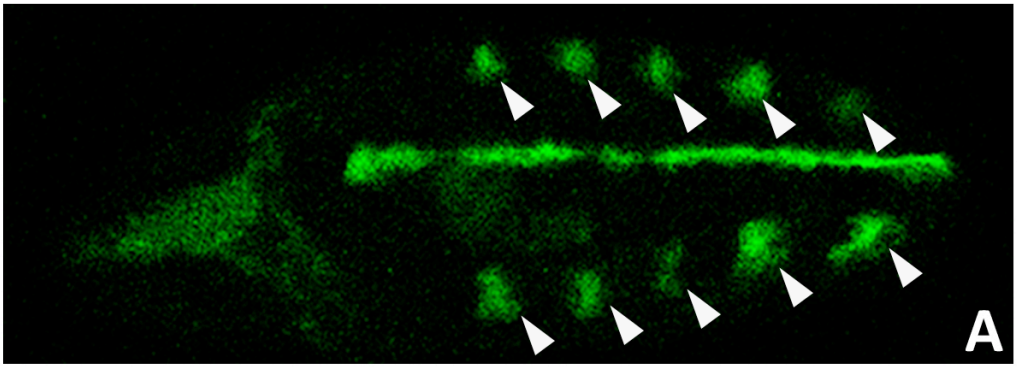
A

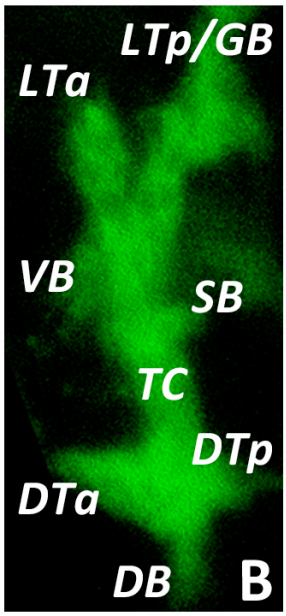
LTp/GB
LTa
VB
SB
TC
DTp
DTa
DB
B

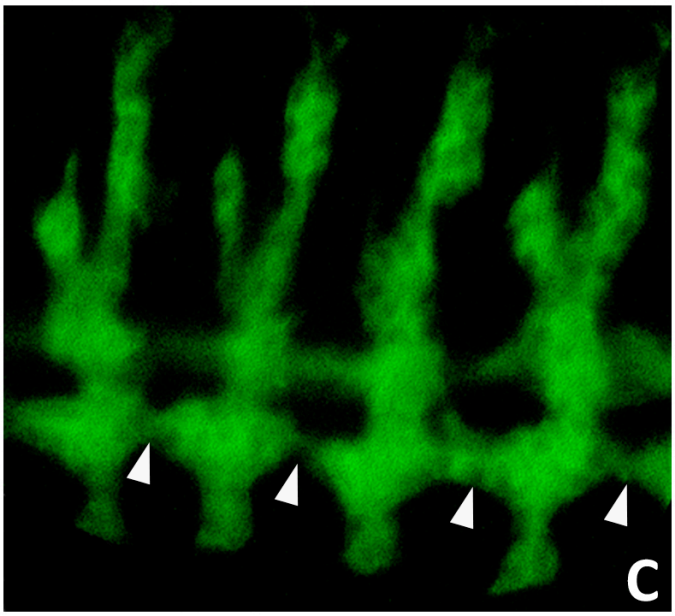
C

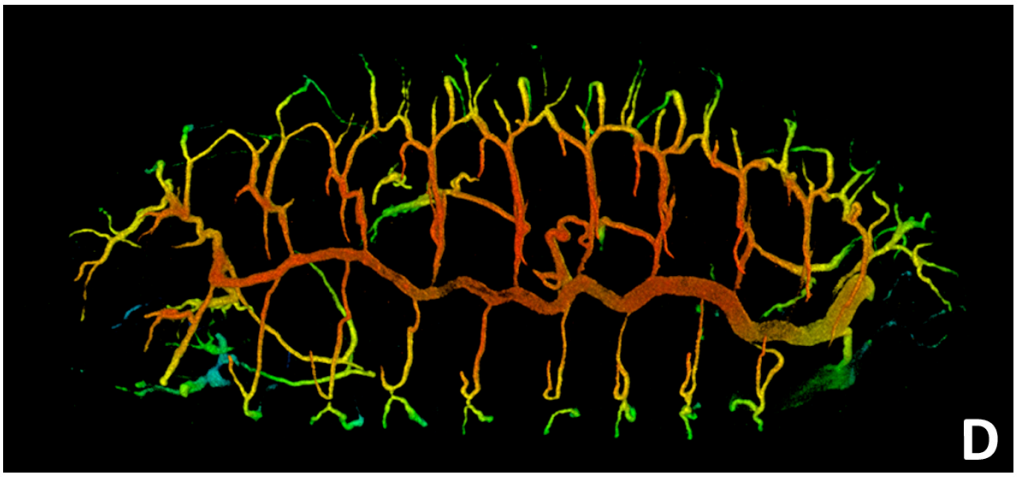
D

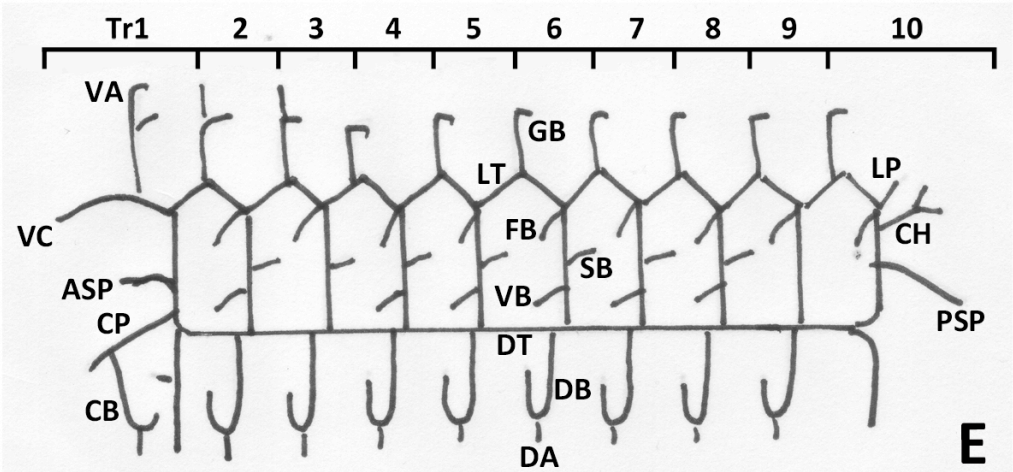
Tr1
2
3
4
5
6
7
8
9
10
VA
GB
LT
LP
VC
FB
CH
SB
ASP
VB
CP
PSP
DT
DB
CB
DA
E

Figure 1.6 Development of the *Drosophila* embryonic tracheal system

Panels A-C: confocal micrographs of the embryonic tracheal system labelled with GFP (*Btl-GAL4, UAS-act5c.GFP*). Panel A: stage 11 embryo demonstrating the 10 paired metameric tracheal sacs, the earliest tracheal structure (arrowed in white) which is evident approximately 6 hours after embryo laying (AEL). Panel B: the 6 primary tracheal branches of a single sac are shown and labelled: dorsal branch (DB), dorsal trunk (DT), transverse connective (TC), visceral branch (VB), spiracular branch (SB) and lateral trunk (LT). The DT and LT branches have paired anterior (a) and posterior (p) elements. Panel C: tracheal system at stage 13 (approximately 10 hours AEL): the dorsal trunk branches in neighbouring metameres have fused together (arrowed in white) to form the dorsal trunk (DT), the main airway of the embryo. Panel D: 3D projection of confocal Z-stacks of an embryo with fully developed tracheal system (stage 16/17). The tracheal system is labelled with the 2A12 antibody (DSHB, University of Iowa) and pseudo-coloured to illustrate depth of its structure. Panel E: Schematic diagram of the fully formed tracheal system. The 10 metameric units are illustrated (Tr1-Tr10) and standard branch names indicated at Tr6: DT, DB, dorsal anastamosis (DA), VB, SB, fat body branch (FB), lateral trunk (LT) and ganglionic branch (GB). Some specialised branches of Tr1: ventral anastamosis (VA); ventral cephalic branch (VC); cerebropharyngeal branch (CP); cerebral branch (CB); anterior spiracular branch (ASP) and Tr10: lateroposterior branch (LP); caudal-hindgut branch (CH) and posterior spiracular branch (PSP) are also illustrated. The lateral aspect of the embryo is shown in each case (anterior to the left, ventral uppermost).

Secondary tracheal branches form a number of hours after primary ones bud: in this process, cells nearest the end of each primary branch form either: (i) *fusion cells*, that join neighbouring tracheal metameres or the paired tracheal hemi-segments; or (ii) *terminal cells,* the blind-ended tracheoles that directly contact target tissues for gas exchange (Samakovlis, Hacohen et al., 1996). This cell-fate determination requires the ETS-family transcription factor Pointed (Pnt) and again relies on iterative Bnl-Btl, Dpp and Wg signalling: furthermore, activation of Delta-Notch signalling plays a role in refining fusion/terminal cell fate, possibly by restricting the fate of neighbouring tracheal cells (Notch mutants display both an increased number of fusion *and* terminal cells) (Ikeya & Hayashi, 1999; Llimargas, 1999; Scholz, Deatrick, Klaes, & Klambt, 1993; Steneberg, Hemphala, & Samakovlis, 1999). There are five fusion cells in each tracheal metamere: one at the end of the DB, which connects with the DB fusion cell of the contralateral hemi-segment, and one each at the anterior and posterior ends of the DT and LT, which contact the fusion cells of the DT and LT in the adjacent tracheal metameres (Figure 1.6). Fusion cells express the transcription factor Escargot, which is required for deposition of the adhesion protein E-cadherin at the contact site between the two adjoining fusion cells (Tanaka-Matakatsu, Uemura, Oda, Takeichi, & Hayashi, 1996). Nineteen of the approximate 80 cells of each tracheal metamere become terminal cells; each terminal branch comprises one cell and targets distinct tissues in the embryo to facilitate gas exchange. Embryonic terminal branches have a fixed path and follow developmental cues, in contrast to those in larvae that are also guided by hypoxia. Two key genes involved in this terminal branching are: (i) *sprouty,* which encodes a cytoplasmic factor activated in response to high-level Btl-signalling at the primary branch tips and functions to antagonize the pathway in neighbouring cells to limit the number of cells that take on a terminal cell fate; and (ii) *pruned,* which encodes *Drosophila* serum response factor (DSRF), a transcription factor required for the establishment of cytoplasmic extensions: DSRF activity must be controlled to prevent ectopic branching and limit the invasion of tracheoles into tissues normally supplied by other tracheal cells (Guillemin et al., 1996; Hacohen, Kramer, Sutherland, Hiromi, & Krasnow, 1998).

The above events, comprising highly stereotyped cell migration, changes in cell shape, selective growth of the apical membrane and intracellular lumen formation (rather than cell proliferation), are sufficient to build the final, complex network of embryonic tracheae (shown in Figure 1.6) by approximately 16 hours AEL (Manning & Krasnow, 1993; Samakovlis, Hacohen et al., 1996). Further to this and prior to embryonic hatching, the tracheal structure undergoes various maturation events and ultimately fills with air to become functional in its role as a respiratory organ: further discussion of tracheal maturation is provided in Chapter 6.

Among tubular organs, the *Drosophila* trachea has emerged as the premier system for understanding the molecular and cellular underpinnings of tube formation (Maruyama & Andrew, 2012). For the purpose of this thesis, *Drosophila* provides a genetically tractable model of airway development where existing genetic tools allow the elegant spatial and temporal manipulation of SERCA function and *in vivo* study of airway morphogenesis.

1.6 Introductory summary and aims of the thesis

Disordered lung development results in death and disease in the young and old: development of novel therapies to target these conditions requires new insights into pulmonary development. SERCA, already explored as a treatment target in asthma and CF, appears to play a key role in regulating aspects of early pulmonary organogenesis: further investigation of this role may be achieved using murine and fly models of airway development.

In view of the striking effects of SERCA inhibition presented above, this thesis aims to further explore this CPA-induced embryonic lung phenotype by assaying changes in gene expression and cell proliferation. In addition, given the coupling of Ca^{2+} dependent AP and branching morphogenesis, it is necessary to separate these two phenomena to ascertain whether SERCA function regulates airway branching morphogenesis itself or whether effects of SERCA inhibition are mediated through changes in airway contractility. By exploiting a *Drosophila* model, this thesis aims to determine the effects of genetic perturbation of SERCA function *in vivo* on airway branching morphogenesis, in the absence of airway contractility.

Chapter 2

MATERIALS AND METHODS

2.1 Bioinformatics

2.1.1 Analysis of SERCA

SERCA genomic and protein data were obtained from the National Center for Biotechnology (NCBI, available at http://www.ncbi.nlm.nih.gov) and Flybase (available at http://flybase.org/) databases. Sequence comparisons against a variety of databases were performed using BLAST (NCBI, available at http://blast.ncbi.nlm.nih.gov/Blast.cgi) which matches short sequence fragments and identifies the best local alignment between unknown sequences and the database. BLASTP was used to align protein sequences with other known SERCA paralogues and splice variants, for a number of model organisms and subsequently retrieve their protein sequences. Multiple alignments of protein sequences were obtained using ClustalW2 at the European Bioinformatics Institute (available at http://www.ebi.ac.uk/Tools/msa/clustalw2/).

2.1.2 RNA interference (RNAi) construct assessment

RNA interference (RNAi) constructs were analysed by aligning the construct's DNA sequence (obtained from the supplier) with the cDNA sequence of the gene of interest, using the BLAST (NCBI) software and assessing the start and end points of the alignment. When the supplier did not provide the DNA sequence, the specified forward and reverse primers were similarly aligned with BLAST. The start point of the forward and end point of the reverse primer was then recorded and used to obtain the predicted DNA sequence of the RNAi construct.

Each RNAi construct was checked for predicted off-target effects by inputting the sequence into dsCheck (available at http://dscheck.rnai.jp/) (Naito et al., 2005). This software predicts genes that the RNAi could potentially interfere with, other than the gene intended for knockdown. It 'dices' the input sequence into 19 nucleotide lengths of small interfering RNA (siRNA) and performs exhaustive scans for each 'diced siRNA' to find off-target gene candidates, simulating the biochemical process of dsRNA-mediated RNAi in vivo. The software then provides the number of hits with a complete match, one mismatch and two mismatches for every off-target gene candidate individually.

2.1.3 Oligonucleotide primer design

In order to design oligonucleotide primers for RT-PCR, the cDNA sequence of the gene of interest was inputted into Primer3Plus software (available at http://www.bioinformatics.nl/cgi-bin/primer3plus/primer3plus.cgi). The software's parameters were specified to provide a primer size of between 18 and 25 bases, a product size of less than 400 base pairs and predicted melting points of both primers within 3°C. The advanced parameters were set to provide a maximum poly-X of 3 bases, maximum number of unknown bases of 0, maximum self-complementarity score of 8 and maximum 3' self-complementarity score of 0. The oligonucleotide primers were then reviewed using BLAST (NCBI). *FGF-10* primer sequences were taken from Unbekandt *et al's* publication where they had been successfully used for PCR analysis (Unbekandt et al., 2008). Primer sequences used in PCR experiments are detailed in Tables 2.1 and 2.2.

Table 2.1 Oligonucleotide primer sequences used in murine PCR

Gene	Forward Primer	Reverse Primer	Product Size
18S	TCCGATAACGAACGAGACTC	CAGGGACTTAATCAACGCAA	315
Fgf-9	CGGCACCAGAAATTTACACA	ATAAGAACCCACCGCATGAA	161
Fgf-10	CACATTGTGCCTCAGCCTTTCC	CCTGCCATTGTGCTGCCAGTTAA	506
Shh	GGAAAACACTGGAGCAGACC	CCACGGAGTTCTCTGCTTTC	308
SM-MHC	AGGAAACACCAAGGTCAAGC	CCCTGACATGGTGTCCAATC	324
Spry2	TTGTGGTTTGCAGTGAGAGG	TCTTCGCCTAGGAGTGTTGG	200
Vegfa	ATGTGACAAGCCAAGGCGGTG	TGGCGATTTAGCAGCCAGATA	298

Table 2.2 Oligonucleotide primer sequences used in Drosophila PCR

Gene	Forward Primer	Reverse Primer	Product Size
18S	CGCAAGATCGTTATATTGGTTG	GCTGCCTTCCTTAGATGTGG	203
Ca-P60A	CGATATCCGTATCACCCACA	CTCACCGAACTCGTCCAGTT	292

2.2 Murine Experiments

2.2.1 Preparation of murine embryonic lung explants

In accordance with Schedule 1 of the UK Animals Act, embryos from timed-pregnant mice (Charles River Ltd, Margate, UK) were harvested on Day 11.5 of gestation (vaginal plug positive = Day 0) by caesarean section. Upon retrieval, embryos were transferred to an isotonic saline bath cooled on ice. Micro-dissected from their extra-embryonic membranes, embryos were secured in a lateral position using cranial and caudal entomology pins (Figure 2.1). Using a Leica MZ6 (Leica Microsystems Ltd., Milton Keynes, UK) stereomicroscope and microsurgical instruments, a thoracic incision was performed to expose the embryonic heart and lungs. The heart was teased from the lung rudiments before the oesophagus was freed carefully from the primitive carina. The trachea was then sectioned and the pulmonary complex transferred by pipette into serum-free culture medium (DMEM/F12 1:1, Gibco; Invitrogen Life Technologies, Paisley, UK).

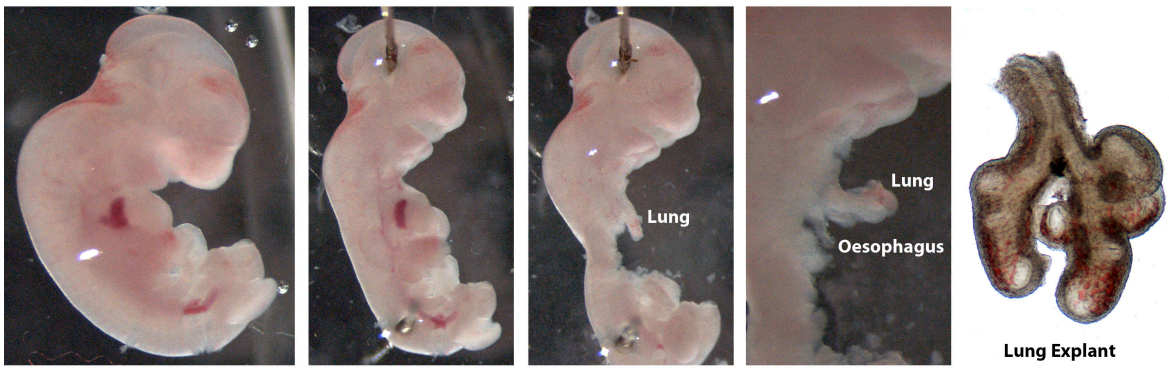

Figure 2.1 Micro-dissection steps used to isolate lung explants from E11.5 mouse embryos

2.2.2 Embryonic lung explant culture

Lung rudiments were positioned on translucent polytetrafluorethylene membrane culture-dish inserts (Millicell; Millipore Corp., Bedford, MA) with serum-free culture media incorporating penicillin (100 IU/ml) and streptomycin (100 µg/ml; Gibco). Cyclopiazonic acid (CPA) (Sigma-Aldrich Company Ltd., Dorset, UK) was filter sterilised and added to the medium at final concentrations of 4 – 20 µM. Lung primordia were incubated at 37°C in 5 % CO_2 for periods up to 78 hours. Using brightfield microscopy, specimens were inspected daily for histologic integrity and viability, and photographed. The culture medium was changed every 48 hours. Lung cultures were either homogenised for RNA extraction or fixed and mounted for histology.

2.2.3 Embryonic lung explant RNA extraction

For each culture condition, lung explants were collected and snap frozen in a micro-centrifuge tube with liquid nitrogen. They were homogenised with a pestle in a micro-centrifuge tube containing 350 µL Buffer RLT (Qiagen Ltd., Crawley, UK) with ß-mercaptoethanol (10 µL per 1 ml). The suspension was then passed 10 times through a 22-gauge needle fitted to a 1 ml RNase-free syringe. The suspension was then transferred to a QIAshredder spin column (Qiagen) and centrifuged at 8,000 x g for 2 min. RNA was extracted from the subsequent lysate using an RNeasy Mini Kit (Qiagen) according to the handbook protocol. Briefly, 1 volume of 70 % ethanol was added to the lysate, mixed by pipetting and the mixture transferred to an RNeasy spin column, which was centrifuged for 15 sec at 8000 x g. After washing the column with 350 µl Buffer RW1 and centrifuging for 15 s at 8000 x g, an on-column DNase digestion was performed, to eliminate genomic DNA contamination. 10 µl DNase I solution (1500 Kunitz units in 550 µl) were added to the spin column membrane along with 70 µL Buffer RDD (Qiagen) and incubated at 25 for 15 minutes. The spin column membrane was further washed with 350 µl Buffer RW1 and then twice with 500 µl Buffer RPE, with the column being centrifuged after each step. Finally, the RNA was eluted from the spin column membrane by adding 50 µl nuclease-free H_2O and then centrifuging for 1 min at 8000 x g. The concentration of extracted RNA was determined at 260 nm using a NanoDrop ND-1000 spectrophotometer. The A260/A280 ratio was assessed as an indicator of RNA purity. The RNA was then stored at -80°C.

2.2.4 Embryonic lung explants fixation and mounting

Cultured lungs were preserved in 4 % paraformaldehyde in PBS, rinsed in PBS, cryoprotected with 20 % (wt/vol) sucrose, gelatine embedded (7.5% [wt/vol] gelatin, 15 % [wt/vol] sucrose in PBS), before being covered in Cryo-M-Bed (Bright, Huntingdon, UK), and snap-frozen at -30°C. Lung frozen sections were taken at 7 µm using a microtome and mounted on slides for storage at -30°C.

2.2.5 Lung explant immuno-histo-chemistry

Frozen sections were allowed to thaw at room temperature and then circled with a hydrophobic pen (Dako UK Ltd., Ely, UK). All subsequent steps were carried out with a drop of solution within each hydrophobic circle. Specimens were first blocked for 30 minutes with 20% goat serum in PBS. Incubation with anti-phospho-Histone H3 (Ser10, Rabbit, Cell Signalling Technologies, Danvers, MA, USA) diluted 1:500 with PBS was carried out at 4°C overnight. Washes used coplin jars and comprised 3 x 10 minute washes in PBS. Alexa Fluor® 555 anti-rabbit (Invitrogen, 1:500 in PBS) secondary antibody and DAPI (1:5000) were incubated with the sample in the dark for 2 hours at room temperature. Washes were carried out as previously stated. The sections were mounted by applying a coverslip over aqueous mountant (Dako).

2.3 Drosophila Experiments

2.3.1 Growth and maintenance of Drosophila

Fly stocks were maintained at 18°C, 25°C or 29°C with a 12 hour light/dark photo cycle, on Drosophila yeast/glucose medium (Table 2.3). Adult flies were anaesthetised with CO_2 gas using an Ultimate Flypad (Genesee Scientific, San Diego, CA, USA) and examined using a Nikon SMZ-645 stereoscopic zoom microscope (Nikon UK Limited, Kingston Upon Thames, UK) and Photonics PL3000 light source (Photonic Optics, Vienna, Austria). Flies were manipulated using a fine artist's paintbrush.

Table 2.3 Drosophila Food Recipe

Mass / Volume	Reagent
6 L	H_2O
72 g	Agar
510 g	Sucrose
120 g	Dried yeast
360 g	Organic maize
150 ml	10% Nipagen solution (in 70% ethanol)
18 ml	Propionic acid

2.3.2 Drosophila stocks and genotypes

Standard markers and chromosomes were as described by Lindsley and Zimm (Lindsley & Zimm, 1992). Stocks were obtained from the Bloomington Drosophila Stock Centre (Indiana University, USA), the Vienna Drosophila RNAi Centre (Institute of Molecular Biotechnology and Research Institute of Molecular Pathology, Vienna, Austria) and the Drosophila Genetic Resource Centre (Kyoto Institute of Technology, Japan). Others were requested from the individual researchers, Daimark Bennett (University of Liverpool, UK), Deborah Andrew (The Johns Hopkins University, USA), Andrea Brand (University of Cambridge, UK), Sanyal Subhabrata (University of Arizona, USA), Dirk Bohmann (University of Rochester, USA), Christos Samakovlis (Unversity of Stockholm, Sweden) and Martin Barron (University of Manchester), as indicated in Table 2.4.

Table 2.4 Fly stocks used or generated

Genotype	Brief Description	Source
w^{1118}	white eyed mini-gene	Bennett
w*; Tft/CyO	2nd chromosome balancer	Bennett
w*; Tft/CyO; MKRS/TM6B	2nd and 3rd chromosome balancer	Bennett
w*; +/ CyO, twi>GFP	Fluorescently tagged CyO balancer	Bennett
w*; Tft/CyO, twi>GFP; MKRS/TM6B	As above but fluorescently labelled 2nd chromosome balancer	Generated
w*; His2Av-mRFP1	Expresses histone:mRFP fusion protein ubiquitously	Bloomington
w*; UAS-histone-YFP	Expresses histone:YFP fusion protein under UAS control	Brand
w*; UAS-dsRed^{nls} 19A	Expresses dsRed nuclear localisation signal under UAS control	Andrew
w*; UAS-Act5C.mRFP	Expresses actin:mRFP fusion protein under UAS control	Bloomington
w*; btl-GAL4, UAS-Act5C.GFP	Expresses actin:GFP fusion protein in *breathless* expressing (tracheal) cells	Bloomington
w; btl-GAL4, UAS-histone. YFP, UAS-act.RFP/CyO	Expresses actin.mRFP and histone.YFP in tracheal cells	Generated
w; Btl-GAL4, UAS-dsRed NLS, UAS-act:GFP/CyO	Expresses actin.GFP and dsRedNLS in tracheal cells	Generated
w^{1118}; UAS-Cameleon.2.1	Expresses Cameleon 2.1 calcium sensor under UAS control	Bloomington
w^{1118}; UAS-Dcr-2.D	Expresses *Dicer-2* under UAS control	Bennett
y^{1}, w^{67c23}, btl-GAL4	Expresses GAL4 in *breathless* expressing (tracheal) cells	DGRC, Kyoto
w*; bnl-GAL4 / TM3, Sb^{1} Ser^{1}	Expresses GAL4 in *branchless* expressing cells	DGRC, Kyoto
w*; ; da.G32-GAL4	Expresses GAL4 ubiquitously	Bennett
w^{1118}/Dp(2;Y)G, w^{+mC}=hs-hidY; wg^{Sp-1}/CyO	Virginiser strain with 2nd chromosome balancer	Bloomington

w^{1118}/Dp(2;Y)G, w^{+mC}=hs-hidY; MKRS/TM2, y^{+}	Virginiser strain with 3rd chromosome balancer	Bloomington
Ca-P60A^{Kum170}/CyO	Conditional, dominant negative mutant form of *SERCA*	Subhabrata
Ca-P60A^{Kum170}/CyO-twi>GFP	Conditional, dominant negative mutant form of *SERCA* with fluorescent balancer	Generated
w^{*}; Ca-P60A$^{Kum(295)}$/CyO-MHC-LacZ	Conditional, dominant negative mutant form of *SERCA*	Subhabrata
w^{*}; Ca-P60A$^{Kum(295)}$/CyO-twi>GFP	Conditional, dominant negative mutant form of *SERCA* with fluorescent balancer	Generated
y^{*}; w^{*}; Ca-P60A$^{Kum170.Scer\UAS}$/CyO; Ca-P60A$^{Kum170.Scer\UAS}$	Conditional, dominant negative mutant form of *SERCA* under UAS control	Subhabrata
w; Ca-P60A^{Kum170}, btl-GAL4, UAS-act:GFP/CyO	Conditional mutant form of *SERCA* and GFP under *btl-GAL4* control	Generated
w^{118}; P{KK107371}v107446	SERCA RNAi construct under UAS control	VDRC
w^{1118}; P{GD436}v4474	SERCA RNAi construct under UAS control	VDRC
w^{118}; P{GD436}v4474, P{KK107371}v107446	Above 2 RNAi constructs recombined on the 2nd chromosome	Generated
w^{1118}; P{GD436}v4474, UAS-dicer	SERCA RNAi construct recombined with *Dicer-2* on the 2nd chromosome under UAS control	Generated
w^{*}; noc^{Sco}/CyO; tubP-GAL80^{ts}	Temperature-sensitive GAL80 under control of *alphaTub84B* promoter	Bloomington
w^{*}; btl-GAL4, UAS-Act5C:GFP; tubGAL80^{ts}	Expresses actin:GFP fusion protein in *breathless* expressing (tracheal) cells and temperature sensitive GAL80	Generated
btl-GAL4, UAS-GFP, tubGAL80^{ts}, esg-LacZ	Expresses actin:GFP fusion protein in tracheal cells and *LacZ* under control of *escargot* promotor	Bohmann

hsFlp; act>y>GAL4, UAS-GFP; btl-mRFPmoe	Flippase recombinase under control of heat shock promotor; GAL4 under control of actin promotor (with yellow cassette); GFP under UAS control and moesin.RFP fusion protein under control of *breathless* promotor	Bohmann
hsFlp^{122}; Tft/CyO; TM2/TM6B	Flippase recombinase (122 allele) under control of heat shock promotor and 2nd/3rd chromome balancers	Bennett
y^{1}, w*; FRT42D, tubGAL80/CyO	GAL80 under control of tubulin promoter with FRT site	Bloomington
w*; +/CyO; Act>CD2>GAL4, UAS-GFP/MKRS	GAL4 under control of actin promotor (with CD2 cassette) and GFP under UAS control	Bennett
w*; FRT42D, tubGAL80; Act>CD2>GAL4, UAS-GFP	Elements from above 2 stocks combined on 2nd/3rd chromosomes	Generated
y^{d2}, w^{1118}; FRT42D, Ca-P60A^{k08308ab} / CyO	Dominant negative *SERCA* mutant with FRT site	DGRC Kyoto
hsFlp^{122}; FRT42D, Ca-P60A^{k08308ab} / CyO; Btl>mRFPmoes	Dominant negative *SERCA* mutant with FRT site, combined with heat shock flippase and moesin.RFP fusion protein under control of *breathless* promotor	Generated
w^{1118}; FRT42D, white-un1	FRT site for making control clones	Bloomington
hsFLP^{122}; FRT42D, white-un1/CyO; Btl>mRFPmoes/TM6B	FRT site for making control clones and moesin.RFP fusion protein under control of *breathless* promotor	Generated
Btl-GAL4, UAS-GcaMP3/CyO	Expresses genetic calcium sensor in *breathless* expressing (tracheal) cells	Samakovolis
UAS-deltex/CyO-GFP	Expresses *deltex* under UAS control	Barron
w; FRT/CyO; UAS-rasV12	Oncogenic *ras* under UAS	Bennett
ptc-GAL4, UAS-GFP/CyO	Expresses GAL4 in *patch* expressing cells and GFP under UAS control	Bennett

2.3.3 Embryo collection

Embryos were collected on apple juice agar plates (Table 2.5) smeared with a small amount of yeast paste and placed at the bottom of fly cages. Firstly a pre-lay collection was performed to encourage females to deposit retained eggs and synchronise subsequent egg collections. Embryo collections were carried out over relatively short periods of time (1-4 hours) to ensure embryos were of a similar developmental stage. Embryos were then aged on the agar plates at 25°C to reach the desired stage of development. Embryos were removed from the plates by washing with distilled water through a fine mesh sieve (Sefar Nitex 120 μM mesh, Sefar Ltd., Bury, UK). The chorion was removed by placing the sieve into thin household bleach for 1-2 mins. The bleach was drained off and the embryos were washed with copious distilled water. The mesh was then dried by blotting on paper towels. The embryos were removed with a damp, fine artist's paintbrush and either placed in fixative, mounted for live imaging or dissociated for RNA extraction or calcium imaging.

Table 2.5 Apple Juice Agar Recipe

Mass / Volume	Reagent
335 ml	H_2O
165 ml	Apple Juice
30 g	Agar
8 g	Sucrose
2 ml	10% Nipagen solution (in 70% ethanol)

2.3.4 Staging embryo development

In order to obtain a number of embryos at the same, known developmental stage, collections were performed over short time windows (as described above) and carefully aged according to standard Bownes stage numbers, using accepted time periods described by Campos-Ortega and Hartenstein (Bownes, 1975; Campos-Ortega & Hartenstein, 1985). For accurate, reproducible assessment of tracheal phenotype, early stage 16 (16.1) was chosen in most cases: at this stage the large majority of the tracheal system has formed and importantly, it is readily identifiable from gut morphology. The onset of stage 16 is characterised by three circular midgut constrictions that subdivide the midgut into four chambers (Figure 2.2), customarily numbered 1-4 antero-posteriorly. These characteristics are identifiable in dechorionated embryos inspected under light or transmitted-light confocal microscopy. Later in stage 16, all four chambers constrict further, resulting in the long, highly convoluted tube that is evident as the larval midgut. Development of the embryonic alimentary tract is complete by stage 17.

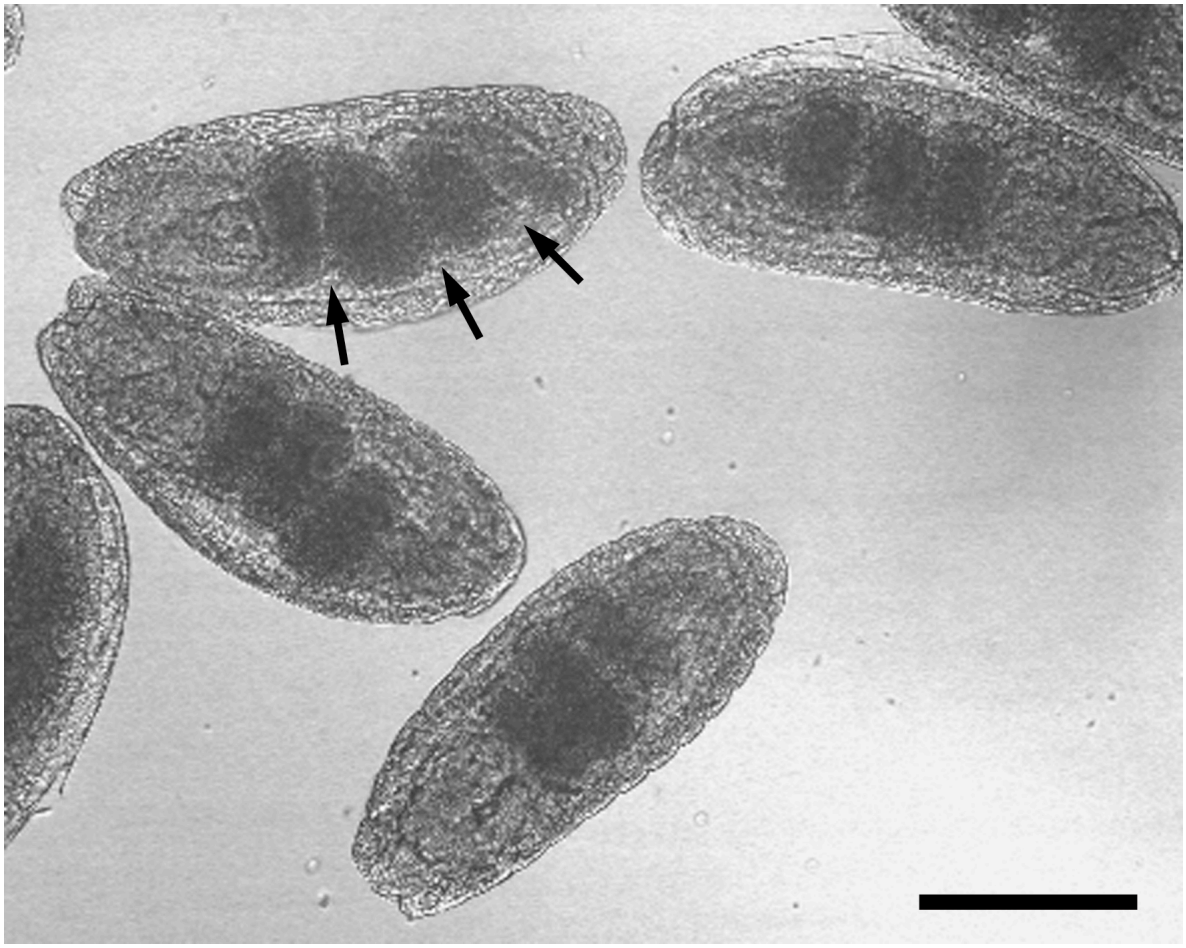

Figure 2.2 Selecting early stage 16 embryos based on gut morphology

Transmitted light confocal micrograph of a number of early stage 16 (16.1) embryos. The midgut is subdivided by 3 circular constrictions (labelled with arrows), leading to the characteristic appearance of parallel chambers of gut that appear ‘stacked’ antero-posteriorly. The most posterior chamber is often more difficult to visualise, but can be clearly seen in the upper left embryo. Scale bar indicates 200 μm.

2.3.5 Determination of developmental stage of lethality

Embryos were collected on apple juice agar plates as described above and then counted using light microscopy (Nikon SMZ-645 stereoscopic zoom microscope and Photonic PL3000 light source). The embryos were then inspected at 12 hour intervals to assess development. Larval developmental stage was determined according to the 3 instars.

2.3.6 Determination of tracheal gas filling

Embryos were selected for stage 16.1 and correct genotype (if necessary) using fluorescent and light microscopy (described above, using Leica MZ10F stereo microscope and EL6000 light source). Embryos were then mounted on double-sided sticky tape on a microscopic slide and covered in halocarbon oil. They were then inspected at 22 hours AEL for tracheal gas filling.

2.3.7 Drosophila embryo RNA extraction

For each genotype, twenty embryos were collected as described above and snap frozen in a micro-centrifuge tube with liquid nitrogen. They were homogenised with a pestle in a micro-centrifuge tube containing 350 µL Buffer RLT (Qiagen) with ß-mercaptoethanol (10 µL per 1 ml). The suspension was then passed 10 times through a 22-gauge needle fitted to a 1 ml RNase-free syringe. The suspension was then transferred to a QIAshredder spin column (Qiagen) and centrifuged at 8,000 x g for 2 min. RNA was extracted from the subsequent lysate using an RNeasy Mini Kit (Qiagen) according to the handbook protocol sd described above. The concentration of extracted RNA was determined at 260 nm using a NanoDrop ND-1000 spectrophotometer. The A260/A280 ratio was assessed as an indicator of RNA purity. The RNA was then stored at -80°C.

2.3.8 Embryo fixation

Embryos were transferred to a small glass jar containing 5ml heptane, in order to puncture the vitelline membrane and 5 ml fixative solution (0.1 M Hepes, pH 6.9, 2 mM $MgSO_4$, 3.7 % formaldehyde) and left for 45 minutes with gentle agitation. The embryos settled at the interface of the heptane and formaldehyde layers. In order to remove the vitelline membrane, the lower aqueous phase was removed using a fine glass Pasteur pipette and 5 ml methanol

was added. The jar was shaken vigorously for around 30 seconds so the devitellinised embryos fall to the bottom of the methanol. They were then transferred to a fresh tube and washed with fresh methanol 4 times. These can then be stored at 4°C in methanol. Embryos were rehydrated with serially decreasing solutions of methanol (80 %, 60 %, 40 %, 20 %, 0 %) in PBS and 0.1 % Triton X-100. For certain immunofluorescent experiments, a short fixation procedure was required. This involved the same steps described above, but the fixative solution contained 33% formaldehyde in 500 mM EGTA (pH 7.5) and the duration of fixation was 5 mins.

2.3.9 Immunofluorescent staining of Drosophila embryos

Staining was carried out in micro-centrifuge tubes and a rotator was used to gently agitate the embryos in all steps. A blocking step was performed whereby rehydrated embryos were placed in a solution of PBS, 0.1 % Triton X-100 and 0.5 % BSA for 30 minutes at 25°C and this step was repeated a further time. Primary antibodies were used as in Table 2.6 and diluted in PBST (PBS and 0.1 % Triton X-100) to the stated working concentrations. Incubation was carried out for either 6 hours at 25°C, or overnight at 4°C. Embryos were then washed in PBST for the following time periods and frequencies: 2 x 30 seconds, 2 x 5 minutes and finally 2 x 30 minutes. Secondary antibodies used are given in Table 2.7 and incubation was for 2 - 4 hours at 25°C or overnight at 4°C. Washes were then carried out with PBST for the durations described above. When red-fluorescent BODIPY® TR-X thapsigargin (Invitrogen) was used, rehydrated embryos were incubated with the fluorophore at a concentration of 5 µM for 2 hours at 25°C and then washes were carried out as above. Embryos were mounted on microscopy slides with VECTASHIELD® Mounting Medium (Vector Laboratories, Peterborough, UK). To avoid crushing the embryos, coverslips were applied in a system where they were raised by 2 further coverslips stuck to the slide with clear nail-polish. Clear nail-polish was also used to seal the edges of the coverslip.

Table 2.6 Primary Antibodies used for Embryo Staining

Antibody	Dilution	Host	Supplier
2A12	1:10	Mouse	DSHB, Iowa, USA
Muscle-myosin	1:250	Rabbit	Kiehart, Duke University, USA
Non-sarcomeric Myosin	1:250	Rabbit	Kiehart, Duke University, USA

Table 2.7 Secondary Antibodies used for Embryo Staining

Antibody	Dilution	Host	Species Against	Supplier
Alexa Fluor® 488	1:500	Goat	Mouse, Rabbit	Invitrogen
Alexa Fluor® 555	1:500	Goat	Mouse, Rabbit,	Invitrogen

2.3.10 Calcium imaging of embryonic cells

For live calcium imaging of embryonic cells, a system was designed using features of a protocol for Drosophila primary embryonic cell culture (Bai, Sepp, & Perrimon, 2009). Embryos were collected and dechorionated as described above. 100-200 embryos were placed in a micro-centrifuge tube containing 800 µL of GIBCO™ Schneider's Drosophila medium (Invitrogen) and dissociated using a sterile pestle. The suspension was then centrifuged at 40 x g for 5 minutes and the process repeated. The cell suspension was then diluted to 1200 µL with further medium. 300 µL of this cell suspension was loaded into each chamber of a 4-well Lab-Tek™ II Chambered Coverglass (Nunc, Thermo Fisher Scientific, Rochester, NY, USA) that had been pre-coated with Poly-L-Lysine (Sigma-Aldrich) for 1 hour and washed off with sterile water.

Cells were then loaded with Fluo-4 (Invitrogen) at a concentration of 1 µM for 1 hour, thus also allowing them to adhere to the coverglass. Imaging was performed with confocal microscopy as described below. When required for stimulation experiments, thapsigargin (Sigma-Aldrich) was added to give a final concentration of 2 µM.

2.3.11 Collection of larvae

Embryos were collected over 4 – 8 hour periods of time on apple juice agar plates as described above, or in large vials containing fly food. Embryos were allowed to hatch and develop into the required stage of larval development at 25°C. When the temperature sensitive GAL80 construct was used to repress GAL4 mediated expression, a permissive (to GAL80) temperature of 18°C and restrictive temperature of 29°C were used.

2.3.12 Generation of flip-out and mitotic clones

For clonal analysis, embryos were kept at 25°C until late L2 larval stage. Vials containing the larvae were then placed in a 37°C water bath for between 15 minutes and 1 hour in order to activate the flippase (FLP) recombinase which is under the control of a heat-shock promoter (hs). The larvae were then returned to 25°C until the late L3 stage when they were dissected. The presence or absence of clones within the imaginal discs was deduced by inspecting the larvae under fluorescence microscopy (as above).

2.3.13 Larval micro-dissection

Larvae at the correct stage of development were first washed and then dissected in ice cold PBS. In order to dissect the imaginal wing disc, larvae were transected at the level of the abdomen and inverted over forceps. The wing disc was then carefully dissected away from the thoracic trachea using fine forceps and transferred to cold PBS. Care was taken to ensure that the tracheal system and air sac were not damaged by excessive traction.

2.3.14 Fixation and fluorescent staining of imaginal discs

Fixation and staining were carried out in 'watch-glass' type glass containers. Wing discs were fixed in 4% paraformaldehyde in PBS for 20 minutes at 25°C. The discs were then washed twice in PBS for 20 minutes. A blocking step was carried out for 2 hours at 25°C using PBST containing 5% fetal calf serum. Primary antibodies were used as in Table 2.8 and diluted in the blocking solution to the specified concentration. Discs were incubated in the primary antibody overnight at 4°C. Four 20 minute washes were carried out with PBST before incubation with the secondary antibody. Secondary antibodies (Table 2.9) were

diluted in blocking solution and incubated for 2 hours at 25°C in the dark. The final wash steps included 20 minutes washes in PBST repeated 4 times in total and then a final wash of 20 minutes in PBS to remove the detergent. Wing discs were mounted on microscopy slides with VECTASHIELD® Mounting Medium (Vector Laboratories). Slides were kept in the dark at 4°C to reduce fading of the fluorophores.

When MAP Kinase (Diphosphorylated ERK-1&2) staining was carried out, the concentration of fixative was increased to 8 %. When Notch intracellular domain staining was carried out, a protocol adapted from Mark Fortini (Thomas Jefferson University, Philadelphia, USA) was used. This comprised a PLP fixation step (2% paraformaldehyde, 75 mM lysine, 37 mM sodium phosphate, 10 mM periodate) for 40 minutes on ice. Washes prior to primary and secondary antibody incubation were carried out with PBS-DT (1 X PBS, 0.3 % Na-deoxycholate, 0.3% Triton X-100). The antibody dilution, incubation and final wash steps were as above.

Table 2.8 Primary Antibodies and Dyes used for Imaginal Disc Staining

Antibody	Dilution	Host	Supplier
Anti-phospho-Histone H3 (Ser10)	1:500	Rabbit	Cell Signalling
17.9C6 Anti-notch ICD	1:100	Mouse	DSHB
2B10 Anti-cut protein	1:100	Mouse	DSHB
Anti-β-Galactosidase	1:1000	Rabbit	Promega
Activated Caspase-3	1:100	Rabbit	Cell Signalling
Anti-MAP Kinase, Activated (Diphosphorylated ERK-1&2)	1:100	Mouse	Sigma
4F3 Anti-discs large	1:100	Mouse	DSHB
TOPRO-3	1:1000	N/A	Invitrogen

Table 2.9 Secondary Antibodies used for Imaginal Disc Staining

Antibody	Dilution	Against	Host	Supplier
Alexa Fluor® 555	1:500	Mouse or Rabbit	Goat	Invitrogen
Alexa Fluor® 633	1:500	Mouse or Rabbit	Goat	Invitrogen

2.3.15 Preparation for live imaging

Live embryos at the correct developmental stage were dechorionated and washed with distilled water as above. Individual embryos were mounted with a damp; extra fine artist's paint brush, with most of the bristles removed. Embryos for confocal imaging using an inverted microscope, were placed on the coverglass of a 4-well Lab-Tek™ II Chambered Coverglass (Nunc, Thermo Fisher Scientific). These dishes have borosilicate glass and embryos loosely adhere to them, whilst still allowing manipulation with a brush to gain the correct orientation for imaging. Once embryos had been mounted, 600 µL of PBS was carefully added to the well. Embryos for live fluorescent, wide-field imaging on an upright microscope were mounted on a gas-permeable membrane stretched over two silicon bars on top of a slide and covered with halocarbon oil to prevent desiccation.

In order to image live imaginal discs, a modified version of the protocol published by Aldaz *et al* was adopted (Aldaz, Escudero, & Freeman, 2010). Shields and Shang M3 insectum medium (Sigma-Aldrich) was supplemented with 2 % fetal calf serum and 0.5 % penicillin-streptomycin. (Invitrogen) In order to make the medium viscous for live imaging, methyl-cellulose (Sigma-Aldrich) was added at a concentration of 2.5% wt/vol. The methyl-cellulose was added to the medium and stirred until dissolved, then left overnight at 4°C to remove bubbles. Aliquots were then stored at -20°C. Late third instar larvae were dissected as stated earlier, except the above culture medium (without methylcellulose) was used in place of PBS. Care was taken to ensure that imaginal discs were undamaged. 300 µL of the viscous medium was placed in a chamber of a 4-well Lab-Tek™ II Chambered Coverglass (Nunc, Thermo Fisher Scientific) and dissected discs carefully transferred to this. Each disc was orientated with it's columnar epithelium facing downwards and peripodial

membrane upwards. The disc was encouraged to sink down in the media and then gently placed against the glass coverslip (previously coated in Poly-L-Lysine, as above).

2.4 Imaging

2.4.1 Confocal microscopy

Slides were imaged using a Zeiss LSM 710 (Carl Zeiss Ltd, Hertfordshire, UK) laser scanning confocal system with an inverted Axio Observer.Z1 microscope. Zeiss Fluor 20x/0,75 air and 40x/1,3 oil immersion objectives were used. An X-CITE® 120PC Q (Lumen Dynamics Group Inc., Ontario, Canada) light source was use for fluorescent microscopy. For live imaging experiments, a cooled stage (Lauda Dr. R, Lauda-Königshofen, Germany) was kept at 25°C.

GFP fusion proteins and Alexa Fluor 488 dyes were excited at 488 nm, using an Argon laser and detected maximally at 509 nm and 519 nm respectively. YFP fusion proteins were excited at 514 nm using an Argon laser and detected maximally at 527 nm. mRFP and DsRed fusion proteins and Alexa Fluor 555 were excited at 543 nm using a GHe/Ne laser and detected maximally at 607, 583 and 565 nm respectively. Alexa Fluor 633 dyes were excited at 633 nm using a GHe/Ne laser and detected maximally at 647 nm. Images were captured using Zen 2010 (Zeiss) software.

The pinhole was usually set at around 1 airy unit (AU) to give optimal signal to noise ratios. When Z-stacks of tissues were taken, the optimal slice thickness for 1 AU, as specified by the software was used (usually between 0.5 – 2 µm).

2.4.2 Calcium imaging

When live imaging of cells loaded with Fluo-4 (Invitrogen) was carried out, a system was used whereby thapsigargin could be added to the dish during imaging with minimal disruption to the solution and cells. A fine, 22G needle, connected to a syringe by fine plastic tubing, was carefully inserted into the well of the dish and the correct amount of thapsigargin infused. In order to collect real-time data during stimulation experiments, the LSM 710 was set-up to scan at maximum speed without averaging. The 20x objective was used to gain good depth of field for a number of cells imaged simultaneously.

2.4.3 Fluorescent Resonance Energy Transfer (FRET)

Confocal spectral scanning microscopy was used to image the genetically encoded calcium indicator cameleon 2.1. This involved using the lambda mode of the Zeiss 710 microscope and Zen 2010 software. Cameleon YC.2.1 was excited at 458 nm using an Argon laser and the emission captured with 13 photo-detectors (at specific wavelengths of 469, 479, 488, 498, 508, 581, 527, 537, 547, 557, 566, 576 and 586 nm). FRET was indicated by the presence of 2 peaks of maximal emission at 485 nm (corresponding to cyan fluorescent protein [CFP]) and 535 nm (corresponding to yellow fluorescent protein [YFP]). In order to confirm FRET, acceptor photo-bleaching was carried out and the recovery in CFP emission observed in the bleached region (Karpova et al., 2003). The Zen software bleach function was used to carry out bleaching of a defined region of interest (ROI) of YFP. The 514 nm laser is used at high power in order to do this. An internal control for the bleaching experiment was established by assessing changes in emission of an unbleached region in parallel (Karpova et al., 2003). The software was used to unmix the spectral channel emission data by extracting the mean intensity for two wavelength ranges, corresponding to CFP and YFP emission (473-493 nm and 522-541 nm respectively). Since background (outside of imaged cells or tissues) pixel fluorescence was low (<10% of signal), background subtraction was not performed in order to minimise data manipulation (Karpova et al., 2003).

2.4.4 Assessment of cameleon FRET System

In order to assess the approximate dynamic range of the cameleon 2.1 system in Drosophila embryonic cells in vitro, embryos ubiquitously expressing cameleon YC2.1 were collected and dechorionated as described above. 100-200 embryos were then placed in a micro-centrifuge tube containing 800 µL of GIBCO™ Schneider's Drosophila medium (Invitrogen) and dissociated using a sterile pestle. The suspension was then centrifuged at 40 x g for 5 minutes and the process repeated. 400 µL of this cell suspension was loaded into each chamber of a 4-well Lab-Tek™ II Chambered Coverglass (Nunc, Thermo Fisher Scientific) that had been pre-coated with Poly-L-Lysine for 1 hour. The cells were allowed to adhere to the coverglass for 1 hour and then the medium replaced with S2 Ringer's Solution (150 mM NaCl, 5 mM KCl, 2 mM $CaCl_2$, 4 mM $MgCl_2$ and 10mM HEPES, pH 7.2) or Ca2+ free Ringer's solution (150 mM NaCl, 5 mM KCl, 6 mM

$MgCl_2$, 1 mM EGTA and 10mM HEPES, pH 7.2) (Zhang et al., 2006). Calibration steps were adapted from Palmer *et al's* protocol (Palmer & Tsien, 2006). In order to assess the maximum YFP/CFP ratio, conditions of high calcium concentration were created by adding $CaCl_2$ (final concentration 10 mM) and ionomycin (final concentration 10 µM) to the well. For assessing the minimum ratio, calcium was chelated by adding EGTA (final concentration 5 mM) and ionomycin 10 µM). Imaging was carried out for at least 15 minutes post addition in order to achieve a steady state.

2.4.5 Live Fluorescent Imaging

For wide-field live imaging, dechorionated embryos were mounted on a gas-permeable membrane stretched over two silicon bars on the top of a slide and covered with halocarbon oil to prevent desiccation. Embryos were imaged on a Zeiss Axio Observer.Z1 microscope, Colibri LED light source and high speed AxioCam CCD camera, controlled by AxioVision software 4.5. Objectives used were Zeiss 20x/0,5 Plan-Neofluar or 63x/1,3 C-Apochromat water-immersion lenses.

2.4.6 Image Processing

Images were exported from Zen 2010 in Tagged Image File Format (TIFF) and edited in Adobe Photoshop CS5 (Adobe Systems Europe Ltd, Maidenhead, UK). When Z-stacks were produced, images are presented as single slices, unless a projection is specified. When a 3-dimensional (3D) projection was required, stacks were rendered using Zen 2010 software (Zeiss). If image brightness required changing in order to achieve satisfactory colour reproduction for publication, this change was standardised between groups to allow valid comparison.

When pixel intensity was quantified in a defined region of interest (for example during single cell calcium imaging), the mean intensity for that region, at individual time points was determined in the Zen software and exported as numerical data. These data were processed and plotted as graphs using SPSS Statistics 18.0 (IBM®).

2.5 Polymerase Chain Reaction (PCR) Experiments

2.5.1 Reverse Transcriptase

First-strand cDNA synthesis was initiated from 0.2 µg total RNA. The oligonucleotide primer was annealed to the RNA by adding 1 µl random hexamers (0.5 µg/µl Promega, Madison, WI, USA) and nuclease-free H_2O to a total volume of 15 µl in a micro-centrifuge tube. The mixture was then incubated at 70°C for 5 mins and then put on ice. For the reverse transcriptase reaction, 1 µl Moloney Murine Leukemia Virus (M-MLV) reverse transcriptase, 5 µl 5x M-MLV reverse transcriptase buffer, 0.5 µl ribonuclease inhibitor (all from Promega), 1.25 µl nucleotides (10 mM ATP, CTP, GTP, UTP) and 2.25 µl nuclease-free H_2O were added to the RNA and oligonucleotide mixture and incubated at 42°C for 1 hour. The cDNA was then diluted to a volume of 100 µl with nuclease-free H_2O and stored at -30°C.

2.5.2 Polymerase Chain Reaction

Oligonucleotide primers were used at a concentration of 10 µM (DST, Sigma-Aldrich). For the PCR reaction, 5 µl cDNA were added to 1 µl forward primer, 1 µl reverse primer, 18 µl nuclease-free H_2O and 25 µl PAQ5000 2X PCR Master Mix (Agilent Technologies UK Ltd, Edinburgh, UK). The PCR conditions were 94°C for 2 min, 94°C for 30 seconds, 58°C for 30 seconds (oligonucleotide annealing) and 72°C for 1 min (primer extension). The last 3 steps were repeated for 25 cycles. The final step was 72°C for 5 min and then the samples were removed and placed on ice. 18 µl PCR product was combined with 2 µl loading buffer and loaded on a 1% agarose electrophoresis gel in 1 x TAE buffer, along with a 50 base pair DNA ladder (New England BioLabs, Hitchin, UK). The gel was run at 110 volts for 30 min and analysed using a InGenius (Syngene UK, Cambridge, UK) gel documentation system with GeneSnap (Syngene) software .

2.5.3 Quantitative Polymerase Chain Reaction (qPCR)

For the qPCR reaction, 5 µl cDNA were added to 0.75 µl forward primer, 0.75 µl reverse primer, 6 µl nuclease-free H_2O and 12.5 µl Brilliant SYBR Green 2X QPCR Master Mix (Agilent). PCR conditions were 95°C for 10 min in order to activate the DNA polymerase and then 40 cycles of: 95°C for 15 seconds and 58°C for 1

minute. A further step of 90°C for 15 seconds, 55°C for 30 seconds and 95°C for 30 seconds was used to generate a dissociation (melting) curve.

An MX3000P® Multiplex Quantitative QPCR System (Agilent) was used for all reactions and corresponding MxPro software for analysis. Transcripts were quantified using the relative standard curve method (Applied Biosystems, 1997). Although this method does not permit absolute quantification of the target gene, it negates the requirement for the absolute quantity of the standard to already be known (as required by an absolute standard curve method) (Agilent Technologies, 2009; Applied Biosystems, 1997). It also has advantages over the ΔCT relative quantification method, of not requiring the reference (housekeeping) gene to uninfluenced by the experimental situation and not relying on the amplification efficiencies of reference and target genes to be broadly the same (Ginzinger, 2002). A standard (calibrator) was produced by pooling cDNA from a large number of samples and this was used as the standard for all experiments. 1:1, 1:2, 1:5, 1:10 and 1:20 dilutions of this standard were used to produce the standard curve for each target gene. An arbitrary value of 1000 copies was assigned to the 1:1 standard for all experiments. All reactions were run in either duplicate or triplicate. 18S expression was monitored as an internal standard on the cDNA template; mRNA expression for each target gene was normalised to this internal standard.

2.6 Statistical Analyses

Data were analysed using SPSS Statistics 18.0 (IBM®). Fisher's exact test was used to compare categorical data. Continuous data were analysed for normality using Kolmogorov-Smirnov and Shapiro-Wilk tests and homogeneity of variance using Levene's test. Normally distributed data with similar variance between groups were compared using an unpaired student t-test. Non-parametric data were compared using the Mann-Whitney U test. Statistical significance was defined as $p<0.05$.

Boxplots were plotted in SPSS using the package's standard algorithm. The median and IQR are displayed as a thick line and box respectively. Values that are between one and a half and three box lengths from either end of the box, are known as 'outliers' and denoted by dots. Values that are more than three box lengths from either end of the box are labelled 'extreme' values and denoted by asterisks.

Chapter 3

SERCA REGULATES GENE EXPRESSION AND CELL PROLIFERATION IN THE DEVELOPING LUNG *IN VITRO*

3.1 Introduction and aims

SERCA inhibition in the embryonic lung *in vitro* has been shown to have striking effects (discussed in Chapter 1). When rodent lung explants are cultured with the specific SERCA inhibitor, cyclopiazonic acid (CPA), there is a dramatic loss of branching morphogenesis, pulmonary myogenesis and airway peristalsis (AP) (N. Featherstone et al., 2005; N. C. Featherstone et al., 2005; Seidler et al., 1989). Furthermore, these effects are: (i) reversible, when CPA is removed from the culture medium, branching morphogenesis, myogenesis and AP resume; and (ii) dose dependent, with higher doses of CPA resulting in a more marked effect (Lansdale, Connell et al., 2010).

The reversibility of the effect is significant: it implies the abrogation of development is not simply due to cellular toxicity from CPA. If CPA treatment was profoundly toxic and resulted in extensive necrosis or apoptosis, it could be expected that that the lung explant would indeed fail to branch and develop normally. However, if this was the case, it is likely the lung explant would reduce in size with time, normal architecture would be lost and branching morphogenesis would fail to restart on removal of the CPA: this pattern is not seen. Since branching morphogenesis and airway peristalsis are complex processes, necessitating cell growth, patterning, migration and proliferation, it seems reasonable to hypothesise that CPA is having a reversible and specific effect on the control of one or more of these. Given the likelihood of changes to these fundamental cellular processes, we hypothesised that CPA's effect on the developing lung was mediated by changes in gene expression and / or cell proliferation and aimed to determine:

(i) How is gene expression in the developing lung affected by SERCA inhibition with CPA?

(ii) What are the effects on cell proliferation from SERCA inhibition with CPA?

3.2 SERCA regulates gene expression in key morphogenic pathways

3.2.1 Selecting genetic pathway candidates

Lung organogenesis involves the interplay of a number of biochemical and biomechanical factors [reviewed in (Warburton et al., 2010)]. These factors are regulated by a complex set of genetic signalling pathways. Much of our understanding of these molecular pathways comes from studies using transgenic mouse technology, where the effects of gene knock out and over-expression on lung organogenesis have been meticulously catalogued (Cardoso & Lu, 2006).

To assess the effect of SERCA inhibition on these genetic pathways, broadly speaking, two approaches could be instigated: (i) a high-dimensional screen of a large number of genes, using so called multiplex techniques; or (ii) a candidate gene approach, where key pathways are focussed on. Given the dramatic changes witnessed upon CPA treatment in the developing lung, and prior to embarking on a more costly and less focussed screening approach, we selected a candidate approach to ascertain whether any key pathways were affected by this treatment. Having observed the abrogation of branching morphogenesis in embryonic lung explants, specific elements of the branching programme were interrogated. Similarly, because CPA treatment also resulted in a cessation of airway smooth muscle (ASM) function, elements of pulmonary myogenesis were also assessed: the specific roles of the selected genes are briefly discussed below.

Fibroblast growth factor (FGF) family members have been shown to play a conserved role in respiratory organ development from *Drosophila* to mammals (Sutherland et al., 1996). There are 23 subgroups of mammalian FGFs, with 4 types of cognate, transmembrane protein tyrosine kinase receptors (FGFRs) (Ornitz & Itoh, 2001). During development, FGFs are known to play key roles in the processes of cell proliferation, migration and differentiation. Within the lung, FGF10 is the most well studied member and is expressed in the peripheral lung mesenchyme in E11-12 mouse lung (the stage of development studied in our culture model) (Bellusci, Grindley et al., 1997). What is more, the pattern of FGF10 expression changes dynamically and appears to occur at the site of lung bud formation (Bellusci, Grindley et al., 1997). FGF10 signals via adjacent

FGFR2IIIb, which is expressed in the distal lung epithelium. This mesenchyme to epithelial, FGF10-FGR signalling pathway is critical for lung formation: *Fgf10* null mutant mice lack lung distal to the trachea, whilst loss of its receptor, *Fgfr2IIIb* also results in severe lung defects (De Moerlooze et al., 2000; Min et al., 1998; Sekine et al., 1999). *In vitro* studies have shown that FGF10 has a chemo-attractant effect on neighbouring lung bud epithelium, inducing it to proliferate and migrate towards the source of FGF10 (Park et al., 1998; Weaver, Dunn, & Hogan, 2000). FGF10 also induces differentiation of the growing epithelium through its effects on other genes such as *Bmp4* and *Sp-C* (Hyatt, Shangguan, & Shannon, 2002). FGF10 is itself regulated by genes such as *Sonic Hedgehog* (*Shh*) and *Sprouty* (*Spry2*), which were also investigated (discussed later).

The Sprouty (Spry) family, coded for by four genes (*Spry1-4*) in mammals, are key regulators of the size and shape of developing lung buds through their control of FGF signalling. *Spry2* is expressed in the distal epithelium of the embryonic lung and is down regulated in clefts between new lung buds (Mailleux et al., 2001). This expression is adjacent to *Fgf10* expression in the neighbouring mesenchyme and is spatially and temporally dynamic. Induced soon after *Fgf10* expression, *Spry2* acts as an *Fgf10*-dependent inhibitor of *Fgfr2b* activity, limiting the proliferation and migration of lung epithelial cells during branching morphogenesis (Mailleux et al., 2001; Tefft et al., 2002). Consistent with these observations, decreasing *Spry2* activity *in vitro* results in increased lung branching, whilst over-expression severely impairs branching (Mailleux et al., 2001; Tefft et al., 2002).

Sonic hedgehog (SHH) signalling plays important roles in embryonic development through its regulation of epithelial to mesenchyme interactions (Bitgood & McMahon, 1995). SHH in the epithelium, binds to the transmembrane protein, Patched 1 (Ptch1) in the adjacent sub-epithelial mesenchyme and results in activation of the *Gli* transcription factors (van Tuyl & Post, 2000). In the lung, *Shh* is expressed at low levels throughout the epithelium, but particularly high levels are found at the growing tip (Bellusci, Furuta et al., 1997). *Shh* null mutants display hypoplastic lungs and a failure of the oesophagus and trachea to separate (Pepicelli, Lewis, & McMahon, 1998). *Shh* over-expression in the lung results in increased proliferation of the mesenchyme and epithelium, but leads to a failure of alveolarisation (Bellusci, Furuta et al., 1997). SHH is proposed to

regulate epithelial branching pattern by spatially suppressing *Fgf10* in the distal mesenchyme and upregulating *Fgf7* (Lebeche, Malpel, & Cardoso, 1999; Pepicelli et al., 1998).

FGF9 is another FGF family member that plays an important role in regulating branching morphogenesis of the developing lung. FGF9 is expressed in the mesothelium (visceral pleura) of the early embryonic lung (again around the stage of our culture model) (J. S. Colvin, Feldman, Nadeau, Goldfarb, & Ornitz, 1999). *Fgf9* null mice display lungs with reduced airway branching and interestingly, reduced pulmonary mesenchyme (J. S. Colvin, White, Pratt, & Ornitz, 2001). This reduction in mesenchyme has a knock-on effect of reducing *Fgf10* expression. FGF9's other effects on the mesenchyme include the repression of peribronchiolar smooth muscle differentiation and stimulation of vascular development in vivo (White et al., 2006).

Airway smooth muscle (ASM) is evident from early in the pseudoglandular stage of development (E11 in the mouse), closely following the emergence of the definitive lung bud (Sparrow, Warwick, & Everett, 1995; Tollet, Everett, & Sparrow, 2001). Prenatal pulmonary myogenesis is thought to play an intimate role in regulating overall organogenesis, both biochemically, through ASM progenitor mediated FGF-10 production, and mechanically, through contraction and maintenance of tone (Harding & Hooper, 1996; Jesudason, 2009; Mailleux et al., 2005). ASM prenatal phasic contractility (airway peristalsis) propels lung liquid, distending the distal bud (where growth is centred) and maintains airway tone, thus permitting stretch-induced signals that are implicated in lung growth (Jesudason et al., 2005; Schittny et al., 2000). Airway peristaltic waves are preceded by spontaneous propagating Ca^{2+} waves in ASM cells and SERCA inhibition with CPA abolishes these Ca^{2+} transients, resulting in airways peristalsis being replaced by tonic contraction (N. C. Featherstone et al., 2005). It therefore appears that SERCA has a key role in ASM function and this may be linked to the effects on morphogenesis seen upon its inhibition with CPA. As a result, we chose to test the impact of SERCA inhibition on ASM gene expression by assessing levels of the smooth muscle variant of myosin heavy chain (*smMHC*), a gene that has been detected at E10.5 in the mouse lung (Jostarndt-Fogen, Djonov, & Draeger, 1998).

In addition to the branched network of airways in the lung, efficacious gas exchange requires the development of a patterned pulmonary vascular network that is intimately related to those airways. Vascular endothelial growth factors (VEGFs) regulate vascular development by promoting endothelial cell viability; cell proliferation and directing cell motility via their signalling with the tyrosine kinase receptors, Flk-1 and Flt-1 (Larrivee & Karsan, 2000). VEGF isoforms are expressed from E11.5 in the developing lung epithelium and mesenchyme (Greenberg et al., 2002). VEGF mutants display abnormal pulmonary vasculature and rats treated with VEGF receptor inhibitors, display a pruned pulmonary arterial tree and decreased alveolarisation (Kasahara et al., 2000; Ng, Rohan, Sunday, Demello, & D'Amore, 2001).

3.2.2 Gross morphology of lung explants for assessment

Before assessing gene expression in CPA-treated lung explants, we first reproduced the observation that CPA halts branching morphogenesis in these explants as reported by Featherstone *et al* (Figure 3.1) (N. Featherstone et al., 2005; N. C. Featherstone et al., 2005). E11.5 murine lung explants were cultured on polytetrafluorethylene membranes at the air/fluid interface +/- 20 μM CPA, using an established model and photographed at 24 hour intervals up to 78 hours (Figure 3.1) (Jesudason et al., 2000). There was an abolishment of epithelial branching in the CPA group and this effect occurred soon after commencement of culture, given that no branching occurred between 0 and 30 hours. In addition, pulmonary mesenchyme was seen to expand in size relative to neighbouring epithelium, compared to controls (Figure 3.1). These findings therefore reproduce the previously discovered phenotype and confirm the samples are appropriate for gene expression analysis.

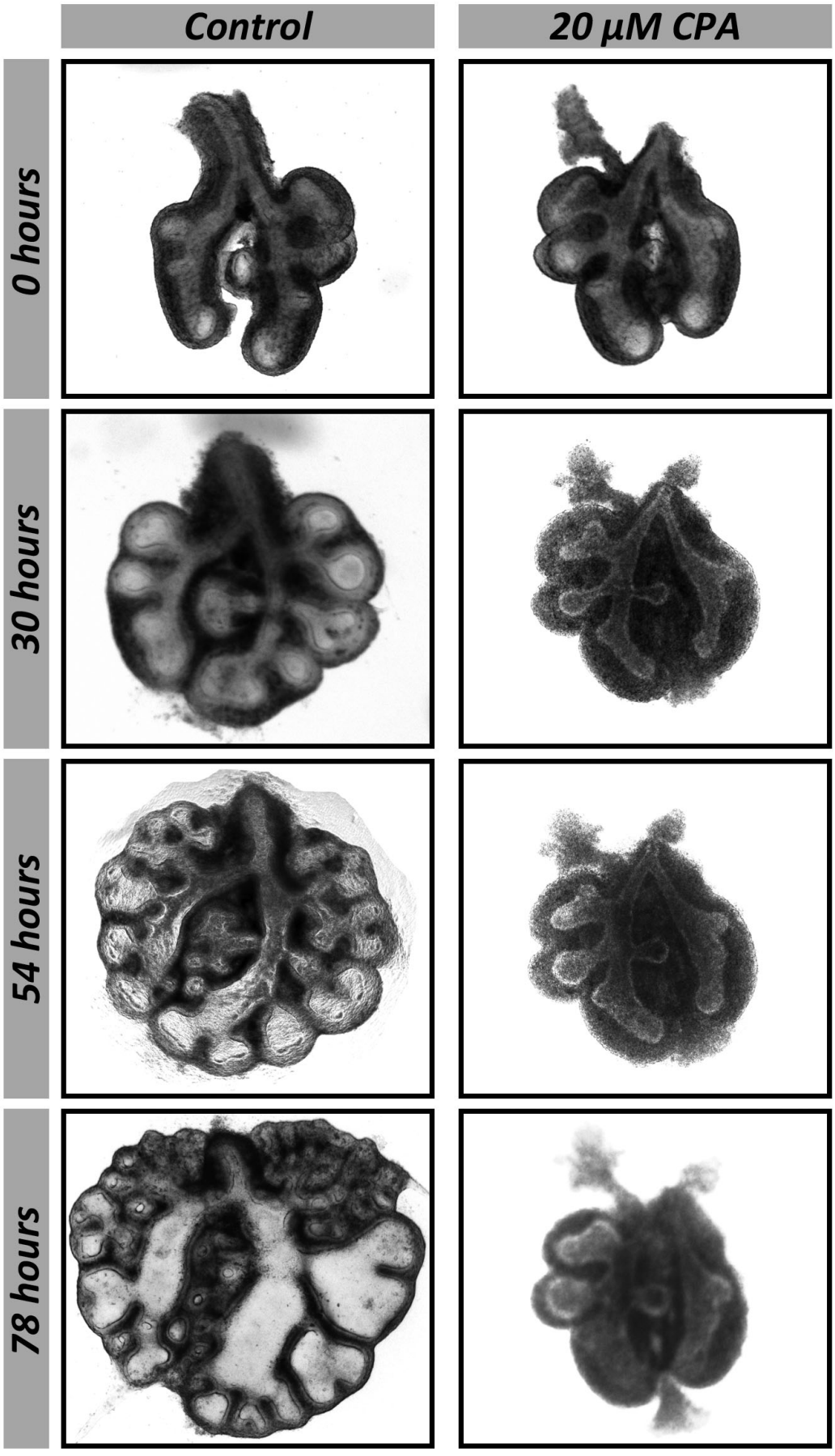

Figure 3.1 Gross morphology of lung explants for assessment

Photomicrographs of whole E11.5 murine lung primordia in organ culture +/- 20 µM CPA at 0 – 78 hours. The trachea is seen superiorly. At 78 hours, whole lungs were homogenised for RNA extraction or fixed for immunohistochemistry

3.2.3 Measuring changes in gene expression in the developing embryonic lung using quantitative RT-PCR

To make a quantitative assessment of gene expression, quantitative RT-PCR (qRT-PCR) was used to measure whole lung mRNA levels of candidate genes outlined above. Real-time qRT-PCR is a sensitive and reliable method with which to quantify mRNA in a sample (Schmittgen et al., 2000). It uses specific technology (such as TaqMan® probes or SYBR Green I dyes) to measure PCR product accumulation in real-time, through continuous detection of generated fluorescence (Heid, Stevens, Livak, & Williams, 1996; Wittwer, Herrmann, Moss, & Rasmussen, 1997). In the case of SYBR Green I (the method of choice in this thesis), the dye binds to double stranded DNA (dsDNA) with a high affinity (compared to single stranded), resulting in approximately 1000-fold increase in fluorescence, thus making it a sensitive indicator of dsDNA quantity (Agilent Technologies, 2009). During the exponential phase of the PCR reaction, a fluorescent signal threshold is determined at which point all samples can be compared (Ginzinger, 2002). The number of PCR cycles required to generate this fluorescent signal is defined as the cycle threshold (Ct). This Ct value is directly proportional to the amount of starting template for the target gene and is the basis for calculating mRNA expression levels.

RNA was extracted from whole lung explants cultured +/- 20 μM CPA, as above. Extracted RNA concentration was higher from control explants (Table 3.1). This difference was standardised during reverse transcriptase when first-strand cDNA synthesis was initiated from a total of 0.2 μg RNA for each sample. The A_{260}/A_{280} absorbance ratio for extracted RNA was within the frequently quoted range of 1.8 - 2.0 (Table 3.1): RNA purity therefore appeared reasonable (Fleige & Pfaffl).

Table 3.1 Median (IQR) concentration and A_{260}/A_{280} absorbance ratio of extracted RNA

Condition	RNA Conc. (ng/uL)	A_{260}/A_{280}
Control	44.5 (17.9)	2.01 (0.06)
CPA	18.3 (5.2)	1.84 (0.12)

A relative standard curve method of qRT-PCR was used for quantification of the initial template (Applied Biosystems, 1997). This relies on high quality standard curve production (through accurate serial dilution), but not absolute PCR efficiency, thus contrasting with the ΔCt method (Applied Biosystems, 1997; Ginzinger, 2002). When reviewing standard curve characteristics, R^2 is an indicator of quality of fit of the curve; slope is directly related to average amplification efficiency. Here, R^2 is >0.989 for all but one target genes, indicating good quality of fit and curve accuracy (Table. 3.2).

Table 3.2 Standard curve characteristics for qRT-PCR experiments

Gene	R^2	Slope	Efficiency (%)
18S	0.995	3.06	112
FGF-9	0.998	3.55	91
FGF-10	0.935	3.03	114
SHH	0.997	3.92	80
smMHC	0.999	4.22	73
SPRY2	0.996	3.29	101
VEGF	0.989	3.06	112

The amplification curves (Figure 3.2) for each experiment were inspected to ensure that: (i) the fluorescent threshold was set within the exponential phase of the PCR reaction; (ii) the curve continued to rise and the reaction was therefore not limited by reagent availability; and (iii) the non-template control (NTC) did not show fluorescence (and hence product formation). The dissociation (melting) curves (Figure 3.2) were inspected to ensure PCR product specificity, as indicated by a single, tall peak at a melting temperature above 80°C (Agilent Technologies, 2009). These criteria were fulfilled in each case.

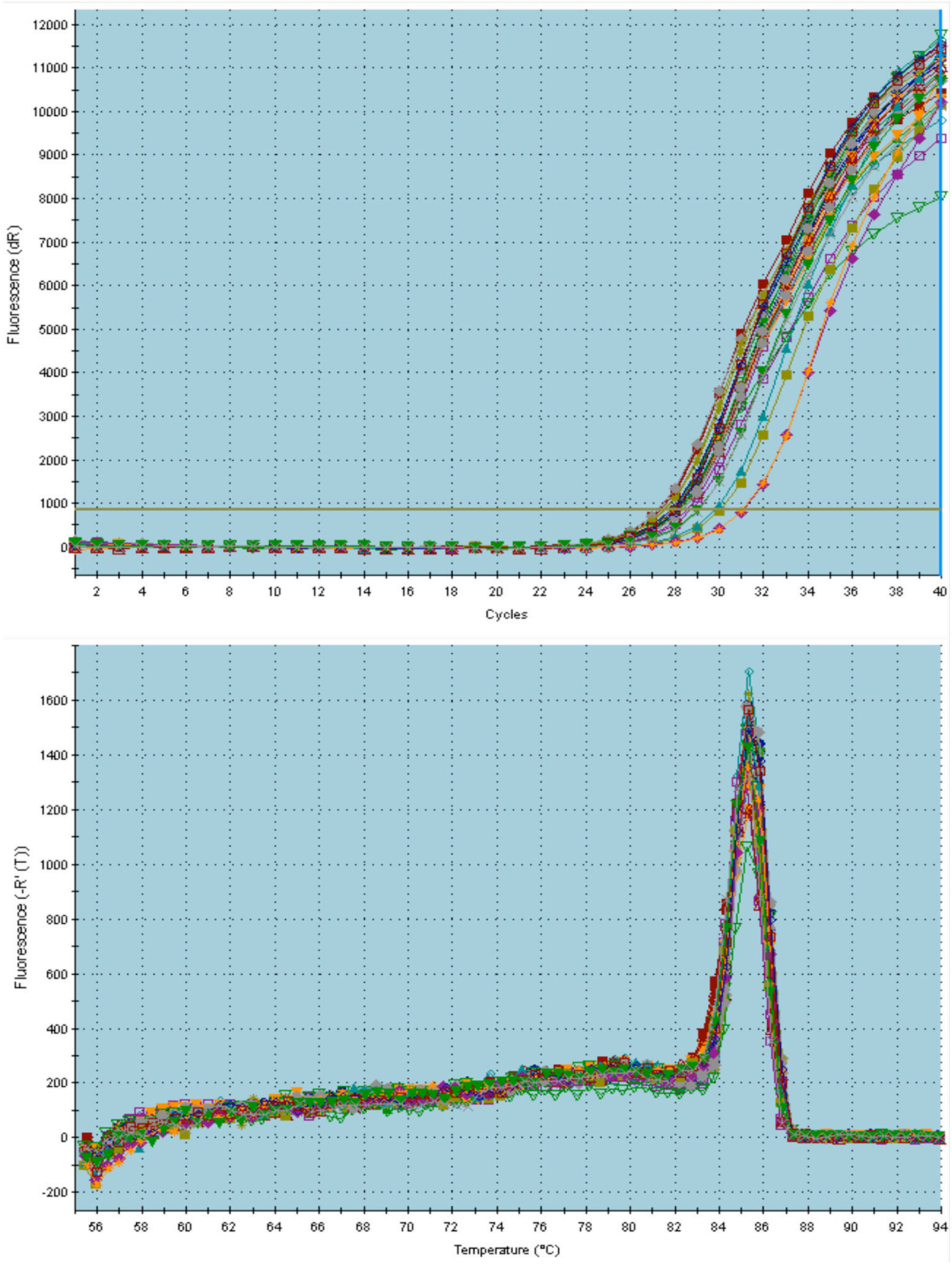

Figure 3.2 Amplification and dissociation curves for qRT-PCR experiments

Top panel: representative amplification curve for relative quantification of genes of interest. Curves indicate the increase in fluorescence with increasing cycle number for each reaction. The horizontal line indicates the threshold fluorescence. The point at which the amplification curve intersects the horizontal line indicates the cycle threshold (Ct) value. Lower panel: representative dissociation (melting) curve produced to confirm specificity of PCR. The first derivative of the fluorescence reading multiplied by –1 (–R´(T)) is plotted against temperature to demonstrate the loss in fluorescence when double stranded DNA product is melted to single stranded DNA.

3.2.4 SERCA inhibition regulates key candidate genes in vitro

SERCA inhibition with CPA had the effect of up or down regulating mRNA levels of target genes, normalised to the reference gene (*18S* ribosomal RNA) (Figure 3.3). These effects were consistent across biological replicates, as indicated by the relatively small variance of these ratios when compared to effect size (data are presented as mean +/- SEM). Normalised *Fgf10* mRNA expression was significantly lower in lung explants in the CPA group, although this difference was relatively modest, being around 3-fold in magnitude (p=0.001). In contrast, the other FGF member, *Fgf9* was expressed at significantly higher levels in the CPA treated group and the size of the difference was greater, approaching 9 fold (p=0.006). Normalised *Shh* mRNA expression was significantly lower in CPA treated lungs, following a similar pattern to that of *Fgf10*, with a fold difference of approximately 6 (p=0.001). Similarly, *smMHC* mRNA was significantly downregulated, with a fold change in the order of 9 (p=0.001). *Spry2* mRNA expression was significantly higher in the CPA treated group, being nearly 10 times greater (p=0.004). Finally, *Vegfa* was upregulated in CPA treated lungs, with a fold change approaching 7 (p=0.001).

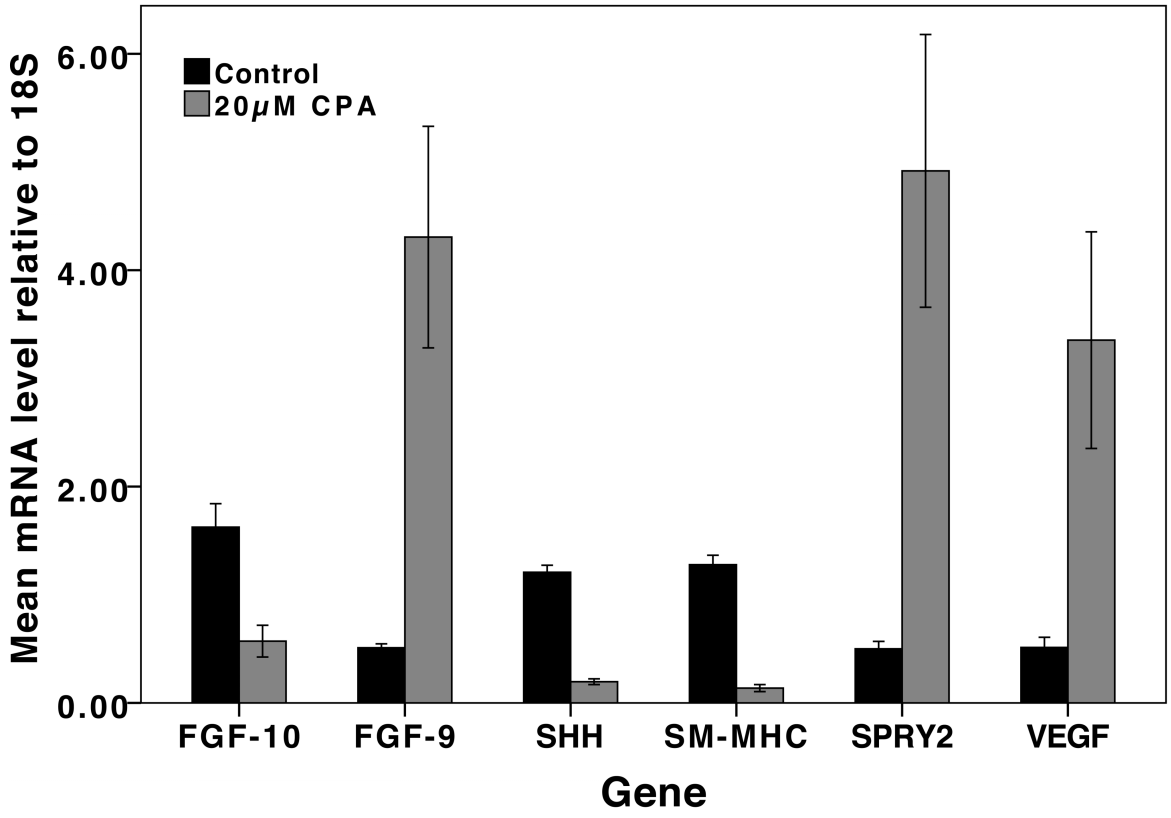

Figure 3.3 SERCA inhibition both up and down regulates candidate genes *in vitro*

Quantitative RT-PCR of whole cultured embryonic murine lungs (E11.5). *Fibroblast-growth-factor-10* (FGF-10), *Fibroblast-growth-factor-9* (FGF-9), *Sonic-hedgehog* (SHH), *smooth-muscle-Myosin-Heavy-Chain* (SM-MHC), *Sprouty-2* (SPRY2) and *Vascular-endothelial-growth-factor-A* (VEGF) mRNA expression levels in CPA treated & control lung cultures at 78h. Levels normalised to *18S* mRNA expression. Error bars indicate +/- SEM. ($n \geq 8$ individual embryos in all groups, except for FGF-9 and SPRY2 when $n \geq 5$). Difference between CPA treated & control groups significant ($p < 0.05$) for all genes.

3.3 SERCA inhibition reduces cell proliferation dose-dependently

3.3.1 Quantifying mitosis in CPA treated lung explants

To test the effect of SERCA inhibition on pulmonary cell proliferation *in vitro*, mitotic activity was assessed in CPA and control groups using established methods. Embryonic lung explants were cultured +/- differing concentrations of CPA (4, 10 and 20 μm), as previously described. Immunohistochemistry of lung frozen sections was carried out for Phospho-Histone-H3, serine 10 (PH3). Histone-H3 is one of four core histone proteins (H2A, H2B, H3, and H4) that undergo various post-translational modifications at their N-termini, as part of their structural and functional roles (Hansen, Tse, & Wolffe, 1998). Phosphorylation at serine 10 is a specific and highly conserved modification that occurs during chromosome condensation, during mitosis (Hendzel et al., 1997). PH3 immuno-staining is therefore widely used to detect mitotic cells.

Once the labelled sections of lung explants had been imaged with confocal microscopy, mitotic activity was quantified with nuclear counting (carried out by MG Connell). Mitotic nuclei (labelled with anti-PH3 and fluorescent secondary antibody) were counted in the pulmonary epithelium and mesenchyme independently, as were the other nuclei (labelled with DAPI). Mitotic activity was therefore quantified as the percentage of total nuclei that were PH3 positive, for the epithelium and mesenchyme alike.

3.3.2 SERCA inhibition with CPA reduces cell proliferation dose-dependently, in vitro

SERCA inhibition with CPA reduced levels of pulmonary cell mitosis (Figure 3.4). The lowest concentration of CPA (4 μM) was sufficient to induce a significant reduction in proliferation compared to controls (0 μM CPA). Reduction in mitosis was seen in both the epithelium and the mesenchyme of lung explants. Cell proliferation reduced further with higher concentration of CPA (10 μM), but no further, significant reduction was witnessed when CPA concentration was raised to 20 μM ($p<0.05$ between all groups, except 10 and 20 μM). These data indicate there is a dose dependent reduction in mitosis until a threshold concentration of CPA is reached at around 10 μM. Reviewing the separate components of epithelium and mesenchyme, there appeared to be a more marked decrease in

mesenchymal cell proliferation at the lower dose of 4 μM CPA, when compared to the epithelium, where a higher dose was required for such a magnitude of effect (Figure 3.4).

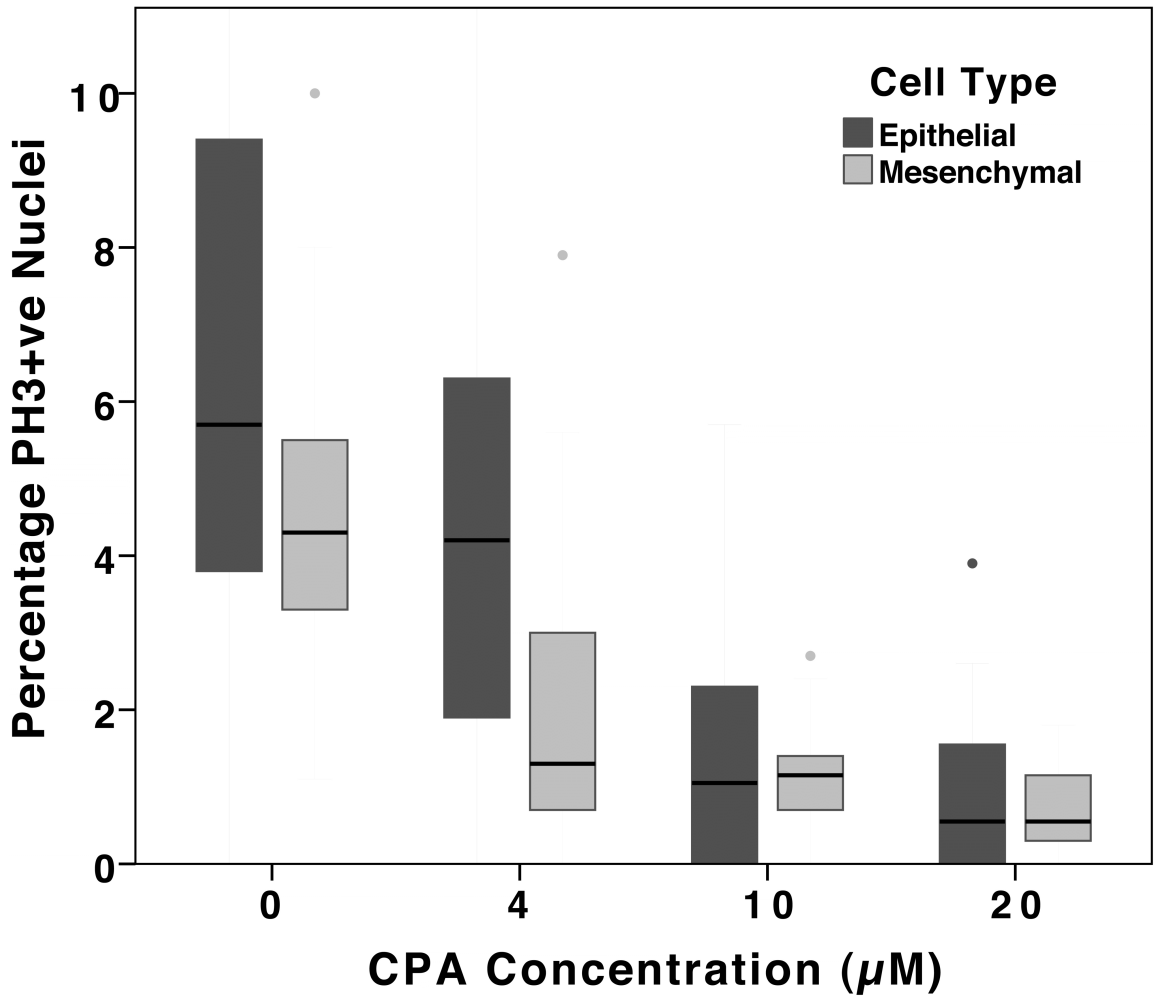

Figure 3.4 SERCA inhibition with CPA reduces cell proliferation does-dependently, *in vitro*

Percentage of PH3+ve nuclei (median & IQR) vs. CPA concentration for epithelial and mesenchymal cells (n=>24 in all groups). E11.5 murine lung explants cultured +/- CPA (4, 10 and 20 μM) for 78 hours. Mitotic cells labelled with Phospho-Histone-H3, serine 10 (PH3) immunohistochemistry and expressed as a percentage of total nuclei (labelled with DAPI) in the epithelium and mesenchyme separately. Difference between CPA concentration groups statistically significant for each cell type ($p<0.05$), with the exception of 10 and 20 μM. Cell counting performed by MG Connell.

3.4 Discussion

3.4.1 SERCA as a regulator of pulmonary gene expression

These data demonstrate that the reversible loss of branching, airway contractility and Smooth Muscle Actin expression that are mediated by CPA inhibition of SERCA function are associated with altered gene expression in key pathways that regulate airway branching, ASM formation, as well as other aspects of lung epithelial and endothelial development (Chapter 1 and Figure 3.3). Given the importance of these closely regulated genetic pathways in dictating normal prenatal development (discussed above), the significant disruption in expression levels witnessed upon SERCA inhibition with CPA is likely to result in consequent changes to essential developmental processes. Whether such changes could explain the striking phenotype remains unclear: given the complexity and frequent interdependency of these genetic pathways, this is likely to be challenging to deduce experimentally in murine knockout studies. The above findings remain important, as the up and down regulation of key candidate genes lends further support (in addition to reversibility and dose-dependency) to the postulate that SERCA plays an important role in pulmonary development, rather than CPA simply inducing global toxicity or cellular quiescence (Figure 3.3). Together, these observations justify further exploration of SERCA's role in airway development and provide a rationale for investigations in this thesis.

Given the paramount importance of the FGF-FGFR-Sprouty axis in airway organogenesis, our observed alterations in this pathway are of particular interest (Figure 3.3). Conservation of airway FGF-FGFR-Sprouty signalling from *Drosophila* to mammals allow us, in the rest of the thesis, to define the role of SERCA in airway development genetically using *Drosophila* (with its single SERCA gene rather than three in mammals; see also Chapter 1) (Sutherland et al., 1996).

3.4.2 SERCA: a link between Ca^{2+} driven airway smooth muscle (ASM) peristalsis and branching morphogenesis?

Propagating Ca^{2+} waves in ASM cells precede waves of airway peristalsis in the prenatal lung (discussed in Chapter 1): SERCA inhibition with CPA abolishes these transients and results in tonic ASM contraction (N. C. Featherstone et al., 2005). A number of roles for these largely unexplained Ca^{2+} waves have been proposed in regulating lung development: (i) a mechanical role, where they drive ASM contraction and induce rhythmic stretch of the airway epithelium; and (ii) a biochemical role, by triggering epithelial Ca^{2+}-activated chloride release and hence lung liquid production (N. C. Featherstone et al., 2005; Jesudason, 2009). Prenatal ASM contraction and lung liquid are intimately related: airway peristalsis induces lung fluid flux, causing phasic distension and relaxation of the growing lung end buds (Jesudason et al., 2005; Schittny et al., 2000). This mechanical stretch, along with the maintenance of airway tone by ASM, are proposed to induce signals that regulate key morphogenic events (Unbekandt et al., 2008; Yang, Beqaj, Kemp, Ariel, & Schuger, 2000). Given ASM peristalsis is coupled to branching morphogenesis *in vitro*, and underpinned by SERCA dependent Ca^{2+} transients, it was important to tease apart, as far as possible, the roles SERCA plays in peristalsis and branching (N. C. Featherstone et al., 2005; Jesudason et al., 2005)?

Data presented here and from others, demonstrate that SERCA inhibition in the lung *in vitro*, has striking effects on: (i) propagating Ca^{2+} waves; (ii) myogenic gene expression and ASM contraction; (iii) morphogenic gene expression and; (iv) branching morphogenesis (N. C. Featherstone et al., 2005; Lansdale, Connell et al., 2010). In addition, these effects on airway peristalsis and branching share a similar dose-response range. One suggestion is that these phenomena are linked by the function of SERCA dependent pulmonary pacemaker cells: SERCA function is essential for pacemaker activity in other tissues (Dixon et al., 2011; Jesudason et al., 2005; Sanyal, Jennings, Dowse, & Ramaswami, 2006).

3.4.3 SERCA as a cell cycle regulator

SERCA also has a role(s) in controlling specific elements of the cell cycle. Cheng *et al* knocked-down SERCA in cell lines, detected slower cell growth and found a delay in the transition from G1 to S phase, with SERCA deficient cells less likely

to enter DNA synthesis (G. Cheng, Liu, Yu, Diglio, & Kuo, 1996). Similarly, Simon *et al* inhibited SERCA pharmacologically using thapsigargin, and reported cells having a prolonged G1 phase (Simon & Moran, 2001). These effects could not be recreated by altering cytosolic Ca^{2+} alone and cells expressing thapsigargin-resistant SERCA progressed normally through the cell cycle, thus indicating that cell cycle effects were SERCA specific. Other studies have reported similar effects, finding decreased proliferation and cells reversibly entering a quiescent, G0-like state upon SERCA inhibition (Legrand et al., 2001; Waldron, Short, Meadows, Ghosh, & Gill, 1994).

These observations may go some way towards explaining the abrogation of branching in the present study. If embryonic lung explant cells were to enter a quiescent (G0 like) state upon CPA treatment, then cell proliferation would be reduced and it is conceivable that normal branching morphogenesis would halt. Indeed, this may also account for the reversibility of the effect on morphogenesis. What is not explained by this hypothesis, however, is the continued increase in size of the pulmonary mesenchyme relative to the epithelium following CPA treatment, indicating there are ongoing changes in cell size or number in this tissue. The upregulation of key morphogenic genes, discussed earlier, also indicates that all cells were not simply quiescent. In addition, studies report contradictory results, with SERCA inhibition actually stimulating cell proliferation and overexpression inducing apoptosis, with cell-cycle arrest in the G2/M phase (Charlesworth & Rozengurt, 1994; Ma, Mann, Lee, & Gallinghouse, 1999). It therefore seems likely that effects of SERCA inhibition on the cell cycle are complex and may be dependent on the intra and extra-cellular environment; the *in vitro* nature of these studies limit the conclusions that may be drawn and may also explain the variation in the published findings. To determine this matter, we undertake *in vivo* investigation of SERCA's role in airway cell proliferation in Chapter 7.

3.4.4 Limits of pharmacological SERCA manipulation

The principal limitation of the murine system here is the reliance on CPA as a specific SERCA inhibitor (Seidler et al., 1989). It is widely known that pharmacological agents may induce off-target effects and these may be occult (MacDonald et al., 2006). CPA is reported to inhibit the SERCA Ca^{2+}-ATPase pump

specifically rather than other ATPases: the diverse phenotypes induced by CPA in species ranging from rats to pigs indicate either SERCA has pleiotropic, fundamental roles in cell signalling and / or that CPA may harbour off-target effects yet to be identified (Cullen, Wilson, Hagler, Ort, & Cole, 1988; Lomax, Cole, & Dorner, 1984; Purchase, 1971).

Genetic models would provide some reassurance about the effects seen with CPA. However, mammals have three SERCA paralogues (*ATP2A 1-3*) each of which may produce numerous mRNAs by alternative splicing: complete SERCA knockout in a mammalian system would therefore be challenging (Wuytack et al., 2002). This task is compounded by the essential developmental requirement for SERCA1&2 (SERCA2-null mice are non-viable, SERCA1-null die as newborns): a tissue specific and / or conditional mutagenesis approach would be required with attention to the problems of redundancy too (Pan et al., 2003; Periasamy et al., 1999). As a simple and elegant alternative, we have studied genetic manipulation of SERCA during Drosophila airway development.

3.4.5 Genetic inhibition of airway epithelial SERCA in vivo

Invertebrates including *Caenorhabditis elegans* and *Drosophila melanogaster* have one SERCA gene, permitting simpler genetic manipulation than for vertebrates (Cho, Bandyopadhyay, Lee, Park, & Ahnn, 2000; Magyar, Bakos, & Varadi, 1995). *Drosophila* affords powerful tools to control gene expression spatially and temporally during respiratory organogenesis, with well-characterised genetic homology to mammals (discussed in Chapters 1, 4 and 7) (Sean E. McGuire, Roman, & Davis, 2004; Metzger & Krasnow, 1999).

3.4.6 SERCA Phylogeny

FlyBase (available at http://flybase.org) reports the *Drosophila* SERCA gene, *Ca-P60A* to have eight different mRNAs (A-H) from alternative splicing: when the predicted translations are aligned, isoforms B–H have identical protein sequences (Appendix I) (Tweedie et al., 2009). It therefore appears *Drosophila* has two protein isoforms (A with 1002 residues and B with 1020), differing only at the final 27 residues (9 of the short isoform) at the C terminus. Multiple protein sequence alignments were undertaken between various paralogues and splice variants of SERCA, in principal model organisms and humans (Appendix I). SERCA

proteins are highly conserved across species, from *Drosophila* to humans: differences in amino acid sequence are few and largely grouped at the C terminus. This high conservation between species of protein sequence, and hence also protein function, indicates that findings from *Drosophila* are likely to be directly applicable to mammals.

3.5 Other potential future directions

The data presented do not provide a proven mechanism linking CPA's effects on gene expression, cell proliferation, pulmonary morphogenesis and ASM contractility: reviewing the data with existing literature provides hypotheses for future testing.

Pulmonary development relies on signalling between lung mesothelium, mesenchyme and epithelium: given SERCA modulates receptor-mediated Ca^{2+} signals in the pancreas and arterial endothelium, it is plausible that SERCA inhibition dysregulates interactions between these pulmonary compartments too (Arredouani et al., 2002; Lynne H. Liu et al., 1997; Warburton et al., 2010; Zhao, Shin, Liu, Shull, & Muallem, 2001)? This could underpin parallel changes in gene expression across these histological compartments, e.g. (i) mesothelial *Fgf9* positively regulates mesenchymal *Vegf*: both were upregulated here; and (ii) epithelial *Spry2*, upregulated here, is a key inducible repressor of mesenchymal *Fgf10,* appropriately downregulated here (Figure 3.3).

Another explanation for CPA's widespread effects is SERCA's role in protein chaperoning/trafficking. The endoplasmic reticulum (ER), a site of protein synthesis, post-translational modification and folding, is highly sensitive to changes in Ca^{2+} homeostasis: the SERCA inhibitor, thapsigargin is well known to induce ER stress (Ellgaard, Molinari, & Helenius, 1999; R. V. Rao et al., 2001). In the interest of protein quality control, ER stress results in an accumulation of unfolded proteins, triggering the coordinated unfolded protein response (UPR) (Kaufman, 1999; Rutkowski & Kaufman, 2004; Stirling, Lundin, & Leroux, 2003). The effect of the UPR is to decrease the burden of proteins in the ER, by reducing translation and increasing protein efflux (e.g. by facilitating their folding through increased chaperone protein synthesis). SERCA is transcriptionally upregulated in ER stress and UPR, and this increase is independent of ER Ca^{2+} depletion (Caspersen, Pedersen, & Treiman, 2000; Hojmann Larsen, Frandsen, & Treiman, 2001). SERCA may therefore have a role in regulating post-translational events such as chaperoning and in keeping with this, it has an essential role in trafficking of several proteins, including notch, in *Drosophila* (Periz & Fortini, 1999). Whether through these or other mechanisms,

SERCA appears critical for development since is it is highly conserved, widely expressed and essential for viability (as shown by SERCA2-null mice) (Periasamy et al., 1999; Wuytack et al., 2002).

Chapter 4

TECHNIQUES TO STUDY THE EFFECTS OF SERCA INHIBITION ON THE *DROSOPHILA* RESPIRATORY ORGAN

4.1 Introduction

The development of the *Drosophila* respiratory organ can be broadly divided into 3 stages: (i) in the embryonic period, a network of tubes develops from 10 pairs of tracheal sacs (each composed of approximately 80 cells), initially formed from the invagination of epidermal epithelial cells: development of this complex, highly stereotyped structure is entirely controlled by genetically determined branching and tube expansion events; (ii) at the end of embryogenesis and through much of the larval period, respiratory tubes grow and subdivide into finer, more random, often terminal branches in response to oxygen demands of target tissues; (iii) during metamorphosis, clusters of imaginal and 'de-differentiated' larval tracheoblasts proliferate and spread, replacing the larval tracheal epithelium and reconfiguring most branches (Guha, Lin, & Kornberg, 2008; Manning & Krasnow, 1993; Sato, Kitada, & Tabata, 2008; Weaver & Krasnow, 2008). Most early studies that set out to elucidate the genetic programming of these events focussed on the first stage, since embryonic tracheal morphogenesis is highly stereotyped (Affolter et al., 1994; Glazer & Shilo, 1991; Samakovlis, Hacohen et al., 1996). More recently, progress has been made in determining the mechanisms behind later events, in larvae and pupae (Cabernard & Affolter, 2005; Pitsouli & Perrimon, 2010; Sato & Kornberg, 2002). In all cases, the study of trachea and its derivatives is dependent on an accurate demonstration of its structure. Non-gas-filled viscera are not readily visualised with light microscopy and hence investigators have used a variety of experimental techniques with which to demonstrate the tracheal system: antibodies (e.g. to tracheal lumenal proteins, such as 2A12), enhancer traps (e.g. *trachealess-lacZ*) and fluorescent proteins (e.g. actin.GFP or moesin.mRFP) (Lin, Buff, Perrimon, & Michelson, 1999; Manning & Krasnow, 1993; Ribeiro, Ebner, & Affolter, 2002; Samakovlis, Hacohen et al., 1996). Fluorescent fusion proteins have been targeted to the trachea by cloning them downstream of a *breathless* promoter or using the *GAL4-UAS* system (discussed later) (Brand & Perrimon, 1993; Ribeiro, Neumann, & Affolter, 2004).

In addition to the advances in imaging techniques that have permitted improved demonstration of *structure*, developmental biology has benefitted from the development of *functional* assays that allow dynamic processes to be studied. Examples of such include, live imaging (from single cells to whole organisms),

cell markers to allow lineage and fate analysis (e.g. using GFP, luciferase or nanoparticles) and molecular reporters (e.g. genetically encoded Ca^{2+} indicators) (Kircher, Gambhir, & Grimm, 2011; Lippincott-Schwartz & Patterson, 2003; Miyawaki et al., 1997). Ca^{2+} signalling is essential to a vast array of biological processes and its study depends on the ability to monitor Ca^{2+} dynamics: resting intracellular free Ca^{2+} is highly heterogeneous yet changes in concentration are key to signalling function (Berridge et al., 2000; Rudolf, Mongillo, Rizzuto, & Pozzan, 2003). Sensors that accurately demonstrate spatiotemporal changes in Ca^{2+} are therefore useful. SERCA is a key regulator of intracellular Ca^{2+}; understanding its role in airway development would therefore benefit from an ability to study airway Ca^{2+} dynamics *in vivo*.

To investigate the effect of SERCA modulation on *Drosophila* airway, I first tested existing research tools to confirm and optimise their efficacy and explore new and relevant applications for them.

4.2 Testing GAL4 drivers in the embryo

The GAL4–upstream activating sequences (UAS) system is the most widely used system with which to spatially restrict ectopic gene expression in *Drosophila* (Figure 4.1) (Brand & Perrimon, 1993). This system has two elements: the *GAL4* gene, encoding the yeast transcription activator protein Gal4, and UAS - a short section of the promoter region, to which, Gal4 specifically binds to activate gene transcription. A *P* element, carrying *GAL4* is randomly inserted throughout the *Drosophila* genome, bringing *GAL4* expression under the control of a range of endogenous, tissue-specific genomic enhancers. Alternatively, the specific promoter can be cloned upstream of *GAL4* in the *P* element construct. In order to create *GAL4*-responsive target transgenes, they are cloned downstream of a UAS sequence. Target genes are hence expressed in the same tissue-specific pattern as the *GAL4* activator.

This study relied upon *GAL4* drivers to activate gene transcription of a host of transgenes (including fluorescent proteins, RNAi constructs and Ca^{2+} indicators) in specific tissues, at specific stages of embryonic development. Experimental design necessitated expression: (i) ubiquitously, throughout the embryo; (ii) in tracheal cells specifically; and, (iii) in cells acting as a source of the FGF branching morphogen, *branchless*. Critically, expression of these transgenes was required to be active at the start of tracheal branching (stage 11) and at the stage of phenotypic assessment (stage 16).

Three GAL4 lines were selected for this purpose: *daughterless-GAL4 (da-GAL4), breathless-GAL4 (btl-GAL4)* and *branchless-GAL4 (bnl-GAL4)*. To confirm the pattern of expression, these lines were crossed to *UAS-histone.YFP*, which encodes a fusion between histone H3 and Yellow Fluorescent Protein (YFP), facilitating rapid visualisation in either fixed samples or by live imaging.

This text box is where the unabridged thesis included the following third party copyrighted material:

St Johnston D et al. (2002). The art and design of genetic screens: Drosophila melanogaster. Nature Reviews Genetics, 3, 176-188.

Figure 4.1 The GAL4–UAS system is used to spatially restrict ectopic gene expression

The yeast transcriptional activator Gal4 can be used to regulate gene expression in *Drosophila* by inserting the upstream activating sequence (UAS) to which it binds next to a gene of interest (gene X). Large libraries of flies expressing GAL4 in an array of cell-type and tissue-specific patterns are available. Expression of the gene of interest (gene X) can be driven in any of these patterns by crossing the appropriate GAL4 line to flies that carry the UAS–gene X transgene. Image adapted from St Johnston D *et al*. The art and design of genetic screens: Drosophila melanogaster. *Nature Reviews Genetics* 2002; 3: 176-188.

4.2.1 Daughterless-GAL4 drives transgene expression in most tissues at stage 11 and throughout the embryo at stage 16

The *da-GAL4* driver was crossed to *UAS-histone.YFP* and live embryos were imaged at stages 11 and 16 (Figure 4.2). At stage 11, YFP expression was present in most somatic tissues, in an almost identical distribution to *daughterless* protein distribution at this stage (Vaessin, Brand, Jan, & Jan, 1994). At stage 16, there was homogenous YFP expression throughout the embryo. These findings confirm the *da-GAL4* driver can be used to drive ubiquitous transgene expression.

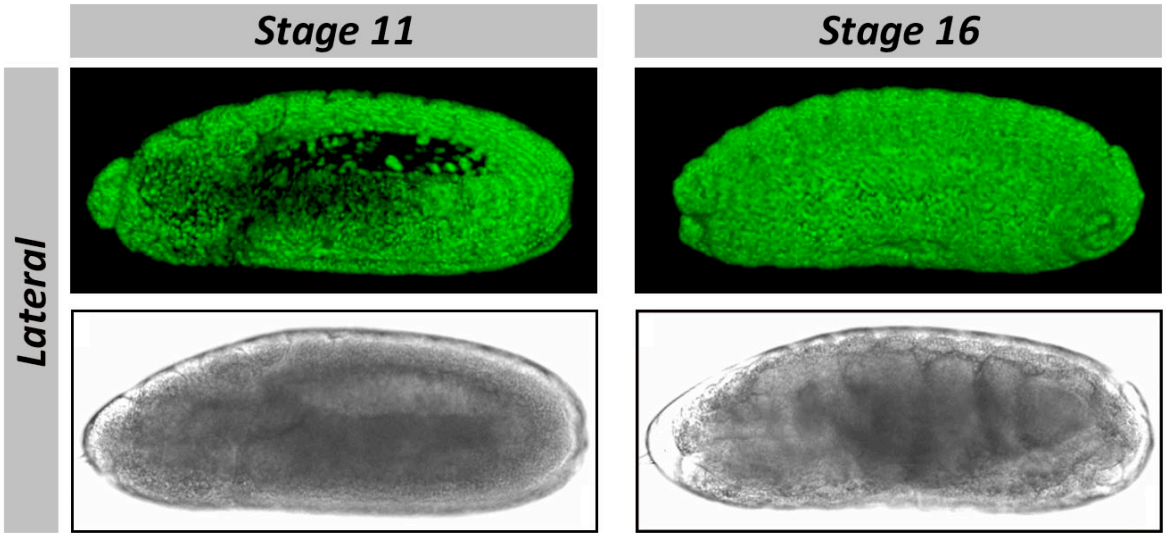

Figure 4.2 *Daughterless-GAL4* drives transgene expression in most tissues at stage 11 and throughout the embryo at stage 16

Confocal micrographs of stage 11 and stage 16 *Drosophila* embryos expressing the histone.YFP fusion protein under the control of the *da-GAL4* driver. 3D projections of z-stacks of the YFP channel are provided (upper panels), along with the transmitted light image (lower panels). The lateral aspect of the embryo is shown in each case (anterior to the left). Embryos are approximately 500 µm in antero-posterior length.

4.2.2 Breathless-GAL4 drives transgene expression in tracheal and midline precursor cells.

The *btl-GAL4* driver was crossed to *UAS-histone.YFP* and embryos imaged at both stages 11 and 16 (Figure 4.3). At stage 11, histone.YFP was expressed in the cells of the 10 metameric tracheal pits and also in a strip along the ventral midline, in cells known as midline precursors (MLP): this conforms with the distribution of *breathless* mRNA and protein reported at this stage (Glazer & Shilo, 1991). Later, YFP was expressed throughout the tracheal system, in major branches (the dorsal and lateral trunks, the dorsal, visceral and ganglionic branches, the transverse connective and dorsal anastomosis) as well as in specialised branches in the first and tenth metameres (Manning & Krasnow, 1993). Hence the *btl-GAL4* driver is suitable for driving transgene expression in tracheal cells. However, expression will also occur in glial and neural MLP cells: phenotypic effects of *btl-GAL4* mediated transgene expression must be interpreted with this caveat.

4.2.3 Branchless-GAL4 driven transgene expression in the embryo is not in-keeping with reported branchless mRNA expression

The *bnl-GAL4* driver was crossed to *UAS-histone.YFP* and embryos imaged at both stages 11 and 16 (Figure 4.4). At stage 11, histone.YFP expression is largely limited to two central areas in the embryo. The distribution of these areas implies they are likely to be the anterior and posterior midgut rudiments but may also include parts of the foregut and hindgut mesoderm. At this stage, *branchless* mRNA expression is known to surround the developing tracheal system: it would be expected that *bnl-GAL4* driven histone.YFP expression would be found in 10 metameric patches, around the tracheal pits (Sutherland et al., 1996). At stage 16, a more widespread, segmental distribution of YFP can be seen, with an abundance of signal anteriorly in the embryo. Again, this does not appear to correlate with reported *branchless* mRNA expression that follows the pattern of tracheal branches, concentrated more posteriorly than anteriorly in the embryo (Sutherland et al., 1996). The commercially available *bnl-GAL4* driver tested in these experiments therefore, does not appear to drive transgene expression in *branchless* expressing cells.

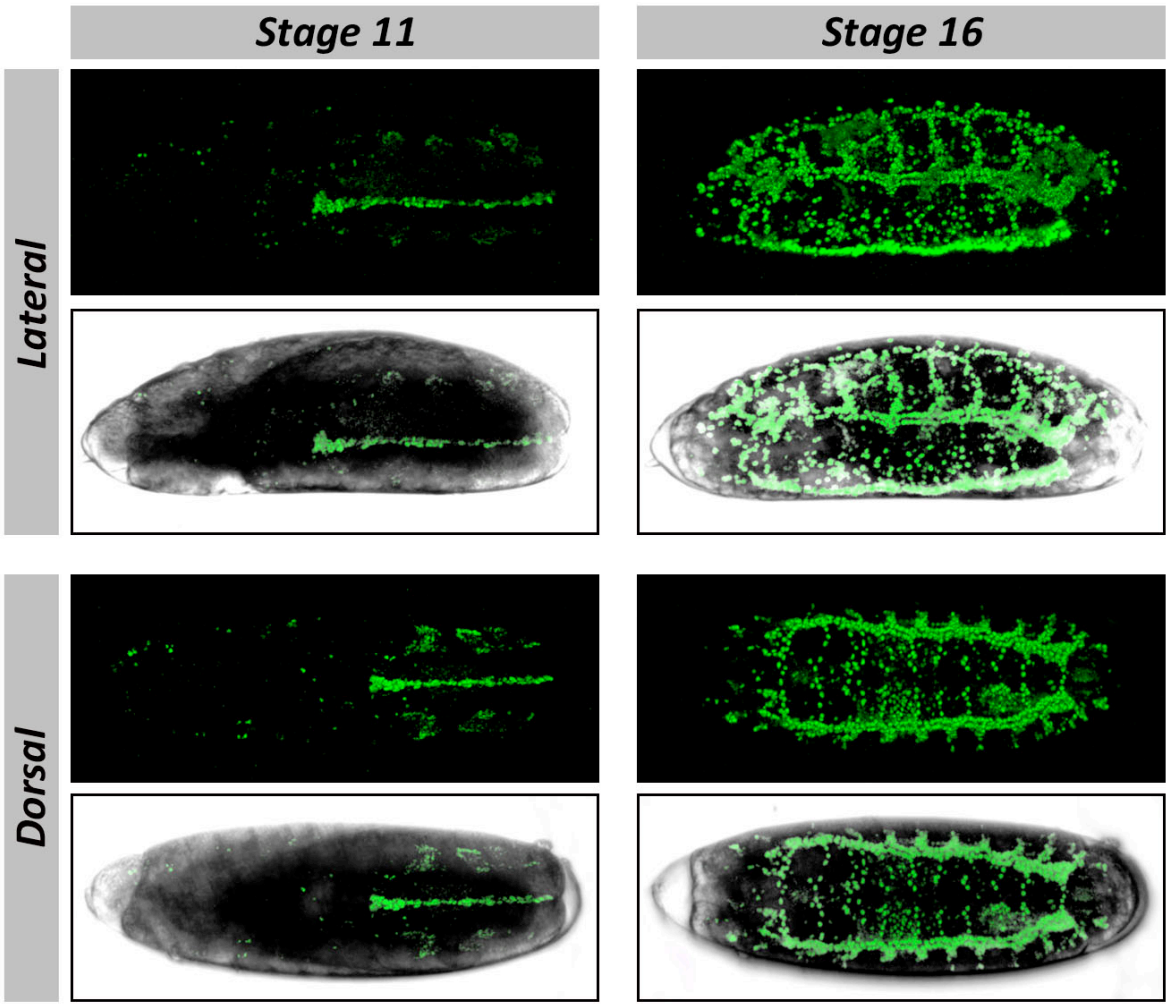

Figure 4.3 *Breathless-GAL4* drives transgene expression in tracheal and midline precursor cells.

Confocal micrographs of stage 11 and stage 16 *Drosophila* embryos expressing the histone.YFP fusion protein under the control of the *btl-GAL4* driver. 3D projections of z-stacks of the YFP channel are provided (upper panels) and merged with the transmitted light image (lower panels). The lateral and dorsal aspects of the embryo are shown in each case (anterior to the left). Embryos are approximately 500 µm in antero-posterior length.

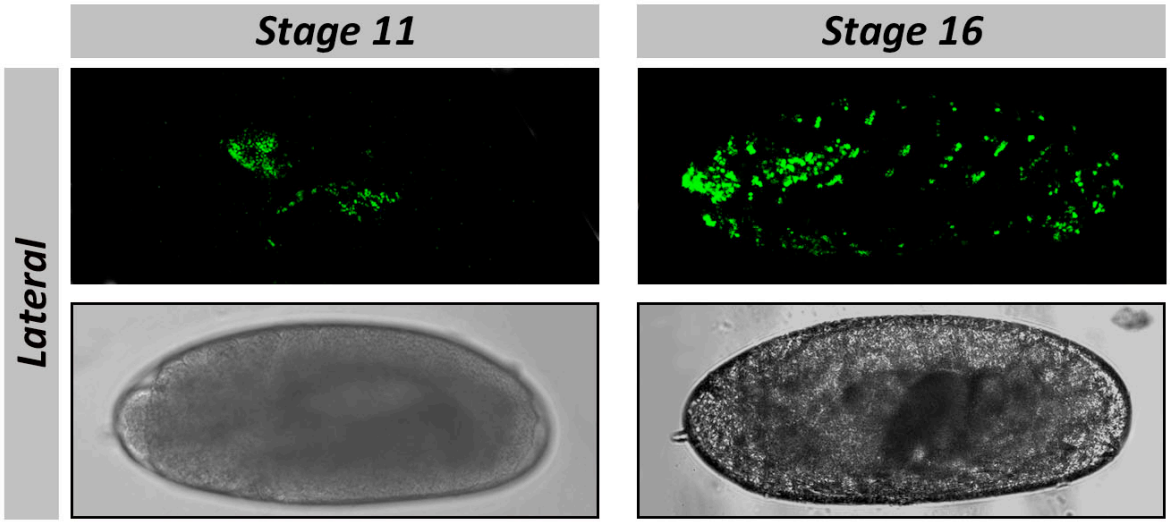

Figure 4.4 *Branchless-GAL4* driven transgene expression in the embryo is not in keeping with reported *branchless* mRNA expression

Confocal micrographs of stage 11 and stage 16 *Drosophila* embryos expressing the histone.YFP fusion protein under the control of the *bnl-GAL4* driver. 3D projections of z-stacks of the YFP channel are provided (upper panels), along with the transmitted light image (lower panels). The lateral aspect of the embryo is shown in each case (anterior to the left). Embryos are approximately 500 µm in antero-posterior length.

4.3 Techniques for imaging development of the tracheal system and embryo

4.3.1 Live imaging of embryonic development may alter timing of events

Embryos expressing histone.YFP under the control of *da-GAL4*, were prepared by adapting Mavrakis *et al's* protocol (Mavrakis, Rikhy, Lilly, & Lippincott-Schwartz, 2008). Live embryos underwent time-lapse confocal microscopy for up to 13 hours (Figure 4.5). This system did not grossly interfere with morphological development since expected transitions were observed. However their timing proceeded faster than expected: stage 6 of embryogenesis begins around 3 h after egg lay (AEL) and at 25°C, stage 16 supervenes no sooner than 10 h later (Bownes, 1975; Campos-Ortega & Hartenstein, 1985). However, embryos imaged from early stage 6 (Figure 4.5) took only 8.5 h to reach stage 16.1 (as confirmed by the characteristic gut morphology of four parallel, divided segments). Thus live imaging protocols can successfully reproduce aspects of morphological development but whilst also altering the rate at which these events occur.

4.3.2 Live imaging protocols allow real time study of developing trachea

Embryos expressing histone.YFP under the control of *btl-GAL4* underwent time lapse confocal microscopy from stage 12 to stage 17 (Figure 4.6). Appropriate tracheal morphogenesis occurred as development proceeded from stage 12 to 16.1 in only 240 minutes (Figure 4.6), compared to the 300–420 min expected at 25°C (Bownes, 1975; Campos-Ortega & Hartenstein, 1985). Again live imaging protocols can therefore provide morphological fidelity at the expense of the temporal.

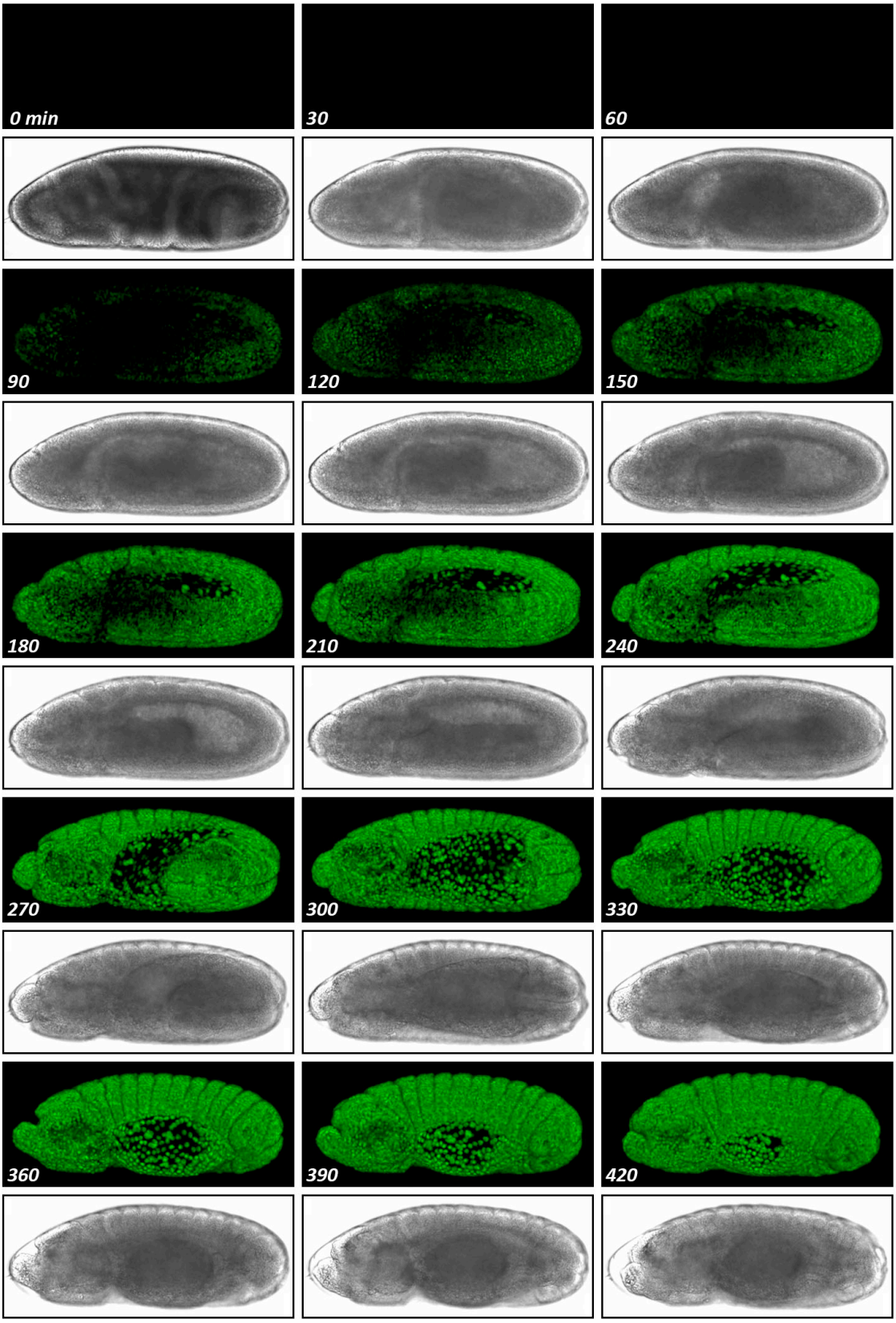

Figure 4.5 Live imaging protocols can be applied to study embryonic development in real time, but rates of development may be altered

Frames from a movie produced by live confocal imaging of a single embryo expressing the histone.YFP fusion protein under the control of the *da-GAL4* driver. 3D projections of the YFP channel (top panels) and transmitted light image (lower panels). Time from the start of imaging is indicated in minutes. The lateral aspect of the embryo is shown in all cases (anterior to the left). The embryo is approximately 500 µm in antero-posterior length.

Figure 4.5 Continued

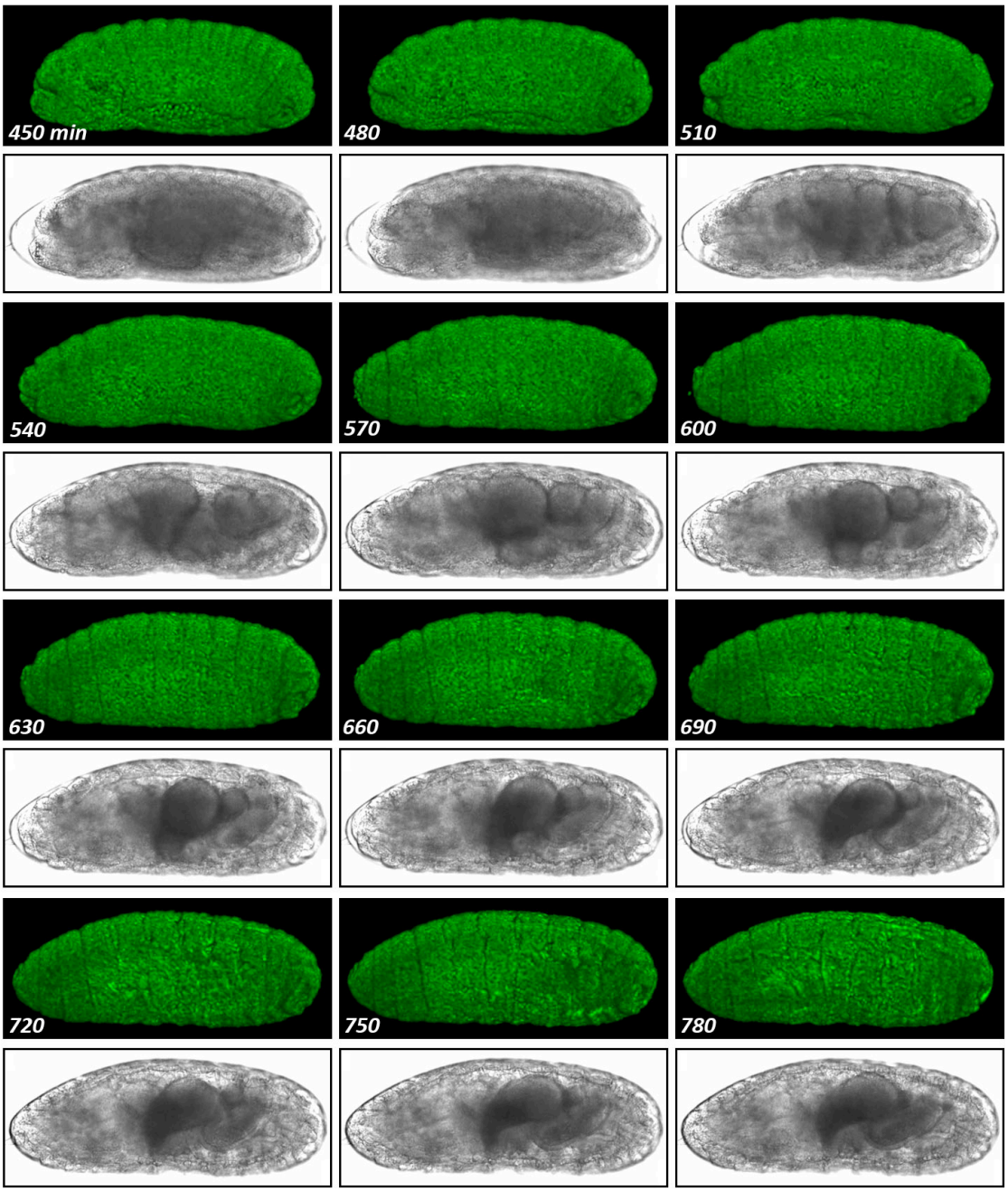

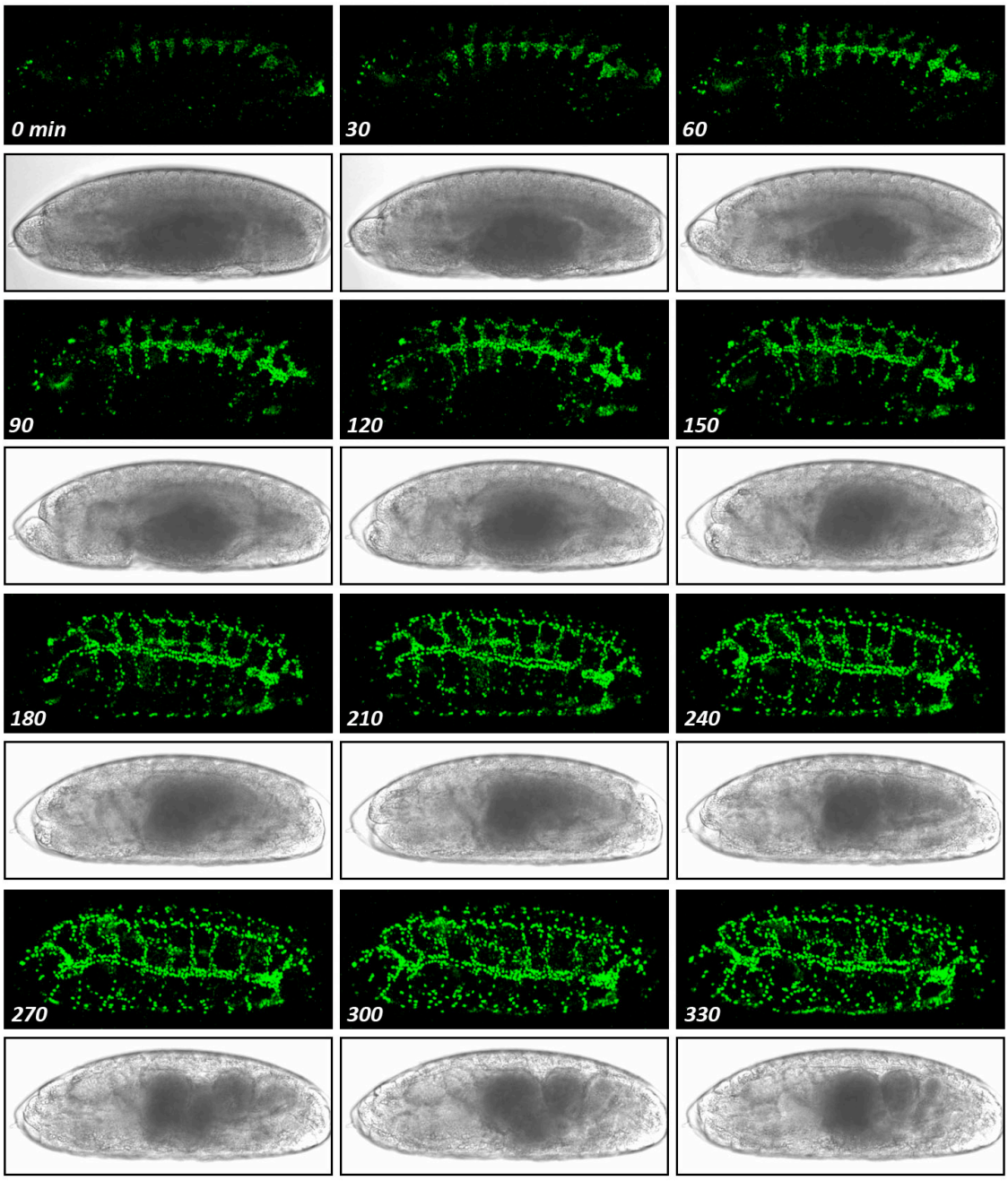

Figure 4.6 Live imaging protocols can be applied to study the developing tracheal system in real time

Frames from a movie produced by live confocal imaging of a single embryo expressing the histone.YFP fusion protein under the control of the *btl-GAL4* driver. 3D projections of the YFP channel (top panels) and transmitted light image (lower panels). Time from the start of imaging is indicated in minutes. The lateral aspect of the embryo is shown in all cases (anterior to the left). The embryo is approximately 500 µm in antero-posterior length.

4.3.3 Fluorescent proteins afford earlier dynamic imaging of embryonic trachea while antibody staining offers better spatial resolution and reproducibility

To test which method of tracheal labelling would best fulfil our different requirements, fluorescent proteins targeted to the tracheal system were compared to antibody staining. Embryos expressing actin.GFP under the control of *btl-GAL4* were compared to ones stained with an antibody to the lumenal protein, 2A12 (DSHB, Iowa) and a fluorescent secondary antibody (Manning & Krasnow, 1993). Confocal imaging was performed at stages of embryo development ranging from 11–16. The tracheal system of embryos labelled with *btl-GAL4, UAS-actin.GFP* could be imaged from stage 11, whereas the earliest stage of development that could be demonstrated with the antibody was stage 14 (Figure 4.7). Antibody staining offered greater spatial definition of finer tracheal branches (such as the ganglionic, spiracular and lateral branches) at stage 16, by which time most embryonic branching events are completed (Figure 4.7) (Manning & Krasnow, 1993). As demonstrated above, targeted fluorescent proteins offer the possibility of dynamic imaging in live embryos, but we found staining of the trachea in fixed embryos to be more reproducible and consistent. In view of this increased spatial resolution and reproducibility, antibody staining was the method of choice for much of this study.

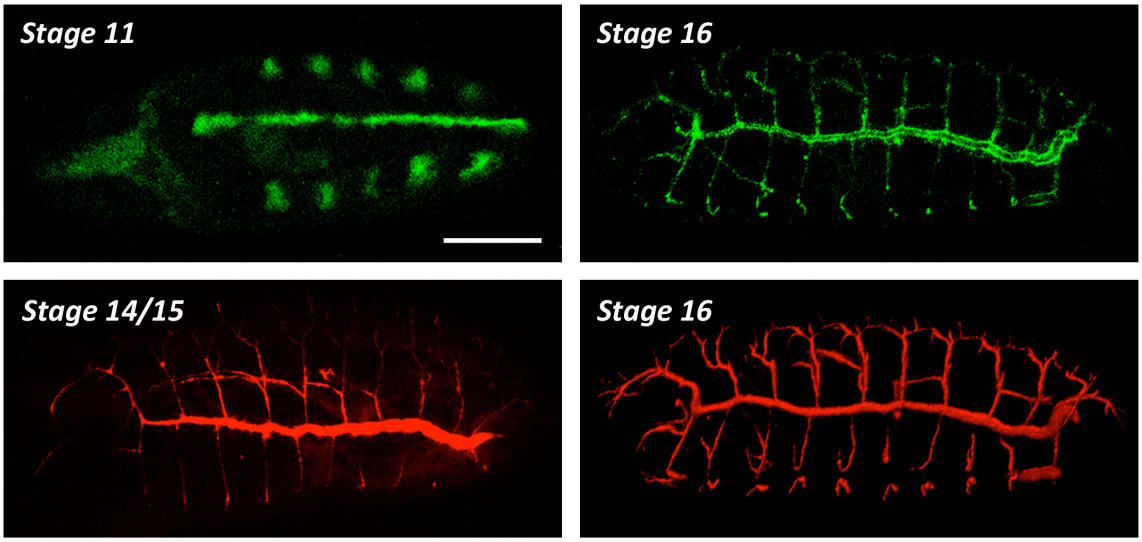

Figure 4.7 Fluorescent proteins offer earlier and dynamic imaging of the embryonic tracheal system; antibody staining offers better spatial resolution and reproducibility

Confocal micrographs (3D projections of z-stacks) of fixed *Drosophila* embryos at the earliest stage that the tracheal system can be imaged with each technique (left panels) and later in embryogenesis (right panels). The tracheal system is labelled with *Btl-GAL4, UAS-act5c.GFP* (upper panels) or the 2A12 antibody (lower panels, DSHB, University of Iowa). The lateral aspect of the embryo is shown in each case (anterior to the left). Scale bar indicates 100 μm.

4.3.4 Fluorescent proteins can be recombined to dual label the tracheal system

To enhance methods for investigating tracheal anatomy, both in embryos and late L3 larvae, *Drosophila* lines with dual labelled tracheal cells /tracheoblasts were developed. Fluorescent fusion proteins and the *btl-GAL4* driver were recombined on the second chromosome, using the crossing scheme given in Figure 4.8. Meiotic recombination in female *Drosophila* was exploited to combine the heterozygously carried transgenes (present on homologous second chromosomes), onto one chromosome. Individual male recombinants were selected based on fluorescence of larvae. Crossing these male recombinants to a second chromosome balancer made stable stocks. Using similar approaches, stocks of flies were generated that expressed either actin.GFP and $DsRed^{NLS}$, or actin.mRFP and histone.YFP under the control of *btl-GAL4*. Tracheal cells and tracheoblasts therefore had both the nucleus and actin cytoskeleton labelled with contrasting red and green fluorescent proteins. (Figure 4.9) These two lines offered individual benefits: actin.GFP is significantly brighter than actin.mRFP and provided better spatial resolution with which to demonstrate tissue architecture; histone.YFP can be used to label nuclei in the embryo (as demonstrated above in Figures 4.2 - 4.6), whereas the slow maturation kinetics of DsRed make it unsuitable for use in *Drosophila* embryos (Akimoto, Wada, & Hayashi, 2005; Campbell et al., 2002). In addition to making use of these dual-labelled lines in this study, they have been distributed to other laboratories to aid their investigations.

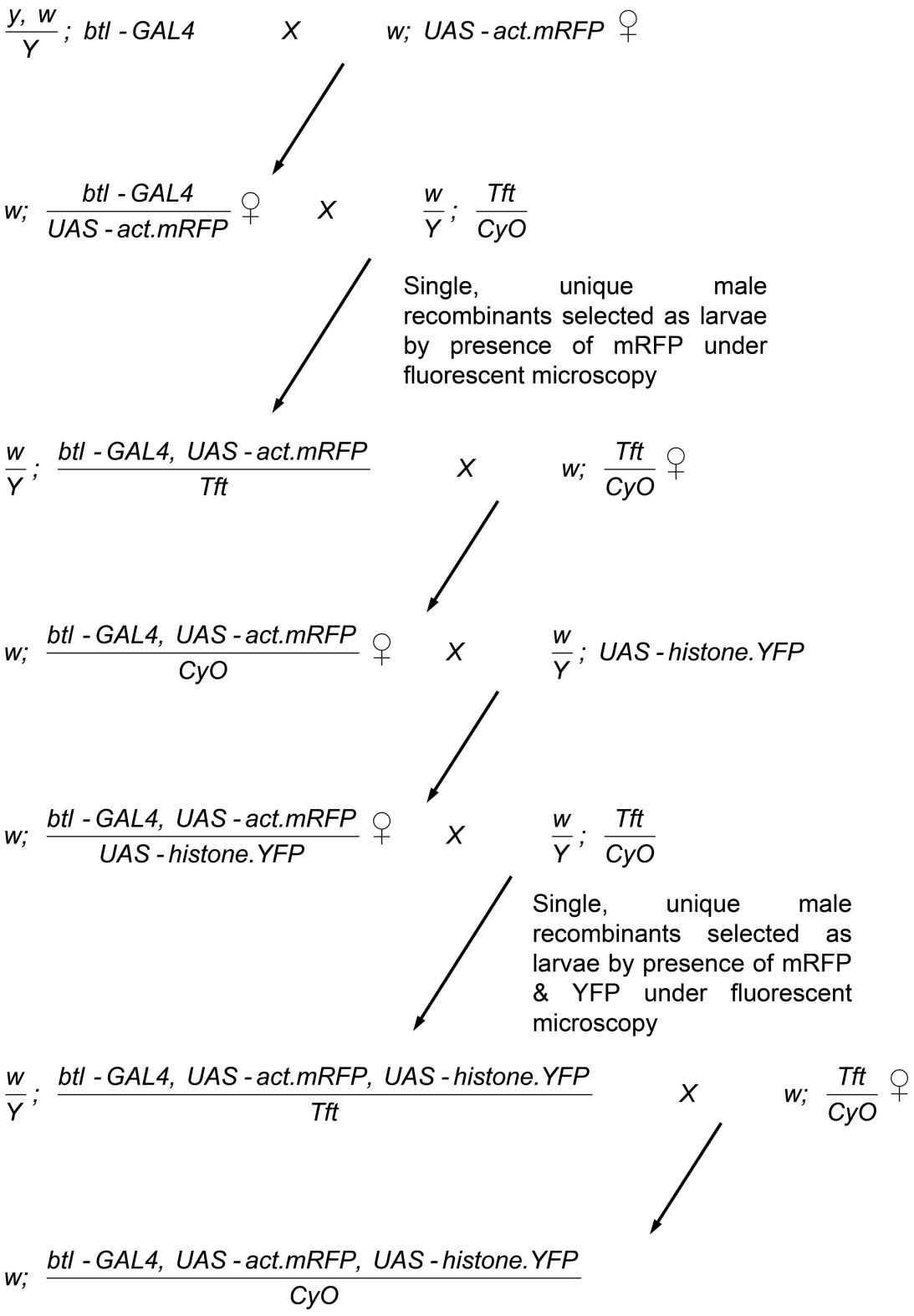

Figure 4.8 Genetic crossing scheme demonstrating the recombination of fluorescent proteins and *btl-GAL4* on the 2nd chromosome,

Meiotic recombination in females was exploited to combine the heterozygously carried transgenes (present on homologous second chromosomes), onto one chromosome. Individual male recombinants were selected based on fluorescence. Stable stocks were then made, by crossing these male recombinants to a second chromosome balancer. A similar scheme was used combine actin.GFP, DsRedNLS and *btl-GAL4* on the second chromosome.

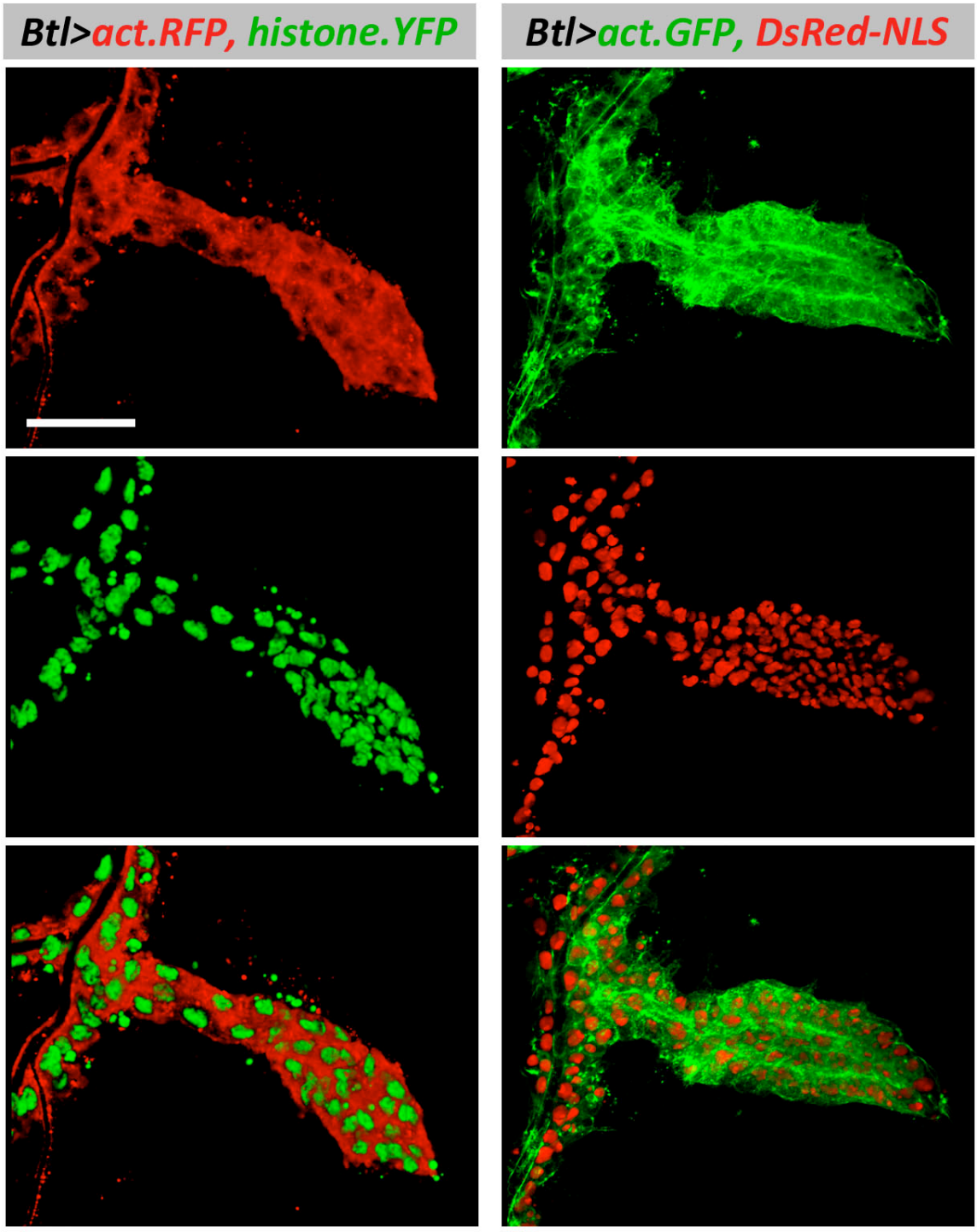

Figure 4.9 Fluorescent proteins can be recombined to dual label the tracheal system

Confocal micrographs of the wing disc air sac and associated trachea, from late third instar *Drosophila* larvae. Stocks expressing two fluorescent proteins and the *btl-GAL4* driver were used as indicated. 3D projections were created from z-stacks taken through the air sac. Scale bar represents 50 μm.

4.4 Calcium imaging in embryonic trachea *in-vivo*

Quantitative assessment of Ca^{2+} dynamics in living cells traditionally relied upon synthetic fluorescent chelators (known as Ca^{2+} indicators, probes, dyes or sensors), applied by intracellular injection or as AM-esters (Tsien, 1980, 1981). Advantages of the most recent versions of these indicators are a high sensitivity and dynamic range, as well as rapid response kinetics to changes in Ca^{2+} concentration (Palmer & Tsien, 2006; Rudolf et al., 2003). Disadvantages include an inability to localise these indicators to specific living cells or tissues, leakage of the dye from cells with time and Ca^{2+} buffering, due to the innate property of the dye as a chelator. Genetically encoded Ca^{2+} indicators (GECIs) offer solutions to some of these problems and provide powerful means with which to study Ca^{2+} dynamics in defined regions (from biochemically defined sub-cellular locations to tissue specific expression in whole organisms) and over prolonged time-courses (Miyawaki et al., 1997; Romoser, Hinkle, & Persechini, 1997).

GECIs can be broadly divided into two classes, dependent on whether they are based upon: (i) a *single* fluorescent protein (e.g. G-CaMPs, camgaroos or pericams), where Ca^{2+} responsive elements, such as calmodulin, are inserted to regulate the protonation state of the chromophore; or, (ii) *double* fluorescent proteins (e.g. cameleons or TN-XL) where Ca^{2+} responsive elements, such as calmodulin or troponin alter the efficiency of fluorescence resonance energy transfer (FRET) between the two fluorescent proteins (Baird, Zacharias, & Tsien, 1999; Mank et al., 2006; Miyawaki et al., 1997; Nagai, Sawano, Eun Sun, & Miyawaki, 2001; Nakai, Ohkura, & Imoto, 2001; Palmer & Tsien, 2006). FRET is a process in which energy is transferred non-radiatively from an excited 'donor' fluorophore, to another 'acceptor' chromophore. Since FRET efficiency is dependent on the inverse-sixth-power of the distance between the donor and acceptor, and this distance is dependent on the molecular conformation of the FRET construct, FRET efficiency can be used to signal changes in conformation of a molecule (Förster, 1965; Ha et al., 1996). In FRET GECIs, the binding of Ca^{2+} to a Ca^{2+} sensitive component (e.g calmodulin), induces a conformational change and hence a change in FRET: FRET efficiency is therefore directly related to Ca^{2+} concentration (Figure 4.10) (Miyawaki et al., 1997).

GECIs have been used extensively in neuroscience research in species ranging from *C. elegans* to mice: they have permitted novel *in-vivo* quantitative assessment of Ca^{2+} transients (Hasan et al., 2004; Kerr et al., 2000). In *Drosophila*, a range of GECIs has been targeted to neurons in adults and larvae, using the *GAL4-UAS* system and successfully used for *in-vivo* assessment (Brand & Perrimon, 1993; Fiala et al., 2002; L. Liu, Yermolaieva, Johnson, Abboud, & Welsh, 2003; Reiff et al., 2005; Reiff, Thiel, & Schuster, 2002; J. W. Wang, Wong, Flores, Vosshall, & Axel, 2003). Cameleon 2.1, an improved, FRET based GECI, has the benefits of being a ratiometric indicator. It has been successfully exploited in *Drosophila* adults and larvae and is available commercially, under *UAS* control (Figure 4.10) (Diegelmann, Fiala, Leibold, Spall, & Buchner, 2002; Fiala et al., 2002; L. Liu et al., 2003; Miyawaki, Griesbeck, Heim, & Tsien, 1999). Although the cAMP FRET-based reporter, GFP-PKA, has been imaged in *Drosophila* embryos, FRET efficiency was not demonstrated, nor measured: I am unable to find any reports of FRET measurement in *Drosophila* embryos, nor reports of cameleon 2.1 expression at this stage (Lissandron et al., 2007).

In view of the exciting potential of GECIs in the *in-vivo* study of SERCA, I aimed to test: (i) the feasibility of expressing cameleon 2.1 in embryonic trachea and, (ii) whether or not FRET occurred in the trachea. Having done this, I proceeded to investigate the dynamic range of the construct in conditions of extreme Ca^{2+} concentration, in order to explore its potential usefulness in our investigations.

This text box is where the unabridged thesis included the following third party copyrighted material:

Diegelmann S et al. (2002). Transgenic flies expressing the fluorescence calcium sensor Cameleon 2.1 under UAS control. Genesis, 34(1-2), 95-98.

Figure 4.10 Schematic illustration of the cameleon 2.1 FRET construct

Illustration taken from Diegelmann *et al*, 2002. Cameleon 2.1 consists of ECFP and EYFP molecules fused to calmodulin and the calmodulin target peptide M13. When Ca^{2+} ions bind, there is a conformational change in the protein: this can be detected by a change in emission ratio of 535/485 nm upon ECFP excitation at 440 nm, due to FRET from ECFP to EYFP.

4.4.1 The cameleon 2.1 FRET construct can be expressed and imaged in the Drosophila embryonic trachea

Flies carrying *UAS-Cameleon2.1* were crossed to those carrying *btl-GAL4* in order to express cameleon in *breathless*-expressing tracheal cells. Embryos were prepared for live imaging as previously described (Mavrakis et al., 2008). Spectral scanning confocal microscopy was used to demonstrate the expression of cameleon 2.1 in tracheal cells (Figure 4.11). When a region of interest (ROI) was defined within the tracheal system, two emission peaks were evident at wavelengths of around 485 nm and 530 nm, approximately equal to the wavelengths of maximal emission of the two fluorescent proteins in cameleon 2.1 (CFP and YFP) (Miyawaki et al., 1999). These findings demonstrate that cameleon can be successfully expressed and imaged in the embryonic trachea and suggest FRET occurrence between the two fluorophores. Further evidence is required in order to confirm 'true' FRET taking place.

4.4.2 FRET occurrence in the cameleon expressing trachea is confirmed by acceptor photobleaching

Reliable analysis of FRET is complicated by factors such as: (i) bleed-through in excitation, when a donor is excited by the acceptor's excitation wavelength and *vice versa*; and (ii) cross talk in emission detection, when the emission of a donor also contributes to the signal measured in acceptor detection, and *vice versa* (Berney & Danuser, 2003; Gordon, Berry, Liang, Levine, & Herman, 1998). Acceptor photobleaching helps to eliminate some of the difficulties in FRET analysis and therefore offers benefits over the simple approach of measuring acceptor emission upon donor excitation: its principle is that energy transfer is eliminated upon bleaching of the acceptor, with a consequent increase in donor fluorescence (so called donor recovery).

Acceptor photobleaching of YFP was carried out in an ROI of the trachea expressing cameleon 2.1, using spectral scanning confocal microscopy and a single laser (Karpova et al., 2003). Changes in emission at 488 and 537 nm (captured using specific detectors) were seen in the bleach ROI, with pixel intensity markedly reducing at 537 nm but appearing to increase slightly at 488 nm (Figure 4.12). Mean emission intensities were extracted from the spectra for two wavelength ranges (473-493 nm and 522-541 nm, corresponding to CFP and

YFP respectively), at the bleached ROI and in a second, internal control (unbleached) ROI. In the bleached ROI, the intensity of YFP emission dramatically dropped upon bleaching and there was an accompanying, small increase in CFP emission, rising from a mean intensity of 147.9, before the bleach, to 164.1 after it (Figure 4.12). The FRET energy transfer efficiency, expressed as a percentage, can be calculated at 9.9% using the equation (efficiency = change in CFP intensity x 100/CFP intensity after bleach) published by Karpova *et al:* this value is in-keeping with published results (Karpova et al., 2003). This FRET efficiency is a quantification of the amount of FRET taking place, however, caution must be exercised in interpreting the significance of any absolute quantification here. It has been recognised that in experiments such as this, the use of negative controls is critical, since 'pseudo' or 'false' FRET has been clearly demonstrated to occur in both non-bleached regions and in bleached regions of non-FRET constructs (Karpova et al., 2003). In the control (unbleached) ROI, YFP emission stayed static during the bleaching process, as expected, but interestingly, CFP emission did appear to increase slightly (Figure 4.12). Mean CFP intensity for the control ROI rose from 125.7 to 132.2 during the time course of the bleaching process. This demonstrates occurrence of a largely unexplained phenomenon, so-called 'pseudo FRET,' in the control ROI, with a calculated efficiency of 4.9%. The FRET efficiency in the bleached ROI was significantly greater than in the control ROI (9.9 vs. 4.9%) and therefore, using published guidance, it is reasonable to conclude that true FRET is occurring in the cameleon expressing tracheal cells (Karpova et al., 2003). These data highlight the significant difficulties in accurately quantifying 'true' FRET.

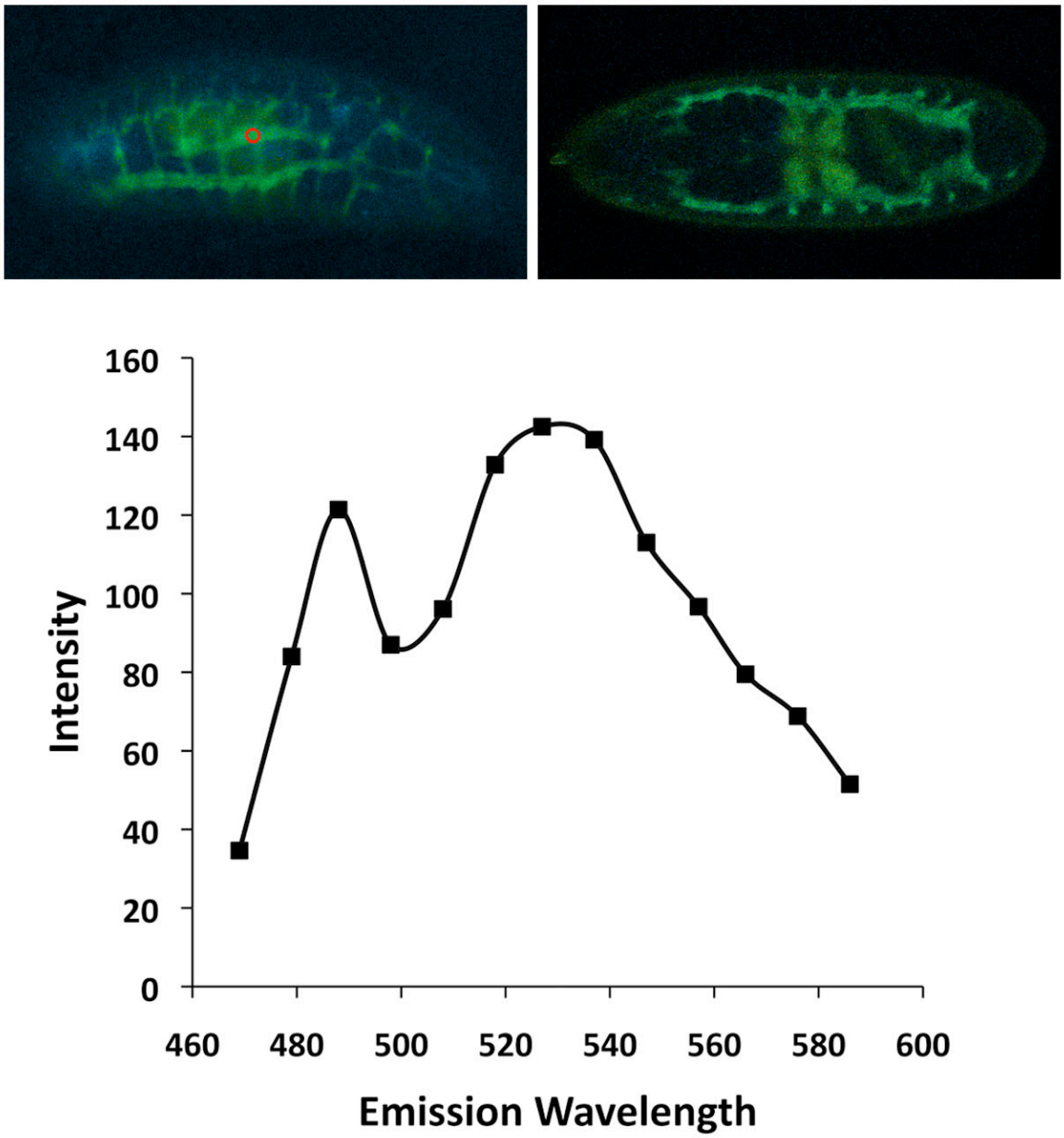

Figure 4.11 The cameleon 2.1 FRET construct can be expressed and imaged in the *Drosophila* embryonic tracheal system

Top panels: confocal micrographs of stage 15/16 embryos (lateral and dorsal views) expressing Cameleon2.1 under the control of *btl-GAL4*. Microscopy used spectral scanning and images are pseudo-coloured by lambda coding using Zen 2010 software (Zeiss).

Lower panel: Emission spectrum for the region of interest (ROI) illustrated in red on the top left panel. Mean intensity for the ROI vs. emission wavelength (nm). 2 peaks of emission are seen, corresponding to those wavelengths of CFP at 488 nm at its peak and YFP at 530 nm.

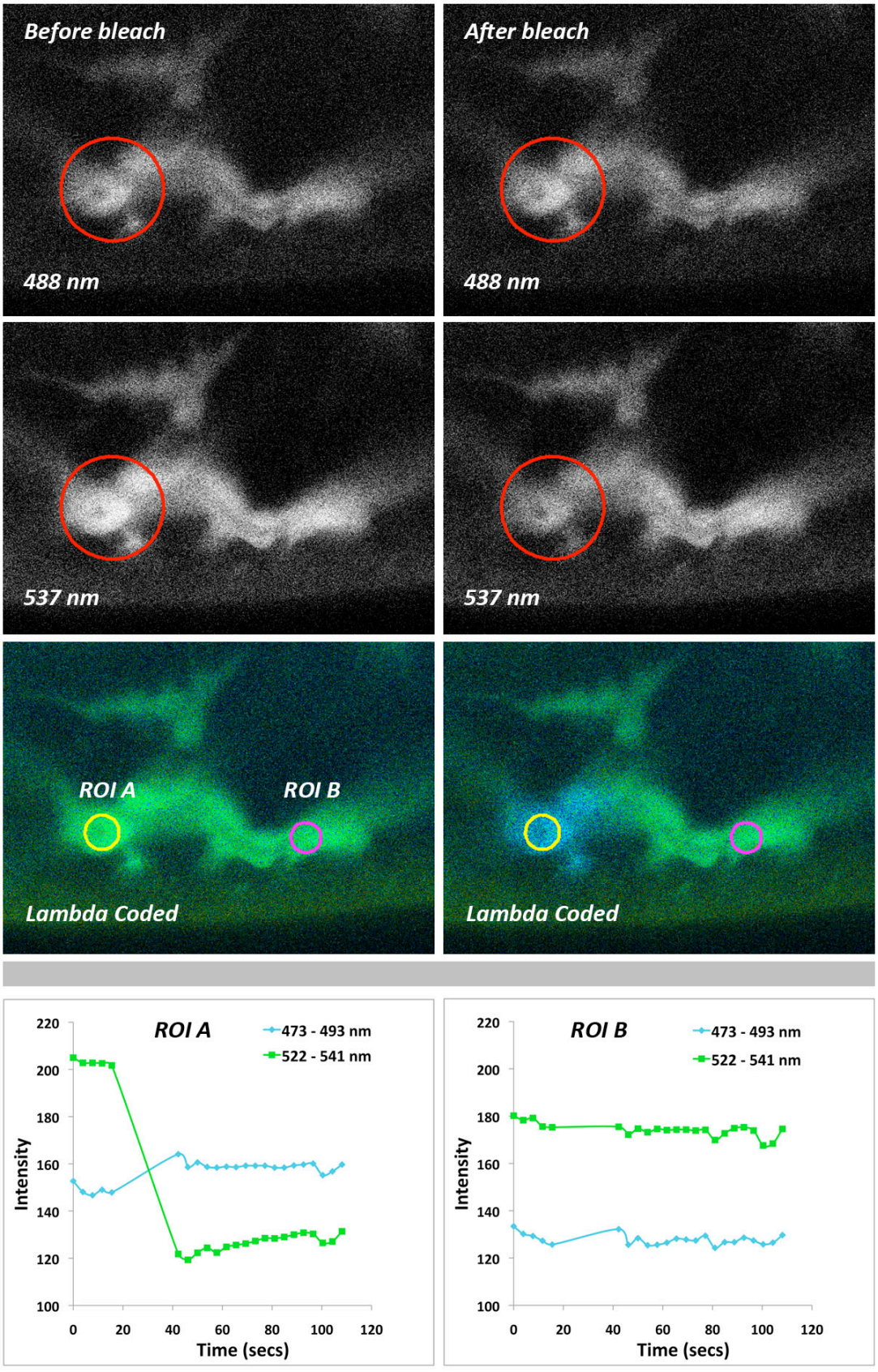

Figure 4.12 FRET occurrence in tracheal cameleon is confirmed by acceptor photobleaching

Confocal spectral scanning micrographs of stage 15/16 *Drosophila* embryo. Top 4 panels show emissions at 488 nm and 537 nm (closest detectors to maximal CFP / YFP emission) before and after acceptor photobleaching (red outline demonstrates bleach region). Lambda coded images demonstrate a region of interest (ROI) within the bleach region (A, yellow) and internal control ROI (B, magenta) The mean emission intensity from these ROIs, between the ranges of 473-493 nm (CFP) and 522-541 nm (YFP) over time, are shown in the graphs in the lower panels.

4.4.3 Cameleon 2.1 in embryonic Drosophila cells responds to changes in calcium concentration, but dynamic range is narrow

To determine how FRET from cameleon 2.1 is affected by changes in Ca^{2+} concentration in *Drosophila* embryos, cells expressing this construct were exposed to very high and low Ca^{2+} concentrations. The vitelline membrane precludes *in-vivo* 'calibration' since it impedes passage of Ca^{2+} and EGTA into intact *Drosophila* embryos. Therefore, embryonic cells were instead dissociated in culture conditions, from embryos expressing cameleon 2.1 ubiquitously under the *da-GAL4* driver. These cells underwent spectral scanning confocal microscopy with 10 mM $CaCl_2$ and 10 µM ionomycin, or 5 mM EGTA and 10 µM ionomycin, in order to submit them to high and low extremes of Ca^{2+} concentration respectively (Palmer & Tsien, 2006).

Changes in Ca^{2+} concentration resulted in a change in the cameleon emission spectrum in embryonic cells (Figure 4.13). As concentrations of Ca^{2+} increased, the maximum intensity of the lower wavelength peak (around 480 nm) decreased and the intensity of the higher wavelength peak (around 535 nm) increased. Although the analysis of FRET using simple quantification of acceptor emission, upon donor excitation, may be susceptible to multiple confounding factors (discussed earlier), this method was used as a simple way to *approximate* changes in FRET with changes in Ca^{2+} concentration. The mean intensities were extracted for two wavelength ranges, corresponding to CFP and YFP, as above. Acceptor (YFP) emission was expressed as a ratio of donor (CFP) emission, as published elsewhere for cameleon 2.1 (Miyawaki et al., 1999). At rest, in physiological S2 Ringer's solution, the mean YFP/CFP ratio (+/- SEM) was 1.53 (+/- 0.04) and rose to 2.21 (+/- 0.09) with addition of $CaCl_2$ and ionomycin. In Ca^{2+} free Ringer's, the ratio was 1.43 (+/- 0.01) and fell to 1.38 (+/- 0.02) with addition of EGTA and ionomycin. The change in ratio from low to high Ca^{2+} concentration was 0.83, a fold change of 1.6. It is acknowledged that these data only *approximate* changes in FRET with changing Ca^{2+} concentration and are susceptible to the influence of factors such as bleed through, cross talk and pseudo/false FRET, discussed and demonstrated earlier. Indeed, they are likely to overestimate true FRET rather than underestimate it (Karpova et al., 2003). However, it appears FRET in cameleon 2.1 changes in response to altered Ca^{2+}

concentration in *Drosophila* embryonic cells and, though not precisely quantified, it does so within a narrow range consistent with other cell types.

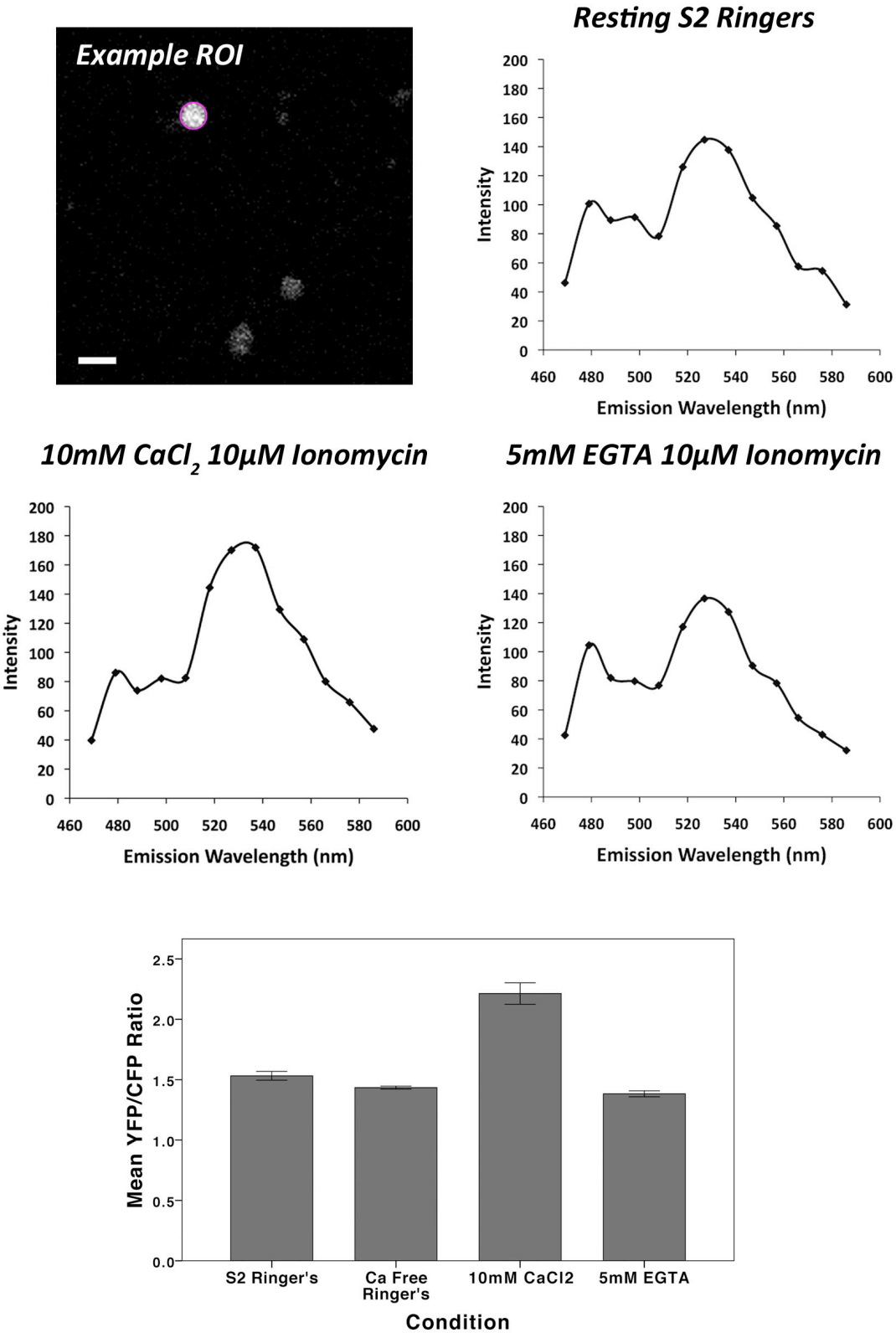

Figure 4.13 Cameleon 2.1 FRET in *Drosophila* embryonic cells responds to changes in Ca^{2+} concentration, but dynamic range is narrow

Upper panels: spectral scanning confocal microscopy of dissociated embryonic cells expressing Cameleon 2.1 under the control of *da-GAL4*. An example ROI of a single cell is shown in magenta and the emission spectra are shown for similar cells in differing culture conditions (S2 Ringer's, 10mM $CaCl_2$ and 5mM EGTA), in order to achieve the resting, maximum and minimum YFP/CFP ratio respectively. Lower panel: Mean YFP/CFP emission ratio (+/- SEM) for each culture condition. n=>6 cells for each condition. Difference between highest (10mM $CaCl_2$) and lowest (5mM EGTA) Ca^{2+}concentrations is significant, p=0.007.

4.5 Concluding remarks

(i) Commercially available *da-GAL4* and *btl-GAL4* lines can be used to express transgenes in the embryo ubiquitously, or in tracheal cells specifically: however *bnl-GAL4* driven expression was inconsistent with known *branchless* mRNA expression patterns.

(ii) Live imaging protocols permit high resolution imaging of embryonic morphogenesis albeit at altered rates of development.

(iii) Fluorescent proteins can be targeted to dual label tracheal cells and offer dynamic imaging capabilities throughout development (from early embryonic to later larval stage). Antibody staining of the trachea in fixed embryos provides superior spatial resolution at later stages. Consequently, in these investigations, antibody staining was the method of choice for demonstrating embryonic tracheal structure; fluorescent proteins were chosen to demonstrate larval trachea and the dorsal air sac primordium.

(iv) The cameleon 2.1 FRET construct can be expressed in embryonic trachea and FRET can be demonstrated. The narrow dynamic range of the cameleon 2.1 response limits its usefulness for quantitative studies, which are further complicated by issues such as pseudo/false FRET. Given these limitations, tracheal expression of cameleon 2.1 was not used further. New generations of GECIs are likely to reduce the impact of such limitations, through the offer of greatly improved dynamic range, faster kinetics and higher signal to noise ratio: improvements have led to one author labelling cameleon 2.1 as 'obsolete,' despite its continued use (Mank et al., 2006; Palmer et al., 2006; Palmer & Tsien, 2006). Cloning of these improved GECIs into vectors such as pUAST will permit similar targeted expression *in-vivo* and may offer future opportunities for studying Ca^{2+} transients in *Drosophila* trachea.

Chapter 5

RNAI MEDIATED *SERCA* KNOCKDOWN IN *DROSOPHILA* EMBRYONIC TRACHEA

5.1 Introduction

First characterised in *Caenorhabditis elegans,* RNA interference (RNAi) is a sequence-specific gene silencing pathway that occurs naturally in organisms ranging from plants to mammals (Elbashir et al., 2001; Fire et al., 1998; van der Krol, Mur, Beld, Mol, & Stuitje, 1990). RNAi is triggered by double-stranded RNA (dsRNA) helices that have been introduced exogenously into cells as small interfering RNAs (siRNAs), or produced endogenously from small, non-coding RNAs known as microRNAs (miRNAs) (R. C. Lee, Feinbaum, & Ambros, 1993). The RNAi pathway is thought to play a diverse range of roles and has been implicated in immunity, development, cell proliferation, haematopoiesis and apoptosis (Olivier, 2001; Rana, 2007). There are at least three levels at which RNAi is mediated: (i) post-transcriptional gene silencing, the best understood pathway, whereby mRNA is degraded in response to siRNA complex binding; (ii) suppression of mRNA translation and protein synthesis; and (iii) pre-transcriptionally, through mechanisms such as chromatin modification (de Carvalho et al., 1992; Fire et al., 1998; Pal-Bhadra, Bhadra, & Birchler, 1997; Tabara et al., 1999; Wightman, Ha, & Ruvkun, 1993; Zeng, Yi, & Cullen, 2003).

5.1.1 The siRNA post-transcriptional gene silencing mechanism

Long dsRNA molecules initiate RNAi when they are cleaved into short, 21-23-nucleotide siRNAs by the RNAse III-type enzyme, Dicer (Figure 5.1) (Bernstein, Caudy, Hammond, & Hannon, 2001; Ketting et al., 2001; Zamore, Tuschl, Sharp, & Bartel, 2000). siRNAs specific to the mRNA targeted for silencing are incorporated into an RNA-induced silencing complex (RISC), along with proteins such as Argonaute-2, the mRNA cleavage enzyme in RISC (J. D. Liu et al., 2004; Meister et al., 2004; Miyoshi, Tsukumo, Nagami, Siomi, & Siomi, 2005). This RISC nuclease complex is the effector unit of RNAi: it finds its target mRNA and uses the antisense nucleotide sequence of the siRNA to guide cleavage of the target (Hamilton & Baulcombe, 1999; Hammond, Bernstein, Beach, & Hannon, 2000; Zamore et al., 2000). The remarkable specificity of RNAi gene silencing is governed by complementarity between the guide strand of the siRNA and the target mRNA: since its discovery in the 1990s, the apparent specificity of RNAi has prompted a range of applications.

This text box is where the unabridged thesis included the following third party copyrighted material:

http://integratedhealthcare.eu/1/en/rna_interference/1498/

Figure 5.1 siRNA post-transcriptional gene silencing

Schematic diagram of the RNA interference (RNAi) mechanism.
Image adapted from http://integratedhealthcare.eu/1/en/rna_interference/1498/

5.1.2 RNAi has found wide technological application

The study of gene function in cell culture and model organisms has been enhanced by RNAi-mediated gene knockdown (Harborth, Elbashir, Bechert, Tuschl, & Weber, 2001; Kennerdell & Carthew, 1998). Generation of RNAi libraries permits genome-wide loss-of-function screens for genes associated with particular phenotypes (Fraser et al., 2000; Paddison et al., 2004; Varsha Wesley et al., 2001). *In-planta* expression of dsRNA has allowed generation of transgenic pest-resistant plants; in opium poppies, morphine can be replaced with a non-narcotic alkaloid, reticuline (Allen et al., 2004; Baum et al., 2007). Finally, clinical use of RNAi is being intensively investigated: the first trials of siRNA have shown promise in areas such as macular degeneration and respiratory syncytial virus immunity (DeVincenzo et al., 2008; DeVincenzo et al., 2010; Singerman, 2009)

5.1.3 RNAi in Drosophila Research

There are now a number of commercially available RNAi libraries, covering much of the *Drosophila* genome (Dietzl et al., 2007; Ni et al., 2008; NIG-Fly; TRiP). For *in vivo* study, RNAi constructs are commonly cloned to vectors such as pUAST and expressed using the *GAL4-UAS* system (Brand & Perrimon, 1993; Dietzl et al., 2007; Ni et al., 2008). This provides powerful tools to induce and control gene knockdown: in addition to spatial restriction with *GAL4* drivers, RNAi expression can be restricted temporally by repressing the transcriptional activity of *GAL4* with the temperature sensitive *GAL80* transgene, the so called TARGET (temporal and regional gene expression targeting) system (S. E. McGuire, Le, Osborn, Matsumoto, & Davis, 2003; S. E. McGuire, Mao, & Davis, 2004). RNAi can also be used to create loss of function mosaics or 'flip-out' clones. Heat-shock induced FLP-recombinase removes a transcriptional-termination cassette that is inserted between a defined promoter and *GAL4,* or between the *UAS* sequence and RNAi construct (Duffy, Harrison, & Perrimon, 1998; Struhl & Basler, 1993).

Calcium dynamics in *Drosophila* have also been investigated with RNAi targeting of components of calcium signalling pathways *in-vitro* and *in-vivo* (Roos et al., 2005; Worrell & Levine, 2008). Given the apparent specificity and efficacy of RNAi gene silencing, this technique was chosen to determine SERCA's role in *Drosophila* tracheal morphogenesis.

5.2 Aims

To determine the effect of spatially restricted *SERCA* inhibition on embryonic tracheal branching morphogenesis, the aforementioned RNAi and *GAL4-UAS* techniques were used to:

(i) Characterise the effects of expressing *SERCA* RNAi constructs in the tracheal system on embryonic branching morphogenesis;

(ii) Increase the efficacy of RNAi mediated *SERCA* knockdown, through co-expression of *Dicer2* or additional RNAi constructs;

(iii) Quantify the effect of RNAi on, *SERCA* mRNA levels, SERCA protein levels and SERCA function in embryonic cells.

5.3 RNAi mediated SERCA knockdown in the embryonic tracheal system

5.3.1 Selection of RNAi constructs

Commercially available RNAi libraries were searched for *Drosophila* lines carrying constructs targeted to the *Drosophila SERCA* gene, *calcium ATPase at 60A (Ca-P60A)*. The Vienna *Drosophila* RNAi Centre (VDRC) had two available lines, with transformant ID numbers, 4474 and 107446 (construct GD436 and KK107371 respectively) (Dietzl et al., 2007). For ease of reference, these lines will be referred to simply as RNAi 4474 or 107446 in future. The DNA sequences of these constructs were used to ascertain the start and end point of alignment with *Ca-P60A* transcripts (Figure 5.2). The alignments of both constructs corresponded to the fourth coding exon, which is common to all *Ca-P60A* transcripts. Their alignments overlapped for a region of 12 nucleotides.

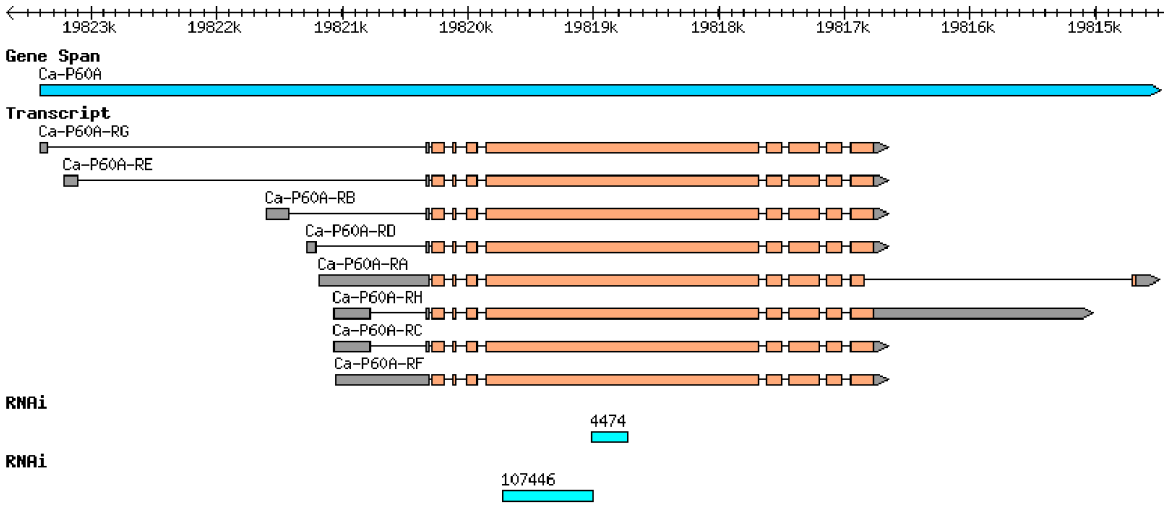

Figure 5.2 Gene map demonstrating the alignment of selected RNAi constructs with *Ca-P60A* transcripts

Created using the Flybase database and GBrowse genome viewer (available at http://flybase.org/cgi-bin/gbrowse/dmel/). Alignment of nucleic acids performed with BLAST software (National Center for Biotechnology, available at http://blast.ncbi.nlm.nih.gov/Blast.cgi)

5.3.2 Potential off-target effects of SERCA RNAi

The most serious limitation of RNAi technology is 'off-target' silencing of unrelated genes with (A. L. Jackson et al., 2003; A. L. Jackson & Linsley, 2004). Off-target silencing effects are caused by siRNA (introduced directly into cells, or produced *in vivo* from long dsRNA) that has sequence similarities with unrelated genes. Therefore the design of RNAi constructs, and interpretation of their phenotypic effects, need to be approached with care.

To check chosen *SERCA* RNAi constructs for vulnerability to off-target effects, we input their cDNA sequences into dsCheck software to predict potentially susceptible non-target genes (dsCheck, at http://dscheck.rnai.jp/) (Naito et al., 2005). This prediction is given by means of the number of hits for a complete match (sequence alignment) of 19 nucleotide length siRNAs and the target gene mRNA, a mismatch of one nucleotide and a mismatch of two nucleotides. RNAi 4474 had 267 hits with a complete match for each *SERCA* transcript: there were no hits for other genes with a complete match. With one mismatch, the highest number of hits for any gene was only three, and with two mismatches, only seven (complete data output in Appendix 2). These data indicate that RNAI 4474 is likely to be highly specific at targeting *SERCA* mRNA. RNAi 107446 had 700 hits for each *SERCA* transcript and two hits for transcripts of *Secretory Pathway Calcium atpase (SPoCk),* with a complete match (complete data output in Appendix 2). These data indicate that RNAi 107446 may affect another Ca^{2+} ATPase pump, although the vastly reduced number of hits (2 vs. 700) for this off-target gene implies the effect may be small, relative to that on *SERCA* mRNA knockdown. In view of these findings, RNAi 4474 was selected for use in all experiments when a single RNAi construct was utilised: RNAi 107446 was only used when dual RNAi expression was required.

5.3.3 Expression of SERCA RNAi 4474 in tracheal cells does not disrupt branching morphogenesis in the embryo

To determine the effect of *SERCA* knockdown on tracheal morphogenesis, RNAi 4474 was expressed in tracheal cells using the *btl-GAL4* driver and compared to a control (w^{1118} crossed to *btl-GAL4*). Embryos were collected over short time intervals and aged to stage 16, when they were fixed and stained with an antibody to the tracheal lumenal protein, 2A12 (DSHB) (Manning & Krasnow,

1993). Confocal microscopy was used to image the tracheal system, using z-stacks with 3D reconstructions for analysis. Stage 16 was chosen for phenotypic assessment, as the vast majority of branching is complete in wild type embyros of this stage, the stage is readily identifiable from gut morphology and it precedes the stage when embryo immunostaining becomes difficult (Manning & Krasnow, 1993).

RNAi 4474 expressed in the trachea did not affect tracheal branching morphogenesis (Figure 5.3). In both *btl>RNAi* and control embryos, the major braches of the tracheal system develop at each appropriate metamere, including the dorsal and lateral trunks, the transverse connectives, the dorsal, visceral, spiracular and ganglionic branches, the dorsal anastomoses, as well as smaller, more variable branches such as the lateral group (Manning & Krasnow, 1993). The specialised branches of the first and tenth metamere are also evident in both groups. Thus RNAi 4474 expression in tracheal cells does not grossly alter embryonic tracheal morphogenesis.

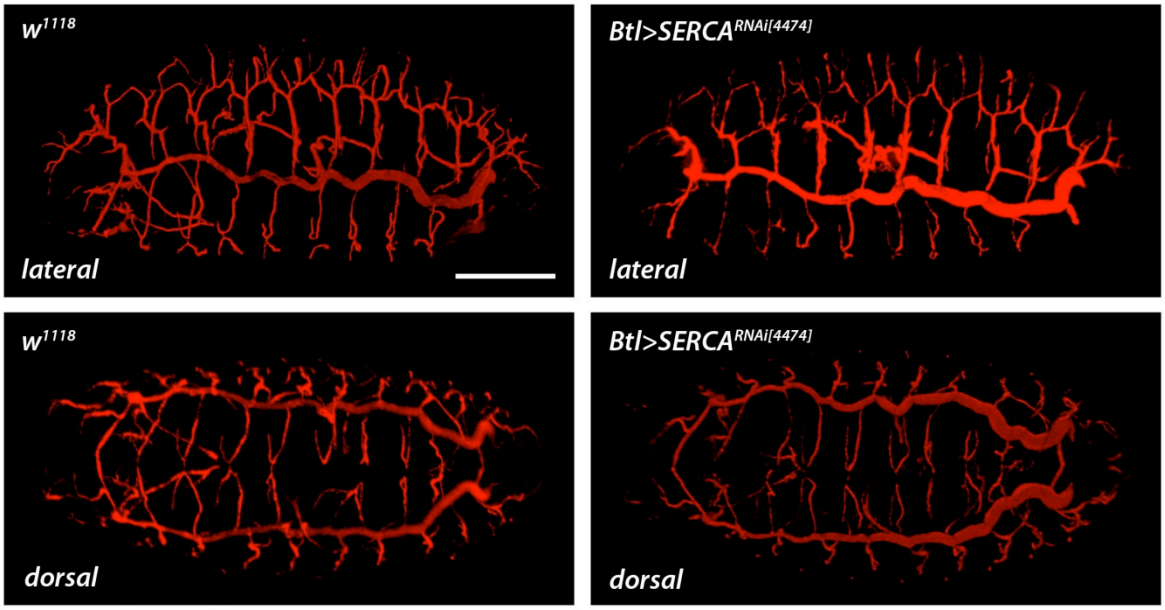

Figure 5.3 Targeted expression of SERCA RNAi 4474 in tracheal cells does not disrupt branching morphogenesis in the embryo

Confocal micrographs (3D projections of z-stacks) of representative stage 16 *Drosophila* embryos expressing the SERCA RNAi construct, VDRC 4474 in tracheal cells (btl>RNAi) vs. control (w1118). The tracheal system is stained with 2A12 antibody (DSHB, Iowa). Upper panels show the lateral aspect of the embryo and lower panels the dorsal aspect (anterior to the left). Scale bar indicates 100 µm.

5.3.4 Recombining SERCA RNAi 4474 with Dicer2 or RNAi 107446, induces lethality at an earlier stage

To try to enhance the RNAi mediated *SERCA* knockdown, RNAi 4474 was recombined with ectopic *Dicer2* or RNAi 107446: co-expression of *Dicer2* has been shown to enhance RNAi potency (Dietzl et al., 2007). Meiotic recombination events that occur in females were exploited to combine the heterozygously carried transgenes (present on homologous second chromosomes), on to one chromosome (Figures 5.4 and 5.5). Potential, individual male recombinants were selected for increased intensity of eye colour, given that flies carrying the individual transgenes and white mutation had a moderate eye colour. Stocks of potential recombinants were made, by crossing them to a second chromosome balancer (Figure 5.4 and 5.5). Interestingly, recombined lines (RNAi 4474 and *Dicer2* or RNAi 107446) were recessively lethal, whereas RNAi 4474 is viable when homozygous: this finding is most likely to be a consequence of insertional inactivation. In order to test *GAL4* mediated effects, the recombined stocks were crossed to *btl-GAL4* and *da-GAL4* drivers and the stage of lethality assessed.

When RNAi 4474 lines recombined with either *Dicer2* or RNAi 107746, were crossed to *da-GAL4,* and hence expressed ubiquitously, the progeny died in the embryonic or early L1 stage (Table 5.1). This is compared to RNAi 4474 or 107446 lines alone, which when crossed to *da-GAL4*, produced progeny that survived until the L2 larval stage. When RNAi 4474 lines recombined with either *dicer2* or RNAi 107746, were crossed to *btl-GAL4,* and hence expressed in tracheal cells, the progeny died at the L1/L2 larval stage. This is compared to RNAi 4474 or 107446 lines alone, which produced viable adult progeny when crossed to *btl-GAL4*. Together, these data demonstrate that recombination of RNAi 4474 with either *dicer2* or RNAi 107446 induces a more potent phenotype and may indicate increased knockdown of *SERCA* compared to individual RNAi constructs used alone. Further evidence of increased *SERCA* knockdown from this recombination is detailed later, when the effects on *SERCA* mRNA expression are reported.

In addition, the lethality seen when more potent RNAi is driven by *btl-GAL4* is significant: lethality is induced by highly specific *SERCA* loss of function in

tracheal cells, thus indicating that the effects of this loss of function on these cells are such to preclude continued survival of the larvae. Whether this phenotype is mediated by a disruption in either tracheal structure or function, or is induced by an extra-tracheal effect, remains to be seen and will be investigated later.

Table 5.1 Recombining SERCA RNAi 4474 with *Dicer2* or RNAi 107446, induces lethality at an earlier stage

Stages of lethality when 2 commercial RNAi lines (VDRC 4474 and 107446) and 2 recombined lines (4474 with *dicer2* and 4474 with 107446) are crossed to *btl-GAL4* and *da-GAL4 drivers*.

	btl-GAL4	***da-GAL4***
RNAi 4474	Viable Adults	L2 Larvae
RNAi 107446	Viable Adults	L2 Larvae
RNAi 4474, *dicer2*	L2 Larvae	Embryo / L1
RNAi 4474, 107446	L1/2 Larvae	Embryo

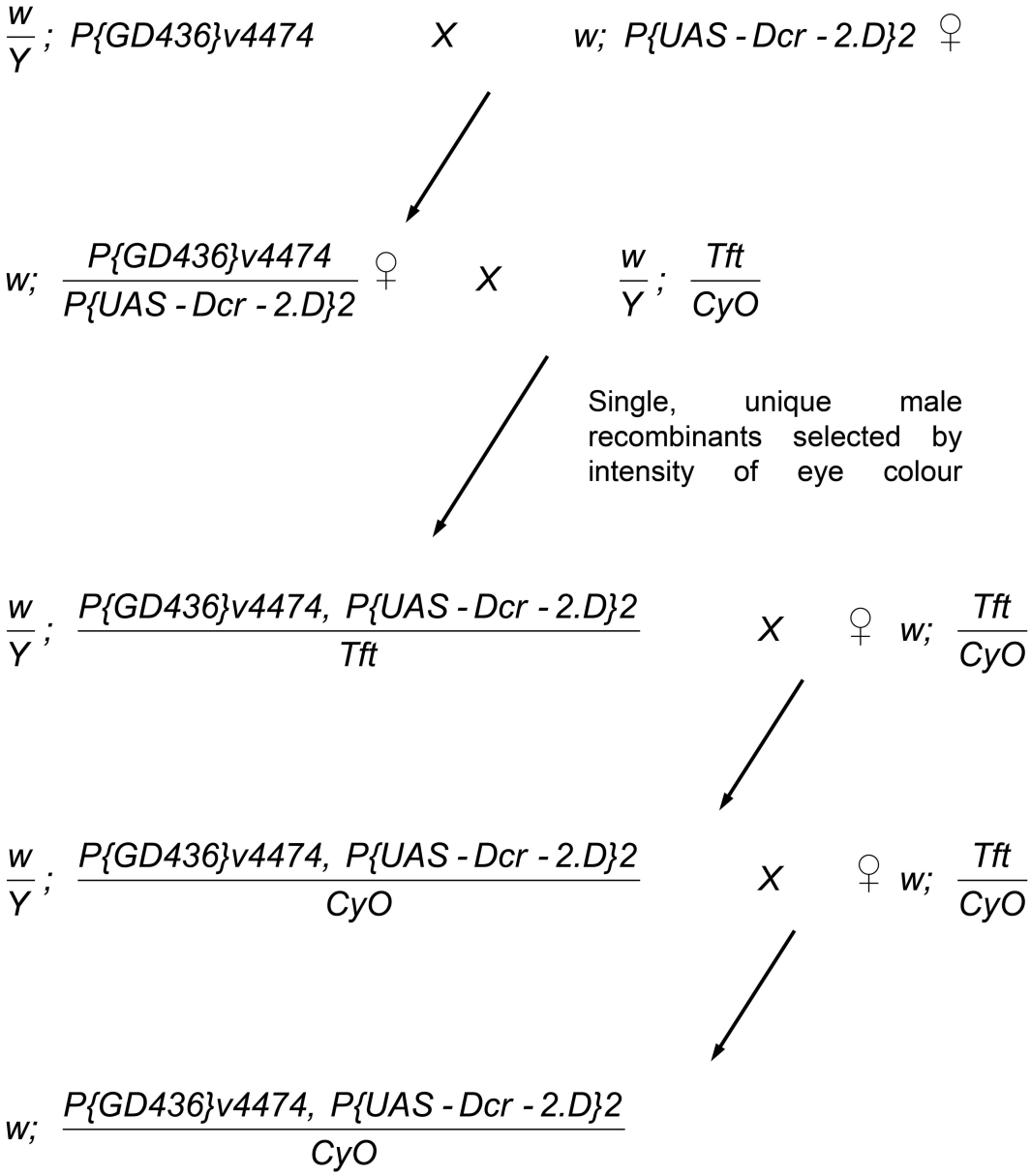

Figure 5.4 Genetic crossing scheme demonstrating the recombination of VDRC RNAi line 4474 with *Dicer2*

Meiotic recombination in females was made use of to combine the heterozygously carried transgenes (present on homologous second chromosomes), onto one chromosome. Potential, individual male recombinants were selected based on increased intensity of eye colour, since the transgenes had originally been inserted in a white-eyed background. Stable stocks were then made, by crossing these male recombinants to a second chromosome balancer.

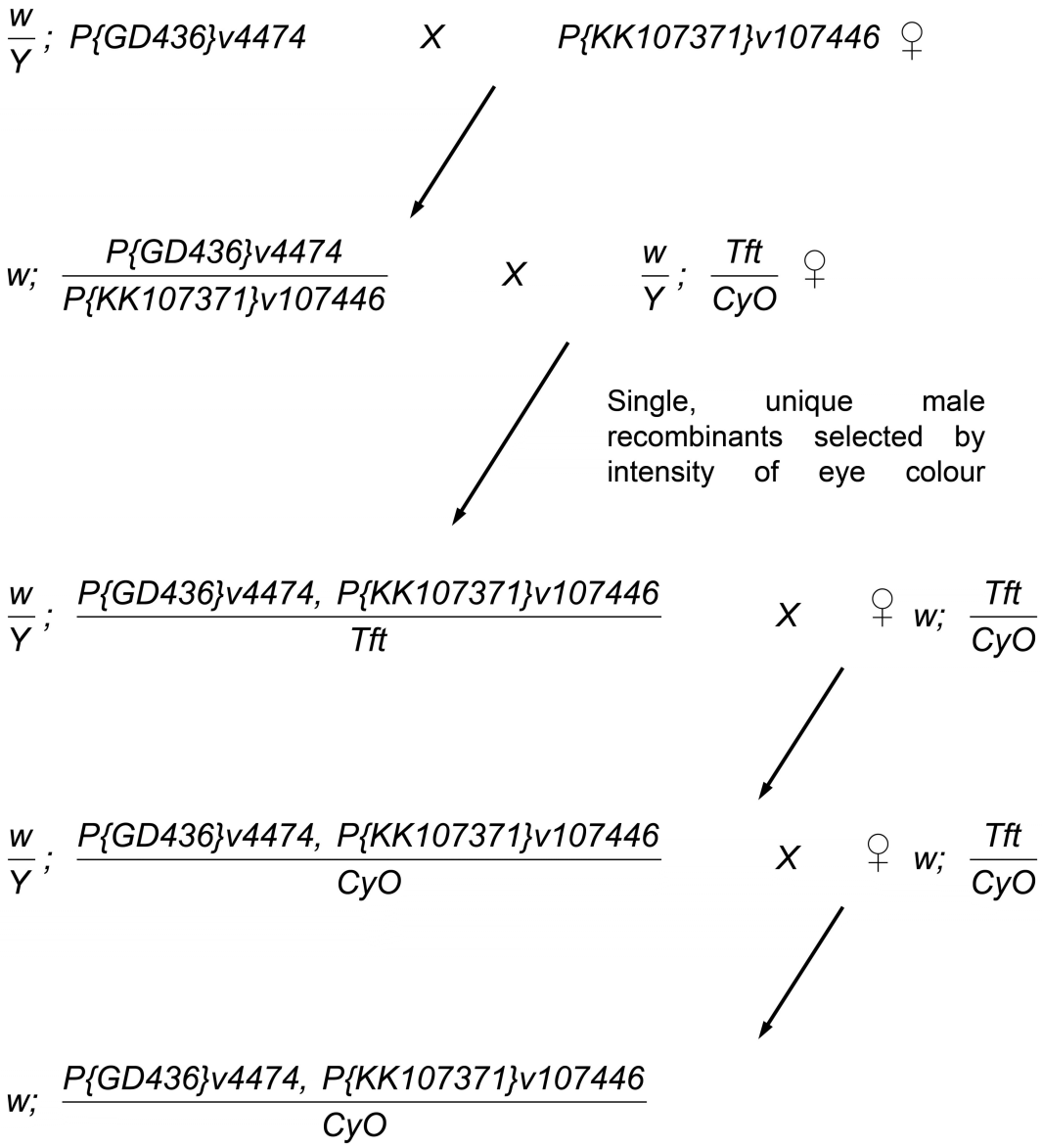

Figure 5.5 Genetic crossing scheme demonstrating the recombination of VDRC RNAi line 4474 with RNAi line 107446

Meiotic recombination in females was made use of to combine the heterozygously carried transgenes (present on homologous second chromosomes), onto one chromosome. Potential, individual male recombinants were selected based on increased intensity of eye colour, since the transgenes had originally been inserted in a white-eyed background. Stable stocks were then made, by crossing these male recombinants to a second chromosome balancer.

5.3.5 SERCA RNAi 4474 recombined with Dicer2 or RNAi 107446 and expressed in tracheal cells, does not disrupt branching morphogenesis in the embryo

RNAi 4474 recombined with *Dicer2* or RNAi 107446 and expressed in tracheal cells with *btl-GAL4,* did not affect gross tracheal morphogenesis (Figure 5.6). In both *btl>RNAi* and control embryos, the major branches of the tracheal system develop at each appropriate metamere, as discussed above (Manning & Krasnow, 1993). The specialised branches of the first and tenth metamere are also evident in both groups. Since our assessment of structure used an antibody to a luminal protein, the presence of a lumen containing 2A12 may be inferred.

The normal gross tracheal structure offers little to explain the intriguing larval lethality observed. The increased potency RNAi may prejudice larval airway structure and/or function and hence survival without affecting embryonic tracheal anatomy; alternatively, the impact on survival may be mediated via an airway independent mechanism. I explore this later in the thesis in Chapter 7.

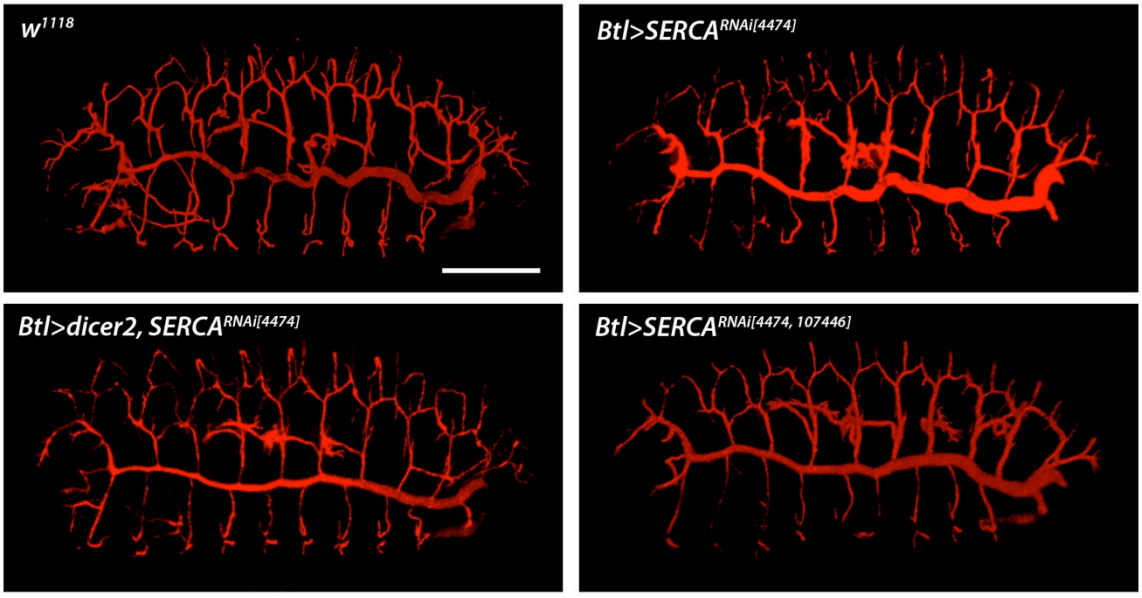

Figure 5.6 SERCA RNAi 4474 recombined with Dicer2 or RNAi 107446, expressed in tracheal cells, does not disrupt branching morphogenesis in the embryo

Confocal micrographs (3D projections of z-stacks) of representative stage 16 *Drosophila* embryos expressing the SERCA RNAi construct, VDRC 4474 with either *Dicer2* or RNAi 107446, in tracheal cells (btl>RNAi) vs. control (w1118). The tracheal system is stained with 2A12 antibody (DSHB, Iowa). The lateral aspect of the embryo is shown in each case (anterior to the left). Scale bar indicates 100 μm.

5.4 Effects of RNAi on SERCA mRNA, protein and function

5.4.1 RNAi mediated SERCA mRNA knockdown does not occur until later in embryogenesis

To determine the effect of RNAi constructs on embryonic *SERCA* mRNA levels, various SERCA RNAi constructs were ubiquitously expressed using the *da-GAL4* driver and RT-PCR performed for *SERCA* mRNA. RNA was extracted from 20 embryos in each group at stage 11 and stage 17 and at least three biological replicates used for each condition. After reverse transcriptase, cDNA was used to carry out quantitative RT-PCR (qRT-PCR, as described in more detail in Chapters 2 and 3) for *SERCA* mRNA and significant differences also confirmed on an electrophoresis gel. The effects of the RNAi constructs were compared to a control (*da-GAL4* crossed to w^{1118}) and results normalised to a reference gene (*18S* mRNA expression).

At stage 11, there was no significant difference in normalised *SERCA* mRNA level between any of the RNAi constructs and the control (Figure 5.7). At stage 17, normalised *SERCA* mRNA levels were significantly reduced by expression of any of the RNAi constructs, compared to the control ($p<0.05$). Reduced *SERCA* mRNA and unaffected *18S* mRNA levels were also confirmed at stage 17 on electrophoresis gel (Figure 5.7). These findings indicate that ubiquitously expressing RNAi in the embryo does not knockdown *SERCA* mRNA levels until later in embryogenesis.

At stage 17, normalised mean (+/- SEM) *SERCA* mRNA levels were reduced in the RNAi 4474/*Dicer2* and RNAi 4474/107446 groups, compared to RNAi 4474 alone (0.33 +/- 0.16 and 0.06 +/- 0.05 vs. 0.68 +/- 0.25 respectively), although this difference did not reach statistical significance. Given the biological difference in lethality between these lines, the lack of statistical significance may overlook a real difference due to small sample size (n=3) and degree of variance relative to effect size. It remains plausible that addition of *Dicer2* overexpression or an extra RNAi construct to RNAi 4474 results in a *biologically* significant increase in *SERCA* mRNA knockdown at stage 17.

Looking at the degree of knockdown, the mean percentage reduction in *SERCA* mRNA, relative to control (w^{1118}) at stage 17, ranged from 71% for RNAi 107446 alone, to 98% for RNAi 4474/107746 recombined together. RNAi 4474 alone resulted in a mean knockdown of 81% and RNAi 4447/*dicer2* recombined together, a 91% reduction.

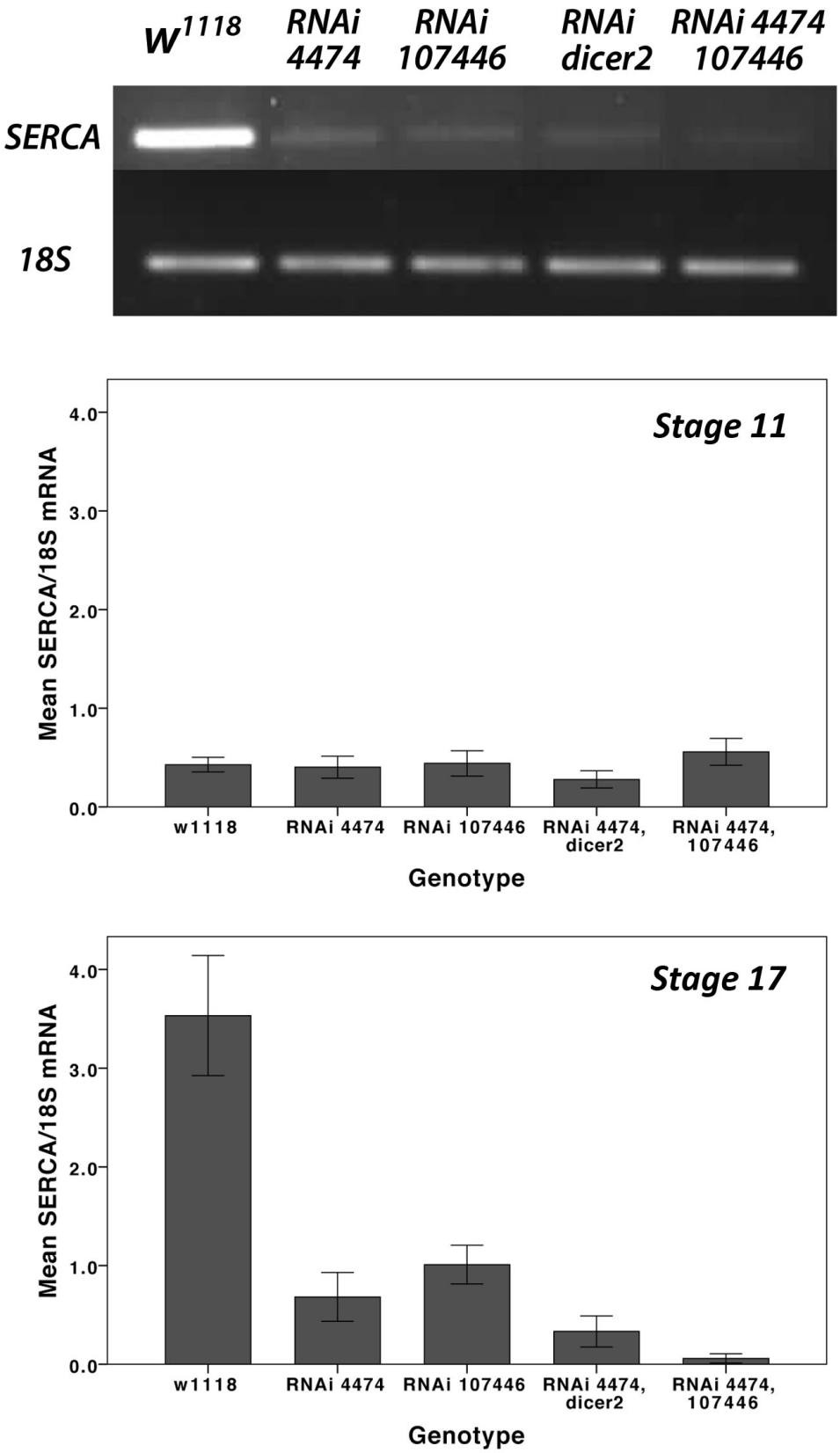

Figure 5.7 RNAi mediated SERCA mRNA knockdown does not occur until later in embryogenesis

RT-PCR of stage 11 and 17 embryos expressing the *da-Gal4* driver and different RNAi constructs +/- *dicer2*. Upper panel: representative gel image of RT-PCR of *SERCA* and *18S* mRNA at stage 17. Lower panels: quantitative RT-PCR of mean *SERCA* mRNA expression relative to *18S* at stages 11 and 17 (error bars indicate +/- 1 SEM). Genotypes used are as indicated

5.4.2 Residual SERCA protein is evident in embryos expressing RNAi ubiquitously

To test the effect of RNAi on SERCA protein levels, RNAi 4474 was expressed ubiquitously throughout the embryo using the *da-GAL4* driver. RNAi 4474 was first balanced over the fluorescent second chromosome balancer, *CyO, twi>GFP,* to generate an easily distinguishable internal control in half of all collected embryos. Stage 11 and 16 embryos were fixed and stained with fluorescently tagged thapsigargin (BODIPY® TR-X thapsigargin, Invitrogen). Thapsigargin avidly and specifically binds SERCA protein and therefore, after excess dye is washed away, fluorescent emission correlates with SERCA protein localisation in the embryo. Embryos were analysed using confocal microscopy with settings standardised between groups.

Diffuse fluorescent emission from TR-X thapsigargin was evident in RNAi and control embryos at both stages 11 and 17 (Figure 5.8). The distribution of the fluorescent signal was very similar between groups. The widespread distribution of SERCA protein in stage 17 embryos, with little or no regional difference, is in-keeping with published data in wild-type embryos (Vazquez-Martinez, Canedo-Merino, Diaz-Munoz, & Riesgo-Escovar, 2003). When Vazquez *et al* carried out similar experiments on embryos pre-treated with unlabelled thapsigargin, to saturate SERCA binding, fluorescent signal was abolished (confirming the specificity of the dye). Hence, in our study, if SERCA protein had been abolished or significantly reduced as a result of RNAi expression, it would be expected that fluorescent signal would also be lost or greatly diminished. These data indicate that there are significant amounts of residual SERCA protein in embryos expressing SERCA RNAi ubiquitously, although this assay only provides a qualitative assessment: relative amounts of protein between groups can not be determined.

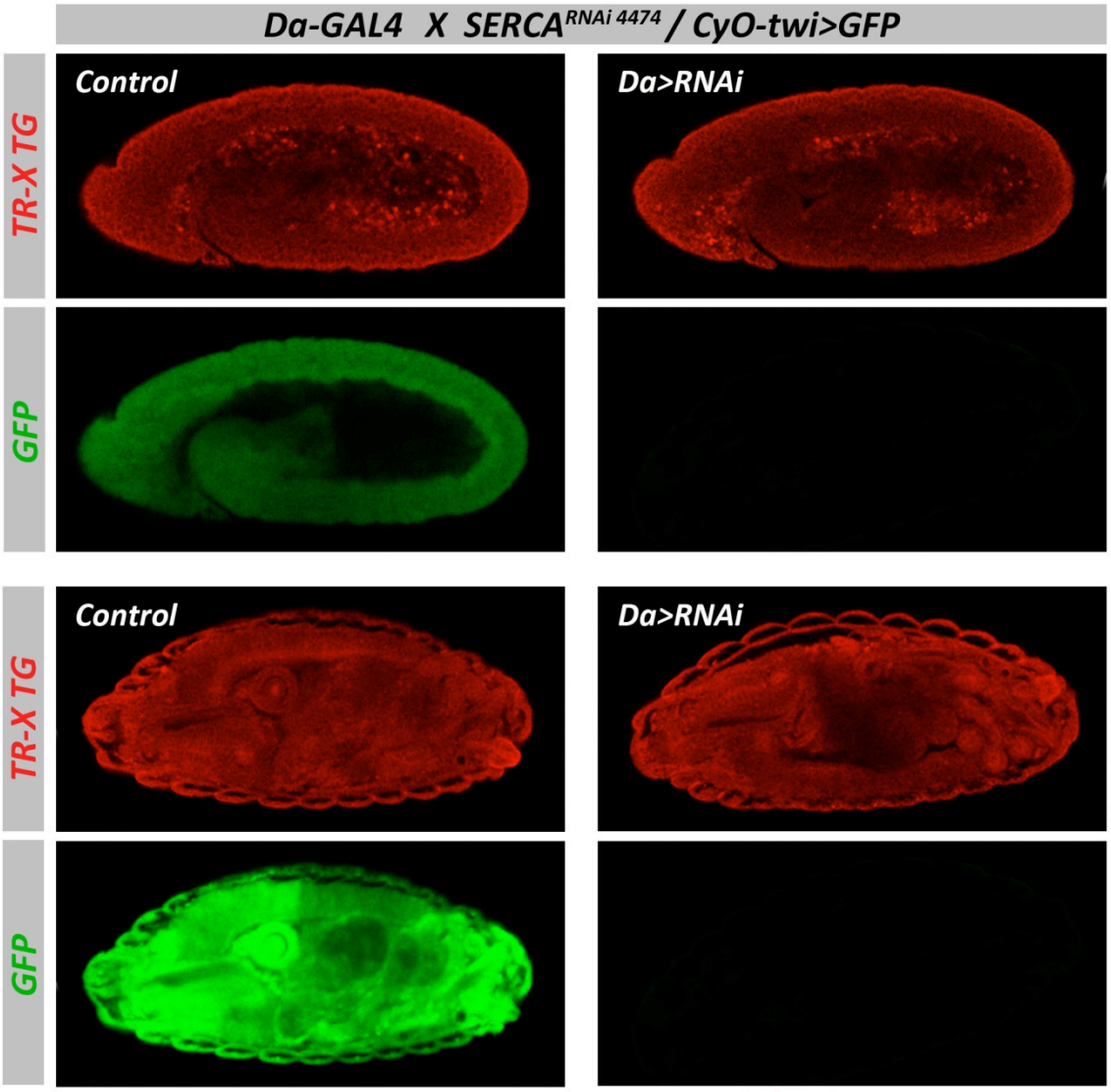

Figure 5.8 Residual SERCA protein is evident in embryos expressing RNAi ubiquitously

Confocal micrographs of stage 11 (upper panels) and stage 16 (lower panels) embryos stained with fluorescent thapsigargin (BODIPY® TR-X, Invitrogen) that specifically binds to SERCA protein. Embryos genotypes are *SERCA* RNAi 4474 under the control of *da-GAL4* vs. an internal control (*CyO-twi>GFP / da-GAL4*) The lateral aspect of the embryo is shown in each case (anterior to the left). Embryos are approximately 500 µm in antero-posterior length.

5.4.3 RNAi reduces SERCA function in late embryogenesis

To test the effect of RNAi on SERCA protein *function*, an assay was developed to assess this in embryonic cells. It is known that when the SERCA pump is inhibited with thapsigargin, there is a sharp rise in intracellular Ca^{2+} concentration, soon after addition of the inhibitor to *Drosophila* S2 cells (Yagodin, Pivovarova, Andrews, & Sattelle, 1999). This rise is due to inhibition of Ca^{2+} re-uptake into cellular stores (and hence store depletion) and triggering of capacitative (store operated) Ca^{2+} entry into the cell (Yeromin, Roos, Stauderman, & Cahalan, 2004). The degree of this rise is known to correlate with the baseline SERCA function within a cell: S2 cells treated with dsRNA targeted to knockdown SERCA i*n-vitro*, display a significantly reduced, or absent rise in intracellular Ca^{2+} on application of thapsigargin (Raymond-Delpech, Towers, & Sattelle, 2004; Zhang et al., 2006). In addition, cells treated with SERCA RNAi have a raised resting intra-cellular Ca^{2+} concentration, compared to controls (Abell, Ahrends, Bandara, Park, & Teruel, 2011; Raymond-Delpech et al., 2004; Zhang et al., 2006).

To apply this system to *Drosophila* embryos expressing RNAi constructs *in-vivo*, a method was required that would permit accurate quantification of intracellular Ca^{2+} concentration and allow simultaneous cell stimulation with thapsigargin. Since the vitelline membrane does not readily permit the passage of molecules such as AM-ester Ca^{2+} indicators into the embryo, an assay was developed where embryos expressing RNAi 4474 ubiquitously (using *da-GAL4*) were dissociated to a single cell suspension. These cells were then loaded with the Ca^{2+} indicator Fluo-4 (Invitrogen) under culture conditions and treated with thapsigargin as previously described. Although an *in-vitro* assay, SERCA RNAi 4474 was expressed in the developing embryo in exactly the same way it had been in other experiments and embryos were only dissociated at the developmental stage when Fluo-4 loading was required.

Cells from stage 11 embryos expressing RNAi 4474 ubiquitously, demonstrated similar intracellular Ca^{2+} characteristics as control (w^{1118}) embryo cells (Figure 5.9). The baseline Ca^{2+} concentration was comparable, as was the amplitude of the thapsigargin-induced rise in concentration. This indicates stage 11 embryos expressing RNAi 4474 ubiquitously do not have significantly reduced levels of SERCA function and hence RNAi has not induced a functional knockdown.

However, at stage 16, the RNAi and control embryonic cells differed markedly: RNAi 4474 cells had higher baseline intra-cellular Ca^{2+} concentration and their response to thapsigargin administration was markedly attenuated compared to control (Figure 5.9). These characteristics are consistent with those of S2 cells treated with *SERCA* dsRNA *in-vitro* and confirm RNAi 4474 reduces SERCA function by stage 16 of embryogenesis (Zhang et al., 2006). Together these data correlate with mRNA knockdown findings detailed above and indicate that RNAi-mediated SERCA inhibition is effective only by late embryogenesis.

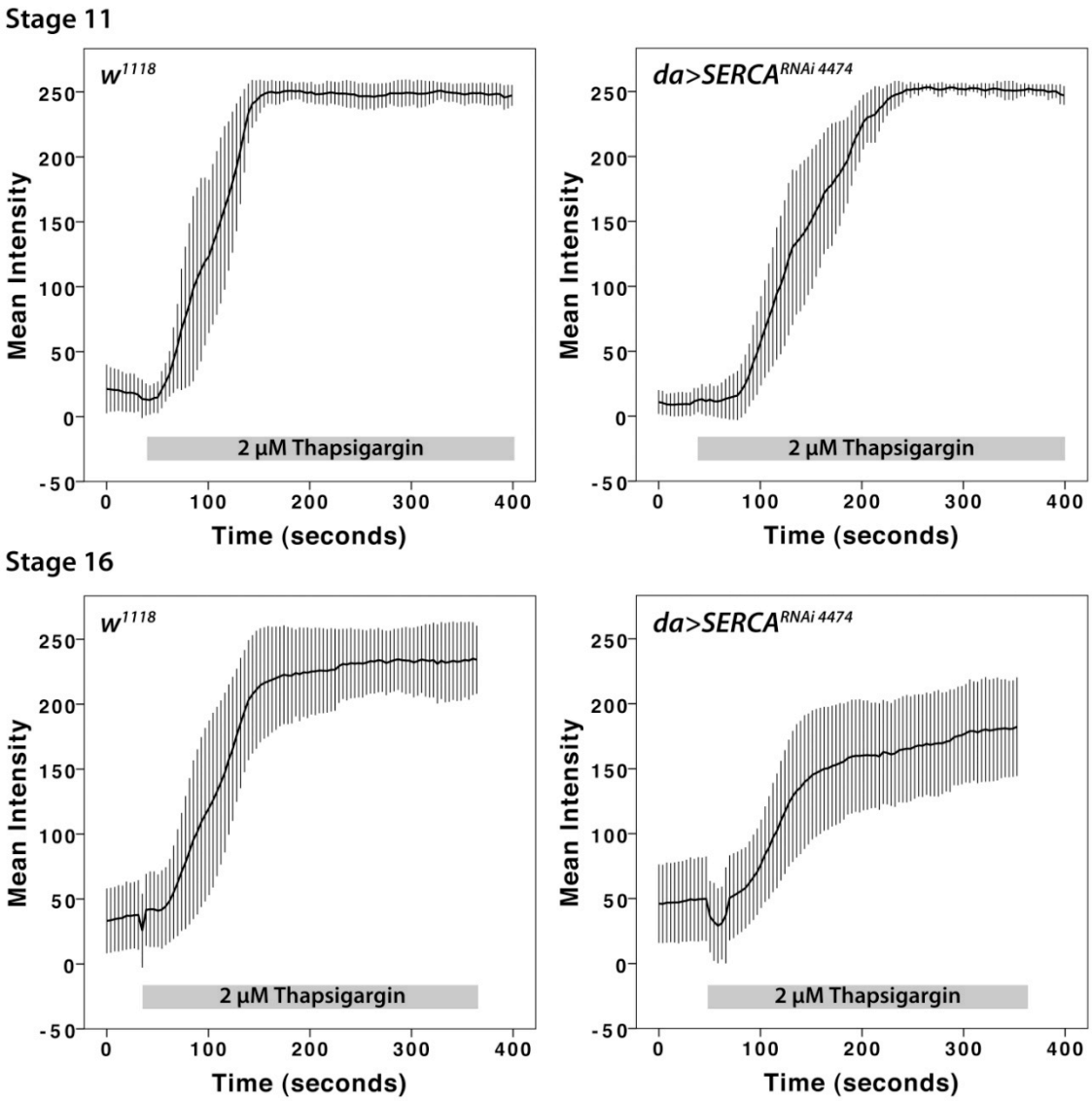

Figure 5.9 RNAi reduces SERCA function in late embryogenesis

Graphs of mean (+/- SD) fluorescent intensity over time of Fluo-4 (Invitrogen) loaded cells, stimulated with thapsigargin at times indicated by the grey bars. *SERCA* RNAi 4474 was expressed ubiquitously in the embryo with the *da-GAL4* driver and compared to w^{1118} controls. Embryos were aged to stages 11 and 16, dissociated into a single cell suspension, loaded with Fluo-4 and imaged with confocal microscopy.

5.5 Discussion

In *Drosophila,* RNAi has been used extensively to interrogate gene loss of function phenotypes, both in S2 cell lines and in targeted, tissue specific *in-vivo* studies (Caplen, Fleenor, Fire, & Morgan, 2000; Goto, Kadowaki, & Kitagawa, 2003; Piccin et al., 2001). Genome wide screens have now similarly been carried out in both manners, taking advantage of available RNAi libraries (discussed above) (Boutros et al., 2004; Cronin et al., 2009; Mummery-Widmer et al., 2009). Despite early, *in-vivo* RNAi studies yielding valuable information about gene function during embryonic development (through the injection of dsRNA into *Drosophila* embryos), most studies of targeted transgenic knockdown (using the *GAL4-UAS* system), have investigated larval and adult phenotypes (Kennerdell & Carthew, 1998; Misquitta & Paterson, 1999). The efficiency of *GAL4-UAS* mediated RNAi knockdown in the embryo has therefore not been well defined. Here I present data that demonstrates transgenic RNAi SERCA knockdown does not occur until later in embryogenesis: once it does occur though, it is considerable, with up to 98% reduction in mRNA and an accompanying significant decrease in protein function. One explanation for the early inefficiency of RNAi is a maternal contribution of SERCA loading (mRNA and/or protein) within the embryo. This hypothesis is supported by RNA-seq and *in-situ* hybridisation data that demonstrate high levels of *SERCA* mRNA throughout embryogenesis (Graveley et al., 2011; Tweedie et al., 2009).

Critically, in this study, significant SERCA knockdown was not achieved until well after tracheal branching morphogenesis commences. Findings of a grossly normal tracheal system *structure* therefore have to be interpreted within the constraints of this temporally limited knockdown. Two obvious explanations for this are: (i) SERCA function is not required for embryonic tracheal morphogenesis or (ii) SERCA function *is* essential for normal tracheal development, but RNAi could not mediate adequate and timely knockdown during the relevant stages of development. Clues to which of these prevail can be gained from considering the larval phenotype: lethality is seen with *btl-GAL4* driven co-expression of RNAi 4474 and either *Dicer2* or RNAi 107446, indicating that SERCA function *is* essential in tracheal cells. What is not clear though, is whether this SERCA requirement in tracheal cells, is for embryonic or larval morphogenic events and whether it is involved in tracheal system structure, function or both; or whether

it is required for tracheal-independent mechanisms. To answer these questions, more efficient, earlier SERCA inhibition is required in the embryo, as well as an interrogation of tracheal structure at the larval stage in SERCA deficient animals: these steps are discussed in later chapters.

Chapter 6

EFFECTS OF A CONDITIONAL *SERCA* MUTATION ON *DROSOPHILA* EMBRYONIC TRACHEAL MORPHOGENESIS

6.1 Introduction

RNAi mediated *SERCA* knockdown was demonstrated to be ineffective until later stages of embryogenesis in Chapter 5. Given that tracheal branching morphogenesis starts at stage 11, a method was sought to inhibit SERCA protein function earlier in embryogenesis.

In addition to being present at high levels in *Drosophila* brain and muscles, *SERCA* mRNA is expressed at lower constitutive levels throughout the adult body (Magyar et al., 1995). RNA-seq and *in situ* hybridisation data also confirm relatively high mRNA expression levels throughout embryogenesis (Graveley et al., 2011; Tweedie et al., 2009). Together, these observations suggest an important housekeeping role for the encoded protein in all, or most cells. This theory is given further credence by demonstration of SERCA playing an essential role in trafficking of a number of proteins: SERCA loss of function cells display mislocalised transmembrane proteins including Notch (Periz & Fortini, 1999). Given this likely housekeeping-type role, strong loss-of-function mutations will likely result in severe, global defects in early embryogenic events. Correspondingly, it has been reported that homozygous SERCA mutants display profoundly abnormal embryo morphology (Sanyal et al., 2005). Significant disturbances to early embryogenesis are likely to be unhelpful in this investigation, as they will preclude the study of later embryonic events, such as tracheal morphogenesis beginning at stage 11. In order to interrogate SERCA's role in tracheal morphogenesis, a conditionally activated, dominant negative mutation was exploited to overcome these constraints.

6.1.1 The conditional SERCA mutant, Kumbhakarna

Named after an eponymous mythological hero who slept for six months of the year, the *Kumbhakarna (Kum)* mutation was discovered in a screen of ethyl methanesulfonate (EMS) induced mutant flies that displayed paralytic behaviour upon heat treatment (Sanyal et al., 2005). Two independent, recessively lethal lines were detected by the screen, both displaying very similar, reversible paralytic phenotypes upon heating to 40°C. Recombination mapping placed the two alleles, named Kum^{170} and Kum^{295}, within the *Ca-P60A* (*Drosophila SERCA* gene) locus, at 60A11–12, on the right arm of the second chromosome. These mutants failed to complement previously described, lethal SERCA mutants, and

sequencing revealed that *Kum*^{170} carries a single-base substitution in the *SERCA* coding sequence, predicted to cause a Glutamic acid 442-to-Lysine mutation. This mutation is located in the hinge domain of the protein and has been hypothesised to potentially influence ATP binding or the conformational state of the molecule (Sanyal et al., 2005; Toyoshima et al., 2000; Toyoshima & Nomura, 2002).

Effects of this mutation on SERCA function were characterised using calcium imaging and electrophysiology of presynaptic motor neuron terminals: heated *Kum*^{170} mutants displayed higher peaks of cytosolic calcium upon nerve stimulation, with a more rapid return to baseline compared to wild-type controls and unheated *Kum*^{170} (Kuromi & Kidokoro, 2002; Sanyal et al., 2005). Importantly, this phenocopied the effects of thapsigargin (a potent, specific SERCA inhibitor) treatment. *Kum*^{170} was therefore confirmed as a conditional, dominant loss of-function allele of *SERCA*.

6.2 Aims

The conditional, dominant negative SERCA mutant allele, *Kum,* was exploited in a variety of experimental systems in order to determine the effects of SERCA inhibition on:

(i) embryonic tracheal branching morphogenesis;

(ii) embryonic tracheal maturation events.

6.3 Effects of the *Kum* mutation on embryonic tracheal morphogenesis

6.3.1 Optimising heat treatment of Kum embryos

Sanyal *et al* induced short (3–5 minute) periods of heat treatment to flies, using a device labelled as a 'sushicooker' by Ramaswami *et al* (Ramaswami, Rao, van der Bliek, Kelly, & Krishnan, 1993; Sanyal et al., 2005). This device comprises a smooth glass chamber surrounded by a water jacket to maintain a controlled temperature. Active flies are loaded into the top and fall from the bottom when paralysed by the effects of the heat. Kum^{170} adults were shown to paralyse within three minutes at 40°C, Kum^{295} similarly, at 39°C. *Kum* larvae displayed a similar paralytic, contracted phenotype within five minutes (Sanyal et al., 2005). The description of an embryonic phenotype was limited to: 'many homozygous Kum^{295}/Kum^{295} mutant embryos also appeared abnormally contracted inside the egg case;' and 'most Kum^{170}/Kum^{170} animals developed normally and hatched into very sluggish first-instar larvae.' It is unclear whether homozygous or heterozygous embryos were heated at all, and if so, how this was achieved. Consequently, in order to take advantage of the heat-sensitive, conditional characteristic of *Kum* in embryos, it was necessary to optimise a protocol for their heat treatment.

Wild-type *Drosophila* embryos exposed to heat-shock conditions (usually 37°C for 15-30 minutes), where the temperature of the embryo is rapidly increased (e.g. by use of liquid incubation medium), have been shown to display a range of cellular and molecular abnormalities, dependent on their developmental stage at heat-shock (Dura, 1981; Graziosi et al., 1983; Graziosi, Micali, Marzari, de Cristini, & Savoini, 1980; Santamaria, 1979). Heat shock has been shown to result in dramatic, irreversible changes when instigated early (e.g. pre-blastoderm), but also induces significant changes later in embryogenesis, such as collapse of the intermediate filament cytoskeleton (Walter, Biessmann, & Petersen, 1990). Even short heat-shocks of a few minutes decrease normal protein synthesis and upregulate heat-shock proteins; they impair development and decrease survival (Eberlein & Mitchell, 1987). Initial attempts to apply such heat-shock methods to *Kum* embryos at around stage 11, at temperatures and over time periods similar to that described by Sanyal *et al*, were limited by gross morphological abnormalities in the embryo (Sanyal et al., 2005). This was

somewhat unsurprising, given the known consequences of heat-shock in embryos and a likely increased sensitivity to heat in *Kum* animals.

To reduce the induction of such global embryonic defects, a different approach was tested, whereby a more gradual increase in temperature was instigated, but for longer periods. Embryos were left on apple juice agar plates and placed in standard 37°C incubators for up to one hour. To test the effects of this treatment on embryo viability, an assay of hatching frequency was employed. Embryos collected from Kum^{170}/CyO or Kum^{295}/CyO stocks were aged to stage 11 and then submitted to a period of one hour in the 37°C incubator, before being returned to 25°C. Heated embryos were significantly less likely to hatch compared to their non-heated controls (Tables 6.1 and 6.2). It would be expected that 25% of these embryos were homozygous for either the *Kum* mutation or *CyO* and hence half of all embryos would be recessively lethal at some point in development: this is consistent with the observation that 50% of embryos failed to hatch in the unheated groups. Given that wild-type embryo hatching is largely unaffected by this type of heat regime, the significant decrease in hatching induced by heat in *Kum* embryos, is likely to be related to specific activation of the conditional mutation. Gross morphology of these embryos was apparently unaffected, when inspected with bright-field and confocal microscopy (Figure 6.1) and hence this type of treatment was used in future experiments.

Table 6.1 Hatching frequency of embryos from *Kum^{170}/CyO* stocks

p=0.0001	Heated	Unheated
Hatched	9	53
Un-hatched	111	67
Total	120	120

Table 6.2 Hatching frequency of embryos from *Kum^{295}/CyO* stocks

p=0.0001	Heated	Unheated
Hatched	7	26
Un-hatched	43	24
Total	50	50

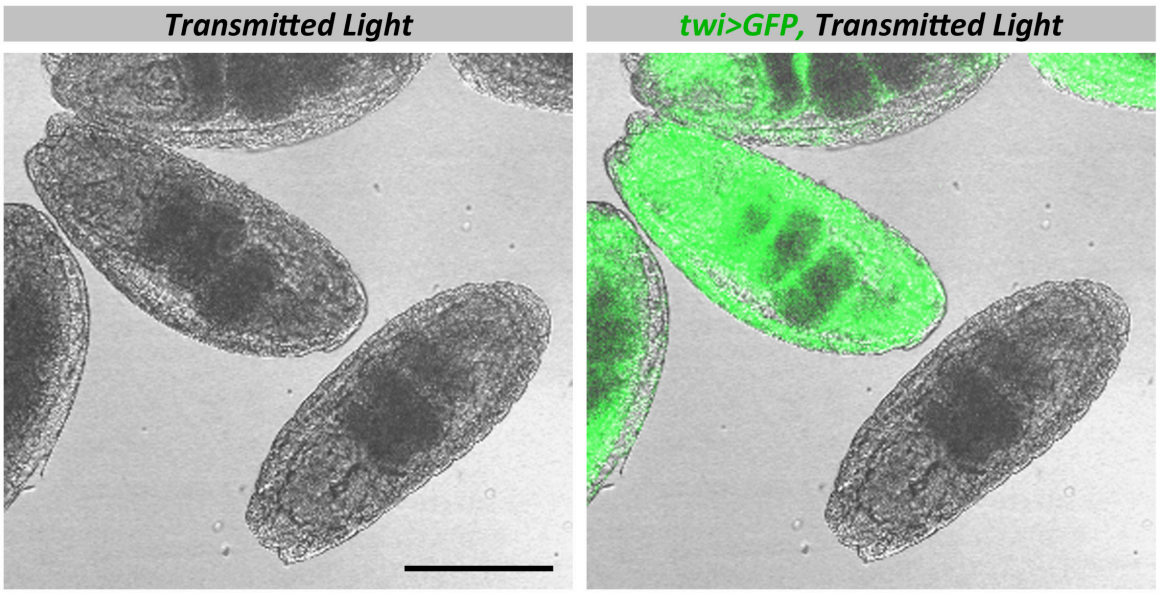

Figure 6.1 Confocal micrographs of embryos from *Kum/CyO, twi>GFP stocks*

Stage 16.1 embryos (confirmed by characteristic gut morphology) are displayed that are heterozygous or homozygous for the *Kum* allele (indicated by the presence or absence of *twi>GFP*). Embryos were submitted to heat treatment at stage 11 to activate the conditional mutation: gross morphology is apparently normal. Scale bar indicates 200 μm.

6.3.2 Embryos homozygous for Kum alleles display grossly normal patterns of tracheal branching morphogenesis

To test the effect of the conditional SERCA mutation *Kum,* on tracheal branching morphogenesis, homozygous embryos were assessed in order to maximise the effect of the dominant negative mutation. Embryos were collected over narrow time intervals and heat treated at stage 11 (as detailed above) and then fixed at stage 16. Homozygous embryos were selected from those laid by stocks of *Kum* flies that had been previously balanced with a fluorescent second chromosome balancer (*CyO, twi>GFP*): selection was based on the absence of GFP (Figure 6.1). The tracheal system was stained with an antibody to the luminal protein, 2A12 (DSHB) and embryos imaged with confocal microscopy. Embryos as close as possible to stage 16.1 were identified from gut morphology (Figure 6.1), to ensure phenotypic comparison between groups was made at equivalent developmental stages.

Embryos homozygous for Kum^{170} or Kum^{295} alleles displayed a grossly normal, branched tracheal system at stage 16, when compared to similarly heated controls (w^{1118}) (Figure 6.2). Major tracheal branches were clearly identified at appropriate positions in all groups, including the dorsal and lateral trunks; dorsal, visceral and ganglionic branches and transverse connectives. Specialised branches of the first and tenth metameres were also present at appropriate positions. The often more variable, finer and shorter branches such as the spiracular, fat body and lateral group, were demonstrated, however, in the Kum^{295} group, these were less well defined (lower panel, Figure 6.2). Although there is evidence that the fundamental cellular events that dictate branch *formation* have occurred in these embryos, the 2A12 antibody has not stained these finer branches as well as in control or Kum^{170} embryos: this may indicate a disturbance to the branch lumen, or protein within the lumen, rather than to the branching event itself. Elements of tracheal maturation, such as this, will be investigated later in this chapter.

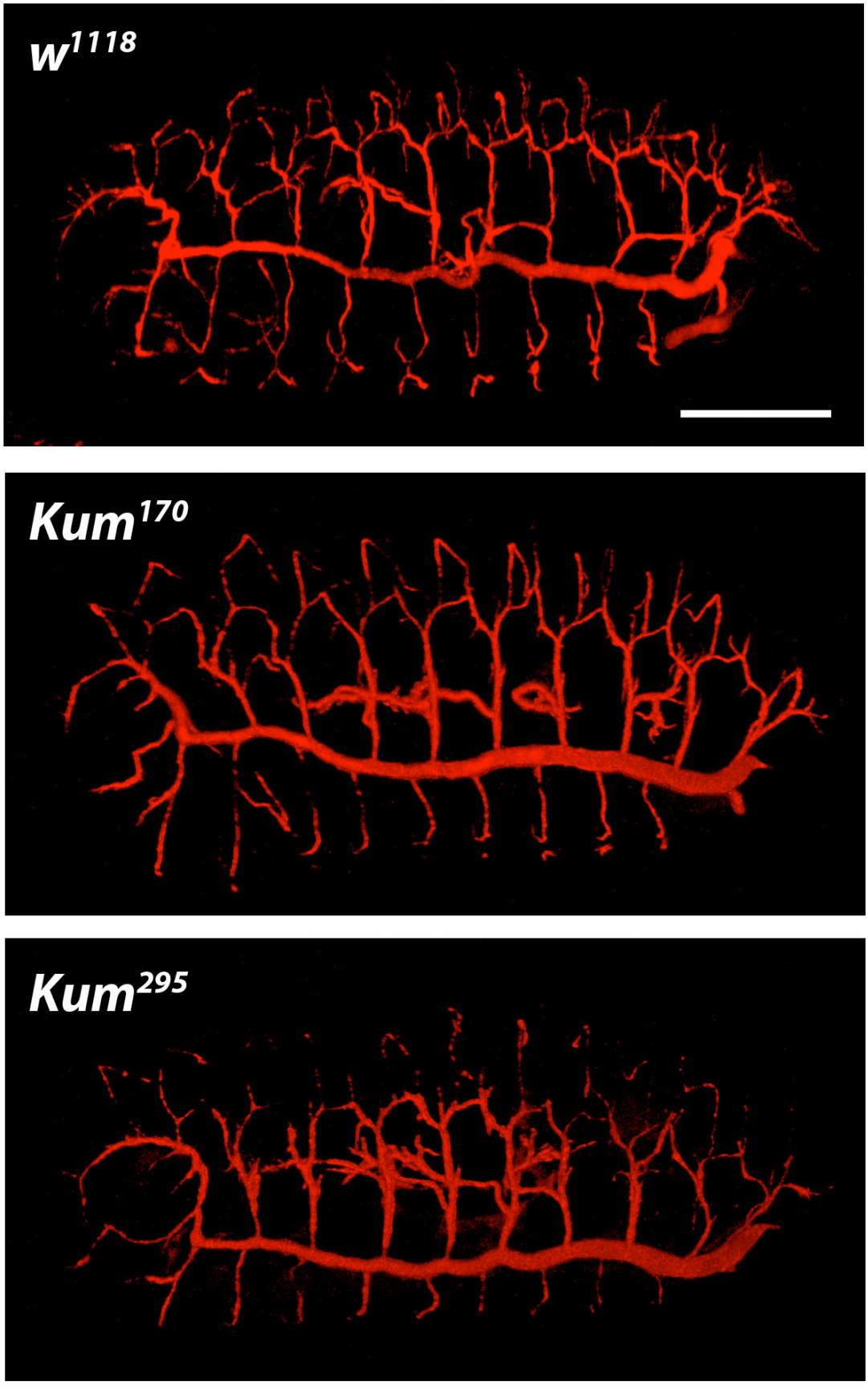

Figure 6.2 Embryos homozygous for *Kum* alleles display grossly normal patterns of tracheal branching morphogenesis

Confocal micrographs (3D projections of z-stacks) of stage 16 *Drosophila* embryos homozygous for *Kum*^{170} or *Kum*^{295} vs. control (*w*^{1118}), exposed to a 1 hour heat treatment at the start of branching morphogenesis (stage 11) . The tracheal system is stained with 2A12 antibody (DSHB, Iowa). The lateral aspect of the embryo is shown (anterior to the left). Scale bar indicates 100 μm.

6.3.3 Embryonic cells homozygous for Kum^{170} display significantly decreased SERCA function

In order to test the effect of the Kum^{170} mutation on SERCA function in embryonic cells, a functional assay of protein activity was performed, as previously described in Chapters 2 and 5. Briefly, embryos homozygous for the Kum^{170} allele were selected as above, aged to stage 11 and submitted to heat treatment as above (thus replicating experimental conditions used for tracheal phenotype assessment). Following heat treatment, embryos were dissociated into a single cell suspension in culture conditions and loaded with the calcium indicator, Fluo-4 AM (Invitrogen). During confocal live imaging, cells were stimulated with thapsigargin and changes in intensity of fluorescence monitored.

Cells from embryos homozygous for the Kum^{170} allele displayed significantly different intracellular Ca^{2+} characteristics, to controls (Figure 6.3). Baseline Ca^{2+} concentration was significantly higher in the Kum^{170} group, as indicated by a higher Fluo-4 intensity (56.1 vs. 26.5, $p=0.001$). The response to thapsigargin stimulation was also significantly attenuated: a smaller increase in intensity was witnessed (147.1 vs. 238.2, $p<0.001$) and this increase occurred at a slower rate (time to maximum intensity, 353.9 vs. 413.7 seconds, $p=0.047$).

These changes in intracellular Ca^{2+} characteristics are in keeping with those in studies of *Drosophila* S2 cells, when SERCA function was inhibited with RNAi (Raymond-Delpech et al., 2004; Zhang et al., 2006). They are also comparable to the effect of *in-vivo* RNAi in late embryogenesis, detailed in Chapter 5. Collectively, this confirms that embryos homozygous for the Kum^{170} allele and treated with heat, have significantly reduced SERCA protein function at stage 11 (around the start of tracheal branching morphogenesis), contrasting starkly with RNAi mediated SERCA knockdown that is not effective at this stage. Given these findings, it seems reasonable to conclude that the dominant negative Kum^{170} allele is effective at reducing the function of maternally loaded SERCA, the presence of which is strongly suggested by transcriptomics and functional assay (Chapter 5) (Graveley et al., 2011; Tweedie et al., 2009). This validation of significant functional inhibition, together with findings of normal tracheal branching (Figure 6.2), confirms that branching morphogenic events can proceed with a considerably decreased level of SERCA function.

Importantly however, residual SERCA function is evident at stage 11: it therefore remains conceivable that SERCA may be required for tracheal branching, but this lower level of activity is sufficient. Further, more potent SERCA knockdown globally across the embryo (such as that mediated by the *Kum* allele) may be precluded by an essential requirement of SERCA in normal embryogenesis, particularly given its putative housekeeping role in most/all cells. Subsequent attempts to increase the potency of SERCA inhibition therefore incorporated an element of targeting to tracheal cells.

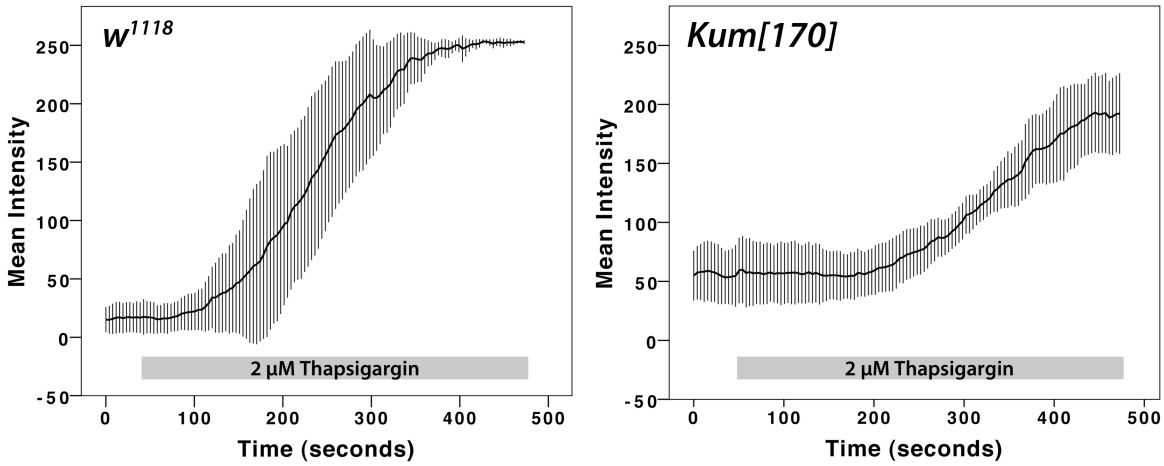

	w^{1118}	Kum^{170}	
Mean Resting Intensity	**16.5 +/- 12.5**	**56.1 +/- 23.8**	**p=0.001**
Mean Maximum Intensity	**254.7 +/- 0.4**	**203.2 +/-30.5**	**p=0.001**
Mean Change	**238.2 +/-12.5**	**147.1 +/- 49.8**	**p<0.001**
Time to Max Intensity (secs)	**353.9 +/- 55.6**	**413.7 +/-32.5**	**p=0.047**
Time to 1/2 Max Intensity (secs)	**191.1 +/- 53.7**	**230.3 +/-42.5**	**p=0.167**

Figure 6.3 Embryonic cells homozygous for Kum^{170} display significantly decreased SERCA function

Upper panels: Graphs of mean (+/- SD) fluorescent intensity over time of Fluo-4 (Invitrogen) loaded cells, stimulated with thapsigargin at times indicated by grey bars. Embryos were homozygous for the *Kum^{170}* allele and compared to *w^{1118}* controls. Embryos were aged to stage 11, dissociated into a single cell suspension, loaded with Fluo-4 and imaged with confocal microscopy.

Lower panel: table of mean (+/- SD) cell fluorescent intensities, along with rates of change for both groups.

6.4 Effects of the *Kum* mutation and SERCA RNAi on embryonic tracheal morphogenesis

6.4.1 Combining the effects of the Kum allele and SERCA RNAi

RNAi mediated SERCA knockdown was ineffective in early embryogenesis: given the seemingly plausible hypothesis that this was a result of maternally loaded SERCA (mRNA and/or protein), efficacious SERCA inhibition must target this maternal contribution. One method used to at least partially achieve this, studied embryos homozygous for *Kum* alleles (discussed above). Residual SERCA function was evident though, making it difficult to draw firm conclusions from findings of a grossly normal tracheal system. A novel way to increase functional inhibition may be to combine the *Kum* allele with RNAi targeted to tracheal cells (*btl>RNAi*, Chapter 5*)*. In theory, the dominant negative *Kum* allele should inhibit maternal SERCA (if *Kum* female flies were used in the cross) and RNAi would target zygotic SERCA specifically in tracheal cells. In order to achieve such a genetic combination, the recessively lethal Kum^{170} allele was recombined on the second chromosome with *btl-GAL4, UAS-act.GFP*.

Meiotic recombination events that occur in female *Drosophila* were exploited to combine the heterozygously carried Kum^{170} allele and *btl-GAL4, UAS-act.GFP* transgenes (present on homologous second chromosomes), onto one chromosome (Figure 6.4). Potential, individual male recombinants were firstly selected based on the presence of tracheal GFP fluorescence in larvae. These larvae were allowed to develop to adults and the presence of the *Kum* allele determined by induction of reversible paralysis with a three minute, 40°C heat-shock. The paralysis witnessed was in-keeping with that described by Sanyal *et al*, indicating that the confirmed dominant negative effect of the *Kum* allele had been retained, and combined with *btl-GAL4, UAS-act.GFP* (Sanyal et al., 2005). The presence of the Kum^{170} allele was further confirmed by a failure of complementation of Kum^{295} (Figure 6.5).

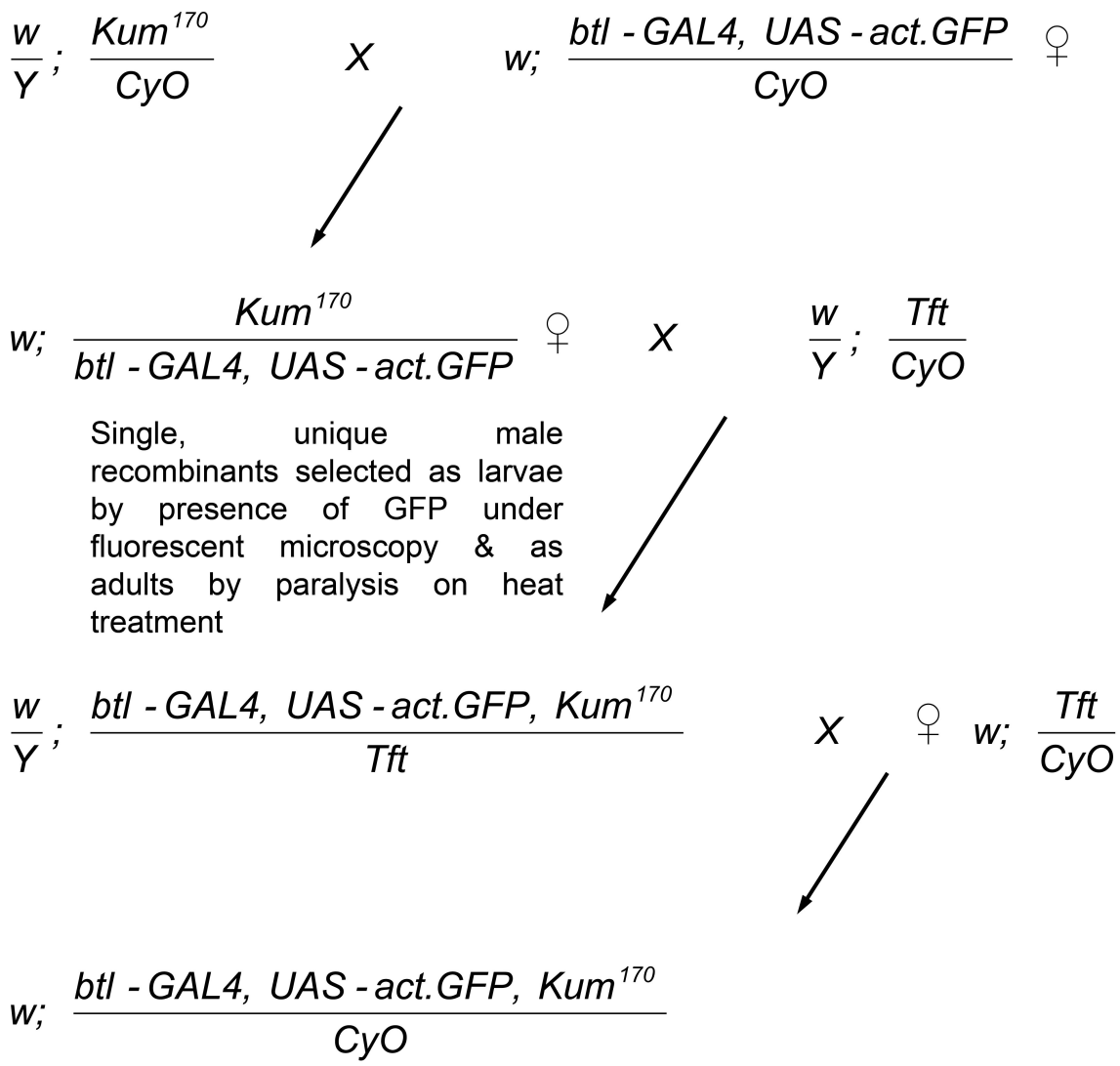

Figure 6.4 Genetic crossing scheme demonstrating recombination of the *Kum^{170}* allele and *btl-GAL4, UAS-act.GFP* on the 2nd chromosome

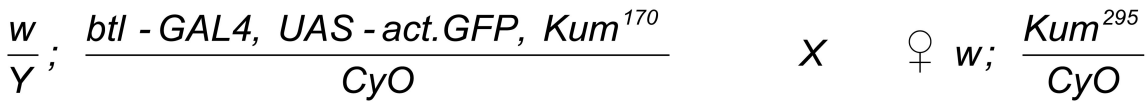

Viability of straight winged progeny assessed

Figure 6.5 Complementation test for the *Kum^{170}* allele

Genetic crossing scheme demonstrating the complementation test used to confirm the presence of the *Kum^{170}* allele on the 2nd chromosome. An absence of viable straight winged flies confirmed the presence of the allele.

6.4.2 Embryos with maternally derived Kum^{170} and expressing SERCA RNAi in tracheal cells, display grossly normal patterns of branching morphogenesis

To test inhibition of maternal SERCA, in parallel to the targeting of tracheal, zygotic SERCA with RNAi, *btl-GAL4, UAS-act.GFP,* Kum^{170} */ CyO* virgin female flies were crossed to homozygous RNAi 4474 males. Given the *Kum* allele was heterozygous in these embryos, it was postulated that a stronger heat-shock might be tolerated, without inducing global defects in embryogenesis. Stage 11 embryos were therefore placed on moist nylon mesh in a ventilated PCR microcentrifuge tube and a PCR thermocycler used to induce a 37°C heat-shock for 30-60 minutes: a method described by Vanario-Alonso *et al* (Vanario-Alonso, O'Hara, McGinnis, & Pick, 1995). Embryos were fixed at stage 16 and stained with an antibody to the tracheal luminal protein, 2A12 (DSHB, Iowa). Embryos of genotype *btl-GAL4, UAS-act.GFP,* Kum^{170} */RNAi 4474* were distinguished from internal controls (*RNAi 4474 /CyO)* based on the presence of tracheal GFP (Figure 6.6).

Control and *Kum* embryos submitted to a 60 minute heat-shock did not develop further and morphologically remained at stage 11 (Figure 6.6). This duration of heat-shock was therefore considered too long and a 30 minute regime used in further experiments. Embryos submitted to a 30 minute heat-shock developed to stage 16 and appeared to have a grossly normal tracheal system (Figure 6.6). All stereotypical tracheal branches were clearly identified in the embryo at appropriate positions, including those finer, shorter and often more variable ones discussed earlier in this chapter. SERCA inhibition comprising the dominant negative Kum^{170} allele (to target maternally contributed SERCA) *and* RNAi 4474 in tracheal cells (targeting zygotic SERCA) therefore did not appear to disrupt tracheal branching morphogenesis. Although it was not possible to quantify the degree of total SERCA inhibition in specific tracheal cells, reviewing the functional effects of Kum^{170} and RNAi used in isolation, it seems likely that when used in combination, they will result in significant reduction in protein function.

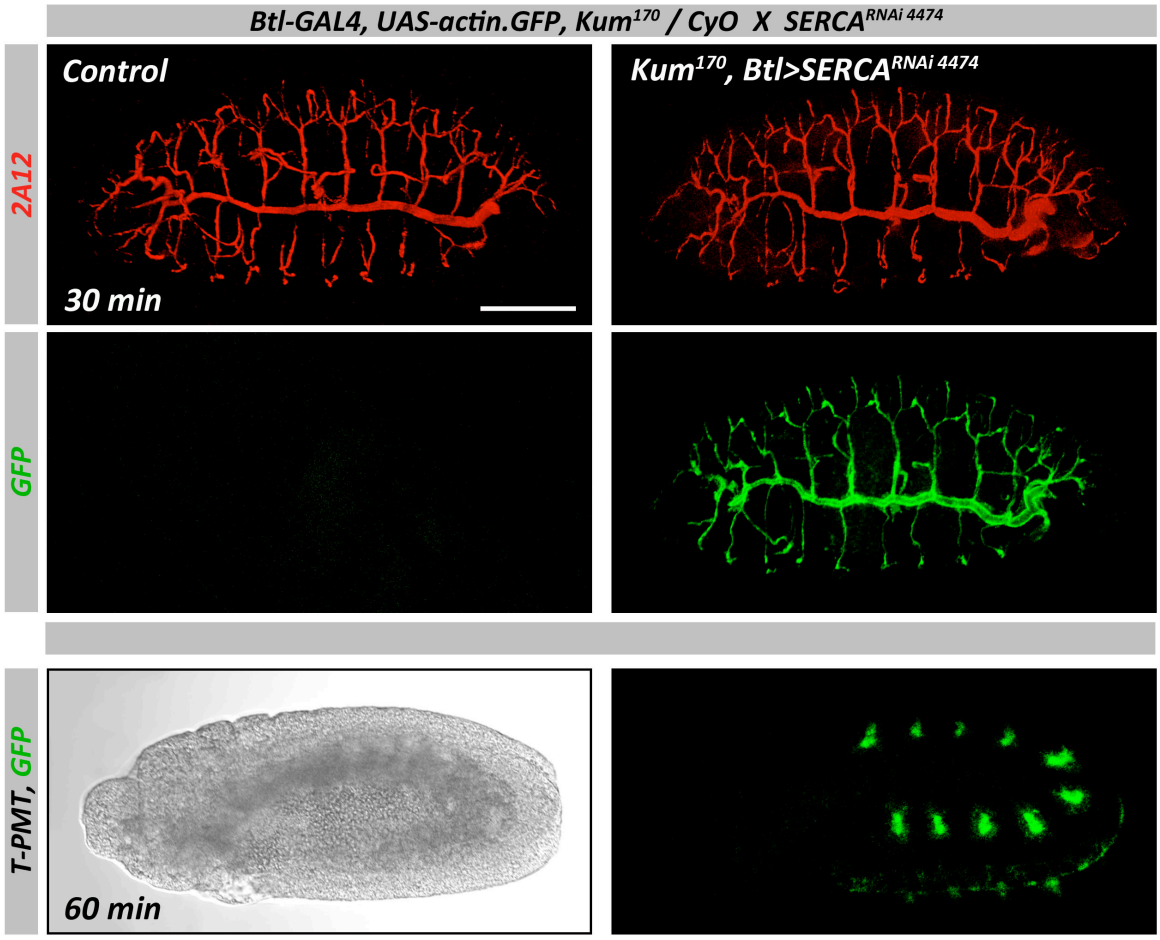

Figure 6.6 Embryos with maternally derived *Kum*^{170} and expressing *SERCA* RNAi in tracheal cells, display grossly normal patterns of branching morphogenesis

Confocal micrographs (3D projections of z-stacks) of stage 16 Drosophila embryos heterozygous for the *Kum*^{170} allele and expressing SERCA RNAi in the embryonic tracheal cells (*btl>RNAi*) vs. internal control (RNAi 4474/CyO). The tracheal system is stained with 2A12 antibody (DSHB, Iowa). The upper 4 panels show embryos subjected to a 30 minute heat-shock at stage 11, going on to develop normally. The lower 2 panels show an embryo subjected to a 60 minute heat-shock at stage 11 and failing to develop any further (imaged at 14 hours AEL). The lateral aspect of the embryo is shown (anterior to the left) in each case. Scale bar indicates 100 μm.

6.5 Effects of targeting *Kum*^{170} to tracheal cells

An alternative method to test the effects on tracheal morphogenesis, of the conditional, dominant negative *Kum* allele, is to specifically target this mutation to tracheal cells. The mutated cDNA from *Kum*^{170} has been previously been cloned into the pUAST vector, permitting misexpression of *Kum*^{170} with *GAL4* drivers (Sanyal et al., 2005). This transgene was made use of to target *Kum*^{170} specifically to tracheal cells, using the *btl-GAL4* driver.

6.5.1 Expression of Kum^{170} *in tracheal cells does not disrupt branching morphogenic events*

Flies carrying the *UAS-Kum*^{170} transgene were crossed to those carrying *btl-GAL4*. Embryos were collected and submitted to heat-shock regimens in order to activate the conditional mutation. The spatially restricted expression of *Kum*^{170} enabled different, more intensive heat regimes to be trialled without inducing global defects in embryogenesis. Given protein turnover and a likelihood that new SERCA may be synthesised in active tracheal cells throughout embryogenesis, it was postulated that repeated heat-shocks to activate newly formed *Kum*^{170} protein, may be most effective at inhibiting SERCA function. A PCR thermocycler was therefore used to submit embryos to a regime similar to that successfully employed elsewhere (Vanario-Alonso et al., 1995). Repeated 37°C heat-shocks, of 5-10 minute duration in each hour, interrupted by recovery periods of 25 °C, were instigated from 6 hours AEL to 14 hours AEL (approximately from stage 11 to 16, the majority of branching morphogenesis). Embryos were then fixed, stained and imaged as previously described.

Embryos submitted to the aforementioned heat regime developed appropriately and gross morphology appeared normal. Tracheal branching morphogenesis also appeared unaffected by *btl>Kum*^{170} expression and repeated heat-shock treatments (Figure 6.7). Major and minor branches (as previously listed) were evident and appeared appropriate in their position, thus indicating that branching events are not influenced by SERCA inhibition with targeted *Kum*^{170} expression. When the diameter of the dorsal trunk was reviewed, there appeared to be some discrepancy between groups (Figure 6.7): further investigation of tube diameter was therefore warranted.

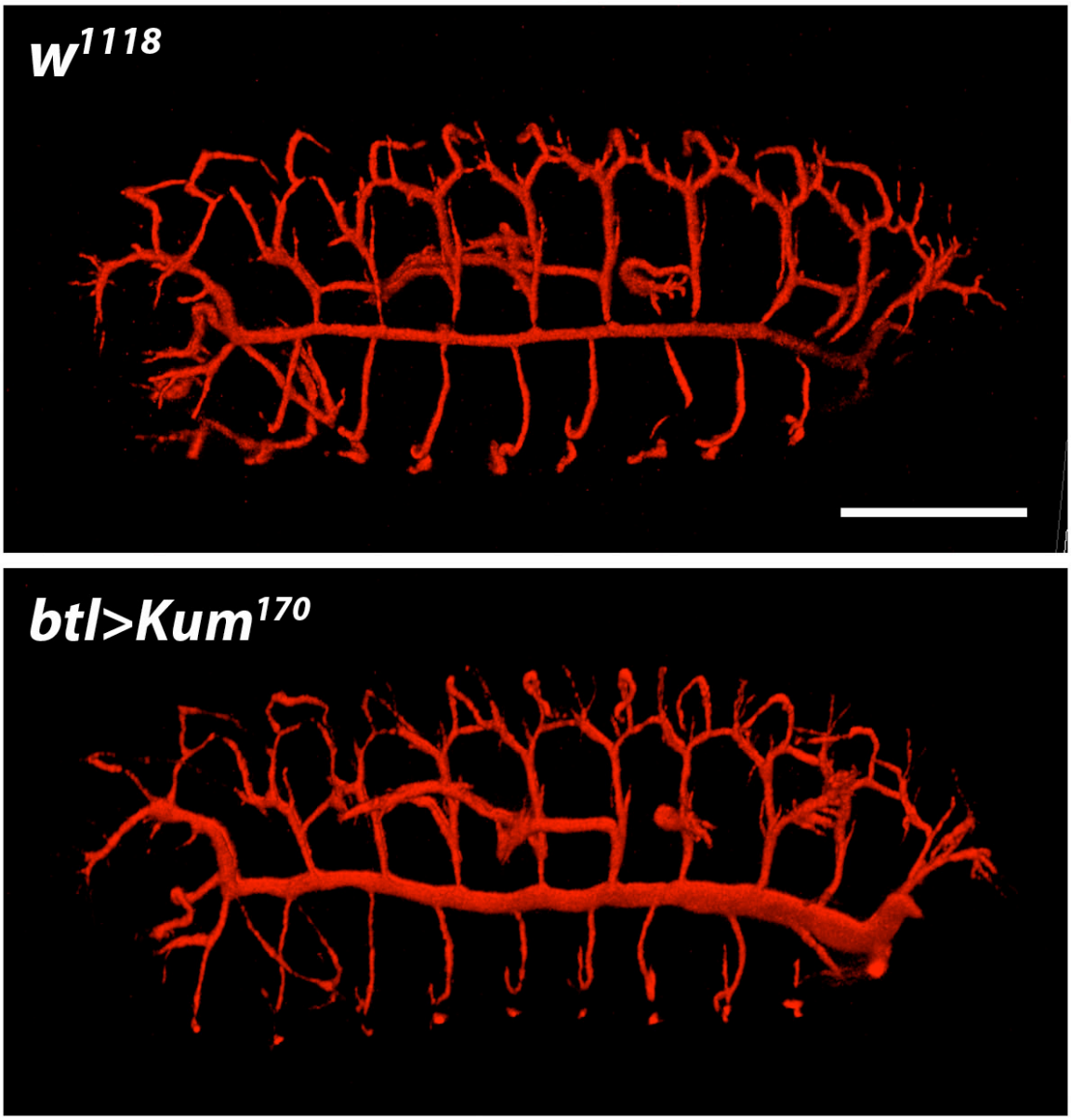

Figure 6.7 Expression of *Kum*^{170} in tracheal cells does not disrupt branching morphogenic events

Confocal micrographs (3D projections of z-stacks) of stage 15/16 *Drosophila* embryos expressing *Kum*^{170} specifically in the embryonic tracheal cells (*btl>Kum*^{170}) vs. control (*w*^{1118}). Embryos were subjected to repeated 5 minute 37°C heat treatments in each hour from 6h AEL until 14h AEL. The tracheal system is stained with 2A12 antibody (DSHB, Iowa). The lateral aspect of the embryo is shown (anterior to the left) in each case. Scale bar indicates 100 µm.

6.5.2 *Kum*^{170} expression in tracheal cells does not alter dorsal trunk diameter or luminal expansion

It is known that respiratory tube size in *Drosophila* is dependent on developmental stage. Relatively small differences in maturity can lead to significant changes in tube diameter and length: dorsal trunk diameter triples over a period of 3 hours, around stages 14 to 16 (Beitel & Krasnow, 2000). Although there was an apparent difference in the dorsal trunk diameter between *btl>Kum*^{170} and *w*^{1118} groups (Figure 6.7), one has to be mindful of any potentially subtle differences in embryonic stage. In addition to the noticeably wider dorsal trunk, the representative *btl>Kum*^{170} example given in Figure 6.7, displays other tracheal features that are indicative of this example being slightly more mature than its *w*^{1118} counterpart. The fine ganglionic and lateral group branches are longer and more complex; the visceral branches also appear wider. Since developmental stage is a spectrum, with a lack of absolute end-points, these features suggest that the *w*^{1118} embryo is closer towards stage 15, whilst the *btl>Kum*^{170} example may be someway through stage 16 (Manning & Krasnow, 1993). These differences are despite every effort being made to ensure equality of developmental stage at the initial assessment, through tight control of embryo laying times. The luminal protein staining method could induce further influence on apparent tube diameter: false-positives may be implied, for example, by tube-size independent changes to protein-antibody interaction.

To further clarify this issue, a different method of determining tracheal diameter was employed, as described by Tsarouhas *et al* (Tsarouhas et al., 2007). The apical surfaces of tracheal cells were labelled with fluorescent protein (*btl>moesin.mRFP*) and live imaging techniques employed to interrogate changes in diameter of the dorsal trunk (Figure 6.8) (Ribeiro et al., 2004). Embryos were mounted for live imaging and selected at stage 16.1 according to distinct gut morphology (discussed earlier). Imaging was carried out for 3 hours to assess changes in diameter throughout stage 16: dorsal trunk diameter was measured at right angles at a number of separate positions within metamere 7, to average tube tapering.

There was no significant difference in dorsal trunk diameter between *btl>Kum*^{170} and *w*^{1118} embryos, either at the beginning or end of imaging (Figure 6.8). The

increase in tube diameter was of a magnitude similar to that of wild-type embryos reported elsewhere, indicating that heat-treatment had not significantly influenced these events (Beitel & Krasnow, 2000; Tsarouhas et al., 2007). Tube expansion, a process that is coupled to secretion of proteins into the tracheal lumen, therefore seems unaffected by inhibition of SERCA through the targeted over expression of the dominant negative *Kum*^{170} allele.

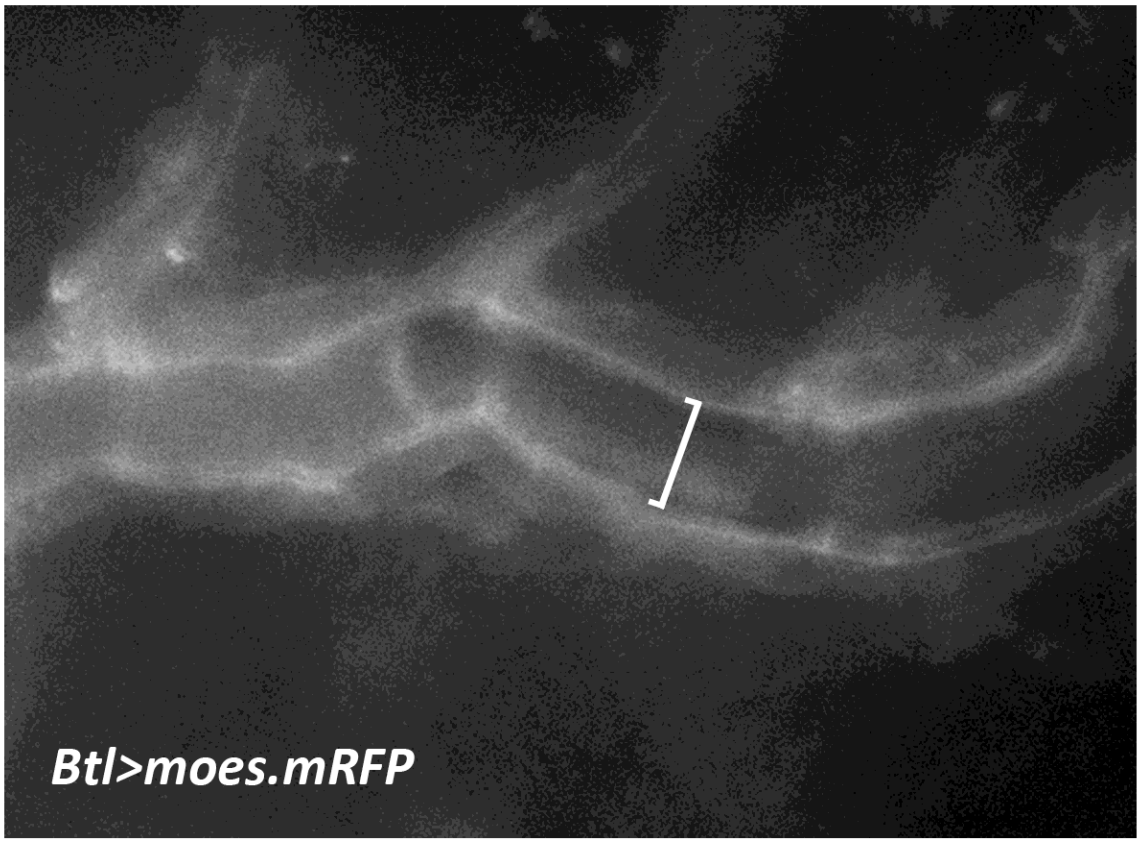

	Diameter (µm)		
	w1118	*Btl>Kum*	
0 min	5.6 +/- 0.5	5.4 +/- 1.0	p=0.708
210 min	8.7 +/- 0.7	8.5 +/- 0.9	p=0.601
Change	3.2 +/- 1.0	3.1 +/- 0.6	p=0.858

Figure 6.8 *Kum*^{170} expression in tracheal cells does not alter dorsal trunk diameter or luminal expansion

Upper panel: frame from live fluorescent microscopy of stage 16 embryo. The apical surfaces of tracheal cells are labelled with *btl>moes.mRFP.* The fifth and sixth metameres are shown and the technique used to measure diameter illustrated with white bars. Lower panel: mean dorsal trunk diameter at the sixth metamere, at the beginning and end of stage 16. Tracheal diameter measurements performed by Dr V Tsarouhas.

6.6 SERCA function is required for tracheal maturation

Tracheal maturation comprises a set of distinct cellular events that occur at stereotypical points in development and result in characteristic morphological changes (Behr, Wingen, Wolf, Schuh, & Hoch, 2007; Beitel & Krasnow, 2000; Manning & Krasnow, 1993; Tsarouhas et al., 2007). Firstly, in late stage 13, there is COP (coat protein complex) mediated secretion of proteins into the lumen: this event is tightly coupled to an expansion in luminal diameter (Grieder et al., 2008; Jayaram et al., 2008; Tsarouhas et al., 2007). Secondly, there is endocytotic clearance of luminal protein material in mid stage 17 (Behr et al., 2007; Tsarouhas et al., 2007). Thirdly, luminal liquid is rapidly cleared, allowing gas filling of the trachea in late stage 17, thus creating functional airways (Kaliss, 1939; Manning & Krasnow, 1993). SERCA inhibition, through targeted over expression of *Kum*^{170} did not appear to disrupt the early event of tracheal lumen expansion. SERCA's role in later maturation events was therefore investigated.

6.6.1 Embryos expressing Kum^{170} in tracheal cells have defects in tracheal gas filling

To test the effect of *Kum*^{170} expression on another, later aspect of tracheal maturation, rates of tracheal gas filling were investigated. Tracheal gas filling is readily assessable with bright-field microscopy at late stage 17 (prior to embryo hatching), due to changes in light refraction. Embryos of genotype *btl>Kum*^{170} and *btl>w*^{1118} were submitted to repeated heat treatments between stages 11 and 16, using a PCR thermocycler, as described above. After dechorionation, stage 16 examples were selected and mounted under halocarbon oil. Gas filling was assessed just prior to embryo hatching.

Tracheal gas filling occurred in 80% of control embryos but only 39% of *btl>Kum*^{170} embryos with heat-activated *Kum*^{170} expression in tracheal cells ($p<0.001$) (Figure 6.9); furthermore, without heat activation of *Kum*^{170} expression, *btl>Kum*^{170} embryos gas-filled at normal rates (84%; $p<0.001$ vs heat-treated). Given that the rate of gas filling in control embryos was unaffected by heat treatment ($p=0.196$) and unheated *Kum* and control embryos did not differ ($p=0.602$), these data indicate that heat treatment is having a specific affect on the *Kum*^{170} mutation and together, these conditions act to disrupt gas filling. The

proportion of heat-treated *btl>Kum*^{170} embryos that do gas fill, might be explained by genotype: the *UAS-Kum*^{170} line obtained from Subhabrata Sanyal, appeared to have *P* elements inserted on the second and third chromosome, but stock viability was maintained with a second chromosome balancer. Half of all collected embryos would therefore have two copies of the *UAS-Kum* transgene, whereas half would only have one copy. If two copies are required to prevent gas-filling, this would explain why only half the expected number of heat-treated *btl>Kum*^{170} embryos gas fill (39% vs 80% in controls). Although, further exploration of this hypothesis could be achieved by introduction of a fluorescent conjoined, second and third chromosome balancer into the line, our data show that SERCA function is required in the embryonic trachea for normal tracheal maturation as manifest by normal rates of gas filling.

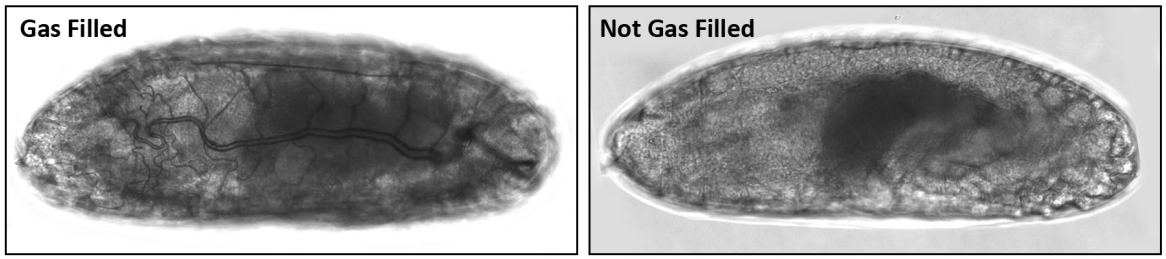

	Gas filling	No Gas Filling	Total
Btl>Kum Heated	**25**	**39**	**64**
w1118 Heated	**71**	**17**	**89**
Btl>Kum No Heat	**48**	**9**	**57**
w1118 No Heat	**62**	**8**	**70**

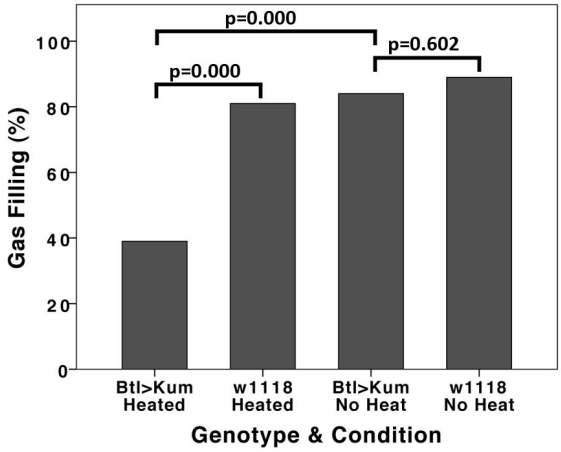

Figure 6.9 Embryos expressing *Kum*^{170} in tracheal cells have defects in tracheal gas filling

Upper panels: Transmitted light micrographs of stage 17 embryos with normal gas filling of the tracheal system (left panel) and failure to gas fill at the expected stage (right).

Table: Numbers of embryos displaying each tracheal gas filling phenotype at late stage 17 (*btl>Kum* vs. control) in heated and unheated groups.

Graph: Heated mutant embryos gas filled with a significantly lower frequency than controls (whether heated or not) and unheated mutants, with the latter three groups all gas filling at similar rates to one another (difference between control groups, p=0.196). Heated mutant embryos survived to late stage 17 with otherwise normal morphology.

6.6.2 Few embryos expressing Kum^{170} in the trachea have defects in luminal protein clearance

Having witnessed an impairment of gas filling, further aspects of tracheal maturation were investigated. Clearance of proteinaceous material from the tracheal lumen at stage 17 occurs prior to tracheal gas filling and this process has been elegantly interrogated using live imaging approaches (Tsarouhas et al., 2007). GFP labelled rat atrial natriuretic factor (ANF) was targeted to the trachea; its secretion and later endocytotic clearance followed using live fluorescent microscopy. ANF is a functionally inert, heterologous secretion marker: in *Drosophila* embryonic trachea, it has been shown to faithfully report the secretion and clearance of endogenous luminal proteins (Rao, Lang, Levitan, & Deitcher, 2001; Tsarouhas et al., 2007). This technique was employed to investigate effects of SERCA inhibition on luminal protein clearance. Strains carrying *btl-GAL4, UAS-ANF-GFP* were crossed to those carrying *UAS-*Kum^{170}: collected embryos were submitted to repeated heat treatments through tracheal morphogenesis, as described above. Embryos were mounted around stage 16 and imaged with live time-lapse fluorescent microscopy. The distribution of ANF-GFP was dynamically tracked over periods of up to eight hours.

Clearance of luminal ANF-GFP failed to occur only in a small number of *btl>*Kum^{170} embryos: this contrasted with the control group where clearance was always witnessed (Figure 6.10). Difference in tracheal protein clearance rate between groups was not statistically significant (Table 6.3). Normal levels of SERCA function in tracheal cells do not, therefore, appear to be critical for endocytotic protein clearance at the apical cell membrane. However, these data are complicated by a number of caveats: (i) residual SERCA function (unaffected by Kum^{170}) may have been sufficient for protein clearance to occur in the majority of embryos; (ii) findings may have been influenced by presence of one vs. two copies of the *UAS-*Kum^{170} transgene (discussed above); (iii) small sample sizes could predispose to type II error (failure to detect a real difference). However, given the marked difference in rates of tracheal gas filling seen with the same experimental conditions, and hence also similar caveats (Figure 6.9), there appears to be a difference in relative SERCA requirement for these distinct tracheal maturation processes.

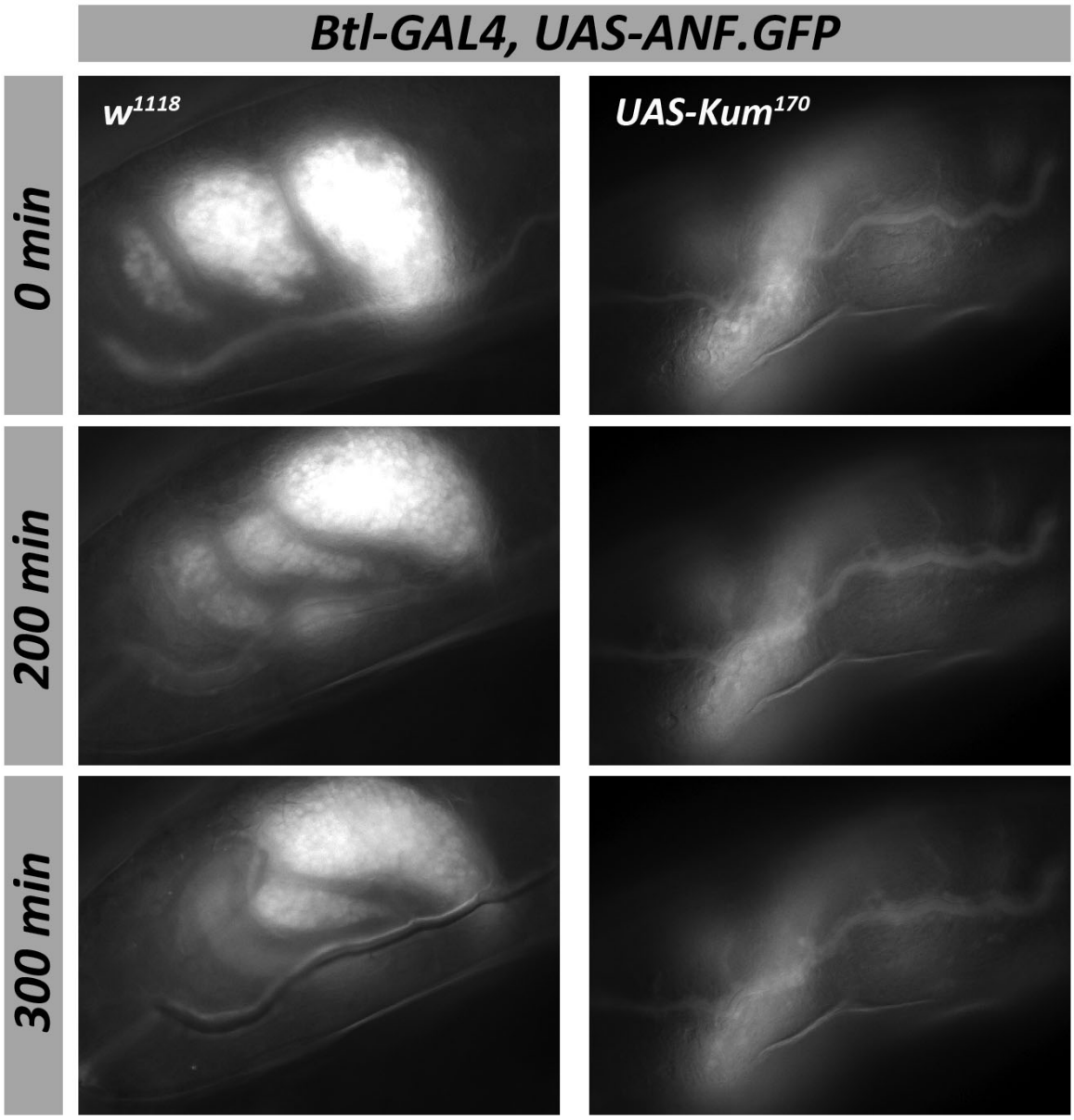

Figure 6.10 Few embryos expressing *Kum*^{170} in the trachea have defects in luminal protein clearance

Live fluorescent microscopy of embryos expressing *ANF-GFP* under the control of the *btl-GAL4* driver. The left hand panels show a control embryo (*w*^{1118}): ANF-GFP is cleared from the tracheal lumen by 200 minutes; followed by tracheal gas filling. All control embryos displayed normal protein clearance (n=12). Right hand panels show an example of the small number (3/17) of *btl>Kum*^{170} embryos failing to clear luminal protein: ANF-GFP remains in the tracheal lumen throughout the period of imaging. Considerable auto-fluorescence from embryonic gut rudiments is also evident.

Table 6.3 Frequency of embryonic tracheal protein clearance

p=0.2463	*btl>Kum*	*w*^{1118}
Protein clearance	14	12
No protein clearance	3	0
Total embryos	17	12

6.7 Discussion

In this chapter a number of approaches to genetically inhibit SERCA function in the embryo have been tested. These have targeted maternal and zygotic SERCA, throughout the embryo (homozygous *Kum* mutants), specifically in tracheal cells (*btl>Kum*) and a combination of the two (*Kum* and *btl>RNAi)*. Dynamic calcium imaging of cells carrying the *Kum* allele confirmed significant reduction in SERCA function. Despite this, all of these approaches failed to significantly perturb tracheal branching. In view of the potential for (and high likelihood of) residual functional protein with all these methods, it is not possible to conclude that SERCA function is unnecessary for embryonic tracheal branching. However, the grossly normal phenotype, despite significant SERCA inhibition, suggests this is a possibility.

What might account for the differences between *Drosophila* embryonic airway branching, that is able to tolerate significant SERCA inhibition, and murine lung branching, with its striking sensitivity to levels of SERCA function (Lansdale, Connell et al., 2010)? One hypothesis is that *Drosophila* embryos apparently lack an organised airway smooth muscle (ASM) layer, in contrast to mammals, who depend on ASM for critical biochemical and mechanical regulation of airway morphogenesis. SERCA is known to be essential for excitation contraction coupling in many systems and is enriched in *Drosophila* muscle (Harding & Hooper, 1996; Jesudason, 2009; Magyar et al., 1995; Mailleux et al., 2005). Could a lack of ASM in *Drosophila* explain this apparent insensitivity to SERCA inhibition? Given this hypothesis, the presence of organised ASM in *Drosophila* embryos was investigated by co-staining for both the trachea and muscle myosin heavy chain (Figure 6.11) (Kiehart & Feghali, 1986). The segmental pattern of muscle myosin fibres was in keeping with other reports, and there was no evidence of myosin being organised around the tracheal system (Bate, 1990). This was somewhat expected, given no previous suggestion of *Drosophila* ASM in detailed characterisations of the system (Manning & Krasnow, 1993). The plausibility of the above hypothesis relies on SERCA's role in mammalian airway branching being solely mediated through ASM function: this seems unlikely given findings of a similar, reversible, CPA induced abolition of airway branching in epithelial-only (lacking ASM) murine lung explants (courtesy of EC Jesudason, unpublished data).

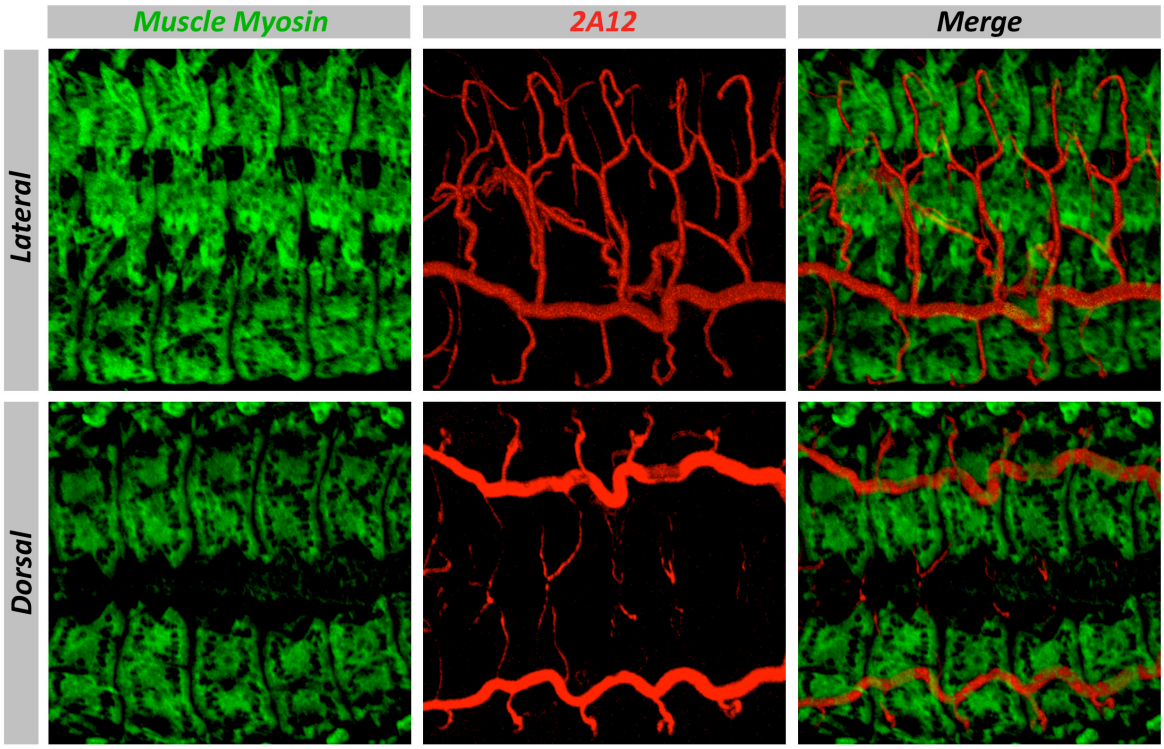

Figure 6.11 Muscle myosin expression in the embryo is not organised around the tracheal system

Confocal micrographs (3D projections of z-stacks) of wild-type stage 16/17 *Drosophila* embryos The embryonic tracheal lumen are stained with the mouse monoclonal antibody, 2A12 (DSHB, Iowa) in red: embryonic muscle is stained with a rabbit polyclonal antibody to muscle myosin heavy chain (Kiehart lab, Duke University, USA) in green. The dorsal and lateral aspects of the central metameres of the embryo are shown, as indicated.

Another fundamental difference between embryonic tracheal morphogenesis in *Drosophila* and airway branching morphogenesis in mammalian embryos, is the requirements for cell proliferation, which is absent from the former but critical in the later. Given SERCA's putative role as a cell cycle regulator, its essential requirement in mouse embryonic branching may be for cell proliferative events, which are not present in the fly (Legrand et al., 2001; Waldron et al., 1994). Further exploration of this hypothesis is performed later in Chapter 7.

In contrast to apparently normal tracheal branching, SERCA inhibition had a marked effect on tracheal maturation, causing a significant aberration of gas filling in late stage 17 (Figure 6.9). Gas filling occurs upon liquid clearance from the embryonic trachea: this process may be of high translational importance, given that human survival is dependent on an ability to rapidly clear the airway of liquid shortly after birth, and problems with this process are implicated in newborn disease (Jain & Eaton, 2006). Currently there is a relative dearth of understanding about the molecular regulation of these fascinating and translationally important events. In ongoing work, investigators have screened the *Drosophila* genome to understand the regulation of these processes (Samakovlis, 2010). Endocytosis is known to play the key role in clearing tracheal luminal proteins *prior* to liquid clearance and gas filling: there is some discordance however, about whether liquid clearance itself is mediated by endocytosis. The novel finding of SERCA as a regulator of liquid clearance/gas filling, (that may be endocytosis dependent) is interesting, and potentially significant, not least because artemisinins (potent anti-malarial drugs) have been shown to inhibit the *Plasmodium falciparum* SERCA orthologue (PfATP6) and markedly inhibit endocytosis (Eckstein-Ludwig et al., 2003; Hoppe et al., 2004). It therefore seems conceivable that SERCA's effects on tracheal liquid clearance in *Drosophila* may be mediated through changes in endocytosis. Contrasting with this is the finding that similar SERCA inhibition did not significantly impair clearance of tracheal luminal proteins, a process that is also dependent on endocytosis. These data therefore indicate that if tracheal liquid clearance/gas filling *is* dependent on endocytosis, these processes are distinct in mechanism from those of endocytotic protein clearance, already known to differ temporally. Further work will directly investigate the effects of SERCA inhibition on specific markers of endocytotic activity.

Another possible explanation for a failure of liquid clearance by SERCA deficient cells, is through disruption of apical membrane Ca^{2+} activated Cl^- ion transport: although not previously linked to tracheal liquid clearance *per se*, these protein channels have been implicated in determining embryonic tracheal size and are likely to be sensitive to changes in SERCA dependent Ca^{2+} levels (A Uv, Tang, & Cavoshi, 2009). Given Cl^- ion flux is a key determinant of mammalian lung liquid (both secretion and absorption), this hypothesis could partly explain a conserved role for SERCA from fly airway maturation events to murine lung morphogenesis (Olver & Strang, 1974; Saumon, 2000).

Chapter 7

SERCA FUNCTION IS ESSENTIAL FOR DORSAL AIR SAC PRIMORDIUM DEVELOPMENT IN *DROSOPHILA*

7.1 Introduction

Drosophila metamorphosis, the process transforming larvae into adult flies, is characterised by consumption of differentiated larval cells and formation of pupal and adult tissues from the proliferation and differentiation of imaginal cells; these tissue-specific progenitors are defined in embryogenesis, but remain quiescent until later larval life (Harbecke et al., 1996; Kylsten & Saint, 1997). During metamorphosis, respiratory organogenesis proceeds in order to meet new aerobic demands of tissues destined for the adult, whilst continuing to satisfy those of existing larval and pupal tissues: the tracheal system is entirely remodelled, a process beginning in the third larval instar (Manning & Krasnow, 1993; Whitten, 1980). Previously thought to exclusively involve imaginal cells, it is now known that this remodelling occurs when two distinct populations of tracheoblasts (dedicated imaginal progenitors and a set derived from previously differentiated larval cells that regain multi-potency), populate the scaffold of the existing larval tracheal system (Guha et al., 2008; T. Matsuno, 1990; Sato et al., 2008; Weaver & Krasnow, 2008).

7.1.1 The dorsal air sac primordium (ASP)

In the second thoracic tracheal segment (Tr2), a stereotypical structure buds close to a point of bifurcation of the first transverse connective branch, during the third larval instar, and extends posteriorly as part of the adepithelial layer of the imaginal wing disc (Figure 7.1A) (Sato & Kornberg, 2002). Known as the dorsal air sac primordium (ASP), this tubular structure further develops in the pupal period to form dorsal air sacs in the adult, the dilated reservoirs that juxtapose flight muscles, supplying them with oxygen (Sato & Kornberg, 2002). In contrast to tracheal remodelling, seen during metamorphosis when the larval system is used as a template, the ASP forms *de novo* from outgrowth of tracheal epithelial cells through the adepithelial layer. ASP development involves cell proliferation, cell migration and directed patterning events, leading to a distinct structure comprising a proximal 'stalk' and distal 'tip' (Figure 7.1B-D) (Cabernard & Affolter, 2005; Sato & Kornberg, 2002). Tracheal cells, retaining epithelial apico-basal polarity, migrate away from the tracheal cuticle to form an ASP apical lumen, filled with secreted proteins; this lumen expands through cell proliferation and migration.

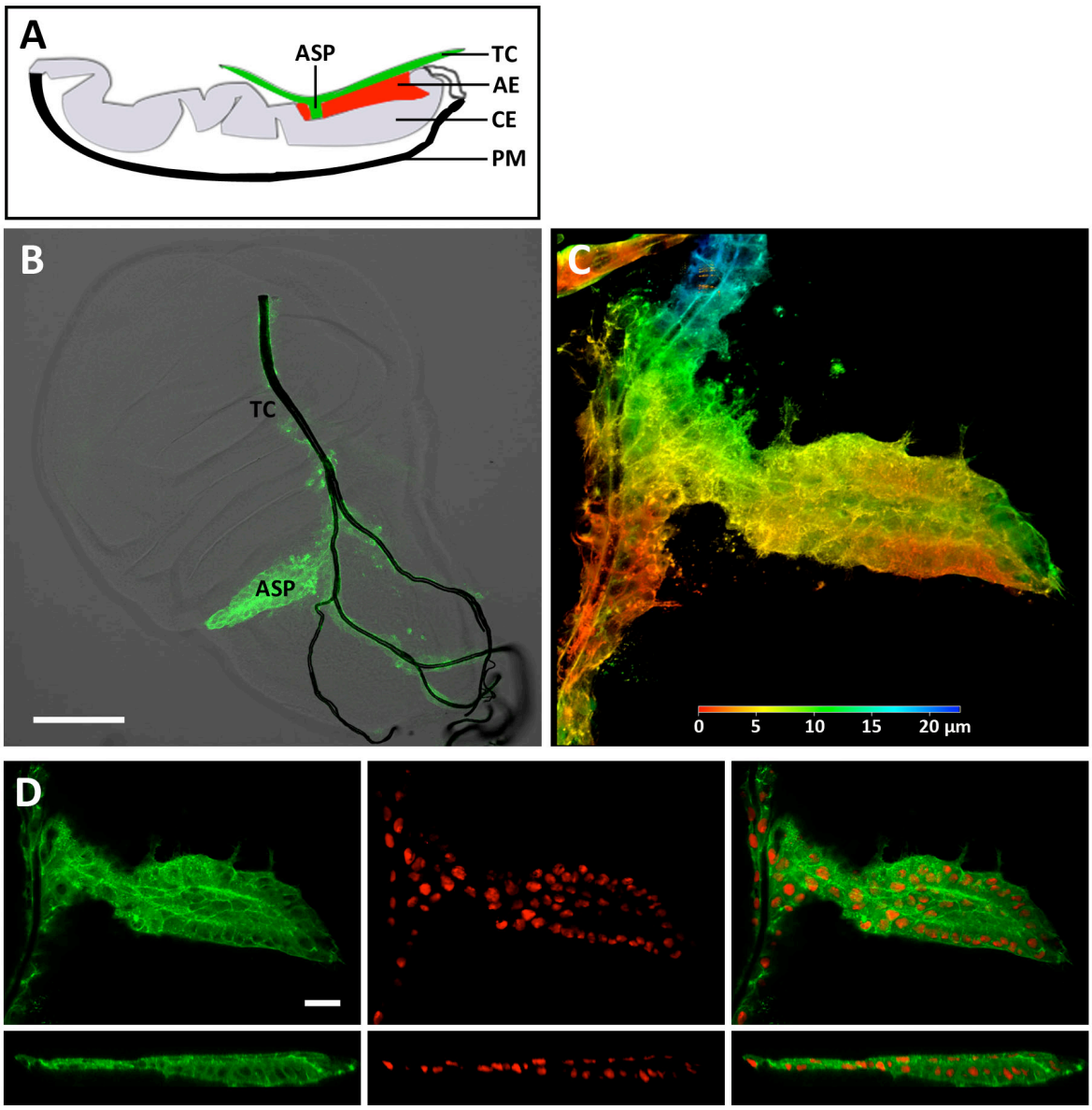

Figure 7.1 The dorsal air sac primordium (ASP) develops late in the third larval instar

Panel A: schematic diagram of a section through the length of the imaginal wing disc. The ASP buds off the first transverse connective (TC, green) tracheal branch; forming in the adepithelial layer (AE, red). The peripodial membrane (PM, black) and columnar epithelium (CE, grey) are also demonstrated. Panels B-D, Confocal micrographs of late third instar imaginal wing discs. Panel B: the position of the ASP within the wing disc is demonstrated, branching off the transverse connective tracheal branch (TC), close to a point of its bifurcation. Tracheoblasts are labelled with *btl-GAL4, UAS-act.GFP*. Scale bar indicates 100 µm. Panel C: 3D projection of z-stack slices through the depth of the ASP. The ASP is pseudo-coloured to illustrate depth of its structure (colour scale indicates depth measurements). Panels D: representative slices through the ASP (upper row) and lateral cross-sectional reconstructions (lower row): tracheoblasts are labelled with *UAS-act.GFP* (cell architecture, left) and *UAS-DsRed*^{NLS} (nuclei, middle): the merged image is also provided (right). Scale bar indicates 20 µm.

7.1.2 Molecular regulation of ASP development

In contrast to the wealth of information available regarding molecular regulation of embryonic airway morphogenesis, relatively little is known about ASP development. Key molecular players have been identified as the epidermal growth factor receptor (EGFR) and fibroblast growth factor (FGF) signalling pathways: the former is required for tracheoblast proliferation and survival, whilst the later, strictly for cell migration at the tip of the ASP (Cabernard & Affolter, 2005; Sato & Kornberg, 2002). In order to elicit their effects on morphogenesis, both pathways utilise the downstream, Ras/Mitogen-activated protein (MAP) kinase signalling cascade (Cabernard & Affolter, 2005). Interestingly, *pointed,* an ETS (E-twenty six) domain transcription factor that mediates Ras/MAP kinase signalling, is essential for FGF dependent cell migration, but not EGFR mediated cell survival and proliferation (Brunner et al., 1994; Cabernard & Affolter, 2005; O'Neill, Rebay, Tjian, & Rubin, 1994).

Cells at the tip of the ASP, marked by *escargot* expression, are key to morphogenic events; they send out actin-based cytoplasmic extensions (cytonemes, types of filipodia), known to be specific to individual signalling pathway proteins (Roy, Hsiung, & Kornberg, 2011; Sato & Kornberg, 2002). Cytonemes expressing the *btl* receptor extend out from the ASP, directly contacting *branchless (bnl)* expressing cells in the columnar epithelium of the wing disc: this *Drosophila* FGF-FGFR (*btl-bnl*) interaction is critical for driving cell migration in ASP morphogenesis. Spatial restriction of this FGF signalling, a key process in determining ASP morphology, is effected by a matrix metalloprotease, Mmp2: *mmp2* deficient ASPs display an extended tip territory, brought about by a failure of repression of FGF-ERK signalling by lateral inhibition pathways (Wang, Uhlirova, & Bohmann, 2010).

7.1.3 The ASP as a model of tubular organogenesis

Until now, this investigation has focussed on SERCA's role in *Drosophila* embryonic development, principally tracheal branching morphogenesis, but also elements of tracheal maturation. Studies of the embryonic trachea have contributed greatly to our understanding of branching morphogenesis and tube formation, but whilst these events are genetically homologous to mammalian airway development, they differ fundamentally: *Drosophila* embryonic tracheal

morphogenesis proceeds without cell division, a critical component of mammalian organogenesis. Investigators have suggested that ASP development, being the only recognised case of tubulogenesis in the fly characterised by cell division and directed morphogenesis, is a better system with which to model mammalian tubular organogenesis, such as that of the lung and kidney (Guha et al., 2008). This system was utilised to further interrogate SERCA's function in airway development.

7.2 Aims

In this chapter, ASP development is used to model mammalian prenatal airway morphogenesis and explore SERCA's role in these events. Effects of SERCA inhibition on the ASP are tested, with specific aims of determining:

(i) What is the effect of SERCA inhibition on ASP morphogenesis?

(ii) Does SERCA inhibition alter ASP cell proliferation or apoptosis?

(iii) How does SERCA inhibition influence cell fate in the ASP?

(iv) How are SERCA's effects on ASP morphogenesis mediated?

7.3 Characterising the dorsal air sac primordium

Prior to investigating effects of SERCA inhibition on ASP development, its normal structure was further characterised. The tubular structure of the ASP forms from directed enlargement of a 'sheet' of tracheal epithelial cells that retain apico-basal polarity to form a respiratory lumen (Cabernard & Affolter, 2005). This process has been elegantly demonstrated by others, but details of epithelial structure, including cell orientation, do not appear to have been well catalogued.

7.3.1 Development of the ASP epithelium

ASP tracheoblasts were dual labelled with nuclear and actin fluorescent proteins described in Chapter 4 (*btl-GAL4, UAS-act.GFP, UAS-DsRed*^{NLS}) and imaged with confocal microscopy. Discs-large (Dlg) staining was employed to aid characterisation of cell polarity. Throughout much of ASP development, cross-sectional reconstructions of z-stacks through its structure, indicate it is composed of a single layer epithelium, with cells arranged apico-basally around the primitive lumen (Figure 7.1). Here, more distal ASP tracheoblasts that are arranged in a layer abutting the columnar epithelium of the wing disc proper, appear columnar in shape themselves: those opposite, adjacent to the outermost surface of the disc, consistently appear more flattened in shape (Figures 7.1 & 7.2). Later on in ASP morphogenesis, just prior to pupation, a lumen proper can just be seen to be emerging; here it becomes evident that the epithelium surrounding this is more than one cell thick (Figure 7.2). The structure of this epithelium is interesting: cells lining the neo lumen appear flattened, almost squamous like in shape, whilst adjacent, more basal cells forming the remaining ASP structure, are more columnar (Figure 7.2). This appearance is reminiscent of respiratory epithelia in other species, providing further evidence that *Drosophila* ASP morphogenesis is a good model for studying airway development. Since structure and function are intimately related in much of biology, it seems plausible that apical epithelial cells have distinct functions, as well as a distinct structures, to those located more basally in the ASP. Given evidence of secreted luminal proteins early in ASP development, specialised apical membrane activity will be required to clear this prior to respiratory function (similar to embryonic tracheal maturation discussed in Chapter 6): more basal, columnar cells may play a more structural, supportive role in the ASP.

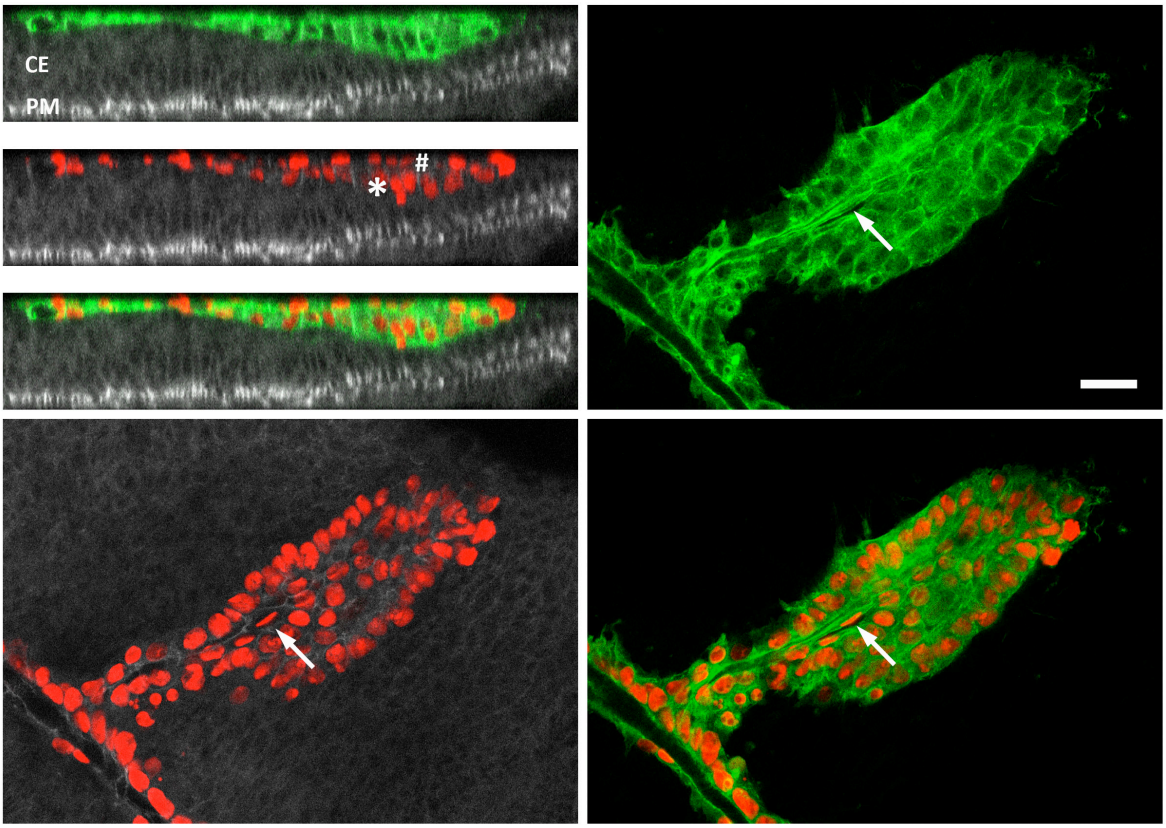

Figure 7.2 Development of the air sac primordium (ASP) respiratory epithelium

Confocal micrographs of late third instar imaginal wing discs. Tracheoblasts are labelled with *btl-GAL4, UAS-act.GFP, UAS-DsRed*^{NLS}: Discs-large (Dlg) antibody staining (DSHB, Iowa) is shown in grey in left panels. Upper left three panels: lateral cross-sectional reconstructions through the wing disc. The position of the ASP in the adepithelial layer is illustrated; the columnar epithelium (CE) of the wing disc proper and peripodial membrane (PM) are labelled. More distal ASP tracheoblasts in a layer abutting the columnar epithelium (labelled *), appear columnar in shape: those close to the outer aspect of the wing disc (labelled #) consistently appear flattened in shape. Remaining panels: section through an ASP present just prior to pupation. The emerging respiratory lumen is evident (labelled with arrows) and appears to be lined by flattened, squamous-like tracheoblasts: adjacent cells, located more basally, appear more columnar in shape. Scale bar indicates 20 μm.

7.4 SERCA is required for dorsal air sac primordium (ASP) development

7.4.1 Targeted SERCA RNAi disrupts ASP development

To test the requirement of SERCA function for ASP morphogenesis, flies carrying the SERCA RNAi construct, VDRC 4474 (discussed in Chapter 5), were crossed to those carrying *btl-GAL4, UAS-act.GFP*. Embryos were collected over short time periods and aged to the wandering third instar, at approximately 120 hours AEL. Wing discs were dissected from larvae and mounted for confocal imaging. ASP morphogenesis in wing discs from RNAi larvae was compared to that of controls (*w^{1118} x btl-GAL4, UAS-act.GFP*). ASP development was disrupted by *btl>RNAi* expression and a spectrum of phenotypes were witnessed (Figure 7.3). Most severely affected examples displayed ASPs that were limited to a number of disordered cytoneme like strands, arising from around the bifurcation of the transverse connective tracheal branch, with no real body of ASP cells. Less affected examples displayed smaller, similarly disordered looking ASPs, that were characterised by being widest at their proximal aspect (immediately adjacent to the trachea), therefore contrasting starkly with control ASPs displaying a thin 'stalk' proximally. The least affected examples appeared more in keeping with control ASPs, although the 'stalk' of the ASP never appeared entirely normal.

Further exploration of this phenotype was carried out by making use of previously characterised, more potent SERCA RNAi lines, created from recombination of RNAi 4474 with *Dicer2* or RNAi 107446 (Chapter 5). Given these lines were shown to induce lethality in the second instar when driven by *btl-GAL4* (Chapter 5), it was necessary to temporally restrict their expression, using temperature sensitive genetic elements. The *tubGAL80^{ts}* transgene, carried on the third chromosome was therefore combined with *btl-GAL4, UAS-act.GFP* on the second, using the crossing scheme detailed in Figure 7.4 (S. E. McGuire et al., 2003; S. E. McGuire et al., 2004). In order to restrict RNAi expression early in development, larvae were kept at 18°C until late in the second instar, when they were transferred to 29°C and aged to the wandering third instar. At 18°C, *tubGAL80^{ts}* represses the transcriptional activity of *btl-GAL4* and effects of the RNAi construct will be limited: at 29°C, *tubGAL80^{ts}* is not active, hence *btl-GAL4* will drive expression of SERCA RNAi in tracheal cells, specifically in the third

instar, during which time the ASP develops. It is also of note that *GAL4* activity (and hence also RNAi expression) will be boosted at 29°C, compared with the standard experimental temperature of 25°C (Brand & Perrimon, 1993; Duffy, 2002).

The more potent SERCA RNAi lines (described earlier) were crossed to *btl-GAL4, UAS-act.GFP; tubGAL80^{ts}*; temperature shifts instigated and ASP phenotype assessed as above. RNAi 4474 recombined with either *Dicer2* or RNAi 107446, resulted in a similar, but more consistently abnormal ASP phenotype, compared to RNAi 4474 alone (Figure 7.3). ASP morphology was always abnormal with no evidence of the 'stalk' and 'tip' phenotype that characterises the wild-type ASP; the SERCA deficient ASP was at its widest proximally, immediately adjacent to the trachea. The border of the ASP also appeared irregular, as opposed to the smooth edge seen in controls. Increased phenotypic consistency is likely to be due to a combination of increased potency of SERCA knockdown, higher *GAL4* activity at 29°C, and tight temporal control of RNAi action with GAL80: RNAi will mediate its actions solely in the third instar, during ASP development, contrasting with RNAi 4474 experiments, when the RNAi will have been active since embryogenesis.

Early in the third instar (approximately 80 hours AEL), the wild-type ASP buds from the trachea, being relatively small and displaying a wide based, rounded, approximately triangular appearance (Cabernard & Affolter, 2005). Possibility of the SERCA deficient, RNAi phenotype being solely explained by this early wild-type ASP appearance was discounted: larvae were carefully aged to at least 120 hours AEL and were seen to 'wander;' the RNAi phenotype was considerably disordered and roughened in appearance compared to the smooth, apico-basally ordered wild-type; many RNAi affected examples failed to display any significant ASP cellular substance other than isolated cytonemes.

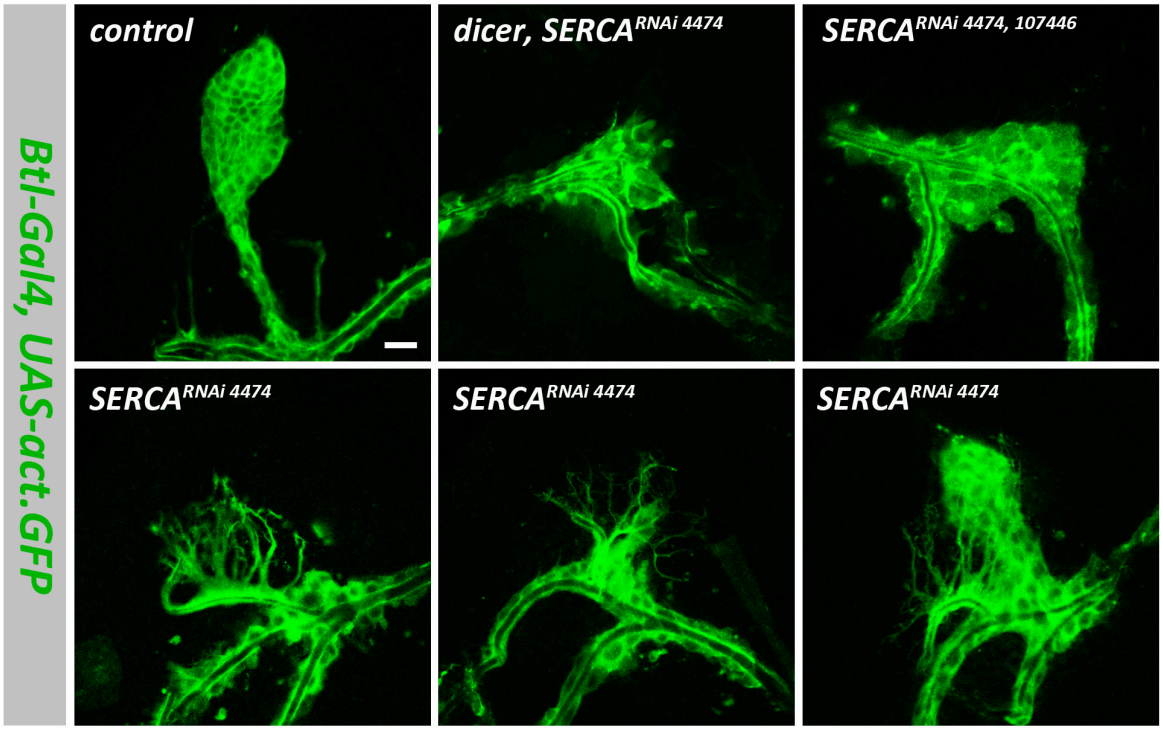

Figure 7.3 Targeted SERCA RNAi disrupts dorsal air sac primordium (ASP) development

Confocal micrographs of third instar larval imaginal wing discs. The tracheal system is demonstrated using *btl-GAL4* driven *UAS-actin.GFP*. Targeted SERCA inhibition is achieved using *btl-GAL4* driven *UAS-RNAi* constructs +/- *UAS-dicer2* and compared to a control (*btl-Gal4, UAS-act.GFP x* w^{1118}). Upper panels show representative phenotypes for the control, and RNAi 4474 recombined with either *Dicer2* or RNAi 107446 (as indicated). Lower panels illustrate the range of phenotypes seen with a weaker degree of knockdown (RNAi 4474 alone). Scale bar indicates 25 µm.

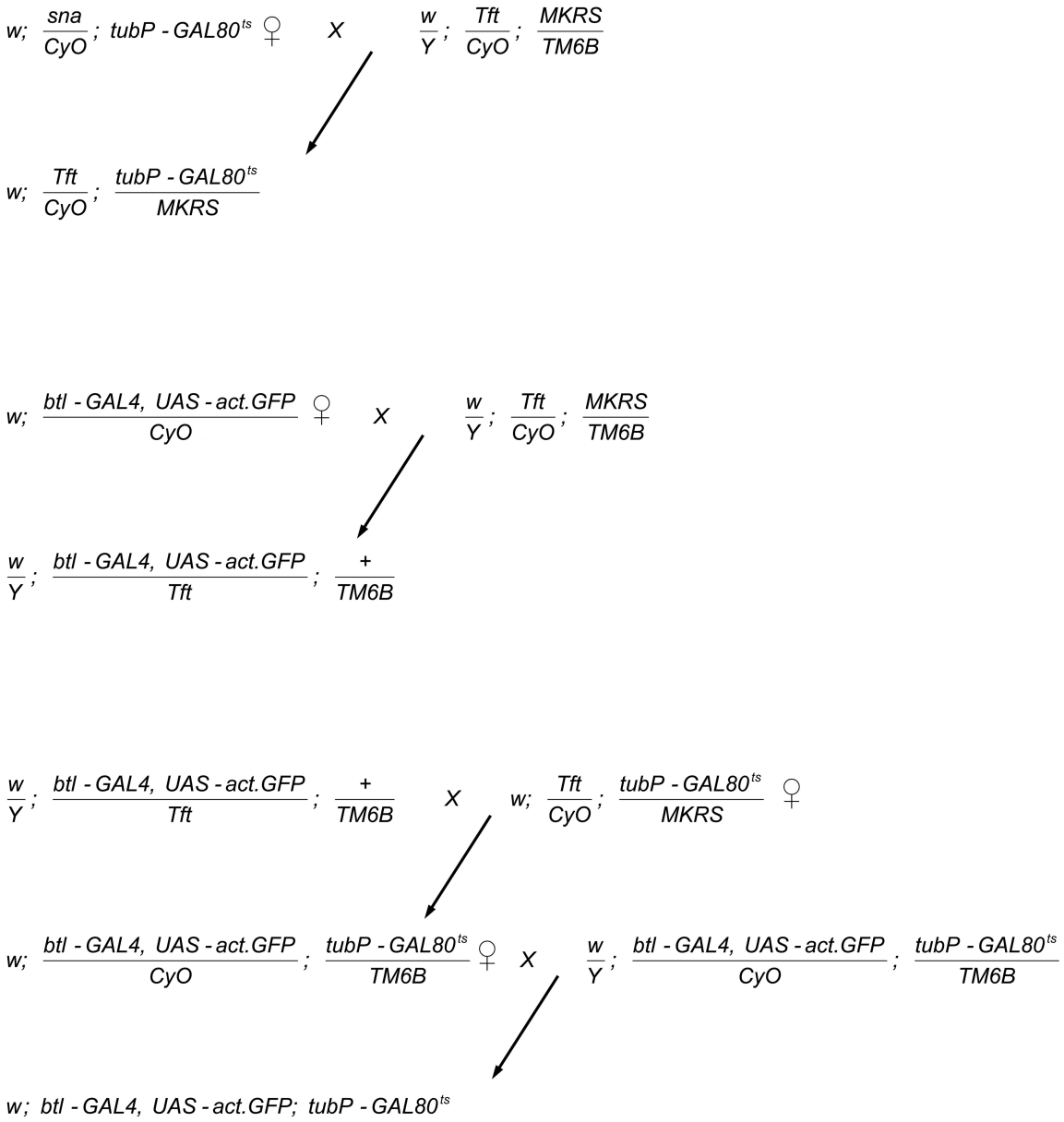

Figure 7.4 Genetic crossing scheme used to generate *Drosophila* to permit spatial and temporal restriction of transgene expression, along with tracheal cell fluorescent labelling.

The heat sensitive *GAL4* repressor, *GAL80*, under control of a *tubulin* promoter (*tubGAL80^{ts}*) on the third chromosome, was combined with *btl-GAL4, UAS-act.GFP* on the second chromosome.

7.4.2 SERCA RNAi decreases G-CaMP3 fluorescence in the ASP

Having previously shown SERCA RNAi to be effective at reducing SERCA function in embryos (Chapter 5), we confirmed that targeted SERCA RNAi expression was effective in the ASP *in vivo* by using the genetically encoded Ca^{2+} indicator (GECI) G-CaMP3. G-CaMP3 is an 'improved' GECI: it is brighter, possesses greater protein stability, and has a larger dynamic range and higher affinity for Ca^{2+} compared to previous versions (Tian et al., 2009). G-CaMP3 has been cloned to the pUAST vector and its targeted expression used to image Ca^{2+} in neurons of *Drosophila in vivo* (Brand & Perrimon, 1993; Tian et al., 2009; Xiang et al., 2010). In an attempt to quantify intracellular Ca^{2+} levels in cells of the ASP, G-CaMP3 expression was driven with *btl-GAL4* and confocal imaging of live imaginal wing discs undertaken, using a protocol adapted from that of Aldaz *et al* (Aldaz et al., 2010). SERCA RNAi 4474 was targeted to the ASP (*btl>RNAi*) and compared to controls (*btl>w^{1118}*).

The intensity of G-CaMP3 fluorescence was markedly and consistently lower in ASP tracheoblasts expressing RNAi 4474, compared to controls: mean +/- SEM fluorescent pixel intensity was 74.5 +/- 6.0 vs. 150.2 +/- 2.8 ($n \geq 6$ in each group, $p=0.000$) (Figure 7.5). Wing discs were imaged for periods up to 30 minutes: there was no suggestion of propagating Ca^{2+} waves in this system over such durations. At first glance, reduced G-CaMP3 emission indicates that intracellular Ca^{2+} concentration is lower in cells expressing RNAi. However, given that this is directly opposite to previous observations in this thesis (Chapter 5) and wholly inconsistent with published reports, this is almost certainly not the case (Abell et al., 2011; Raymond-Delpech et al., 2004; Zhang et al., 2006). The most likely explanation for these findings is that SERCA knockdown with RNAi alters the expression level of mature G-CaMP3 protein. G-CaMP GECIs are based on single fluorescent proteins and do not offer the benefits of ratiometric measurement; their emission is therefore dependent on expression level (Nakai et al., 2001). Given that SERCA is likely to play fundamental roles in post-translational modifications, e.g. protein folding, it is probable that significant SERCA knockdown with RNAi alters expression of the circular permuted G-CaMP molecule (Caspersen et al., 2000; Hojmann Larsen et al., 2001). Despite this limitation precluding accurate Ca^{2+} quantification, markedly reduced G-CaMP fluorescence does indicate that SERCA RNAi is having a substantial effect in cells

of the ASP. In view of previous confirmation of RNAi 4474 inducing specific SERCA knockdown in embryonic cells (Chapter 5), this effect is highly likely to be a result of similar, effective SERCA knockdown in ASP tracheoblasts.

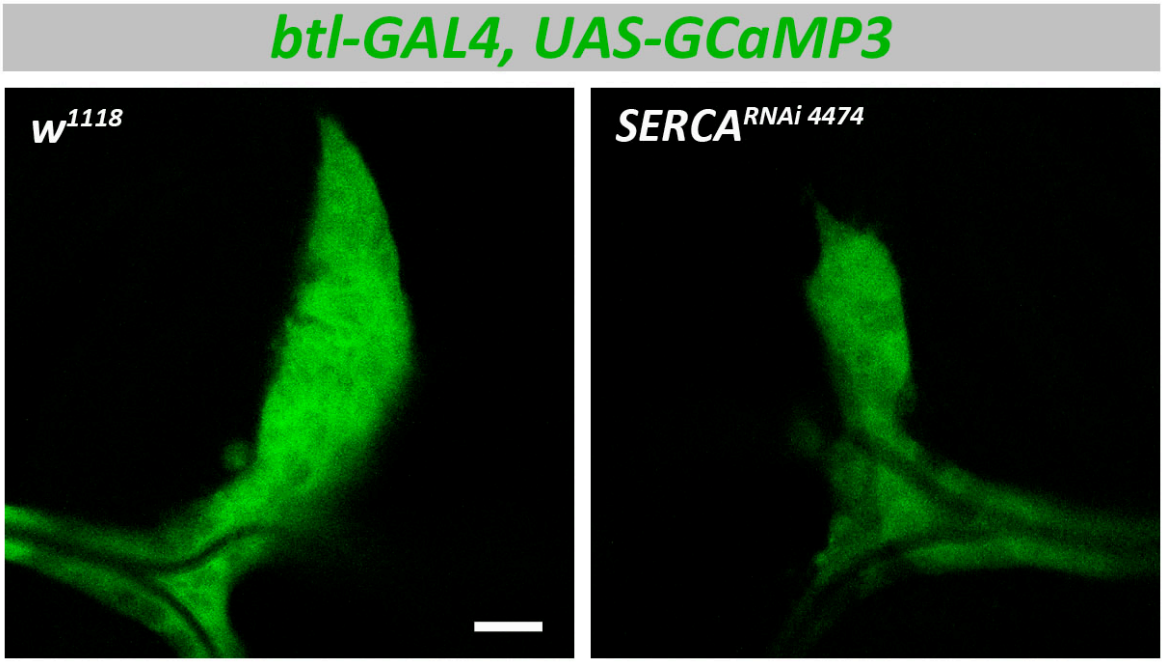

Figure 7.5 SERCA RNAi decreases G-CaMP3 fluorescence in the dorsal air sac primordium

Confocal micrographs of third instar larval imaginal wing discs. The genetically encoded calcium indicator G-CaMP3 (green) is expressed within cells of the dorsal air sac primordium (ASP) using *btl-GAL4*. Targeted SERCA inhibition is achieved using *btl-GAL4* driven *UAS-RNAi 4474* and compared to a control (w^{1118}). Scale bar indicates 20 µm.

7.4.3 Effects of SERCA inhibition on ASP development are dependent on number of deficient cells

To test whether effects on ASP development from SERCA knockdown are: (i) specifically due to SERCA deficient tracheoblasts; and (ii) dependent on the number of deficient cells, random, 'flip-out' clones were generated (Figure 7.6). In this technique, heat-shock induced FLP-recombinase removes a transcriptional-termination cassette that is inserted between a defined promoter and *GAL4*: in this case, *act>y>GAL4* was used (Duffy et al., 1998; Struhl & Basler, 1993). Random SERCA loss of function clones (expressing RNAi 4474) were produced, labelled with GFP (*UAS-GFP*), and the trachea/ASP labelled with *btl>moesin.RFP* (a construct that places moesin.RFP directly under the control of the *btl* promoter) (Ribeiro et al., 2004). ASP morphology was assessed in wing discs dissected from wandering third instar larvae, as above.

RNAi 4474 flies were crossed to those of genotype *hsFLP; act>y>GAL4, UAS-GFP; btl>moes.RFP* and the FLP-recombinase activated with a late second instar 37°C heat-shock (Wang et al., 2010). When relatively short heat-shocks were used (15-30 minutes), the ASP developed fairly normally (Figure 7.7), with a defined 'stalk' and 'tip' morphology being evident. GFP-labelled RNAi clones were seen at various points in the ASP; their distribution is considered later in Section 7.6.2. When larvae were subjected to 60 minute heat-shocks, ASP morphology was grossly disrupted; an abundance of GFP-labelled clones were evident, collected in a group at the point of tracheal branch bifurcation where the ASP should form. This phenotype was not dissimilar to that witnessed in *btl>RNAi* experiments described above (Figure 7.3). Given that longer duration heat-shocks will induce more cells to 'flip-out,' express RNAi, and be SERCA deficient early in ASP development (from the beginning of L3), it is apparent that SERCA deficient cell number is critical in determining ASP morphology. These data also indicate that the observed ASP phenotype is specifically due to ASP tracheoblasts being SERCA deficient, rather than being a more generalised effect of RNAi expression elsewhere in the tracheal system.

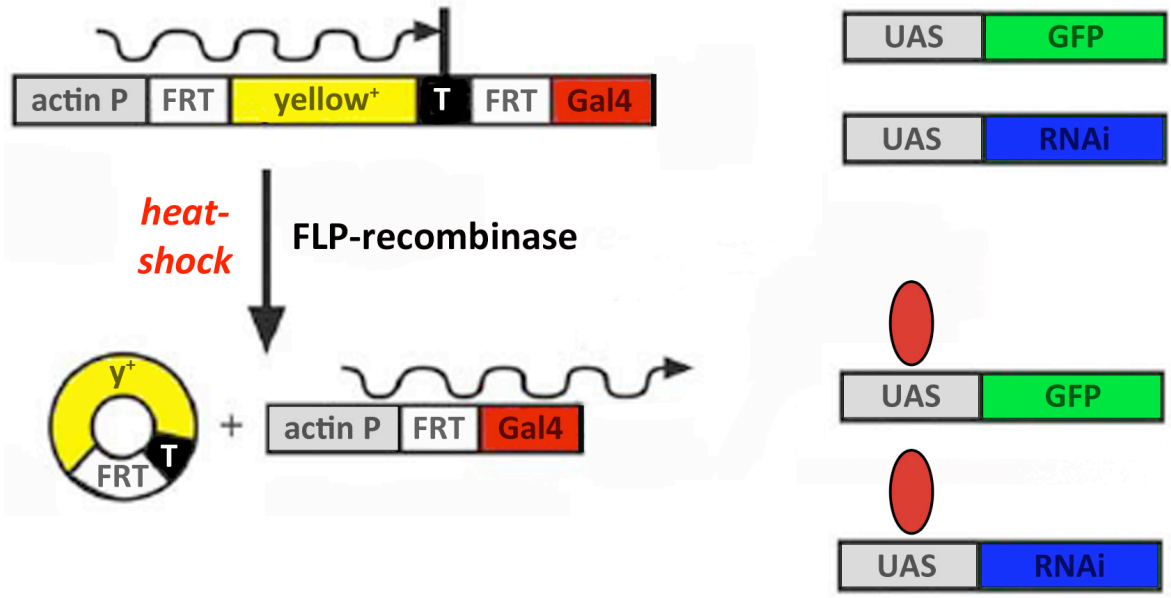

Figure 7.6 Schematic illustration of 'flip-out' clone generation

Two FLP recombination target (FRT) sites flank a wild-type copy of *yellow* and a transcriptional-termination cassette (T), inserted between an *actin* promoter and the *GAL4* coding region: transcription therefore terminates before *GAL4*. In cells where heat-shock treatment induces FLP-recombinase to catalyze recombination between the FRT sites, the *yellow+* termination cassette is excised and *GAL4* transcription occurs under the control of an *actin* promoter (*actin>GAL4*). In these cells, Gal4 can therefore bind to the UAS transgenes (GFP and RNAi in this case), resulting in their transcriptional activation.

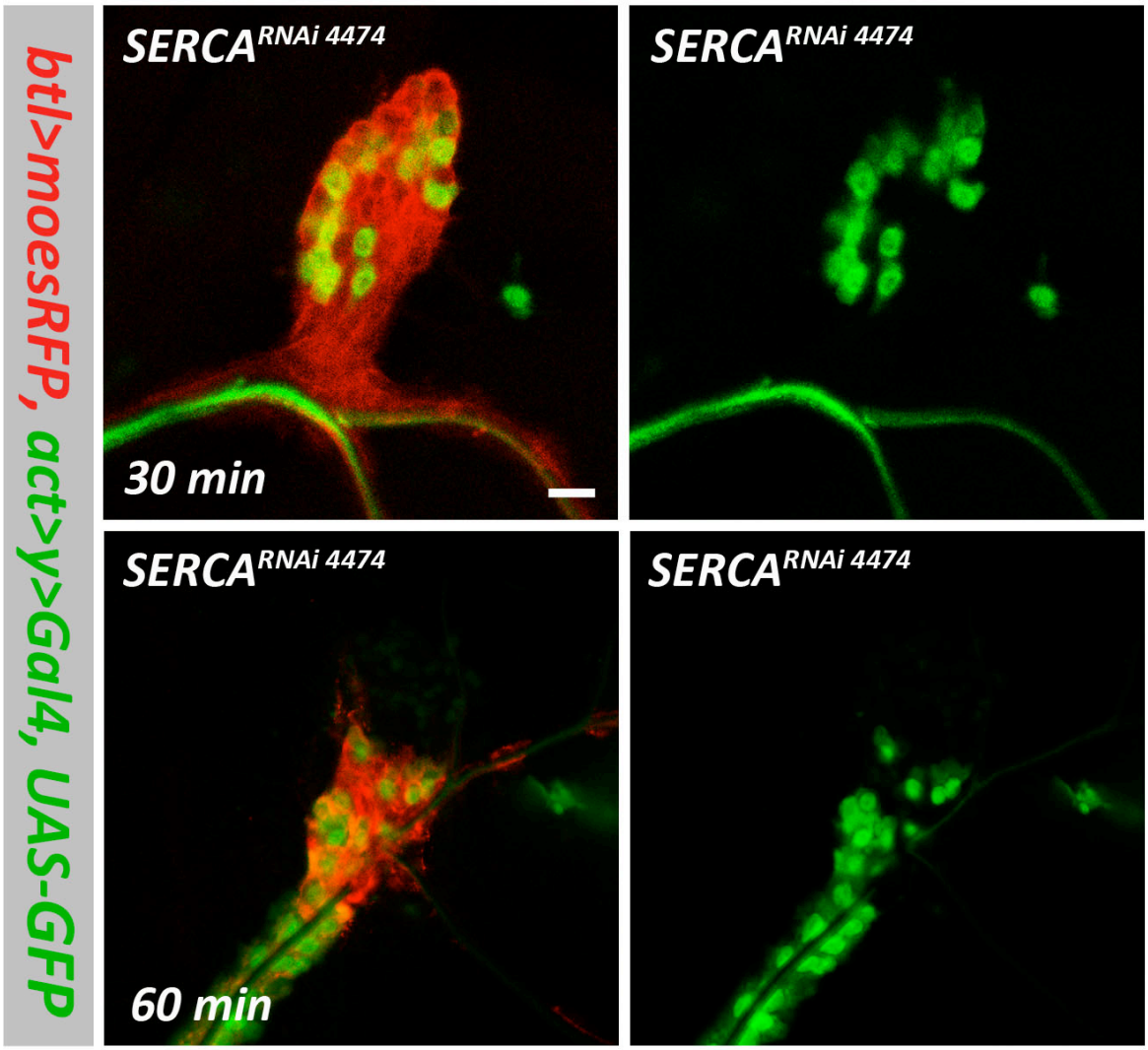

Figure 7.7 Effects of SERCA inhibition on dorsal air sac primordium (ASP) development are dependent on the number of deficient cells

Confocal micrographs (representative slice through the ASP) of third instar larval imaginal wing discs. Random SERCA RNAi flip-out clones were generated using *hsFLP* recombinase and *actin>y>GAL4*. Clones are marked using *UAS-GFP*. The tracheal system is demonstrated using *btl>moesRFP*. Larvae were submitted to a heat-shock of either 30 mins (Top Panels) or 60 mins (Bottom panels) at late second instar. Scale bar indicates 25 μm.

7.4.4 Presence of SERCA mutant clones in the ASP territory disrupts its development

To confirm that disrupted ASP morphology is due to SERCA loss of function, rather than a non-specific effect of RNAi, SERCA mutant clones were studied. The mosaic analysis with a repressible cell marker (MARCM) technique was exploited to randomly generate cells homozygous for the hypomorphic SERCA mutant allele *k08308ab*, and positively mark them with GFP (T. Lee & Luo, 1999, 2001; Periz & Fortini, 1999). MARCM relies on specific recombination events at FRT sites during mitosis, and produces cells that are either, homozygous for the mutation of interest, but lack *tubGAL80* (and hence express *act-GAL4, UAS-GFP*), or are homozygous for *tubGAL80* (therefore do not express *GAL4* dependent GFP) but lack the mutant allele (Figure 7.8) (Wu & Luo, 2006). In order to induce GFP marked mitotic clones and fluorescently label the ASP with a contrasting colour, *hsFLP, FRT42D, Ca-P60A*^{k08308ab} (SERCA mutation) and *btl>moes.RFP* were combined in one fly line and *FRT42D, tubGAL80, A>CD2>GAL4 and UAS-GFP* in another (Figure 7.9).

This text box is where the unabridged thesis included the following third party copyrighted material:

Wu JS & Luo L. (2006). A protocol for mosaic analysis with a repressible cell marker (MARCM) in Drosophila. Nature Protocols, 1(6), 2583-2589.

Figure 7.8 Schematic illustration of the mosaic analysis with a repressible cell marker (MARCM) technique

Illustration taken from Wu *et al.* 2007. Mitotic recombination occurs at specific FRT sites (black arrowheads), producing two daughter cells, each of which is homozygous for the chromosome arm distal to the FRT sites. Ubiquitous *GAL80* expression represses *GAL4* driven GFP expression (*UAS-GFP*) in cells without the mutation. Loss of *GAL80* expression in homozygous mutant cells results in specific expression of GFP.

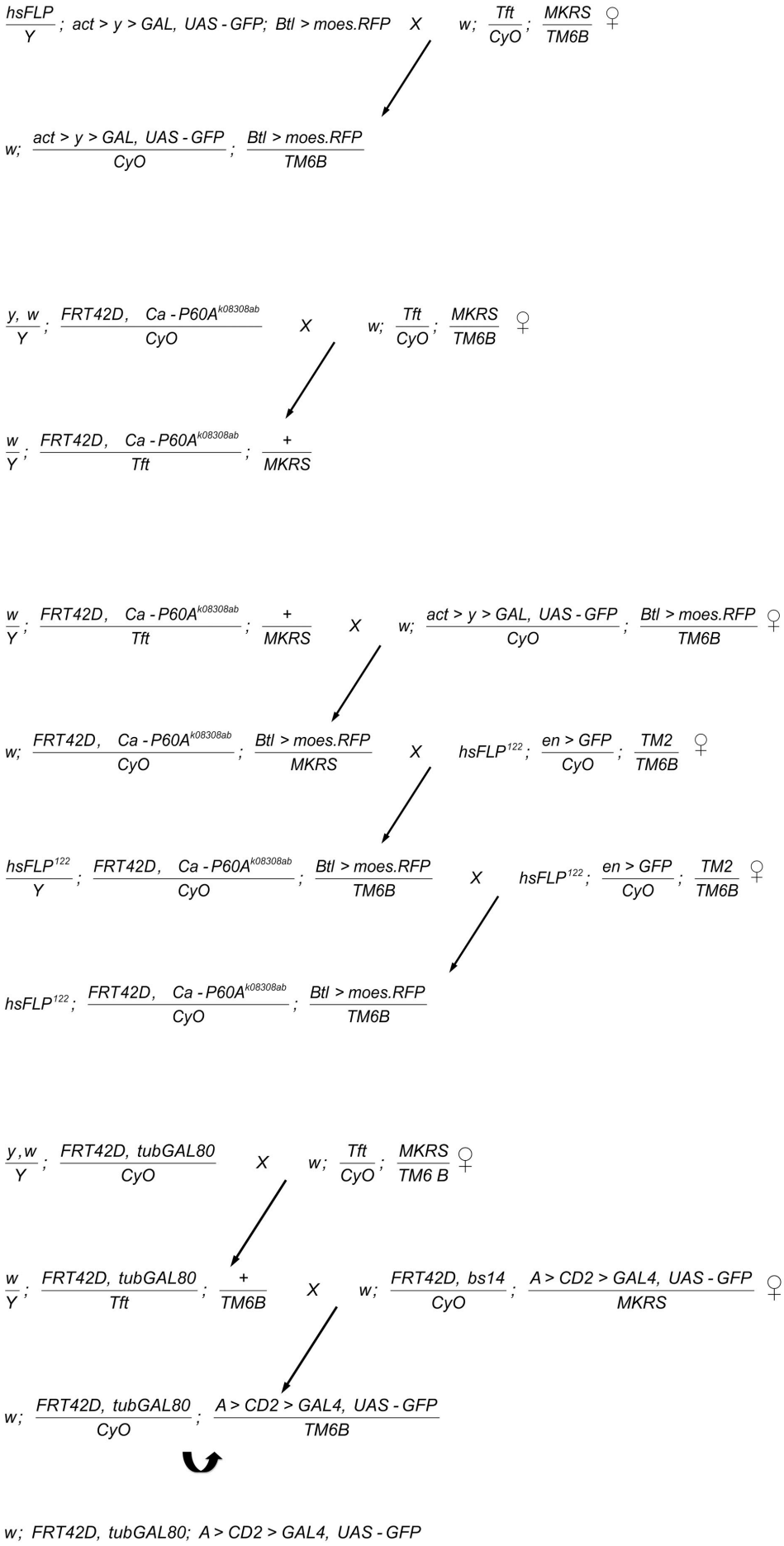

Figure 7.9 Genetic crossing scheme used to produce stable stocks of *Drosophila* for generation of positively labelled SERCA mutant clones.

Clones were produced in larvae by crossing *hsFLP^{122}; FRT42D, Ca-P60A^{k08308ab} / CyO; btl>moes.RFP / TM6B* with *FRT42D, tubGAL80; A>CD2>GAL4, UAS-GFP*. Embryos were collected over short time periods and allowed to develop to second instar, when FLP-recombinase was activated with a one hour 37°C heat-shock. Wandering third instar larvae were selected for dissection by presence of GFP marked clones in thoracic imaginal discs, using fluorescent microscopy. SERCA mutant clones were compared to controls (*FRT42D, whiteun-1*).

In both groups, few clones were seen within the ASP or tracheal system, compared to other regions of the imaginal wing disc (Figure 7.10). When sufficient SERCA mutant cells were present within or directly adjacent to the ASP, an abnormal morphology was evident (Figure 7.10). This proximally 'wide-based' appearance of the ASP approximately phenocopied the RNAi experiments above and contrasted to ASPs containing control clones, that appeared relatively normal (Figure 7.10). These findings indicate that when sufficient tracheoblasts lack SERCA function, the ASP is unable to develop normally, in-keeping with the results of *btl>RNAi and* RNAi flip-out clones described above. Collectively, these data indicate that SERCA function is essential for normal ASP development. It is important to acknowledge however, that in these MARCM experiments, although clearly abnormal ASP morphology was seen, there were relatively few clonal cells within the ASP itself, particularly when compared to the surrounding tissues. This observation raises the question of whether or not SERCA is required in the surrounding, *bnl* expressing cells for normal ASP development: this hypothesis has not been tested in this thesis. Importantly, RNAi experiments above (Figures 7.3 and 7.7) confirm that SERCA deficiency in the ASP alone is sufficient to induce the phenotype. The small size of clones (often single cells) relative to previous reports of MARCM in the ASP, is probably explained by different timings of FLP-recombinase activation: heat-shock was applied in the second instar here, as opposed to late in embryogenesis in other studies (Cabernard & Affolter, 2005; Chanut-Delalande et al., 2007).

Further analysis of mitotic clones was aided by Discs-large (Dlg) staining (4F3, DSHB); during imaging, z-stacks were taken through the full thickness of the disc. It was apparent that most clones within, or directly adjacent to the ASP, were small in size (usually single cells) and predominantly in a single layer at the interface of the ASP and columnar epithelium of the wing disc proper: clones in

other regions contrasted markedly, being much larger and extending through the depth of the disc (Figure 7.11). It is not entirely clear why this specific phenotype was evident in both control and mutant groups, but it appears most likely to be due to higher mitotic activity in these regions. Another explanation may be that clone cells are extruded from the ASP epithelium at this junctional region: this seems much less likely though, given that 'wild-type' clone cells displayed this pattern. Findings of negligible levels of apoptosis in ASP clones, discussed later in Section 7.5.2, also support the proposal that high rates of clone extrusion from the epithelium are unlikely.

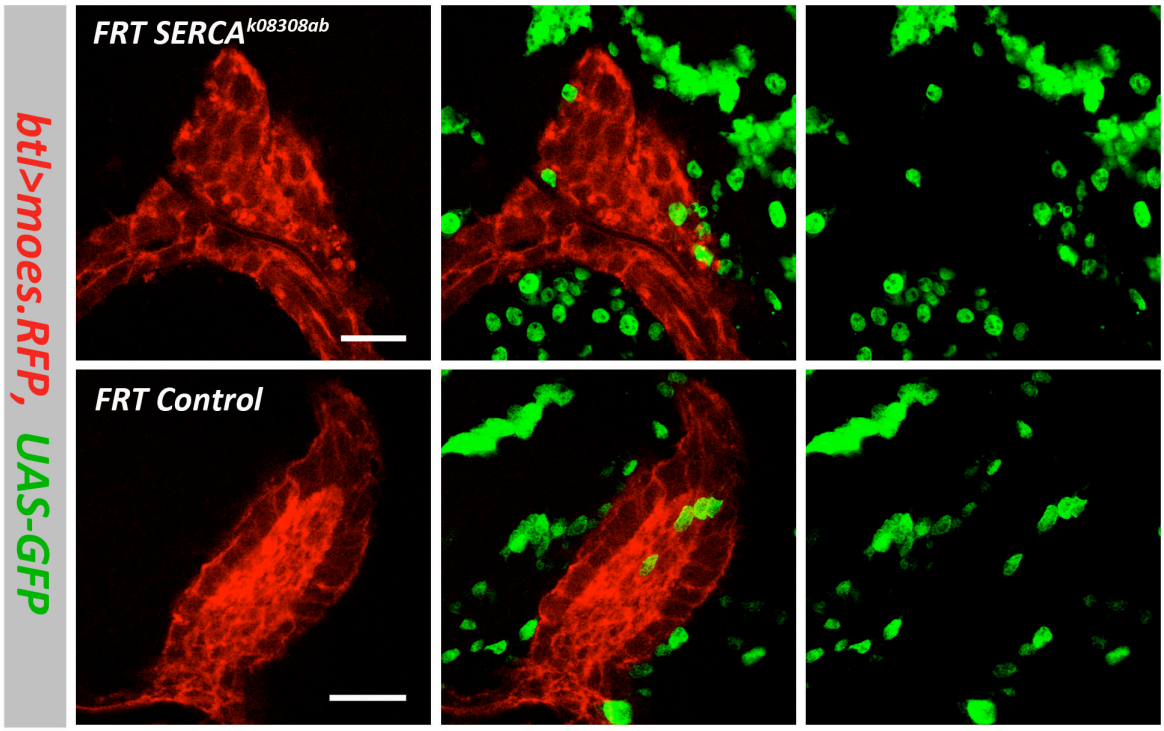

Figure 7.10 Presence of SERCA mutant clones in the dorsal air sac primordium (ASP) territory disrupts its development

Confocal micrographs (representative slice through the ASP) of third instar larval imaginal wing discs. The tracheal system is demonstrated using *btl>moes.RFP*. Random positively marked mitotic clones were generated using *hsFLP* recombinase and *FRT, GAL80, A>CD2>GAL4, UAS-GFP* crossed to either *FRT, SERCA*^{k08308ab} (mutant) or *FRT, whiteun-1* (control). Scale bar indicates 20 µm.

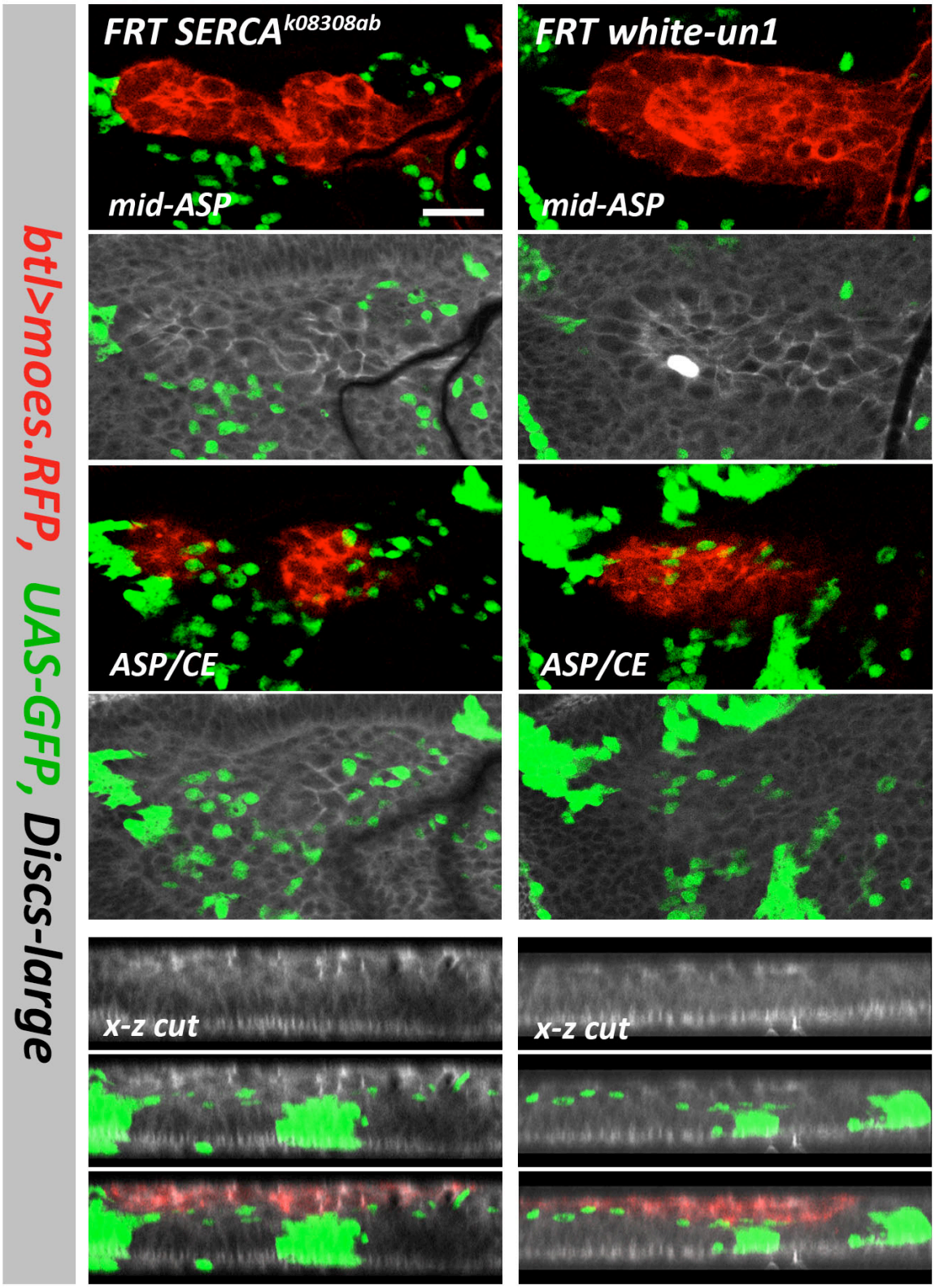

Figure 7.11 Control and SERCA mutant clones related to the air sac primordium (ASP) are small and most frequently found in a single layer at the interface of the ASP epithelium and columnar epithelium.

Confocal micrographs of third instar larval imaginal wing disc (representative slices from z-stacks). The tracheal system is demonstrated using *btl>moes.RFP*. Random positively marked mitotic clones were generated using *hsFLP* recombinase and *FRT, GAL80, A>CD2>GAL4, UAS-GFP* crossed to either *FRT, SERCA*^{k08308ab} (mutant) or *FRT, whiteun-1* (control). Discs large is labelled with 4F3 anti-discs large antibody (DSHB, Iowa) (grey). Upper four panels are slices at approximately the mid-point of the ASP (mid-ASP): middle four, at the interface of the ASP and the columnar epithelium (ASP/CE): lower panels are x-z reconstructions through the imaginal disc. Scale bar indicates 20 μm for each panel.

7.5 Effect of SERCA inhibition on ASP cell proliferation and apoptosis

Having demonstrated that SERCA loss of function results in a consistently abnormal ASP phenotype, it was hypothesised that this may be due, in part, to consequent changes in cell proliferation and / or apoptosis.

7.5.1 SERCA inhibition reduces ASP tracheoblast proliferation

To test the effect of SERCA knockdown on ASP cell proliferation, RNAi 4474 was targeted to the tracheal system and ASP, using the *btl-GAL4* driver and proliferating cells were labelled with Phospho-Histone H3 (Ser10) antibody (Cell Signaling, Inc), referred to as PH3 hereafter. Phosphorylation at serine 10 is a specific and highly conserved modification that occurs during chromosome condensation, during mitosis: PH3 staining is a reliable and widely used method to demonstrate mitosis (Hendzel et al., 1997). The tracheal system and ASP were labelled with *btl-GAL4, UAS-act.GFP*. The ASP was imaged through its full thickness, with z-stack confocal microscopy and compared to controls (*btl>w*^{1118}). Mitotic (PH3 positive) cells in each ASP were counted in both groups: the ASP was defined as the region distal to the transverse connective branch lumen, marked with GFP.

When SERCA knockdown was induced with *btl>RNAi,* mitotic cells were rarely seen within the ASP structure, contrasting markedly with control ASPs that frequently contained a number of mitotically active cells (Figure 7.12). When quantified, the difference in proliferating tracheoblasts between groups was highly significant (median 0 vs. 2.5, p=0.000, Figure 7.12). This finding indicates that when tracheoblasts lack SERCA function, they are unable to proliferate normally; consistent with studies in other systems and also with murine lung explant findings reported in Chapter 3 (Legrand et al., 2001; Waldron et al., 1994). Given ASP morphogenesis relies upon cell proliferation, inadequate tracheoblast proliferation may partly explain the disrupted ASP phenotype witnessed upon SERCA inhibition (Cabernard & Affolter, 2005; Sato & Kornberg, 2002). Given that SERCA deficient ASPs display abnormal shape as well as size, it seems likely that abnormalities in cell migration and / or patterning also play a role in this phenotype (discussed in Section 7.6.2).

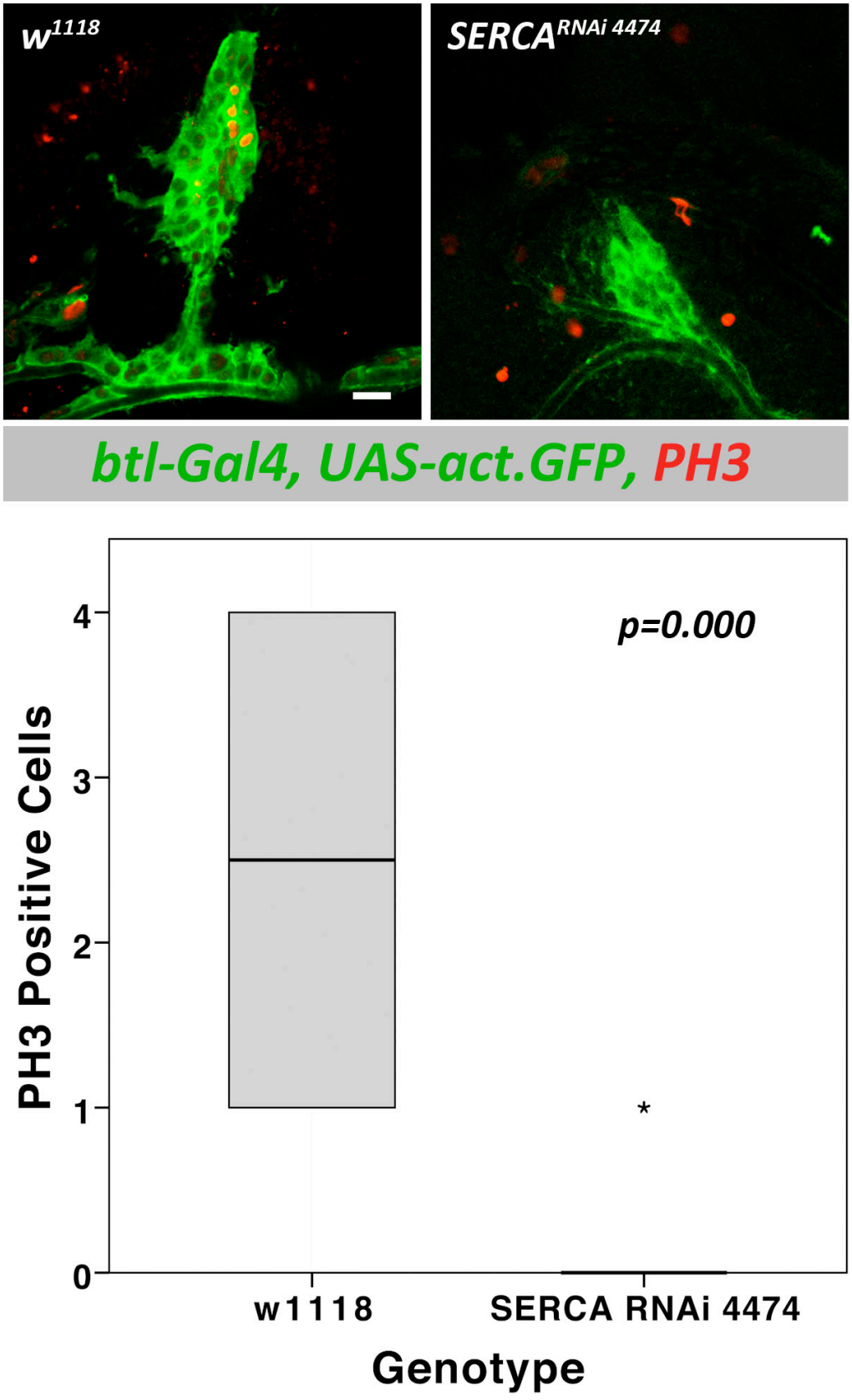

Figure 7.12 SERCA inhibition reduces air sac primordium (ASP) tracheoblast proliferation

Upper panel: Confocal micrographs of third instar larval imaginal wing discs (representative slices). The tracheal system is demonstrated using *btl-GAL4* driven *UAS-actin.GFP*. Mitotic cells are labelled with anti-phospho-Histone H3 (ser10) antibody (Cell Signalling Technology) SERCA inhibition is achieved using *btl-GAL4* driven RNAi 4474 and compared to controls (w^{1118}).

Lower panel: Mitotic cells per air sac (median and IQR) for RNAi and control groups. Difference between groups is statistically significant, p=0.000. n=18 in both groups.

7.5.2 SERCA inhibition does not affect apoptosis in the ASP

To test the effect of SERCA knockdown on ASP cell apoptosis, cells were labelled with Cleaved Caspase-3 (Asp175) antibody (Cell Signaling Inc.). Caspase-3 plays a key role in the execution phase of apoptosis, its active form being responsible for proteolytic cleavage of important cellular proteins (Fernandes-Alnemri, Litwack, & Alnemri, 1994). Activated caspase-3 staining is a specific and widely used method to detect apoptotic cells. Caspase-3 staining of imaginal wing discs from larvae with targeted SERCA knockdown (*btl>RNAi*) was compared to controls (*btl>w*^{1118}), and also carried out in animals containing SERCA mutant clones (MARCM), as described earlier. ASP phenotype was assessed as previously indicated.

In all groups, apoptotic cells were almost never seen in the ASP or tracheal system (Figure 7.13). From a total of 42 wing discs imaged, only one demonstrated a single apoptotic cell in the ASP. To confirm that Caspase-3 staining was efficiently detecting apoptotic cells, a positive control was analysed: a region of the disc known to have higher rates of apoptosis at this stage, the wing/notum border was used (Milan, Campuzano, & Garcia-Bellido, 1997). Strong staining of compact, rounded cells was evident in the positive control group, confirming efficacy of the staining protocol (Figure 7.13). These data indicate that apoptosis does not play an important role in dictating ASP dysmorphogenesis in SERCA deficient environments.

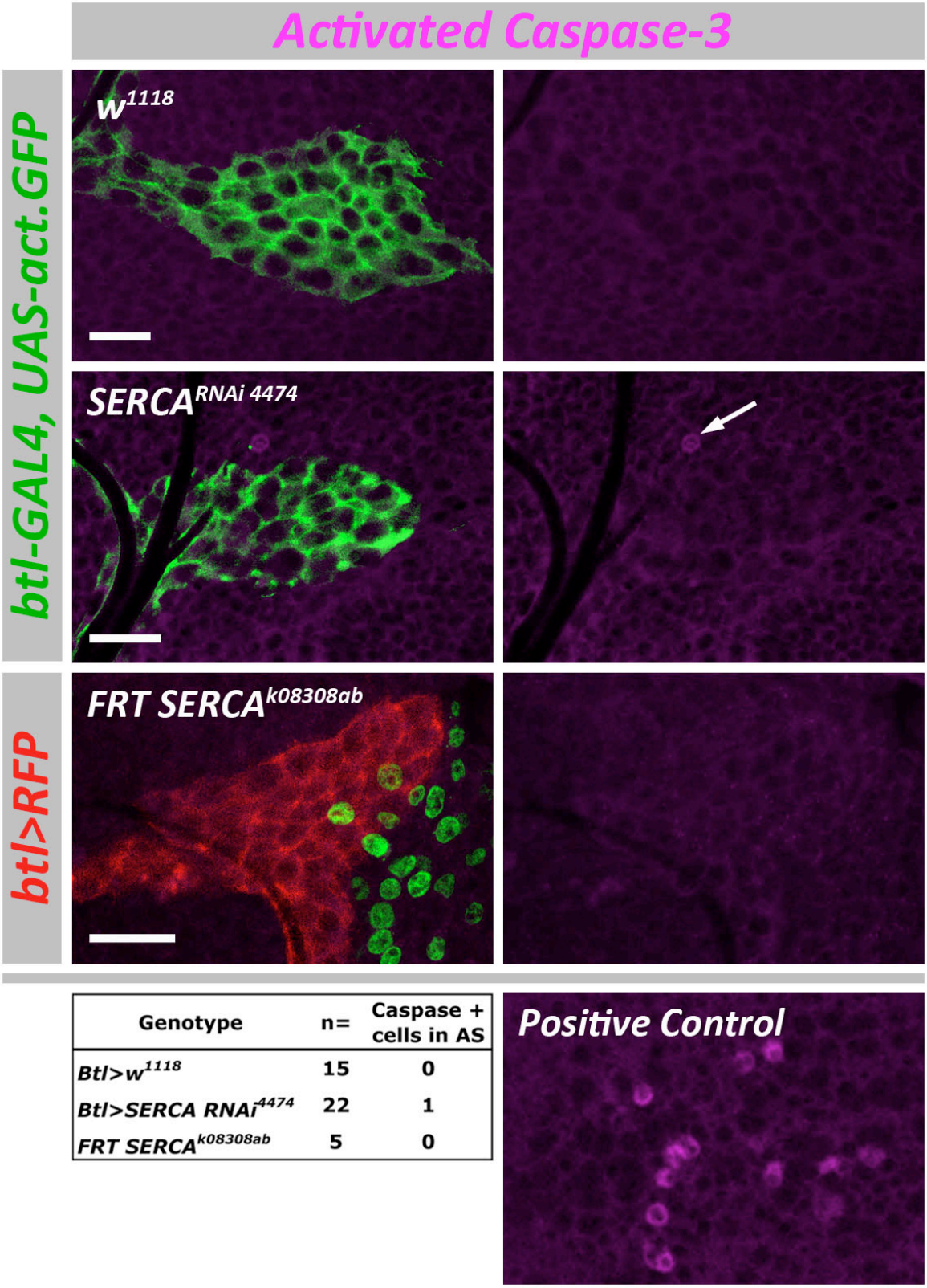

Genotype	n=	Caspase + cells in AS
Btl>w^{1118}	15	0
Btl>SERCA RNAi^{4474}	22	1
FRT SERCA^{k08308ab}	5	0

Figure 7.13 SERCA inhibition does not affect apoptosis in the air sac primordium (ASP)

Confocal micrographs of third instar larval imaginal wing discs. The tracheal system is demonstrated using *btl-GAL4, UAS-actin.GFP* or *btl>moes.RFP*. Upper row: control ASP. Second row: targeted SERCA inhibition with *btl-GAL4* driven RNAi 4474. Third row: random *Ca-P60A^{k08308ab}* mutant mitotic clones (MARCM). Clones are marked using *UAS-GFP*. Apoptotic cells are labelled with Cleaved Caspase-3 (Asp175) antibody (Cell Signaling Technology, Inc.), shown in magenta. The white arrow demonstrates an apoptotic cell outside of the air sac. The scale bars represent 20 μm for each row. Table illustrates the number of biological repeats in each group and number of activated caspase-3 positive cells seen per ASP. Positive control confirms efficacy of apoptotic cell labelling.

7.6 Effect of SERCA inhibition on ASP cell fate

To explore the effect of SERCA inhibition on ASP tracheoblast fate, random 'flip-out' clones were produced, as described above (SERCA RNAi 4474 vs. control). Given that clones were frequently seen to be confluent, making determination of individual clone identity difficult, a shorter, 15 minute heat-shock was employed in late second instar larvae, to active FLP-recombinase in fewer cells. In view of previous findings (Figure 7.7), this relatively small number of 'flipped' cells ensured that ASP morphogenesis proceeded normally: individual SERCA deficient cells were in an otherwise normal, 'wild-type' background.

7.6.1 Similar proportions of ASPs contained SERCA RNAi or control 'flip-out' clones

Firstly, the proportion of ASPs in each group that contained any clonal cells was determined. Larvae that apparently contained GFP marked clones in thoracic imaginal discs were selected for dissection under fluorescent microscopy. Once imaginal wing discs were mounted and imaged with confocal microscopy, the proportion with clones in the ASP was determined. There was no significant difference in proportion of ASPs containing clone cells in the SERCA RNAi or control group (Table 7.1). This indicates that the process of clone formation itself is not unduly influenced by SERCA deficiency. It also confirms that SERCA deficient cells do not appear to be eliminated from the ASP epithelium to any significant degree: findings supported by absence of any significant levels of apoptosis (Figure 7.13).

Table 7.1 Proportion of air sac primordia (ASPs) containing clone cells.

Genotype	Clones in dorsal air sac primordium (ASP)		Total
	Yes	No	
RNAi 4474	13	22	**35**
w^{1118}	12	12	**24**
Total	**25**	**34**	***p=0.423***

7.6.2 SERCA deficient cells rarely populate the ASP tip domain

The distribution of clone cells within the ASP was determined by arbitrarily dividing it into three distinct domains: the 'stalk' being most proximal, the 'mid-zone' and the 'tip' most distally (Figure 7.14). These distinctions were based on observations of previous studies that demonstrated an *escargot* defined tip territory occupying approximately one third of the wild-type ASP (Wang et al., 2010). GFP-labelled clone cells in each domain were counted for RNAi 4474 and w^{1118} groups and expressed as a ratio of total clone cells: the nuclei of all cells was labelled with TO-PRO-3 (Invitrogen) to aid cell counting.

The distribution of SERCA deficient, RNAi clones was markedly different to that of controls (Figure 7.14). SERCA RNAi clones were significantly less likely to be in the ASP tip domain than control cells ($p=0.002$): they were significantly more frequently found in the stalk region ($p=0.006$). There was no significant difference between RNAi and control groups in the proportion of cells found in the mid-zone of the ASP ($p=0.310$). These data indicate that SERCA deficient cells have their fate restricted and are frequently unable to populate the ASP tip. Adoption of tip position in the ASP has previously been studied as an indicator of cell migratory behaviour: in approximately 70% of ASPs, wild-type cells labelled with MARCM techniques are known to contribute to the tip domain (Cabernard & Affolter, 2005; Chanut-Delalande et al., 2007). Although slightly different methods of assessment have been used here, findings of SERCA deficient cells being significantly less likely to reach the tip are largely comparable to those in studies demonstrating essential roles for FGF and Ras/MAP kinase signalling, as well as other genes such as *Mhc* and *stam* (Cabernard & Affolter, 2005; Chanut-Delalande et al., 2007). SERCA function therefore appears essential for normal ASP tracheoblast migration.

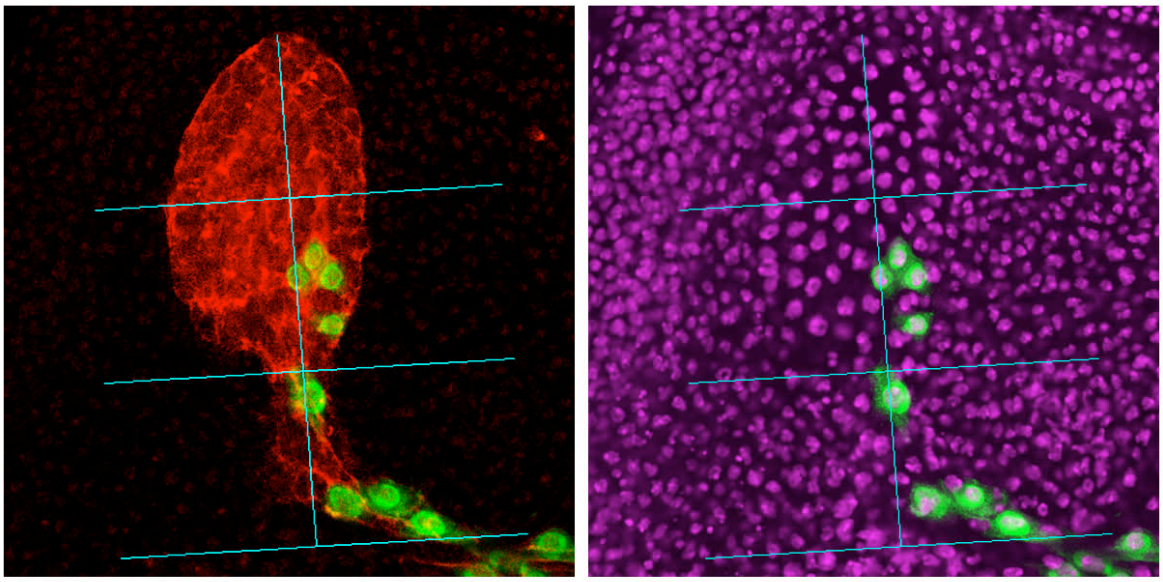

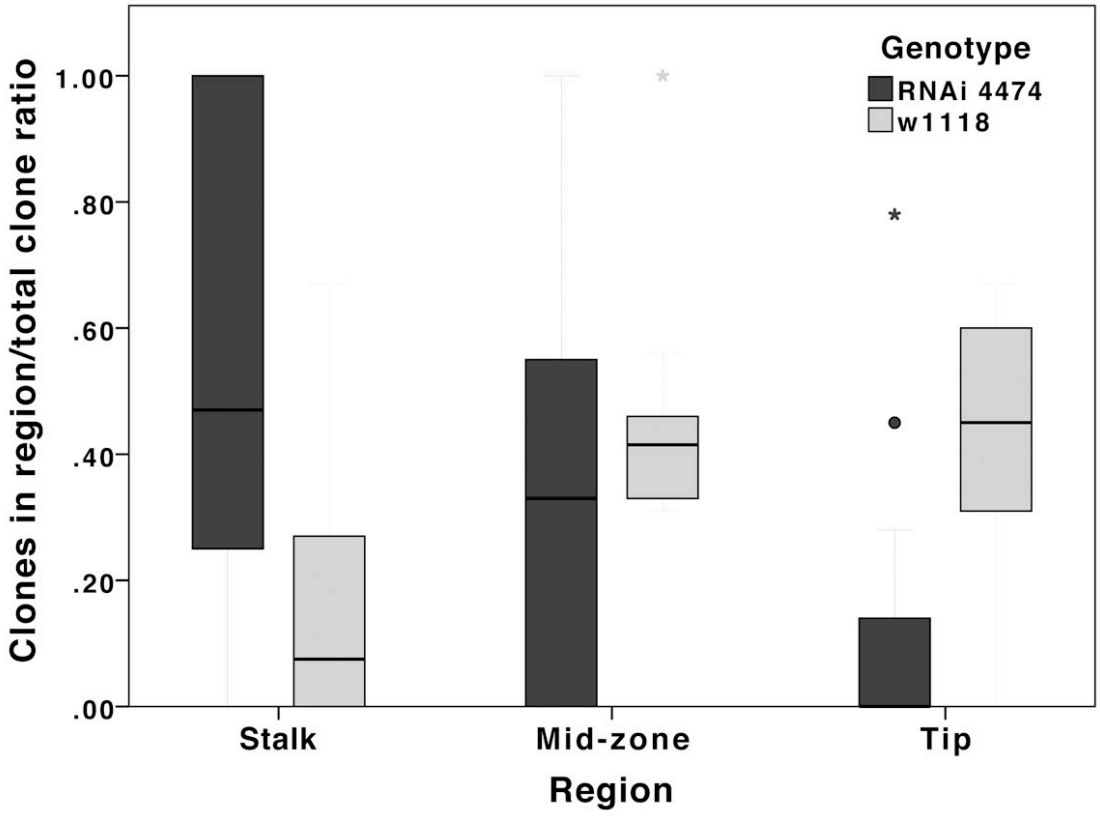

Figure 7.14 SERCA deficient cells rarely populate the air sac primordium (ASP) tip domain

Upper panel: confocal micrographs (representative slice through the ASP) of third instar larval imaginal wing discs. Random SERCA RNAi or control (*w1118*) flip-out clones were generated using *hsFLP* recombinase and *actin>y>GAL4*. Clones are marked using *UAS-GFP*. The tracheal system is demonstrated using *btl>moesRFP*. All nuclei are labelled with TO-PRO-3 (Invitrogen, shown in magenta) to aid cell counting. The air sac is divided into 3 regions of equal length (stalk, mid-zone and tip).

Lower panel: Proportion of flip out clone cells found per region of ASP (median and IQR) for RNAi and control groups. n=14 air sacs in both groups.

7.6.3 SERCA deficient ASP clones comprise fewer cells

Given findings of reduced levels of mitosis in SERCA deficient ASPs (Figure 7.12), the ability of these cells to replicate was further investigated. The relative sizes of SERCA RNAi and control flip-out clones was determined by counting the number of individual cells in each clone 'patch.' Clones were induced and assessed in the same way as for clone distribution experiments discussed above: individual clones were defined as a 'patch' of GFP labelled cells in continuity with each other and surrounded by non-GFP labelled cells.

SERCA deficient clones were significantly smaller in size than controls: median (IQR) number of GFP labelled cells in clone patches was 2 (3) vs. 6 (19), p=0.001 (Figure 7.15). Given the likelihood of the largest patches of GFP labelled cells actually representing two or more clones becoming confluent, a sub-analysis was carried out of those clones with less than 12 cells, after reviewing the distribution of raw data, plotted in clone size frequency histograms (Figure 7.15) Despite this sub-analysis, the difference in clone size remained significantly different between groups (2 [2] vs. 5 [5], p=0.000) The ability of clones to expand during development relies on proliferation and clone size will be inversely related to cell-doubling time. SERCA RNAi clones were significantly smaller and hence SERCA deficient cells appear to have prolonged cell-doubling times. These data are entirely in keeping with those from PH3 staining in SERCA RNAi expressing ASPs (Figure 7.12) and CPA treated murine lung experiments (Chapter 3). Furthermore, these novel *in vivo* findings lend further credence to previous *in vitro* studies and confirm SERCA function is required for normal cell proliferative events (Legrand et al., 2001; Waldron et al., 1994).

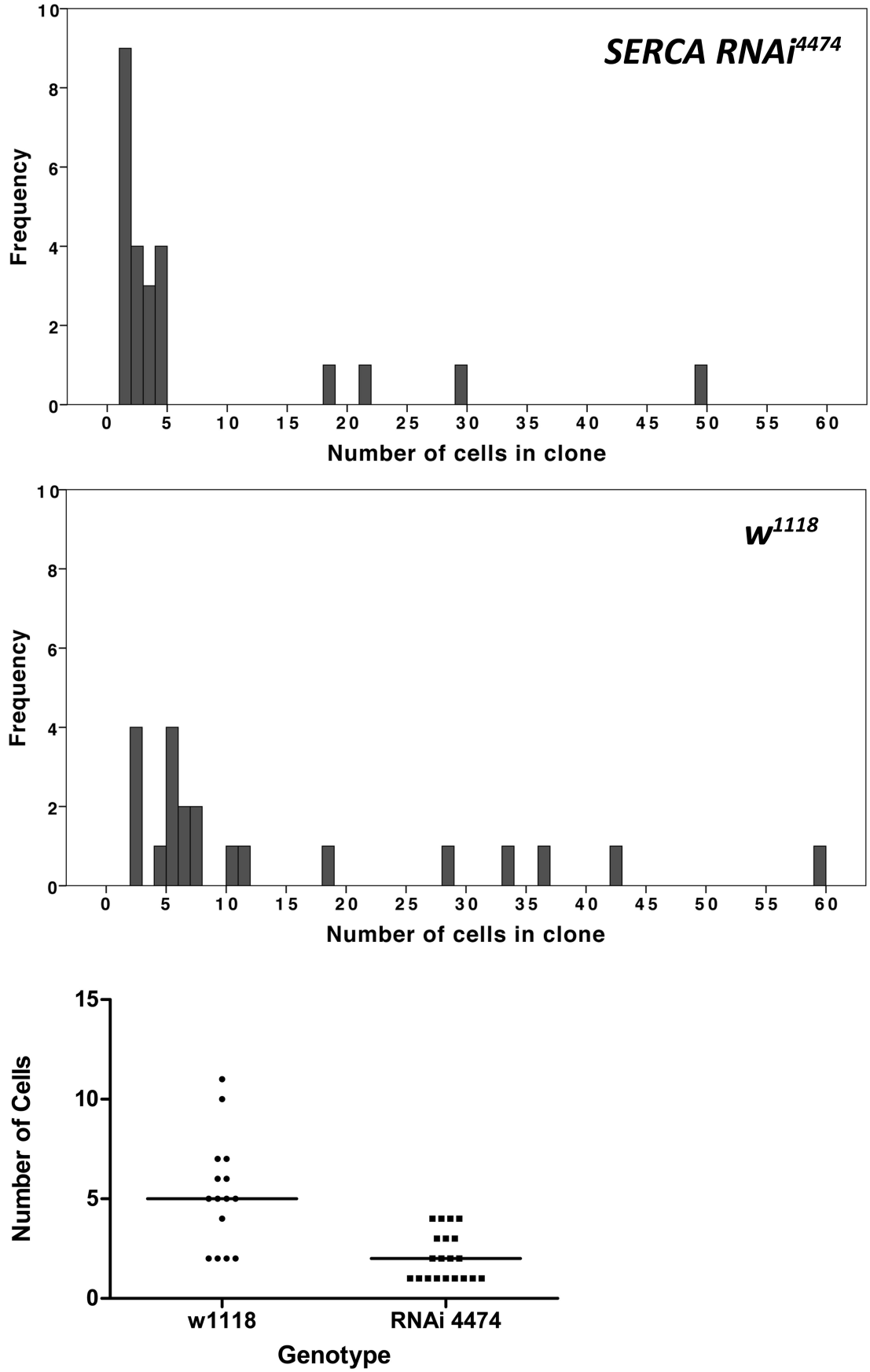

Figure 7.15 SERCA deficient ASP clones comprise fewer cells

Upper panels: histograms of frequency vs. clone size (number of cells) for SERCA RNAi and control (w^{1118}) groups. 14 ASPs were analysed in each group. Lower panel: sub-analysis for clones <12 cells in size: scatter plot of individual clones and group median (horizontal line) are shown.

7.7 Exploring mechanisms of SERCA dependent ASP morphogenesis

Given suggestions of ASP development serving as a superior model for tubular organogenesis e.g. lung or kidney, further insight into the molecular regulation of these events is desirable. Data presented here show SERCA function is essential for normal ASP development; when lacking, defects in cell proliferation and migration occur. The underlying mechanism(s) behind these findings are important: further elaboration of SERCA's role in tubular organogenesis may have high translational importance. To determine further the molecular events surrounding these effects, candidate pathways were selected based on prior findings in *Drosophila* ASPs and interrogated with established techniques.

7.7.1 Targeted SERCA inhibition expands the escargot expressing ASP tip domain

The zinc-finger transcription factor coded for by *escargot (esg)*, is known to be strongly expressed in imaginal cells and functions to inhibit endoreplication and maintain diploidy (Fuse, Hirose, & Hayashi, 1994). In the embryonic trachea, *esg* is essential for epithelial tube fusion; it has been shown to regulate cell adhesion and motility, inducing tip cell fusion through E-Cadherin recruitment (Samakovlis, Manning et al., 1996; Tanaka-Matakatsu et al., 1996). In ASP development, *esg* is expressed in the distal part (tip) of the ASP from around mid-third instar (Sato & Kornberg, 2002). It has been shown that over-expression of *esg* in the ASP can lead to a multi-tipped phenotype, indicating it plays an important role in determining tip cell fate (Wang et al., 2010). Interestingly, we occasionally witnessed a multi-tipped ASP phenotype when SERCA was inhibited with RNAi.

To test what effect SERCA inhibition has on *esg* expression, the *esg-lacZ* enhancer trap was utilised in SERCA deficient (*btl>RNAi*) and control ASPs. Flies of genotype *btl-GAL4, UAS-act.GFP, esg-LacZ* were crossed to RNAi 4474 or w^{1118} (controls). To determine the *esg* expression pattern, late third instar wing discs were stained with an anti-ß-galactosidase antibody and imaged by confocal microscopy. In the SERCA RNAi group, *esg* expression was considerably expanded relative to that in controls, being evident throughout the dysmorphic ASP, including in most proximal locations, adjacent to the trachea (Figure 7.16).

Controls were seen to express *esg* only in the distal half/one third of the ASP, as previously reported (Sato & Kornberg, 2002; Wang et al., 2010). SERCA deficient ASP tracheoblasts therefore display markedly different *esg* expression. This ectopic expression pattern likely indicates a failure to repress *esg*, and therefore also a failure to repress tip cell identity, in more proximal cells. Previous reports have proposed that tip cells expressing *esg*, restrict the fate of more proximal stalk cells, preventing them from becoming tip cells; given *esg* regulates cell adhesion and motility, these findings may also go some way to explaining differences in the distribution of SERCA deficient cells compared to controls (Figure 7.14) (Tanaka-Matakatsu et al., 1996; Wang et al., 2010). Failure of SERCA deficient ASP tracheoblasts to restrict the fate of their more proximal neighbours may also explain witnessed defects in ASP shape: an abundance of 'tip' cells and lack of 'stalk' cells would conceivably result in a wide-based structure, with all cells sending out *btl* expressing cytonemes towards foci of *bnl* expression; a situation not dissimilar to that in the displayed phenotype (Figure 7.3).

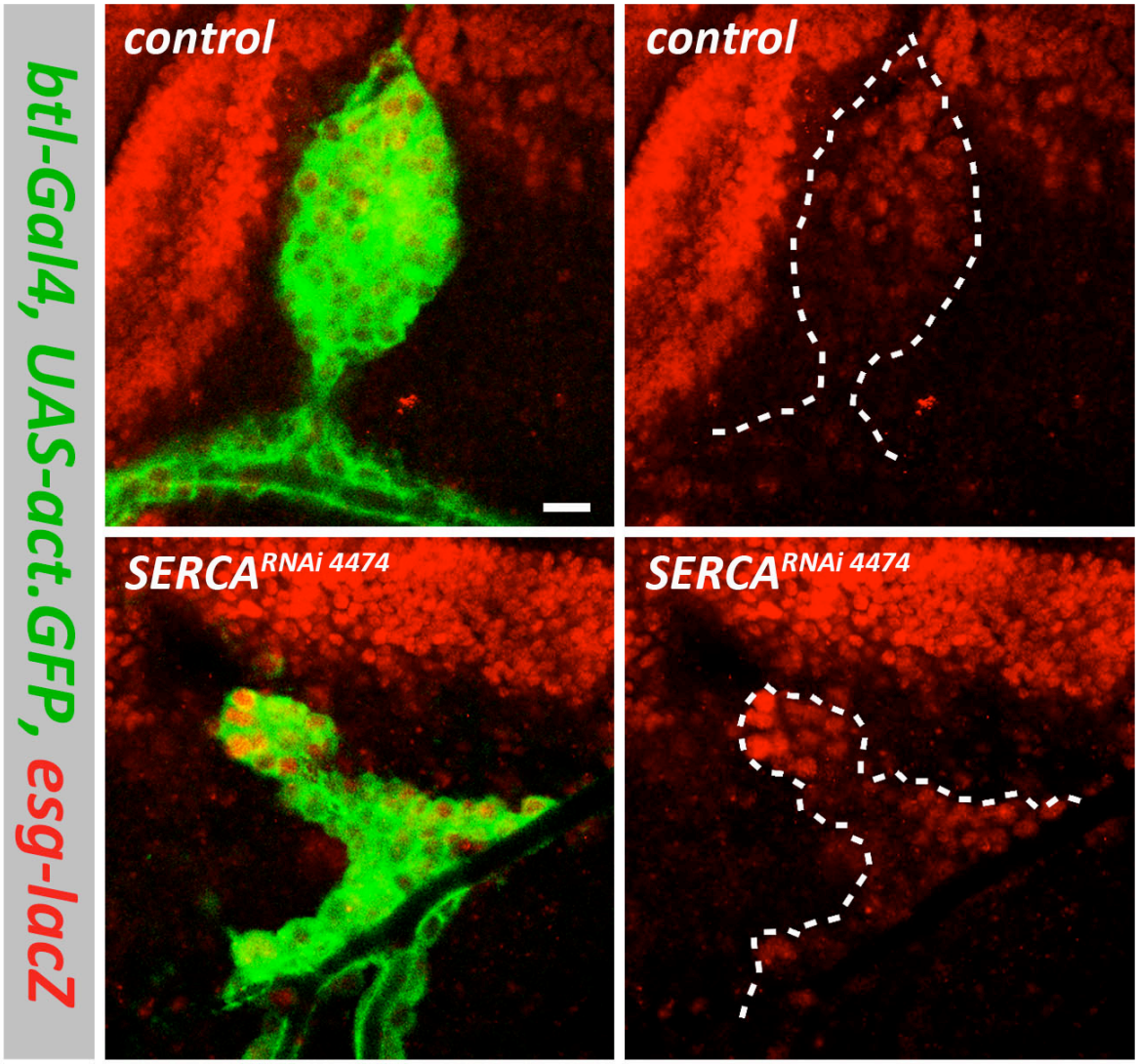

Figure 7.16 Targeted SERCA inhibition expands the *escargot* expressing ASP tip domain.

Confocal micrographs of third instar larval imaginal wing discs (representative slices). The tracheal system is demonstrated using *btl-GAL4* driven *UAS-actin.GFP*. Targeted SERCA inhibition is achieved using the *btl-Gal4* driven SERCA RNAi 4474 construct. *Escargot* expression is demonstrated using *esg-lacZ* and anti β-galactosidase immuno-histo-chemistry. Top panels: control (w^{1118}). Lower panels: *blt> RNAi*. Scale bar indicates 20 µm.

7.7.2 Targeted SERCA inhibition reduces Cut expressing 'stalk' cells in the ASP

Cut proteins are a highly conserved group of homeodomain proteins containing one or more DNA binding domains; in *Drosophila*, *cut* functions to specify cell fate (Nepveu, 2001). Cut proteins play important roles during *Drosophila* respiratory organogenesis: (i) in the embryonic trachea, *cut* mutants fail to undergo normal gas filling and have defective spiracles; (ii) during metamorphosis, *cut* appears to determine cell fate in tracheal remodelling: graded Cut expression in the spiracular tracheal branch correlates with differential growth activity and differentiation (Blochlinger, Bodmer, Jan, & Jan, 1990; Pitsouli & Perrimon, 2010; Wieschaus, Nüsslein-Volhard, & Jürgens, 1984). Given these roles, it was hypothesised that SERCA inhibition induced changes in ASP cell fate, demonstrated by an expanded *esg* expressing tip domain, may be accompanied by changes in Cut expression. To test what effect SERCA inhibition has on Cut levels and distribution, SERCA deficient (*btl>RNAi*) and control ASPs were stained with the monoclonal antibody, 2B10 Anti-cut protein (DSHB).

In both groups (RNAi and control), the majority of ASP tracheoblasts did not stain with Cut antibody, contrasting with surrounding cells of the wing disc that were strongly positive (Figure 7.17). Cut expression was weak and limited to more proximal, 'stalk' cells of the wild-type ASP, whereas no real expression was seen in any part of SERCA deficient (RNAi 4474) ASPs that displayed significantly abnormal morphology. Although relatively weak, patterns of Cut positivity appear approximately reciprocal to that of *esg* (Figure 7.16), indicating that Cut may be a marker of 'stalk' cell identity in the ASP. In the spiracular tracheal branch of larvae undergoing metamorphic remodelling, distinct groups of cells, displaying distinct behaviours are characterised by differential *esg* and *cut* expression (Pitsouli & Perrimon, 2010). Based on data presented here, this may also be the case in the ASP. Collectively, findings of expanded *esg* positivity and absence of proximal Cut protein expression in SERCA deficient ASPs, support the hypothesis that SERCA function is required for ASP 'tip' and 'stalk' cell determination. Given *esg* positive tip cells have distinct functions during ASP morphogenesis, through cytoneme dependent signalling, alterations in tip/stalk cell fate may be responsible for ASP dysmorphogenesis seen in SERCA loss of function environments.

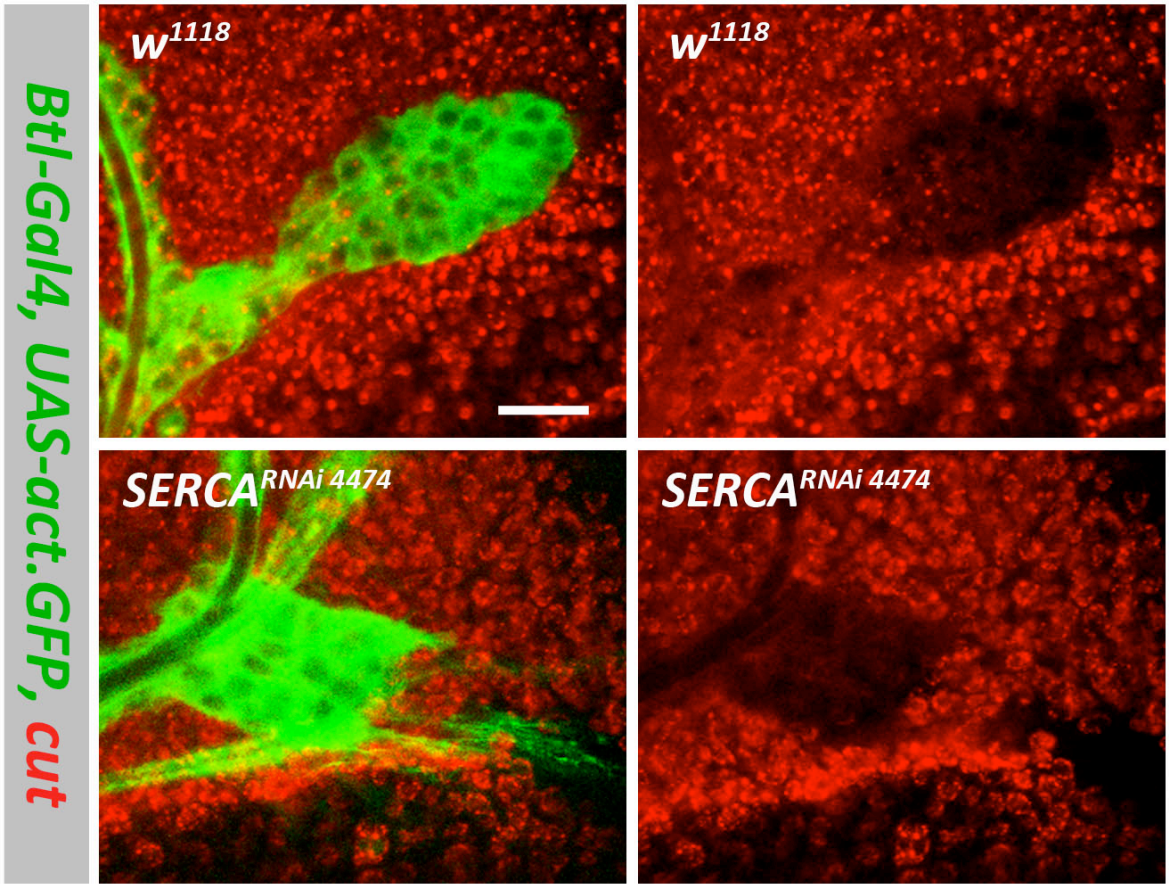

Figure 7.17 Targeted SERCA inhibition reduce Cut expressing 'stalk' cells in the ASP

Confocal micrographs of third instar larval imaginal wing discs (representative slices). The tracheal system is demonstrated using *btl-GAL4* driven *UAS-actin.GFP*. Targeted SERCA inhibition is achieved using the *btl-Gal4* driven SERCA RNAi 4474 construct. Cut protein is labelled with the 2B10 Anti-cut protein antibody in red (DSHB, Iowa). Top panels: control (w^{1118}). Lower panels: *blt> RNAi*. Scale bar indicates 20 μm.

7.7.3 SERCA's effects on ASP morphogenesis appear independent of MAP kinase signalling

Two key aspects of ASP morphogenesis, cell proliferation and migration, are driven by FGF and EGFR growth factors that both rely on the MAP kinase signalling cascade (Cabernard & Affolter, 2005). Given profound effects of SERCA inhibition on ASP morphogenesis, cell migration and proliferation, it was hypothesised that these effects were mediated via changes in MAP kinase signalling. To test what effect SERCA deficiency had on this pathway, SERCA RNAi 'flip-out' and mutant mitotic clones were produced and cells stained for an active, dually-phosphorylated form of MAP kinase (dpERK), using a monoclonal Anti-MAP Kinase, Activated (Diphosphorylated ERK-1&2) antibody (Sigma) (Yung et al., 1997). dpERK staining has been shown to provide a reliable, spatiotemporal readout of receptor tyrosine kinase signalling activity in *Drosophila*, including FGF and EGFR pathways (Gabay, Seger, & Shilo, 1997; Vincent, Wilson, Coelho, Affolter, & Leptin, 1998).

SERCA deficient cells (RNAi or mutant) did not display significantly different dpERK staining to their wild-type neighbours (Figure 7.18). The distribution of staining appeared normal, being largely cytoplasmic; levels of activated MAP kinase also appeared relatively constant between SERCA deficient and wild-type cells. To confirm that antibody staining was efficiently and specifically detecting altered levels of MAP kinase, a positive control was analysed whereby 'flip-out' clones expressing oncogenic Ras (Ras^{V12}) were produced in the wing disc (Karim & Rubin, 1998). In these cells, levels of activated MAP kinase staining were increased compared to wild-type neighbours, consistent with previous reports and thus confirming efficacy of the staining protocol (Figure 7.18) (Prober & Edgar, 2002). Collectively these data indicate that SERCA inhibition-induced ASP dysmorphogenesis is unlikely to be mediated through changes in MAP kinase signalling. The key ASP regulators, EGFR and FGF are principally mediated downstream through the MAP kinase cascade; it therefore appears that SERCA's role in ASP morphogenesis is independent of these pathways. Clearly this assumption relies on adequate sensitivity of the MAP kinase assay: SERCA inhibition could theoretically induce small changes in MAP kinase activity sufficient for dysmorphogenesis, but not detectable by dpERK staining.

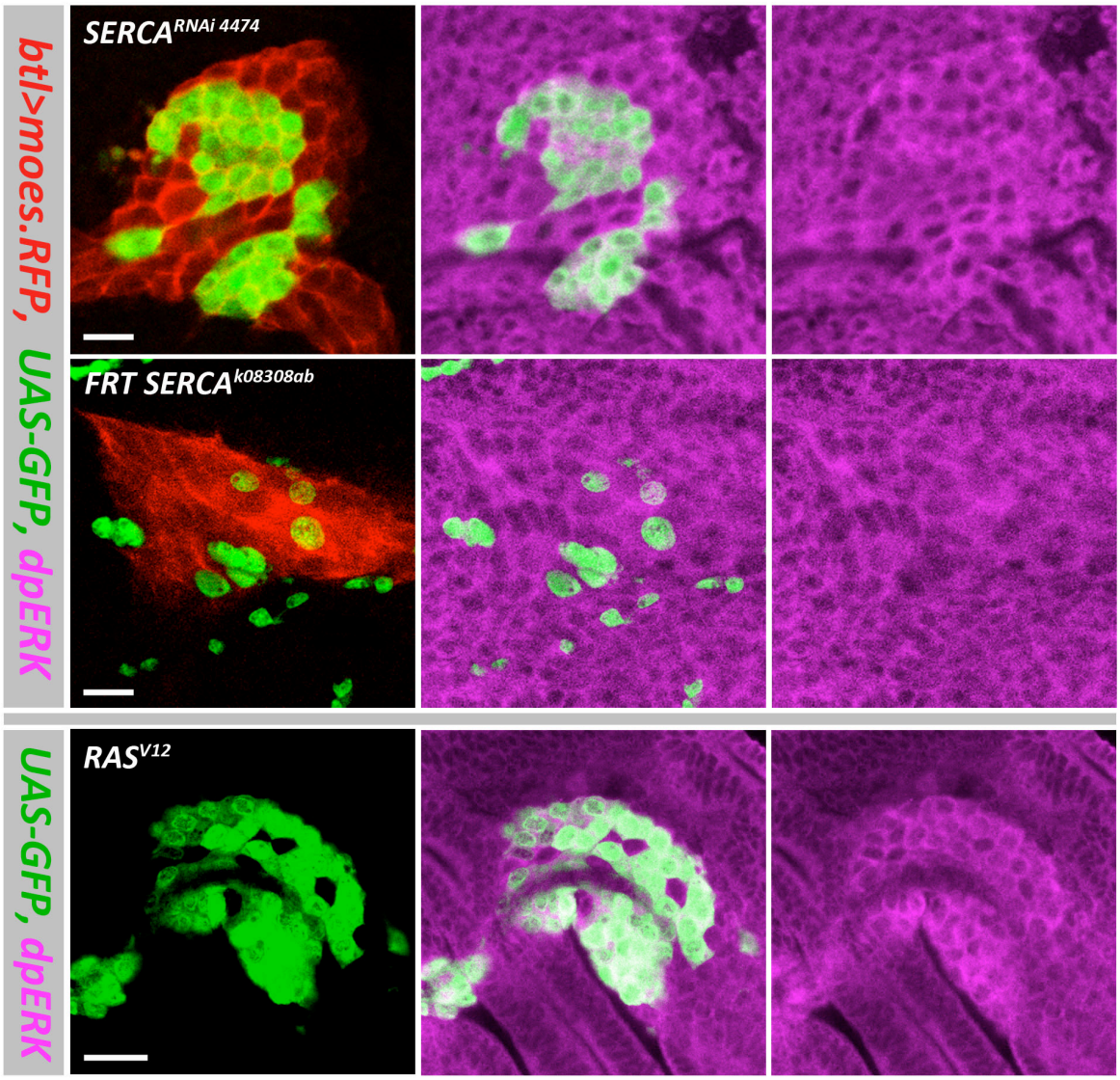

Figure 7.18 SERCA's effects on ASP morphogenesis appear independent of MAP kinase signalling

Upper two rows: confocal micrographs of third instar larval imaginal wing discs (representative slices). The tracheal system is demonstrated using *btl>RFP*. Random SERCA RNAi 'flip-out' clones and SERCA^{k08308ab} mutant mitotic clones are positively labelled with GFP as previously indicated. The active, dually-phosphorylated form of MAP kinase (dpERK) is labelled using a monoclonal Anti-MAP Kinase, Activated (Diphosphorylated ERK-1&2) antibody (Sigma) in magenta. Lower row: positive control demonstrating increased dpERK staining in oncogenic Ras (RasV12), positively marked (GFP) 'flip-out' clones. Scale bars in each row indicate 20 μm.

7.7.4 SERCA's effects on ASP morphogenesis appear independent of Notch signalling

The Notch receptor is part of a highly conserved signalling pathway, playing fundamental roles in determination of developmental cell fate (Artavanis-Tsakonas, Rand, & Lake, 1999). A classical example of Notch-dependent development is lateral inhibition, the process whereby a single cell is chosen to adopt a distinct fate from within a cluster of similar cells, the other cells of which adopt different fates: local Notch signalling between neighbouring cells underpins lateral inhibition (Heitzler & Simpson, 1991). A number of pieces of evidence implicated Notch signalling as a candidate in SERCA dependent ASP morphogenesis: (i) the morphology of SERCA deficient ASPs, comprising a wide base and abundance of tip cells, implied a failure of lateral inhibition signalling between tip cells and neighbouring stalk precursors; (ii) Notch signalling spatially restricts *esg* expression, therefore disruptions in Notch could conceivably explain the demonstrated expansion in ASP *esg* expression; and (iii) SERCA function is essential for intracellular trafficking of the Notch receptor (Ikeya & Hayashi, 1999; Periz & Fortini, 1999). Given this seemingly strong association of SERCA and Notch, it was hypothesised that witnessed ASP dysmorphogenesis may be due to a loss of SERCA-dependent, Notch-signalled lateral inhibition between tip and stalk cells.

To test what effect SERCA deficiency had on Notch signalling in the ASP, SERCA RNAi 'flip-out' and mutant mitotic clones were produced and cells stained for the intra-cellular domain (ICD) of the Notch receptor using a monoclonal antibody (C17.9C6, DSHB). SERCA deficient cells (RNAi or mutant) labelled with GFP, did not display significant differences in Notch ICD staining, compared to their wild-type (GFP negative) neighbours (Figure 7.19). Not only were levels of Notch ICD approximately equivalent between cells, but importantly, the distribution of Notch also appeared unaffected by SERCA loss of function. These data infer that Notch signalling was unchanged between SERCA deficient and control cells. To confirm antibody staining was efficiently and specifically detecting altered levels of Notch ICD, a positive control was analysed whereby *deltex* was over-expressed along the antero-posterior boundary of the wing disc (*Ptc-GAL4*, *UAS-deltex*). *deltex* is an X-linked gene, coding for a cytoplasmic protein Deltex, which is known to be a positive regulator of Notch (K. Matsuno,

Diederich, Go, Blaumueller, & Artavanis-Tsakonas, 1995; Xu & Artavanis-Tsakonas, 1990). Cells over-expressing *deltex*, also labelled with GFP (*UAS-GFP*), displayed increased levels of Notch staining that appeared abnormally distributed (Figure 7.19), consistent with previous reports, where *deltex* over-expression resulted in Notch ICD accumulation in endosomes (Hori et al., 2004). This confirms efficacy of the assay at detecting changes in Notch ICD distribution and abundance, and strongly suggests that findings of apparently unchanged Notch ICD in SERCA deficient cells are a 'true negative' finding.

These results contrast with those of Periz and Fortini, where SERCA mutant clones in the eye disc induced gross changes in Notch localisation; grossly abnormal intracellular accumulation of Notch ICD was demonstrated in these clones using similar staining protocols to those adopted here (Periz & Fortini, 1999). The most likely explanation for this discrepancy is the relative potency of SERCA inhibition between studies: Periz and Fortini used a strong SERCA mutant allele (*Ca-P60A*^{S5}) to generate such effect, demonstrated by cells homozygous for this allele failing to survive in the adult retina; conversely, mutant and RNAi clones used in this investigation result in less severe SERCA knockdown, as confirmed by their continued viability. Importantly however, ASP dysmorphogenesis demonstrated here, was induced with these less severe SERCA knockdown methods (Figures 7.3, 7.7 and 7.10) and therefore appears independent of significant changes in Notch signalling.

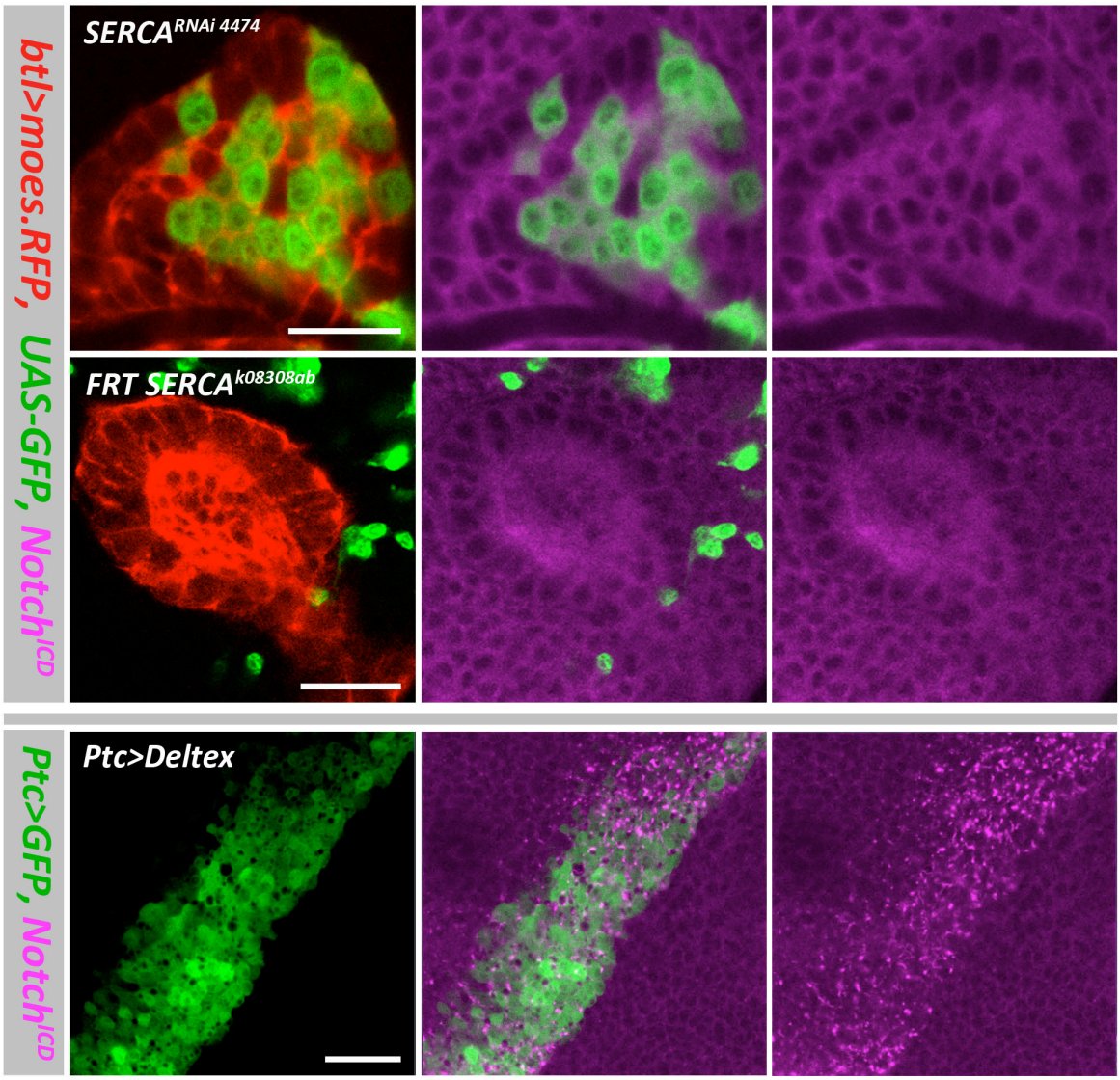

Figure 7.19 SERCA's effects on ASP morphogenesis appear independent of Notch signalling

Upper two rows: confocal micrographs of third instar larval imaginal wing discs (representative slices). The tracheal system is demonstrated using *btl>RFP*. Random SERCA RNAi 'flip-out' clones and SERCA^{k08308ab} mutant mitotic clones are positively labelled with GFP as previously indicated. The intracellular domain (ICD) of the Notch receptor is labelled using a monoclonal anti-notch antibody (C17.9C6, DSHB) in magenta. Lower row: positive control demonstrating an accumulation of Notch ICD staining in cells over-expressing *deltex* under control of the *Ptc-GAL4* driver. *UAS-GFP* is also driven by *Ptc-GAL4* to illustrate the distribution of these cells in the wing disc. Scale bars in each row indicate 20 μm.

7.8 Conclusions

Data presented here allow a number of conclusions to be drawn regarding SERCA's role in ASP morphogenesis; given SERCA's role in murine lung development, some of these points may also be more generally applicable to epithelial tubulogenesis in other organs and in other species.

7.8.1 ASP morphogenesis requires SERCA function for cell proliferation and migration events

RNAi and mutant loss of function data presented here demonstrate that normal ASP morphogenesis depends on adequate SERCA function in tracheoblasts cells (Figures 7.3, 7.7 and 7.10). This requirement is for two distinct processes known to be essential for ASP development: (i) cell proliferation: SERCA deficient ASPs display reduced numbers of proliferating cells and SERCA loss of function clones are reduced in size compared to wild type controls (Figures 7.12 and 7.15); and (ii) cell migration: SERCA deficient clones are unable to populate the tip domain of the ASP at an expected frequency; this inability to reach the tip has been characterised by others to represent a change in cell migration (Figure 7.14) (Cabernard & Affolter, 2005; Chanut-Delalande et al., 2007). Interestingly, SERCA's role in these two processes appears to be independent of Notch and MAP kinase signalling (Figures 7.18 and 7.19).

Control of cell proliferation is known to depend on intracellular Ca^{2+} levels: extracellular signals that induce mitosis (mitogens, e.g. growth factors, hormones and signalling molecules) depend on Ca^{2+} influx via plasma membrane channels to mediate their action (Barbiero et al., 1995; Husain et al., 1997; Kotturi, Carlow, Lee, Ziltener, & Jefferies, 2003). There is increasing evidence that Ca^{2+} influx necessary for cell proliferation is store operated, dependent on channels such as TRPC and Orai, known to be activated upon endoplasmic reticulum (ER) Ca^{2+} depletion; it is through this mechanism that SERCA is likely to regulate mitosis [reviewed in (Lipskaia & Lompr♪©, 2004)]. In addition to the essential role of inositol-1,4,5-triphosphate (IP3R) in activating store operated rises in cytosolic Ca^{2+}, SERCA, through its control of store refilling, probably 'fine-tunes' these Ca^{2+} transients (Camacho & Lechleiter, 1993; Moccia et al., 2003). Whether SERCA function, necessary for replenishing ER Ca^{2+} stores, promotes or inhibits cell proliferation is variably reported and may depend on

factors such as cell type, SERCA isoform and degree of Ca^{2+} store depletion [reviewed in (Lipskaia, Hulot, & Lompr✓©, 2009)]. A number of studies suggest that ER Ca^{2+} store depletion from SERCA inhibition, leads to calcium influx and promotes cell proliferation; others report opposite findings, consistent with data presented here. In prostate cancer cell lines, SERCA inhibition with RNAi or thapsigargin inhibits growth and prevents growth factor stimulation of cell proliferation; furthermore, SERCA is upregulated during stimulated cell proliferation and reciprocally downregulated when proliferation is reduced (Crepin et al., 2007; Humez et al., 2004; Legrand et al., 2001). Similar findings have also been reported in smooth muscle cells (Magnier et al., 1992; Waldron et al., 1994). Given these *in vitro* reports, as well as findings in CPA treated murine lung explants (Chapter 3), novel *in vivo* data here strongly indicate a conserved requirement for SERCA function in the mitotic cycle. Whether this requirement is specifically for SERCA *per se*, rather than one simply for adequate intracellular Ca^{2+} stores, is not entirely clear and is difficult to conclusively establish. However, specific SERCA requirements for cell cycle progression are indicated by an inability to recreate SERCA inhibition induced cell cycle effects, through alterations of cytosolic Ca^{2+} alone (Simon & Moran, 2001).

Effects of SERCA inhibition on cell migration are less well documented, but given the ubiquity of calcium's role in biology and the requirement for SERCA in its regulation, data presented here demonstrating reduced migration seem plausible (Berridge et al., 2000). Support is leant from reports of calcium playing fundamental roles in cell migration: (i) eosinophils migrating toward chemotactic stimuli display an intracellular Ca^{2+} gradient, with levels being low at the leading edge and high at the trailing edge, this polarisation being required for migratory cytoskeletal changes; (ii) integrins, key effectors of cell adhesion and migration, are known to be highly sensitive to changes in Ca^{2+} e.g. through actions of their Ca^{2+} dependent inhibitor, calpain; and (iii) when intracellular Ca^{2+} transients are blocked in migrating neutrophils, they become stuck to extracellular matrix proteins (Brundage, Fogarty, Tuft, & Fay, 1991; Huttenlocher et al., 1997; Lawson & Maxfield, 1995; Marks, Hendey, & Maxfield, 1991).

Looking specifically at tubular organogenesis, calcium transients are required for angiogenesis and SERCA appears to have a specific role here; blockage with

thapsigargin or CPA results in defects in endothelial cell migration (Kimura, Oike, Koyama, & Ito, 2001; Kohn, Alessandro, Spoonster, Wersto, & Liotta, 1995). These *in vitro* findings, support novel *in vivo* data here and suggest an essential role for SERCA in tubular epithelial cell migration. A putative mechanism for this role involves a requirement for SERCA dependent ER Ca^{2+} stores to maintain intracellular Ca^{2+} gradients necessary for the continual replenishment of cell adhesion receptors e.g. integrins, at the leading edge of the migrating cell (Kimura et al., 2001; Lawson & Maxfield, 1995).

7.8.2 SERCA function is required for determination of ASP cell fate

SERCA inhibition resulted in an expansion of the *escargot* labelled 'tip' domain and absence of Cut protein labelled 'stalk' cells in the developing ASP. Given reported roles of 'tip' cells in morphogenic signalling, this tip/stalk cell fate imbalance is likely, in part, to explain structural changes in the ASP: a wide-based ASP morphology, such as that witnessed during SERCA inhibition, removes the normal restraint on number of tracheoblasts able to stem cytoneme processes towards surrounding foci of *bnl* expression. Tip/stalk cell fate determination and ASP morphogenesis therefore appears tightly coupled, as supported by reports of ectopic *esg* expression induced manipulation of cell fate, resulting in changes to ASP morphology (Wang et al., 2010). One explanation for an apparent abundance of tip cells in SERCA deficient ASPs, is a failure of 'tip' cells to restrict the fate of their more proximal neighbours, a mechanism proposed to be dependent on a competitive lateral inhibition mechanism (Q. Wang et al., 2010). If this restrictive feedback mechanism is dependent on SERCA function, SERCA deficiency would result in a lack of feedback and hence cells not adopting a stalk fate. Given Notch is a key mediator of lateral inhibition, spatially restricts *esg* expression and has a strong association with SERCA, it was speculated that its dysregulation upon SERCA inhibition was responsible for a lack of tip cell lateral inhibition: RNAi and mutant clone data here do not support this potential mechanism (Figure 7.19).

A further putative mechanism behind SERCA inhibition induced aberrations in ASP cell fate, may depend on differential activation of transcription factors, as suggested by altered *esg* and Cut protein expression (Figure 7.16 and 7.17).

Activation of transcription factors is known to depend on increases in intracellular Ca^{2+} concentration; furthermore, specificity of individual transcription factor activation depends on characteristics of Ca^{2+} transients, such as amplitude and duration (Dolmetsch, Lewis, Goodnow, & Healy, 1997). SERCA therefore appears to regulate Ca^{2+}-dependent transcription pathways, through control of Ca^{2+} wave amplitude and kinetics (Camacho & Lechleiter, 1993; Lipskaia et al., 2009; Lipskaia & Lompr♂©, 2004; Moccia et al., 2003). A well-characterised example of this mechanism is the activation of the transcription factor NFAT (nuclear factor of activated T-lymphocytes): SERCA function inhibits store operated Ca^{2+} entry and downstream calcineurin/NFAT activity by modifying agonist-induced intracellular Ca^{2+} transients from a steady-state to an oscillatory mode (Bobe et al., 2011). SERCA is therefore able to finely tune gene transcription through spatial and temporal alterations in Ca^{2+}. Similar mechanisms might regulate *escargot* and *cut* transcription factors in the ASP epithelium.

7.8.3 SERCA function has a conserved role in airway morphogenesis

This thesis has demonstrated SERCA function is essential for *Drosophila* ASP morphogenesis *in vivo* and murine embryonic lung development *in vitro*, confirming a conserved role for SERCA in respiratory organogenesis. The key similarity in airway development between these two evolutionarily disparate organisms is a dependence on FGF signalling to induce fundamental morphogenic events. Given that FGF signalling underpins development of a number of branched tubular organs in vertebrates, including the kidney, endocrine and exocrine glands, and blood vessels, it seems possible that demonstrated requirements for SERCA in airway development might also apply to epithelial tubulogenesis more widely (Alarid et al., 1994; Celli, LaRochelle, Mackem, Sharp, & Merlino, 1998; Folkman & Klagsbrun, 1987; D. Jackson et al., 1997).

Another similarity between species is the reduction in cell proliferation seen when SERCA is inhibited in the airway (Chapter 3; Figures 7.12 and 7.15). Interestingly, *Drosophila* embryonic branching morphogenesis, a process independent of cell proliferation, did not appear to have a requirement for significant SERCA function. This conserved SERCA requirement for airway

development processes that are dependent on cell proliferation is particularly significant, given the opposite effect of SERCA inhibition in other systems (e.g. SERCA mutations in humans and mice resulting in increased rates of malignancy (Korosec, Glavaç, Rott, & Ravnik-Glavaç, 2006; L. H. Liu et al., 2001)). Although supported by findings in prostate cancer and smooth muscle cell lines (discussed above), the reason for this dependence is unclear. When SERCA inhibition has been shown to have the opposite effect and stimulate cell proliferation, this consequence has been mediated through the calcineurin/NFAT pathway. One explanation for the conserved, seemingly reverse effect in respiratory organogenesis is that this pathway does not operate similarly in this context: further investigation is needed to test this (Bobe et al., 2011).

Chapter 8

SUMMARY AND CONCLUDING REMARKS

8.1 Disorders of lung development are a global health problem

Defects in lung organogenesis result in a spectrum of disease that presents as structural lung anomalies and/or inadequate respiratory function. A number of comparatively common problems that manifest in the infant, e.g. respiratory distress syndrome (1:100 births) or pulmonary hypoplasia associated with congenital diaphragmatic hernia (1:2500 births), feature inadequate or disordered pulmonary development: the short and long-term outcomes of such are frequently poor (e.g. high mortality, impaired respiratory function and persistent oxygen dependency) (Baraldi & Filippone, 2007; J. Colvin et al., 2005; Muratore et al., 2001; Rodriguez et al., 2002). Development of new treatments for these conditions e.g. surfactant replacement or fetal endoscopic tracheal occlusion (FETO), relied upon novel insights into biochemical and biomechanical regulators of lung development (Avery & Mead, 1959; Wilson et al., 1993). There is now increasing evidence to suggest a number of 'adult' diseases also have their origins in fetal life. Asthma and COPD, both characterised as global epidemics, result in a considerable burden of acute mortality and long-term morbidity, as well as high levels of healthcare expenditure (Masoli et al., 2004; World Health Organization, 2008). Factors responsible for early lung development have been implicated in the pathogenesis of asthma and COPD; it is recognised that these may present future treatment targets (Bousquet et al., 2000; H. Chen et al., 2005). Understanding normal pulmonary development is therefore paramount to discovery of novel therapeutics for a range of pulmonary diseases that commonly afflict the young and old.

8.2 SERCA appears a promising novel target

SERCA, a P-type ATPase, pumps Ca^{2+} ions from the cytoplasm to the lumen of the ER and other specialised compartments (e.g. SR and Golgi): SERCA is therefore responsible for both returning cytosolic free Ca^{2+} concentration back to its resting level following cell activation, and also maintaining high concentrations of Ca^{2+} in organellar lumens (creating important Ca^{2+} gradients across the cell) (Skou, 1957; Wuytack et al., 2002).

A number of pieces of evidence link SERCA to lung function. Firstly, SERCA appears to have an important role in pulmonary development: SERCA blockade,

with the specific inhibitor cyclopiazonic acid (CPA), reduces both airway branching and peristalsis reversibly and dose dependently, whilst also reversibly halting pulmonary myogenesis *in vitro* (N. Featherstone et al., 2006; N. Featherstone et al., 2005; N. C. Featherstone et al., 2005; Lansdale, Connell et al., 2010; Seidler et al., 1989). Secondly, SERCA has been implicated in the pathogenesis of asthma and explored as a potential treatment target: SERCA2 mRNA and protein expression is reduced in airway smooth muscle (ASM) of patients with asthma; this reduction correlates with disease severity and is associated with corresponding changes in Ca^{2+} homeostasis (Mahn et al., 2009). Interestingly, ASM taken from asthmatics, or healthy subjects then subjected to siRNA mediated SERCA knockdown, displays a similar asthmatic-like phenotype (increased cell proliferation, cell-spreading and cytokine secretion). Finally, SERCA pump inhibitors (thapsigargin, curcumin and cyclopiazonic acid) have been explored for use clinically, with the aim of correcting the cystic fibrosis phenotype, by depleting ER Ca^{2+} stores, inhibiting chaperone proteins retaining the CFTR and hence allowing it to function as a Cl^- ion channel at the cell surface (Dalemans et al., 1991; Egan et al., 2002; Rubenstein et al., 1997).

There is therefore evidence for SERCA playing diverse roles in the lung in health and disease: this thesis further explored its role in airway development by exploiting an established murine culture model and developing a range of tools in *Drosophila* embryos and larvae. *Drosophila* provided a genetically tractable model of airway development, where existing genetic tools (including RNAi, conditional mutants; 'flip-out' and MARCM clonal analysis) allowed the elegant spatial and temporal manipulation of SERCA function. The *in vivo* study of airway morphogenesis and quantification of SERCA function was achieved using fixed and live confocal imaging techniques, immunostaining, single and dual-labelled fluorescent proteins and dynamic calcium imaging (Chapters 4-7).

8.3 SERCA has an essential, conserved role in airway development across species

Data presented here and from others, show that SERCA function is essential for *Drosophila* air sac progenitor (ASP) morphogenesis and murine embryonic lung development, confirming a conserved role for SERCA in respiratory organogenesis. The abrogation of larval air sac budding, seen upon targeted

SERCA inhibition with RNAi (Chapter 7), provides *in vivo* support for those *in vitro* findings already described (N. Featherstone et al., 2006; N. Featherstone et al., 2005; N. C. Featherstone et al., 2005; Lansdale, Connell et al., 2010). Importantly, these data also negate the possibility that previous findings were due to off-target effects of the SERCA inhibitor CPA, given they result from genetic SERCA 'knock-down.'

Further conservation of SERCA's role in airway development is seen when cell proliferation is considered: SERCA function regulates the number of mitotic cells in the murine lung epithelium and mesenchyme *in vitro* (Chapter 3), whilst in the *Drosophila* air sac, a similar pattern is seen *in vivo* (Chapter 7). This relationship is maintained when studies of random 'flip-out' clones are reviewed (Chapter 7): SERCA-deficient cells have a cell autonomous proliferation defect, since 'clumps' of SERCA RNAi cells comprised fewer cells than control clones (rates of apoptosis were negligible in each). Given similar reports in smooth muscle and cancer cell lines, as well as an inability to recreate SERCA inhibitor induced cell-cycle arrest through alterations of Ca^{2+} alone, it appears SERCA has a specific role in regulating aspects of the cell cycle (Legrand et al., 2001; Simon & Moran, 2001; Waldron et al., 1994).

SERCA-dependent cell proliferation could explain the stark difference between embryonic and larval phenotypes in the fly airway: mutant and RNAi induced SERCA knockdown in the embryo failed to disrupt tracheal branching morphogenesis (known to proceed without cell proliferation) (Chapters 5 & 6), whereas cell proliferation-dependent ASP development was severely disrupted upon targeted SERCA inhibition (Chapter 7). However, this difference more likely reflects demonstrated residual SERCA function during embryogenesis upon knockdown (Chapters 5 & 6), particularly given preliminary findings of CPA induced tracheal branching defects in the embryo (courtesy of EC Jesudason, unpublished work). If SERCA *is* required for airway morphogenesis in a cell proliferation free system such as the embryo, demonstrated changes in cell proliferation alone seem unlikely to explain the complex, conserved phenotypes associated with SERCA loss-of-function in mouse and fly air sac: other changes in fundamental cell processes are therefore likely e.g. cell migration.

Data presented here demonstrate that cell migration appears to be regulated by SERCA in the *Drosophila* airway: SERCA RNAi cells have a cell autonomous migration defect, with proportionately fewer reaching the air sac tip and commensurately more remaining in the maldeveloped stalk, compared to control clones (Chapter 7). These findings are supported by those of others, both in a monolayer wound closure model where CPA reduces basal and EGF-stimulated migration in a dose-related manner and in zebrafish vasculature where CPA also reduces cell migration (courtesy of EC Jesudason, unpublished work). A plausible, but as of yet untested explanation for these findings, is requirement for SERCA dependent Ca^{2+} stores to maintain intracellular Ca^{2+} gradients required for the continual replenishment of cell adhesion receptors e.g. integrins, critical for cell migration (Kimura et al., 2001; Lawson & Maxfield, 1995).

Witnessed expansion in the expression of the ASP tip cell marker *escargot*, could indicate that SERCA deficient cells preferentially adopt a 'tip' cell type fate, rather than the usual balance of 'tip' and 'stalk' fates seen in control ASPs (Chapter 7). This difference in *escargot* expression is supported by a paradoxical reduction in *cut* expression (a 'stalk' cell marker). Alterations in tip/stalk cell balance such as this could explain changes in ASP morphogenesis seen upon SERCA inhibition, owing to the purported roles that tip cells play in morphogenic signalling (Roy et al., 2011; Sato & Kornberg, 2002). This hypothesis is further supported by findings of ectopic *escargot* expression-induced manipulation of cell fate, resulting in changes to ASP morphology (Wang et al., 2010).

SERCA knockdown in the larval ASP was associated with abnormal expression of *escargot* in *some* cells of the proximal air sac, but maintenance of typical expression distally (Chapter 7): normal SERCA function therefore does not appear necessary for distal *escargot* expression and *escargot* expression in the proximal region is not a necessary outcome of SERCA knockdown. An alternative interpretation of changes in the spatial expression pattern may therefore be that SERCA inhibition does not dysregulate *escargot* expression so much as the migration of cells that happen to be expressing it, thus lending further support to the above findings of SERCA as a key regulator of airway epithelial cell migration (rather than a determinant of cell fate *per se*).

8.4 SERCA's role in airway branching morphogenesis may have wider significance

A key similarity between airway development in the mouse and fly is a reliance on FGF signalling to induce fundamental morphogenic events. Given that FGF signalling underpins development of a number of other branched tubular organs (e.g. kidney, endocrine and exocrine glands and blood vessels), it seems plausible that demonstrable requirements for SERCA in airway development might also apply to epithelial tubulogenesis in other organs, with obvious implications for wider research.

Ca^{2+} cycling has been indicated as a regulator of budding in fungi and plants (Torralba & Heath, 2001; Trewavas & Knight, 1994): could this system also apply to animal species and provide a generic mechanism to explain the control of iterative biological branching in diverse tissue types with differing growth factors? This type of mechanism could shed light onto previously unexplained propagating Ca^{2+} waves that are present in *Drosophila* trachea (courtesy of C Samakovlis, unpublished data) and mammalian lung (known to be SERCA dependent) (N. C. Featherstone et al., 2005). Furthermore, the generic regulation of branching via SERCA dependent Ca^{2+} cycling/gradients would explain SERCA's conserved role in the fly and mouse airway (Chapters 3 & 7) and imply SERCA's role is independent of specific morphogens. Indeed, data here indicate that the effect of SERCA inhibition on branching morphogenesis may be independent of FGF. When random SERCA loss of function clones were produced, defects in ASP morphology were observed and cell autonomous changes in proliferation and migration were present (Chapter 7), despite surrounding tissues being 'wild-type' and hence presumably having normal levels of FGF (implying compensation from surrounding cells did not occur). Findings here of SERCA as a regulator of branching, may therefore have wider relevance across biology, whenever iterative epithelial bud formation occurs.

Finally, demonstrated SERCA regulation of cell proliferation and cell migration also has implications for research into proliferative disease, metastasis and tissue regeneration.

Appendix 1

SERCA Phylogeny

Drosophila melanogaster SERCA isoforms

```
FBpp0072121     MEDGHSKTVEQSLNFFGTDPERGLTLDQIKANQKKYGPNELPTEEGKSIWQLVLEQFDDL 60
FBpp0072122     MEDGHSKTVEQSLNFFGTDPERGLTLDQIKANQKKYGPNELPTEEGKSIWQLVLEQFDDL 60
FBpp0072125     MEDGHSKTVEQSLNFFGTDPERGLTLDQIKANQKKYGPNELPTEEGKSIWQLVLEQFDDL 60
FBpp0072127     MEDGHSKTVEQSLNFFGTDPERGLTLDQIKANQKKYGPNELPTEEGKSIWQLVLEQFDDL 60
FBpp0072126     MEDGHSKTVEQSLNFFGTDPERGLTLDQIKANQKKYGPNELPTEEGKSIWQLVLEQFDDL 60
FBpp0072123     MEDGHSKTVEQSLNFFGTDPERGLTLDQIKANQKKYGPNELPTEEGKSIWQLVLEQFDDL 60
FBpp0072120     MEDGHSKTVEQSLNFFGTDPERGLTLDQIKANQKKYGPNELPTEEGKSIWQLVLEQFDDL 60
FBpp0072124     MEDGHSKTVEQSLNFFGTDPERGLTLDQIKANQKKYGPNELPTEEGKSIWQLVLEQFDDL 60
                ************************************************************

FBpp0072121     LVKILLLAAIISFVLALFEEHEETFTAFVEPLVILLILIANAVVGVWQERNAESAIEALK 120
FBpp0072122     LVKILLLAAIISFVLALFEEHEETFTAFVEPLVILLILIANAVVGVWQERNAESAIEALK 120
FBpp0072125     LVKILLLAAIISFVLALFEEHEETFTAFVEPLVILLILIANAVVGVWQERNAESAIEALK 120
FBpp0072127     LVKILLLAAIISFVLALFEEHEETFTAFVEPLVILLILIANAVVGVWQERNAESAIEALK 120
FBpp0072126     LVKILLLAAIISFVLALFEEHEETFTAFVEPLVILLILIANAVVGVWQERNAESAIEALK 120
FBpp0072123     LVKILLLAAIISFVLALFEEHEETFTAFVEPLVILLILIANAVVGVWQERNAESAIEALK 120
FBpp0072120     LVKILLLAAIISFVLALFEEHEETFTAFVEPLVILLILIANAVVGVWQERNAESAIEALK 120
FBpp0072124     LVKILLLAAIISFVLALFEEHEETFTAFVEPLVILLILIANAVVGVWQERNAESAIEALK 120
                ************************************************************

FBpp0072121     EYEPEMGKVVRQDKSGIQKVRAKEIVPGDLVEVSVGDKIPADIRITHIYSTTLRIDQSIL 180
FBpp0072122     EYEPEMGKVVRQDKSGIQKVRAKEIVPGDLVEVSVGDKIPADIRITHIYSTTLRIDQSIL 180
FBpp0072125     EYEPEMGKVVRQDKSGIQKVRAKEIVPGDLVEVSVGDKIPADIRITHIYSTTLRIDQSIL 180
FBpp0072127     EYEPEMGKVVRQDKSGIQKVRAKEIVPGDLVEVSVGDKIPADIRITHIYSTTLRIDQSIL 180
FBpp0072126     EYEPEMGKVVRQDKSGIQKVRAKEIVPGDLVEVSVGDKIPADIRITHIYSTTLRIDQSIL 180
FBpp0072123     EYEPEMGKVVRQDKSGIQKVRAKEIVPGDLVEVSVGDKIPADIRITHIYSTTLRIDQSIL 180
FBpp0072120     EYEPEMGKVVRQDKSGIQKVRAKEIVPGDLVEVSVGDKIPADIRITHIYSTTLRIDQSIL 180
FBpp0072124     EYEPEMGKVVRQDKSGIQKVRAKEIVPGDLVEVSVGDKIPADIRITHIYSTTLRIDQSIL 180
                ************************************************************

FBpp0072121     TGESVSVIKHTDAIPDPRAVNQDKKNILFSGTNVAAGKARGVVIGTGLSTAIGKIRTEMS 240
FBpp0072122     TGESVSVIKHTDAIPDPRAVNQDKKNILFSGTNVAAGKARGVVIGTGLSTAIGKIRTEMS 240
FBpp0072125     TGESVSVIKHTDAIPDPRAVNQDKKNILFSGTNVAAGKARGVVIGTGLSTAIGKIRTEMS 240
FBpp0072127     TGESVSVIKHTDAIPDPRAVNQDKKNILFSGTNVAAGKARGVVIGTGLSTAIGKIRTEMS 240
FBpp0072126     TGESVSVIKHTDAIPDPRAVNQDKKNILFSGTNVAAGKARGVVIGTGLSTAIGKIRTEMS 240
FBpp0072123     TGESVSVIKHTDAIPDPRAVNQDKKNILFSGTNVAAGKARGVVIGTGLSTAIGKIRTEMS 240
FBpp0072120     TGESVSVIKHTDAIPDPRAVNQDKKNILFSGTNVAAGKARGVVIGTGLSTAIGKIRTEMS 240
FBpp0072124     TGESVSVIKHTDAIPDPRAVNQDKKNILFSGTNVAAGKARGVVIGTGLSTAIGKIRTEMS 240
                ************************************************************

FBpp0072121     ETEEIKTPLQQKLDEFGEQLSKVISVICVAVWAINIGHFNDPAHGGSWIKGAIYYFKIAV 300
FBpp0072122     ETEEIKTPLQQKLDEFGEQLSKVISVICVAVWAINIGHFNDPAHGGSWIKGAIYYFKIAV 300
FBpp0072125     ETEEIKTPLQQKLDEFGEQLSKVISVICVAVWAINIGHFNDPAHGGSWIKGAIYYFKIAV 300
FBpp0072127     ETEEIKTPLQQKLDEFGEQLSKVISVICVAVWAINIGHFNDPAHGGSWIKGAIYYFKIAV 300
FBpp0072126     ETEEIKTPLQQKLDEFGEQLSKVISVICVAVWAINIGHFNDPAHGGSWIKGAIYYFKIAV 300
FBpp0072123     ETEEIKTPLQQKLDEFGEQLSKVISVICVAVWAINIGHFNDPAHGGSWIKGAIYYFKIAV 300
FBpp0072120     ETEEIKTPLQQKLDEFGEQLSKVISVICVAVWAINIGHFNDPAHGGSWIKGAIYYFKIAV 300
FBpp0072124     ETEEIKTPLQQKLDEFGEQLSKVISVICVAVWAINIGHFNDPAHGGSWIKGAIYYFKIAV 300
                ************************************************************

FBpp0072121     ALAVAAIPEGLPAVITTCLALGTRRMAKKNAIVRSLPSVETLGCTSVICSDKTGTLTTNQ 360
FBpp0072122     ALAVAAIPEGLPAVITTCLALGTRRMAKKNAIVRSLPSVETLGCTSVICSDKTGTLTTNQ 360
FBpp0072125     ALAVAAIPEGLPAVITTCLALGTRRMAKKNAIVRSLPSVETLGCTSVICSDKTGTLTTNQ 360
FBpp0072127     ALAVAAIPEGLPAVITTCLALGTRRMAKKNAIVRSLPSVETLGCTSVICSDKTGTLTTNQ 360
FBpp0072126     ALAVAAIPEGLPAVITTCLALGTRRMAKKNAIVRSLPSVETLGCTSVICSDKTGTLTTNQ 360
FBpp0072123     ALAVAAIPEGLPAVITTCLALGTRRMAKKNAIVRSLPSVETLGCTSVICSDKTGTLTTNQ 360
FBpp0072120     ALAVAAIPEGLPAVITTCLALGTRRMAKKNAIVRSLPSVETLGCTSVICSDKTGTLTTNQ 360
FBpp0072124     ALAVAAIPEGLPAVITTCLALGTRRMAKKNAIVRSLPSVETLGCTSVICSDKTGTLTTNQ 360
                ************************************************************
```

```
FBpp0072121     MSVSRMFIFDKVEGNDSSFLEFEMTGSTYEPIGEVFLNGQRIKAADYDTLQELSTICIMC 420
FBpp0072122     MSVSRMFIFDKVEGNDSSFLEFEMTGSTYEPIGEVFLNGQRIKAADYDTLQELSTICIMC 420
FBpp0072125     MSVSRMFIFDKVEGNDSSFLEFEMTGSTYEPIGEVFLNGQRIKAADYDTLQELSTICIMC 420
FBpp0072127     MSVSRMFIFDKVEGNDSSFLEFEMTGSTYEPIGEVFLNGQRIKAADYDTLQELSTICIMC 420
FBpp0072126     MSVSRMFIFDKVEGNDSSFLEFEMTGSTYEPIGEVFLNGQRIKAADYDTLQELSTICIMC 420
FBpp0072123     MSVSRMFIFDKVEGNDSSFLEFEMTGSTYEPIGEVFLNGQRIKAADYDTLQELSTICIMC 420
FBpp0072120     MSVSRMFIFDKVEGNDSSFLEFEMTGSTYEPIGEVFLNGQRIKAADYDTLQELSTICIMC 420
FBpp0072124     MSVSRMFIFDKVEGNDSSFLEFEMTGSTYEPIGEVFLNGQRIKAADYDTLQELSTICIMC 420
                ************************************************************

FBpp0072121     NDSAIDYNEFKQAFEKVGEATETALIVLAEKLNSFSVNKSGLDRRSAAIACRGEIETKWK 480
FBpp0072122     NDSAIDYNEFKQAFEKVGEATETALIVLAEKLNSFSVNKSGLDRRSAAIACRGEIETKWK 480
FBpp0072125     NDSAIDYNEFKQAFEKVGEATETALIVLAEKLNSFSVNKSGLDRRSAAIACRGEIETKWK 480
FBpp0072127     NDSAIDYNEFKQAFEKVGEATETALIVLAEKLNSFSVNKSGLDRRSAAIACRGEIETKWK 480
FBpp0072126     NDSAIDYNEFKQAFEKVGEATETALIVLAEKLNSFSVNKSGLDRRSAAIACRGEIETKWK 480
FBpp0072123     NDSAIDYNEFKQAFEKVGEATETALIVLAEKLNSFSVNKSGLDRRSAAIACRGEIETKWK 480
FBpp0072120     NDSAIDYNEFKQAFEKVGEATETALIVLAEKLNSFSVNKSGLDRRSAAIACRGEIETKWK 480
FBpp0072124     NDSAIDYNEFKQAFEKVGEATETALIVLAEKLNSFSVNKSGLDRRSAAIACRGEIETKWK 480
                ************************************************************

FBpp0072121     KEFTLEFSRDRKSMSSYCTPLKASRLGTGPKLFVKGAPEGVLERCTHARVGTTKVPLTSA 540
FBpp0072122     KEFTLEFSRDRKSMSSYCTPLKASRLGTGPKLFVKGAPEGVLERCTHARVGTTKVPLTSA 540
FBpp0072125     KEFTLEFSRDRKSMSSYCTPLKASRLGTGPKLFVKGAPEGVLERCTHARVGTTKVPLTSA 540
FBpp0072127     KEFTLEFSRDRKSMSSYCTPLKASRLGTGPKLFVKGAPEGVLERCTHARVGTTKVPLTSA 540
FBpp0072126     KEFTLEFSRDRKSMSSYCTPLKASRLGTGPKLFVKGAPEGVLERCTHARVGTTKVPLTSA 540
FBpp0072123     KEFTLEFSRDRKSMSSYCTPLKASRLGTGPKLFVKGAPEGVLERCTHARVGTTKVPLTSA 540
FBpp0072120     KEFTLEFSRDRKSMSSYCTPLKASRLGTGPKLFVKGAPEGVLERCTHARVGTTKVPLTSA 540
FBpp0072124     KEFTLEFSRDRKSMSSYCTPLKASRLGTGPKLFVKGAPEGVLERCTHARVGTTKVPLTSA 540
                ************************************************************

FBpp0072121     LKAKILALTGQYGTGRDTLRCLALAVADSPMKPDEMDLGDSTKFYQYEVNLTFVGVVGML 600
FBpp0072122     LKAKILALTGQYGTGRDTLRCLALAVADSPMKPDEMDLGDSTKFYQYEVNLTFVGVVGML 600
FBpp0072125     LKAKILALTGQYGTGRDTLRCLALAVADSPMKPDEMDLGDSTKFYQYEVNLTFVGVVGML 600
FBpp0072127     LKAKILALTGQYGTGRDTLRCLALAVADSPMKPDEMDLGDSTKFYQYEVNLTFVGVVGML 600
FBpp0072126     LKAKILALTGQYGTGRDTLRCLALAVADSPMKPDEMDLGDSTKFYQYEVNLTFVGVVGML 600
FBpp0072123     LKAKILALTGQYGTGRDTLRCLALAVADSPMKPDEMDLGDSTKFYQYEVNLTFVGVVGML 600
FBpp0072120     LKAKILALTGQYGTGRDTLRCLALAVADSPMKPDEMDLGDSTKFYQYEVNLTFVGVVGML 600
FBpp0072124     LKAKILALTGQYGTGRDTLRCLALAVADSPMKPDEMDLGDSTKFYQYEVNLTFVGVVGML 600
                ************************************************************

FBpp0072121     DPPRKEVFDSIVRCRAAGIRVIVITGDNKATAEAICRRIGVFAEDEDTTGKSYSGREFDD 660
FBpp0072122     DPPRKEVFDSIVRCRAAGIRVIVITGDNKATAEAICRRIGVFAEDEDTTGKSYSGREFDD 660
FBpp0072125     DPPRKEVFDSIVRCRAAGIRVIVITGDNKATAEAICRRIGVFAEDEDTTGKSYSGREFDD 660
FBpp0072127     DPPRKEVFDSIVRCRAAGIRVIVITGDNKATAEAICRRIGVFAEDEDTTGKSYSGREFDD 660
FBpp0072126     DPPRKEVFDSIVRCRAAGIRVIVITGDNKATAEAICRRIGVFAEDEDTTGKSYSGREFDD 660
FBpp0072123     DPPRKEVFDSIVRCRAAGIRVIVITGDNKATAEAICRRIGVFAEDEDTTGKSYSGREFDD 660
FBpp0072120     DPPRKEVFDSIVRCRAAGIRVIVITGDNKATAEAICRRIGVFAEDEDTTGKSYSGREFDD 660
FBpp0072124     DPPRKEVFDSIVRCRAAGIRVIVITGDNKATAEAICRRIGVFAEDEDTTGKSYSGREFDD 660
                ************************************************************

FBpp0072121     LSPTEQKAAVARSRLFSRVEPQHKSKIVEFLQSMNEISAMTGDGVNDAPALKKAEIGIAM 720
FBpp0072122     LSPTEQKAAVARSRLFSRVEPQHKSKIVEFLQSMNEISAMTGDGVNDAPALKKAEIGIAM 720
FBpp0072125     LSPTEQKAAVARSRLFSRVEPQHKSKIVEFLQSMNEISAMTGDGVNDAPALKKAEIGIAM 720
FBpp0072127     LSPTEQKAAVARSRLFSRVEPQHKSKIVEFLQSMNEISAMTGDGVNDAPALKKAEIGIAM 720
FBpp0072126     LSPTEQKAAVARSRLFSRVEPQHKSKIVEFLQSMNEISAMTGDGVNDAPALKKAEIGIAM 720
FBpp0072123     LSPTEQKAAVARSRLFSRVEPQHKSKIVEFLQSMNEISAMTGDGVNDAPALKKAEIGIAM 720
FBpp0072120     LSPTEQKAAVARSRLFSRVEPQHKSKIVEFLQSMNEISAMTGDGVNDAPALKKAEIGIAM 720
FBpp0072124     LSPTEQKAAVARSRLFSRVEPQHKSKIVEFLQSMNEISAMTGDGVNDAPALKKAEIGIAM 720
                ************************************************************

FBpp0072121     GSGTAVAKSAAEMVLADDNFSSIVSAVEEGRAIYNNMKQFIRYLISSNIGEVVSIFLTAA 780
FBpp0072122     GSGTAVAKSAAEMVLADDNFSSIVSAVEEGRAIYNNMKQFIRYLISSNIGEVVSIFLTAA 780
FBpp0072125     GSGTAVAKSAAEMVLADDNFSSIVSAVEEGRAIYNNMKQFIRYLISSNIGEVVSIFLTAA 780
FBpp0072127     GSGTAVAKSAAEMVLADDNFSSIVSAVEEGRAIYNNMKQFIRYLISSNIGEVVSIFLTAA 780
FBpp0072126     GSGTAVAKSAAEMVLADDNFSSIVSAVEEGRAIYNNMKQFIRYLISSNIGEVVSIFLTAA 780
FBpp0072123     GSGTAVAKSAAEMVLADDNFSSIVSAVEEGRAIYNNMKQFIRYLISSNIGEVVSIFLTAA 780
FBpp0072120     GSGTAVAKSAAEMVLADDNFSSIVSAVEEGRAIYNNMKQFIRYLISSNIGEVVSIFLTAA 780
FBpp0072124     GSGTAVAKSAAEMVLADDNFSSIVSAVEEGRAIYNNMKQFIRYLISSNIGEVVSIFLTAA 780
                ************************************************************

FBpp0072121     LGLPEALIPVQLLWVNLVTDGLPATALGFNPPDLDIMEKPPRKADEGLISGWLFFRYMAI 840
FBpp0072122     LGLPEALIPVQLLWVNLVTDGLPATALGFNPPDLDIMEKPPRKADEGLISGWLFFRYMAI 840
FBpp0072125     LGLPEALIPVQLLWVNLVTDGLPATALGFNPPDLDIMEKPPRKADEGLISGWLFFRYMAI 840
FBpp0072127     LGLPEALIPVQLLWVNLVTDGLPATALGFNPPDLDIMEKPPRKADEGLISGWLFFRYMAI 840
FBpp0072126     LGLPEALIPVQLLWVNLVTDGLPATALGFNPPDLDIMEKPPRKADEGLISGWLFFRYMAI 840
FBpp0072123     LGLPEALIPVQLLWVNLVTDGLPATALGFNPPDLDIMEKPPRKADEGLISGWLFFRYMAI 840
```

```
FBpp0072120      LGLPEALIPVQLLWVNLVTDGLPATALGFNPPDLDIMEKPPRKADEGLISGWLFFRYMAI 840
FBpp0072124      LGLPEALIPVQLLWVNLVTDGLPATALGFNPPDLDIMEKPPRKADEGLISGWLFFRYMAI 840
                 ************************************************************

FBpp0072121      GFYVGAATVGAAAWWFVFSDEGPKLSYWQLTHHLSCLGGGDEFKGVDCKIFSDPHAMTMA 900
FBpp0072122      GFYVGAATVGAAAWWFVFSDEGPKLSYWQLTHHLSCLGGGDEFKGVDCKIFSDPHAMTMA 900
FBpp0072125      GFYVGAATVGAAAWWFVFSDEGPKLSYWQLTHHLSCLGGGDEFKGVDCKIFSDPHAMTMA 900
FBpp0072127      GFYVGAATVGAAAWWFVFSDEGPKLSYWQLTHHLSCLGGGDEFKGVDCKIFSDPHAMTMA 900
FBpp0072126      GFYVGAATVGAAAWWFVFSDEGPKLSYWQLTHHLSCLGGGDEFKGVDCKIFSDPHAMTMA 900
FBpp0072123      GFYVGAATVGAAAWWFVFSDEGPKLSYWQLTHHLSCLGGGDEFKGVDCKIFSDPHAMTMA 900
FBpp0072120      GFYVGAATVGAAAWWFVFSDEGPKLSYWQLTHHLSCLGGGDEFKGVDCKIFSDPHAMTMA 900
FBpp0072124      GFYVGAATVGAAAWWFVFSDEGPKLSYWQLTHHLSCLGGGDEFKGVDCKIFSDPHAMTMA 900
                 ************************************************************

FBpp0072121      LSVLVTIEMLNAMNSLSENQSLITMPPWCNLWLIGSMALSFTLHFVILYVDVLSTVFQVT 960
FBpp0072122      LSVLVTIEMLNAMNSLSENQSLITMPPWCNLWLIGSMALSFTLHFVILYVDVLSTVFQVT 960
FBpp0072125      LSVLVTIEMLNAMNSLSENQSLITMPPWCNLWLIGSMALSFTLHFVILYVDVLSTVFQVT 960
FBpp0072127      LSVLVTIEMLNAMNSLSENQSLITMPPWCNLWLIGSMALSFTLHFVILYVDVLSTVFQVT 960
FBpp0072126      LSVLVTIEMLNAMNSLSENQSLITMPPWCNLWLIGSMALSFTLHFVILYVDVLSTVFQVT 960
FBpp0072123      LSVLVTIEMLNAMNSLSENQSLITMPPWCNLWLIGSMALSFTLHFVILYVDVLSTVFQVT 960
FBpp0072120      LSVLVTIEMLNAMNSLSENQSLITMPPWCNLWLIGSMALSFTLHFVILYVDVLSTVFQVT 960
FBpp0072124      LSVLVTIEMLNAMNSLSENQSLITMPPWCNLWLIGSMALSFTLHFVILYVDVLSTVFQVT 960
                 ************************************************************

FBpp0072121      PLSAEEWITVMKFSIPVVLLDETLKFVARKIADGESPIYKMHGIVLMWAVFFGLLYAMML 1020
FBpp0072122      PLSAEEWITVMKFSIPVVLLDETLKFVARKIADGESPIYKMHGIVLMWAVFFGLLYAMML 1020
FBpp0072125      PLSAEEWITVMKFSIPVVLLDETLKFVARKIADGESPIYKMHGIVLMWAVFFGLLYAMML 1020
FBpp0072127      PLSAEEWITVMKFSIPVVLLDETLKFVARKIADGESPIYKMHGIVLMWAVFFGLLYAMML 1020
FBpp0072126      PLSAEEWITVMKFSIPVVLLDETLKFVARKIADGESPIYKMHGIVLMWAVFFGLLYAMML 1020
FBpp0072123      PLSAEEWITVMKFSIPVVLLDETLKFVARKIADGESPIYKMHGIVLMWAVFFGLLYAMML 1020
FBpp0072120      PLSAEEWITVMKFSIPVVLLDETLKFVARKIADGESPIYKMHGIVLMWAVFFGLLYAMML 1020
FBpp0072124      PLSAEEWITVMKFSIPVVLLDETLKFVARKIADVPDVVVDRM------------------ 1002
                 ********************************  . : .
```

Alignment of predicted protein sequences for *Drosophila melanogaster's reported eight Ca-P60A* mRNAs

FlyBase (available at http://flybase.org) reports the Drosophila SERCA gene, Ca-P60A to have eight different mRNAs (A-H). When the predicted translations are aligned using ClustalW2 at the European Bioinformatics Institute (available at http://www.ebi.ac.uk/Tools/msa/clustalw2/), isoforms B–H have identical protein sequences: *Drosophila* therefore has two protein isoforms (A with 1002 residues and B with 1020), differing only at the final 27 residues (9 of the short isoform) at the C terminus.

Drosophila melanogaster protein sequences in principal model organisms and humans

```
SERCA_3e_Homo.s      MEAAHLLPAADVLRHFSVTAEGGLSPAQVTGARERYGPNELPSEEGKSLWELVLEQFEDL 60
SERCA_3c_Homo.s      MEAAHLLPAADVLRHFSVTAEGGLSPAQVTGARERYGPNELPSEEGKSLWELVLEQFEDL 60
SERCA_3f_Homo.s      MEAAHLLPAADVLRHFSVTAEGGLSPAQVTGARERYGPNELPSEEGKSLWELVLEQFEDL 60
SERCA_2d_Homo.s      MEAAHLLPAADVLRHFSVTAEGGLSPAQVTGARERYGPNELPSEEGKSLWELVLEQFEDL 60
SERCA_3b_Homo.s      MEAAHLLPAADVLRHFSVTAEGGLSPAQVTGARERYGPNELPSEEGKSLWELVLEQFEDL 60
SERCA_3a_Homo.s      MEAAHLLPAADVLRHFSVTAEGGLSPAQVTGARERYGPNELPSEEGKSLWELVLEQFEDL 60
SERCA_3c_Mus.m       MEEAHLLSAADVLRRFSVTAEGGLSLEQVTDARERYGPNELPTEEGKSLWELVVEQFEDL 60
SERCA_3b_Mus.m       MEEAHLLSAADVLRRFSVTAEGGLSLEQVTDARERYGPNELPTEEGKSLWELVVEQFEDL 60
SERCA_3a_Mus.m       MEEAHLLSAADVLRRFSVTAEGGLSLEQVTDARERYGPNELPTEEGKSLWELVVEQFEDL 60
SERCA_3_Xeno_t       MDSAHAKTVSEVLRHFEVNENCGLSSEQVRRSREKYGLNELPAEEGKSLWELVLEQFEDL 60
SERCA_3_Danio.r      MENAHTKSASEVLANFGVNENTGLTLEQVKNNFDKYGPNELPAEEGKSLWELVVEQFEDL 60
SERCA_2b_Homo.s      MENAHTKTVEEVLGHFGVNESTGLSLEQVKKLKERWGSNELPAEEGKTLLELVIEQFEDL 60
SERCA_2a_Mus.m       MENAHTKTVEEVLGHFGVNESTGLSLEQVKKLKERWGSNELPAEEGKTLLELVIEQFEDL 60
SERCA_2b_Mus.m       MENAHTKTVEEVLGHFGVNESTGLSLEQVKKLKERWGSNELPAEEGKTLLELVIEQFEDL 60
SERCA_2a_Homo.s      MENAHTKTVEEVLGHFGVNESTGLSLEQVKKLKERWGSNELPAEEGKTLLELVIEQFEDL 60
SERCA_2_Xeno_t       MENAHTKTVEEVLAHFNVNESTGLSLEQVKKQKERWGANELPAEEGKTLWELVIEQFEDL 60
SERCA_2a_Danio.r     MENAHTKSVEEVYSNFSVNESTGLTLDQVKRNRDKWGPNELPAEEGKSIWELVIEQFEDL 60
SERCA_2b_Danio.r     MENAHTKTVEEVYSFFAVNESTGLGLEQVKRQREKWGPN------GKSLWELVVEQFEDL 54
SERCA_1a_Homo.s      MEAAHAKTTEECLAYFGVSETTGLTPDQVKRNLEKYGLNELPAEEGKTLWELVIEQFEDL 60
SERCA_1b_Homo.s      MEAAHAKTTEECLAYFGVSETTGLTPDQVKRNLEKYGLNELPAEEGKTLWELVIEQFEDL 60
SERCA_1_Mus.m        MEAAHSKSTEECLSYFGVSETTGLTPDQVKRHLEKYGPNELPAEEGKSLWELVVEQFEDL 60
SERCA_1_Xeno_t       MEAAHTKTTEECLAYFGVNENTGLSPEIVKKNFDKFGPNELPAEEGKSIWELVAEQFEDL 60
SERCA_1_Danio.r      MENAHTKETPECLAYFGVSESTGLTPEQVKKNQAKYGFNELPAEEGKSIWELVVEQFEDL 60
SERCA_b_Dros.m       MEDGHSKTVEQSLNFFGTDPERGLTLDQIKANQKKYGPNELPTEEGKSIWQLVLEQFDDL 60
SERCA_a_Dros.m       MEDGHSKTVEQSLNFFGTDPERGLTLDQIKANQKKYGPNELPTEEGKSIWQLVLEQFDDL 60
SERCA_Caen.e         MEDAHAKDANEVCKFFGTGPE-GLTPQQVETLRNKYGENEMPAEEGKSLWELILEQFDDL 59
                     *: .*   . :    * .    **    :     ::* *      **:: :*: ***:**

SERCA_3e_Homo.s      LVRILLLAALVSFVLAWFEEGEET---TTAFVEPLVIMLILVANAIVGVWQERNAESAIE 117
SERCA_3c_Homo.s      LVRILLLAALVSFVLAWFEEGEET---TTAFVEPLVIMLILVANAIVGVWQERNAESAIE 117
SERCA_3f_Homo.s      LVRILLLAALVSFVLAWFEEGEET---TTAFVEPLVIMLILVANAIVGVWQERNAESAIE 117
SERCA_2d_Homo.s      LVRILLLAALVSFVLAWFEEGEET---TTAFVEPLVIMLILVANAIVGVWQERNAESAIE 117
SERCA_3b_Homo.s      LVRILLLAALVSFVLAWFEEGEET---TTAFVEPLVIMLILVANAIVGVWQERNAESAIE 117
SERCA_3a_Homo.s      LVRILLLAALVSFVLAWFEEGEET---TTAFVEPLVIMLILVANAIVGVWQERNAESAIE 117
SERCA_3c_Mus.m       LVRILLLAALVSFVLAWFEEGEET---TTAFVEPLVIMLILVANAIVGVWQERNAESAIE 117
SERCA_3b_Mus.m       LVRILLLAALVSFVLAWFEEGEET---TTAFVEPLVIMLILVANAIVGVWQERNAESAIE 117
SERCA_3a_Mus.m       LVRILLLAALVSFVLAWFEEGEET---TTAFVEPLVIMLILVANAIVGVWQERNAESAIE 117
SERCA_3_Xeno_t       LVRILLLAAFVSFILAWFEEGEET---TTAFVEPIVIIMILVINAFVGVWQERNAESAIE 117
SERCA_3_Danio.r      LVRILLLAACVSFVLALFEEGEES---TTAFVEPIVILLILVANAVIGVWQERNAENAIE 117
SERCA_2b_Homo.s      LVRILLLAACISFVLAWFEEGEET---ITAFVEPFVILLILVANAIVGVWQERNAENAIE 117
SERCA_2a_Mus.m       LVRILLLAACISFVLAWFEEGEET---ITAFVEPFVILLILVANAIVGVWQERNAENAIE 117
SERCA_2b_Mus.m       LVRILLLAACISFVLAWFEEGEET---ITAFVEPFVILLILVANAIVGVWQERNAENAIE 117
SERCA_2a_Homo.s      LVRILLLAACISFVLAWFEEGEET---ITAFVEPFVILLILVANAIVGVWQERNAENAIE 117
SERCA_2_Xeno_t       LVRILLLAACISFVLAWFEEGEET---ITAFVEPFVILLILVANAIVGVWQERNAENAIE 117
SERCA_2a_Danio.r     LVRILLLAACISFVLAWFEEGEET---ITAFVEPFVILLILIANAIVGVWQERNAENAIE 117
SERCA_2b_Danio.r     LVRILLLAACISFVLAWFEEGEET---ITAFVEPFVILLILIANAIVGVWQERNAENAIE 111
SERCA_1a_Homo.s      LVRILLLAACISFVLAWFEEGEET---ITAFVEPFVILLILIANAIVGVWQERNAENAIE 117
SERCA_1b_Homo.s      LVRILLLAACISFVLAWFEEGEET---ITAFVEPFVILLILIANAIVGVWQERNAENAIE 117
SERCA_1_Mus.m        LVRILLLAACISFVLAWFEEGEET---VTAFVEPFVILLILIANAIVGVWQERNAENAIE 117
SERCA_1_Xeno_t       LVRILLLAACISFVLAWFEEGEET---VTAFVEPFVILLILIANAVVGVWQERNAEDAIE 117
SERCA_1_Danio.r      LVRILLLAACISFVLAWFEEGEET---VTAFVEPFVILLILIANAVVGVWQERNAESAIE 117
SERCA_b_Dros.m       LVKILLLAAIISFVLALFEEHEET---FTAFVEPLVILLILIANAVVGVWQERNAESAIE 117
SERCA_a_Dros.m       LVKILLLAAIISFVLALFEEHEET---FTAFVEPLVILLILIANAVVGVWQERNAESAIE 117
SERCA_Caen.e         LVKILLLAAIISFVLALFEEHEDQTEAVTAFVEPFVILLILIANATVGVWQERNAESAIE 119
                     **:****** :**:** *** *:     ******:**::**: ** :*********.***

SERCA_3e_Homo.s      ALKEYEPEMGKVIRSDRKGVQRIRARDIVPGDIVEVAVGDKVPADLRLIEIKSTTLRVDQ 177
SERCA_3c_Homo.s      ALKEYEPEMGKVIRSDRKGVQRIRARDIVPGDIVEVAVGDKVPADLRLIEIKSTTLRVDQ 177
SERCA_3f_Homo.s      ALKEYEPEMGKVIRSDRKGVQRIRARDIVPGDIVEVAVGDKVPADLRLIEIKSTTLRVDQ 177
SERCA_2d_Homo.s      ALKEYEPEMGKVIRSDRKGVQRIRARDIVPGDIVEVAVGDKVPADLRLIEIKSTTLRVDQ 177
SERCA_3b_Homo.s      ALKEYEPEMGKVIRSDRKGVQRIRARDIVPGDIVEVAVGDKVPADLRLIEIKSTTLRVDQ 177
SERCA_3a_Homo.s      ALKEYEPEMGKVIRSDRKGVQRIRARDIVPGDIVEVAVGDKVPADLRLIEIKSTTLRVDQ 177
```

```
SERCA_3c_Mus.m        ALKEYEPEMGKVIRSDRKGVQRIRARDIVPGDIVEVAVGDKVPADLRLIEIKSTTLRVDQ 177
SERCA_3b_Mus.m        ALKEYEPEMGKVIRSDRKGVQRIRARDIVPGDIVEVAVGDKVPADLRLIEIKSTTLRVDQ 177
SERCA_3a_Mus.m        ALKEYEPEMGKVIRSDRKGVQRIRARDIVPGDIVEVAVGDKVPADLRLIEIKSTTLRVDQ 177
SERCA_3_Xeno_t        ALKEYEPEMGKVIRGDRSGVQRIRARDIVPGDIVEVAVGDKVPADIRITEIRSTTLRVDQ 177
SERCA_3_Danio.r       ALKEYEPEMGKVYRMNRTAVQRIKARDIVPGDIVEISVGDKVPADIRITSIKSTTLRVDQ 177
SERCA_2b_Homo.s       ALKEYEPEMGKVYRQDRKSVQRIKAKDIVPGDIVEIAVGDKVPADIRLTSIKSTTLRVDQ 177
SERCA_2a_Mus.m        ALKEYEPEMGKVYRQDRKSVQRIKAKDIVPGDIVEIAVGDKVPADIRLTSIKSTTLRVDQ 177
SERCA_2b_Mus.m        ALKEYEPEMGKVYRQDRKSVQRIKAKDIVPGDIVEIAVGDKVPADIRLTSIKSTTLRVDQ 177
SERCA_2a_Homo.s       ALKEYEPEMGKVYRQDRKSVQRIKAKDIVPGDIVEIAVGDKVPADIRLTSIKSTTLRVDQ 177
SERCA_2_Xeno_t        ALKEYEPEMGKVYRQDRKSVQRIKARDIVPGDIVEVAVGDKVPADIRLTSIKSTTLRVDQ 177
SERCA_2a_Danio.r      ALKEYEPEMGKVYRQDRKSVQRIKAKDIVPGDIVEVAVGDKVPADIRISAIKSTTLRVDQ 177
SERCA_2b_Danio.r      ALKEYEPEMGKVYRQDRKTVQRIKARDIVPGDIVEVAVGDKVPADIRLTSIKSTTLRVDQ 171
SERCA_1a_Homo.s       ALKEYEPEMGKVYRADRKSVQRIKARDIVPGDIVEVAVGDKVPADIRILAIKSTTLRVDQ 177
SERCA_1b_Homo.s       ALKEYEPEMGKVYRADRKSVQRIKARDIVPGDIVEVAVGDKVPADIRILAIKSTTLRVDQ 177
SERCA_1_Mus.m         ALKEYEPEMGKVYRADRKSVQRIKARDIVPGDIVEVAVGDKVPADIRILSIKSTTLRVDQ 177
SERCA_1_Xeno_t        ALKEYEPEMGKVYRSDRKSVQRIKAREIVPGDIVEVAVGDKVPADIRLISIKSTTLRIDQ 177
SERCA_1_Danio.r       ALKEYEPEMGKVYRSDRKSVQRIKAREIVPGDIVEVSVGDKVPADIRITAIRSTTLRVDQ 177
SERCA_b_Dros.m        ALKEYEPEMGKVVRQDKSGIQKVRAKEIVPGDLVEVSVGDKIPADIRITHIYSTTLRIDQ 177
SERCA_a_Dros.m        ALKEYEPEMGKVVRQDKSGIQKVRAKEIVPGDLVEVSVGDKIPADIRITHIYSTTLRIDQ 177
SERCA_Caen.e          ALKEYEPEMAKVIRSGHHGIQMVRAKELVPGDLVEVSVGDKIPADLRLVKIYSTTIRIDQ 179
                      *********.** * .:  :* ::*:::****:**::****:***:*:  * ***:*:**

SERCA_3e_Homo.s       SILTGESVSVTKHTEAIPDPRAVNQDKKNMLFSGTNITSGKAVGVAVATGLHTELGKIRS 237
SERCA_3c_Homo.s       SILTGESVSVTKHTEAIPDPRAVNQDKKNMLFSGTNITSGKAVGVAVATGLHTELGKIRS 237
SERCA_3f_Homo.s       SILTGESVSVTKHTEAIPDPRAVNQDKKNMLFSGTNITSGKAVGVAVATGLHTELGKIRS 237
SERCA_2d_Homo.s       SILTGESVSVTKHTEAIPDPRAVNQDKKNMLFSGTNITSGKAVGVAVATGLHTELGKIRS 237
SERCA_3b_Homo.s       SILTGESVSVTKHTEAIPDPRAVNQDKKNMLFSGTNITSGKAVGVAVATGLHTELGKIRS 237
SERCA_3a_Homo.s       SILTGESVSVTKHTEAIPDPRAVNQDKKNMLFSGTNITSGKAVGVAVATGLHTELGKIRS 237
SERCA_3c_Mus.m        SILTGESVSVTKHTDAIPDPRAVNQDKKNMLFSGTNIASGKALGVAVATGLQTELGKIRS 237
SERCA_3b_Mus.m        SILTGESVSVTKHTDAIPDPRAVNQDKKNMLFSGTNIASGKALGVAVATGLQTELGKIRS 237
SERCA_3a_Mus.m        SILTGESVSVTKHTDAIPDPRAVNQDKKNMLFSGTNIASGKALGVAVATGLQTELGKIRS 237
SERCA_3_Xeno_t        SILTGESVSVIKHTDPIPDPRAVNQDKKNMLFSGTNIAAGKAVGIVIATGIYTEIGKIRN 237
SERCA_3_Danio.r       SILTGESVSVIKHTDPVPDPRAVNQDKKNMLFSGTNIAAGRAIGVVVSTGVSTEIGKIRN 237
SERCA_2b_Homo.s       SILTGESVSVIKHTDPVPDPRAVNQDKKNMLFSGTNIAAGKAMGVVVATGVNTEIGKIRD 237
SERCA_2a_Mus.m        SILTGESVSVIKHTDPVPDPRAVNQDKKNMLFSGTNIAAGKAMGVVVATGVNTEIGKIRD 237
SERCA_2b_Mus.m        SILTGESVSVIKHTDPVPDPRAVNQDKKNMLFSGTNIAAGKAMGVVVATGVNTEIGKIRD 237
SERCA_2a_Homo.s       SILTGESVSVIKHTDPVPDPRAVNQDKKNMLFSGTNIAAGKAMGVVVATGVNTEIGKIRD 237
SERCA_2_Xeno_t        SILTGESVSVIKHTDPVPDPRAVNQDKKNMLFSGTNIAAGKAIGVVVATGVNTEIGKIRD 237
SERCA_2a_Danio.r      SILTGESVSVIKHTDPVPDPRAVNQDKKNMLFSGTNIAAGKAIGVVVATGVNTEIGKIRD 237
SERCA_2b_Danio.r      SILTGESVSVIKHTDPVPDPRAVNQDKKNMLFSGTNIAAGKAVGVVVATGVNTEIGKIRD 231
SERCA_1a_Homo.s       SILTGESVSVIKHTEPVPDPRAVNQDKKNMLFSGTNIAAGKALGIVATTGVGTEIGKIRD 237
SERCA_1b_Homo.s       SILTGESVSVIKHTEPVPDPRAVNQDKKNMLFSGTNIAAGKALGIVATTGVGTEIGKIRD 237
SERCA_1_Mus.m         SILTGESVSVIKHTDPVPDPRAVNQDKKNMLFSGTNIAAGKAVGIVATTGVSTEIGKIRD 237
SERCA_1_Xeno_t        SILTGESVSVIKHTEAVPDPRAVNQDKKNMLFSGTNVGAGKAIGVVIATGPNTEIGKIRD 237
SERCA_1_Danio.r       SILTGESVSVIKHTESVPDPRAVNQDKKNMLFSGTNIAAGKAIGVVVATGVSTEIGKIRD 237
SERCA_b_Dros.m        SILTGESVSVIKHTDAIPDPRAVNQDKKNILFSGTNVAAGKARGVVIGTGLSTAIGKIRT 237
SERCA_a_Dros.m        SILTGESVSVIKHTDAIPDPRAVNQDKKNILFSGTNVAAGKARGVVIGTGLSTAIGKIRT 237
SERCA_Caen.e          SILTGESVSVIKHTDSVPDPRAVNQDKKNCLFSGTNVASGKARGIVFGTGLTTEIGKIRT 239
                      ********** ***:.:************ ******: :*:* *:.  **  * :****

SERCA_3e_Homo.s       QMAAVEPERTPLQRKLDEFGRQLSHAISVICVAVWVINIGHFADPAHGGSWLRGAVYYFK 297
SERCA_3c_Homo.s       QMAAVEPERTPLQRKLDEFGRQLSHAISVICVAVWVINIGHFADPAHGGSWLRGAVYYFK 297
SERCA_3f_Homo.s       QMAAVEPERTPLQRKLDEFGRQLSHAISVICVAVWVINIGHFADPAHGGSWLRGAVYYFK 297
SERCA_2d_Homo.s       QMAAVEPERTPLQRKLDEFGRQLSHAISVICVAVWVINIGHFADPAHGGSWLRGAVYYFK 297
SERCA_3b_Homo.s       QMAAVEPERTPLQRKLDEFGRQLSHAISVICVAVWVINIGHFADPAHGGSWLRGAVYYFK 297
SERCA_3a_Homo.s       QMAAVEPERTPLQRKLDEFGRQLSHAISVICVAVWVINIGHFADPAHGGSWLRGAVYYFK 297
SERCA_3c_Mus.m        QMAAVEPERTPLQRKLDEFGRQLSHAISVICVAVWVINIGHFADPAHGGSWLRGAVYYFK 297
SERCA_3b_Mus.m        QMAAVEPERTPLQRKLDEFGRQLSHAISVICVAVWVINIGHFADPAHGGSWLRGAVYYFK 297
SERCA_3a_Mus.m        QMAAVEPERTPLQRKLDEFGRQLSHAISVICVAVWVINIGHFADPAHGGSWLRGAVYYFK 297
SERCA_3_Xeno_t        QMVATEPEKTPLQQKLDEFGQQLSKVISLICVAVWVINIGHFNDPVHGGSWFRGAIYYFK 297
SERCA_3_Danio.r       QMAATEQEKTPLQQKLDEFGQQLSKVISLICIAVWVINIGHFADPVHGGSWIRGAIYYFK 297
SERCA_2b_Homo.s       EMVATEQERTPLQQKLDEFGEQLSKVISLICIAVWIINIGHFNDPVHGGSWIRGAIYYFK 297
SERCA_2a_Mus.m        EMVATEQERTPLQQKLDEFGEQLSKVISLICIAVWIINIGHFNDPVHGGSWIRGAIYYFK 297
SERCA_2b_Mus.m        EMVATEQERTPLQQKLDEFGEQLSKVISLICIAVWIINIGHFNDPVHGGSWIRGAIYYFK 297
SERCA_2a_Homo.s       EMVATEQERTPLQQKLDEFGEQLSKVISLICIAVWIINIGHFNDPVHGGSWIRGAIYYFK 297
SERCA_2_Xeno_t        EMVATEQERTPLQQKLDEFGEQLSKVISLICIAVWIINIGHFNDPVHGGSWIRGAIYYFK 297
SERCA_2a_Danio.r      EMASTEQERTPLQQKLDEFGEQLSKVISLICIAVWIINIGHFNDPVHGGSWIRGAVYYFK 297
SERCA_2b_Danio.r      EMASTEQERTPLQQKLDEFGQQLSKVISLICIAVWIINIGHFNDPVHGGSWVRGAVYYFK 291
SERCA_1a_Homo.s       QMAATEQDKTPLQQKLDEFGEQLSKVISLICVAVWLINIGHFNDPVHGGSWFRGAIYYFK 297
SERCA_1b_Homo.s       QMAATEQDKTPLQQKLDEFGEQLSKVISLICVAVWLINIGHFNDPVHGGSWFRGAIYYFK 297
SERCA_1_Mus.m         QMAATEQDKTPLQQKLDEFGEQLSKVISLICVAVWLINIGHFNDPVHGGSWFRGAIYYFK 297
SERCA_1_Xeno_t        EMAATEQEKTPLQQKLDEFGEQLSKVISLICVAVWLINIGHFNDPIHGGSWIKGAIYYFK 297
SERCA_1_Danio.r       QMAATEQEKTPLQQKLDEFGEQLSKVISLICVAVWLINIGHFNDPVHGGSWIRGAVYYFK 297
SERCA_b_Dros.m        EMSETEEIKTPLQQKLDEFGEQLSKVISVICVAVWAINIGHFNDPAHGGSWIKGAIYYFK 297
SERCA_a_Dros.m        EMSETEEIKTPLQQKLDEFGEQLSKVISVICVAVWAINIGHFNDPAHGGSWIKGAIYYFK 297
SERCA_Caen.e          EMAETENEKTPLQQKLDEFGEQLSKVISVICVAVWAINIGHFNDPAHGGSWVKGAIYYFK 299
                      :*  .*  :****:******.***:.**:**:*** ****** ** *****.:**:****
```

```
SERCA_3e_Homo.s      IAVALAVAAIPEGLPAVITTCLALGTRRMARKNAIVRSLPSVETLGCTSVICSDKTGTLT 357
SERCA_3c_Homo.s      IAVALAVAAIPEGLPAVITTCLALGTRRMARKNAIVRSLPSVETLGCTSVICSDKTGTLT 357
SERCA_3f_Homo.s      IAVALAVAAIPEGLPAVITTCLALGTRRMARKNAIVRSLPSVETLGCTSVICSDKTGTLT 357
SERCA_2d_Homo.s      IAVALAVAAIPEGLPAVITTCLALGTRRMARKNAIVRSLPSVETLGCTSVICSDKTGTLT 357
SERCA_3b_Homo.s      IAVALAVAAIPEGLPAVITTCLALGTRRMARKNAIVRSLPSVETLGCTSVICSDKTGTLT 357
SERCA_3a_Homo.s      IAVALAVAAIPEGLPAVITTCLALGTRRMARKNAIVRSLPSVETLGCTSVICSDKTGTLT 357
SERCA_3c_Mus.m       IAVALAVAAIPEGLPAVITTCLALGTRRMARKNAIVRSLPSVETLGCTSVICSDKTGTLT 357
SERCA_3b_Mus.m       IAVALAVAAIPEGLPAVITTCLALGTRRMARKNAIVRSLPSVETLGCTSVICSDKTGTLT 357
SERCA_3a_Mus.m       IAVALAVAAIPEGLPAVITTCLALGTRRMARKNAIVRSLPSVETLGCTSVICSDKTGTLT 357
SERCA_3_Xeno_t       IAVALAVAAIPEGLPAVITTCLALGTRRMAKKNAIVRSLPSVETLGCTSVICSDKTGTLT 357
SERCA_3_Danio.r      IAVALAVAAIPEGLPAVITTCLALGTRRMAKKNAIVRSLPSVETLGCTSVICSDKTGTLT 357
SERCA_2b_Homo.s      IAVALAVAAIPEGLPAVITTCLALGTRRMAKKNAIVRSLPSVETLGCTSVICSDKTGTLT 357
SERCA_2a_Mus.m       IAVALAVAAIPEGLPAVITTCLALGTRRMAKKNAIVRSLPSVETLGCTSVICSDKTGTLT 357
SERCA_2b_Mus.m       IAVALAVAAIPEGLPAVITTCLALGTRRMAKKNAIVRSLPSVETLGCTSVICSDKTGTLT 357
SERCA_2a_Homo.s      IAVALAVAAIPEGLPAVITTCLALGTRRMAKKNAIVRSLPSVETLGCTSVICSDKTGTLT 357
SERCA_2_Xeno_t       IAVALAVAAIPEGLPAVITTCLALGTRRMAKKNAIVRSLPSVETLGCTSVICSDKTGTLT 357
SERCA_2a_Danio.r     IAVALAVAAIPEGLPAVITTCLALGTRRMAKKNAIVRSLPSVETLGCTSVICSDKTGTLT 357
SERCA_2b_Danio.r     IAVALAVAAIPEGLPAVITTCLALGTRRMAKKNAIVRSLPSVETLGCTSVICSDKTGTLT 351
SERCA_1a_Homo.s      IAVALAVAAIPEGLPAVITTCLALGTRRMAKKNAIVRSLPSVETLGCTSVICSDKTGTLT 357
SERCA_1b_Homo.s      IAVALAVAAIPEGLPAVITTCLALGTRRMAKKNAIVRSLPSVETLGCTSVICSDKTGTLT 357
SERCA_1_Mus.m        IAVALAVAAIPEGLPAVITTCLALGTRRMAKKNAIVRSLPSVETLGCTSVICSDKTGTLT 357
SERCA_1_Xeno_t       IAVALAVAAIPEGLPAVITTCLALGTRRMAKKNAIVRSLPSVETLGCTSVICSDKTGTLT 357
SERCA_1_Danio.r      IAVALAVAAIPEGLPAVITTCLALGTRRMAKKNAIVRSLPSVETLGCTSVICSDKTGTLT 357
SERCA_b_Dros.m       IAVALAVAAIPEGLPAVITTCLALGTRRMAKKNAIVRSLPSVETLGCTSVICSDKTGTLT 357
SERCA_a_Dros.m       IAVALAVAAIPEGLPAVITTCLALGTRRMAKKNAIVRSLPSVETLGCTSVICSDKTGTLT 357
SERCA_Caen.e         IAVALAVAAIPEGLPAVITTCLALGTRRMAKKNAIVRSLPSVETLGCTSVICSDKTGTLT 359
                     ******************************:****************************

SERCA_3e_Homo.s      TNQMSVCRMFVVAEADAGSCLLHEFTISGTTYTPEGEVRQGDQPVR--CGQFDGLVELAT 415
SERCA_3c_Homo.s      TNQMSVCRMFVVAEADAGSCLLHEFTISGTTYTPEGEVRQGDQPVR--CGQFDGLVELAT 415
SERCA_3f_Homo.s      TNQMSVCRMFVVAEADAGSCLLHEFTISGTTYTPEGEVRQGDQPVR--CGQFDGLVELAT 415
SERCA_2d_Homo.s      TNQMSVCRMFVVAEADAGSCLLHEFTISGTTYTPEGEVRQGDQPVR--CGQFDGLVELAT 415
SERCA_3b_Homo.s      TNQMSVCRMFVVAEADAGSCLLHEFTISGTTYTPEGEVRQGDQPVR--CGQFDGLVELAT 415
SERCA_3a_Homo.s      TNQMSVCRMFVVAEADAGSCLLHEFTISGTTYTPEGEVRQGDQPVR--CGQFDGLVELAT 415
SERCA_3c_Mus.m       TNQMSVCRMFVVAEAEAGTCRLHEFTISGTTYTPEGEVRQGEQPVR--CGQFDGLVELAT 415
SERCA_3b_Mus.m       TNQMSVCRMFVVAEAEAGTCRLHEFTISGTTYTPEGEVRQGEQPVR--CGQFDGLVELAT 415
SERCA_3a_Mus.m       TNQMSVCRMFVVAEAEAGTCRLHEFTISGTTYTPEGEVRQGEQPVR--CGQFDGLVELAT 415
SERCA_3_Xeno_t       TNQMSVSRMFVIEKIEGVNCSFHEFSITGSTYAPVGQVLKDEQPVN--CGQFDGLVELAT 415
SERCA_3_Danio.r      TNQMSVCRMFVVNKADDSSCSLHEFTISGSTYAPEGEVLKADKQVQ--CGDYDGLVELAT 415
SERCA_2b_Homo.s      TNQMSVCRMFILDRVEGDTCSLNEFTITGSTYAPIGEVHKDDKPVN--CHQYDGLVELAT 415
SERCA_2a_Mus.m       TNQMSVCRMFILDKVEGDTCSLNEFSITGSTYAPIGEVQKDDKPVK--CHQYDGLVELAT 415
SERCA_2b_Mus.m       TNQMSVCRMFILDKVEGDTCSLNEFSITGSTYAPIGEVQKDDKPVK--CHQYDGLVELAT 415
SERCA_2a_Homo.s      TNQMSVCRMFILDRVEGDTCSLNEFTITGSTYAPIGEVHKDDKPVN--CHQYDGLVELAT 415
SERCA_2_Xeno_t       TNQMSVCR-------------VRNCFIFSLKSLPXREVLKDDKLVK--CHQYDGLVELAT 402
SERCA_2a_Danio.r     TNQMSVCRMFIIDKAEGENCSLTEFTISGSTYAPEGDVCLDNRIVK--CSQYDGLVELAT 415
SERCA_2b_Danio.r     TNQMSVCRMFIVDQANGNTCSLKEFSISGSTYAPDGQVCHEGKPVQ--CSKFDALVEMAS 409
SERCA_1a_Homo.s      TNQMSVCKMFIIDKVDGDICLLNEFSITGSTYAPEGEVLKNDKPVR--PGQYDGLVELAT 415
SERCA_1b_Homo.s      TNQMSVCKMFIIDKVDGDICLLNEFSITGSTYAPEGEVLKNDKPVR--PGQYDGLVELAT 415
SERCA_1_Mus.m        TNQMSVCKMFIIDKVDGDVCSLNEFSITGSTYAPEGEVLKNDKPVR--AGQYDGLVELAT 415
SERCA_1_Xeno_t       TNQMSVCRMFVLDKVDGDICSLNEFSITGSTYAPEGEVLKNDKSVK--AGQYDGLVELAT 415
SERCA_1_Danio.r      TNQMCVTKMFVIEKVEGESVTLDQYDISGSKYTPEGEVTKNGLPVK--CGQFDGLVELAT 415
SERCA_b_Dros.m       TNQMSVSRMFIFDKVEGNDSSFLEFEMTGSTYEPIGEVFLNGQRIK--AADYDTLQELST 415
SERCA_a_Dros.m       TNQMSVSRMFIFDKVEGNDSSFLEFEMTGSTYEPIGEVFLNGQRIK--AADYDTLQELST 415
SERCA_Caen.e         TNQMSVSKMFIAGQASGDNINFTEFAISGSTYEPVGKVSTNGREINPAAGEFESLTELAM 419
                     ****.* :             . :  : . .  *  .*      :.    .:: * *::

SERCA_3e_Homo.s      ICALCNDSALDYNEAKGVYEKVGEATETALTCLVEKMNVFDTDLQALSRVERAGACNTVI 475
SERCA_3c_Homo.s      ICALCNDSALDYNEAKGVYEKVGEATETALTCLVEKMNVFDTDLQALSRVERAGACNTVI 475
SERCA_3f_Homo.s      ICALCNDSALDYNEAKGVYEKVGEATETALTCLVEKMNVFDTDLQALSRVERAGACNTVI 475
SERCA_2d_Homo.s      ICALCNDSALDYNEAKGVYEKVGEATETALTCLVEKMNVFDTDLQALSRVERAGACNTVI 475
SERCA_3b_Homo.s      ICALCNDSALDYNEAKGVYEKVGEATETALTCLVEKMNVFDTDLQALSRVERAGACNTVI 475
SERCA_3a_Homo.s      ICALCNDSALDYNEAKGVYEKVGEATETALTCLVEKMNVFDTDLQALSRVERAGACNTVI 475
SERCA_3c_Mus.m       ICALCNDSALDYNEAKGVYEKVGEATETALTCLVEKMNVFDTDLKGLSRVERAGACNSVI 475
SERCA_3b_Mus.m       ICALCNDSALDYNEAKGVYEKVGEATETALTCLVEKMNVFDTDLKGLSRVERAGACNSVI 475
SERCA_3a_Mus.m       ICALCNDSALDYNEAKGVYEKVGEATETALTCLVEKMNVFDTDLKGLSRVERAGACNSVI 475
SERCA_3_Xeno_t       ICALCNDSSLDFNESKGVYEKVGEATETALTCLVEKMNVFNTDLSTLSKVERANACNSVI 475
SERCA_3_Danio.r      ICSLCNDSSLDYNEAKGVYEKVGEATETALTTLVEKMNVFKTDLSGLSKVDRAAACNLII 475
SERCA_2b_Homo.s      ICALCNDSALDYNEAKGVYEKVGEATETALTCLVEKMNVFDTELKGLSKIERANACNSVI 475
SERCA_2a_Mus.m       ICALCNDSALDYNEAKGVYEKVGEATETALTCLVEKMNVFDTELKGLSKIERANACNSVI 475
SERCA_2b_Mus.m       ICALCNDSALDYNEAKGVYEKVGEATETALTCLVEKMNVFDTELKGLSKIERANACNSVI 475
SERCA_2a_Homo.s      ICALCNDSALDYNEAKGVYEKVGEATETALTCLVEKMNVFDTELKGLSKIERANACNSVI 475
SERCA_2_Xeno_t       ICALCNDSSLDFNEAKGVYEKVGEATETALTCLVEKMNVFDTDLKGLSRIERANACNSVI 462
SERCA_2a_Danio.r     ICALCNDSSLDFNESKGVYEKVGEATETALTCLVEKMNVFDTDVRNLSKIERANACNAVI 475
SERCA_2b_Danio.r     ICALCNDSSLDYNEAKGVYEKVGEATETALTCLVEKMNVFDTELKGLSKVERANACNSVI 469
SERCA_1a_Homo.s      ICALCNDSSLDFNEAKGVYEKVGEATETALTTLVEKMNVFNTDVRSLSKVERANACNSVI 475
SERCA_1b_Homo.s      ICALCNDSSLDFNEAKGVYEKVGEATETALTTLVEKMNVFNTDVRSLSKVERANACNSVI 475
SERCA_1_Mus.m        ICALCNDSSLDFNETKGVYEKVGEATETALTTLVEKMNVFNTEVRSLSKVERANACNSVI 475
SERCA_1_Xeno_t       ICALCNDSSLDYNESKGVFEKVGEATETALTTLVEKMNVFNTEVRSLSKVERANACNSVI 475
```

```
SERCA_1_Danio.r      ICALCNDSSLDYNESKGIYEKVGEATETALCCLVEKMNVFNTDVRGLSKVERANTCCAVI 475
SERCA_b_Dros.m       ICIMCNDSAIDYNEFKQAFEKVGEATETALIVLAEKLNSFSVNKSGLDRRSAAIACRGEI 475
SERCA_a_Dros.m       ICIMCNDSAIDYNEFKQAFEKVGEATETALIVLAEKLNSFSVNKSGLDRRSAAIACRGEI 475
SERCA_Caen.e         ICAMCNDSSVDYNETKKIYEKVGEATETALIVLAEKMNVFGTSKAGLSPKELGGVCNRVI 479
                     ** :****::*:** *  :***********  *.**:* * ..   *.  . . .*   *

SERCA_3e_Homo.s      KQLMRKEFTLEFSRDRKSMSVYCTPTRPHPTGQGSKMFVKGAPESVIERCSSVRVGSRTA 535
SERCA_3c_Homo.s      KQLMRKEFTLEFSRDRKSMSVYCTPTRPHPTGQGSKMFVKGAPESVIERCSSVRVGSRTA 535
SERCA_3f_Homo.s      KQLMRKEFTLEFSRDRKSMSVYCTPTRPHPTGQGSKMFVKGAPESVIERCSSVRVGSRTA 535
SERCA_2d_Homo.s      KQLMRKEFTLEFSRDRKSMSVYCTPTRPHPTGQGSKMFVKGAPESVIERCSSVRVGSRTA 535
SERCA_3b_Homo.s      KQLMRKEFTLEFSRDRKSMSVYCTPTRPHPTGQGSKMFVKGAPESVIERCSSVRVGSRTA 535
SERCA_3a_Homo.s      KQLMRKEFTLEFSRDRKSMSVYCTPTRPHPTGQGSKMFVKGAPESVIERCSSVRVGSRTA 535
SERCA_3c_Mus.m       KQLMRKEFTLEFSRDRKSMSVYCTPTRADPKVQGSKMFVKGAPESVIERCSSVRVGSRTA 535
SERCA_3b_Mus.m       KQLMRKEFTLEFSRDRKSMSVYCTPTRADPKVQGSKMFVKGAPESVIERCSSVRVGSRTA 535
SERCA_3a_Mus.m       KQLMRKEFTLEFSRDRKSMSVYCTPTRADPKVQGSKMFVKGAPESVIERCSSVRVGSRTA 535
SERCA_3_Xeno_t       KKLMKKECTLEFSRDRKSMSVYCNSVAPNSGQSASKMFVKGAPESVIERCNYVRVGSTKL 535
SERCA_3_Danio.r      RQLMQKKFTLEFSRDRKSMSVYCTPNGTNSQ---SKMFVKGAPEGVIDRCQFVRVGKERF 532
SERCA_2b_Homo.s      KQLMKKEFTLEFSRDRKSMSVYCTPNKPSRTSMS-KMFVKGAPEGVIDRCTHIRVGSTKV 534
SERCA_2a_Mus.m       KQLMKKEFTLEFSRDRKSMSVYCTPNKPSRTSMS-KMFVKGAPEGVIDRCTHIRVGSTKV 534
SERCA_2b_Mus.m       KQLMKKEFTLEFSRDRKSMSVYCTPNKPSRTSMS-KMFVKGAPEGVIDRCTHIRVGSTKV 534
SERCA_2a_Homo.s      KQLMKKEFTLEFSRDRKSMSVYCTPNKPSRTSMS-KMFVKGAPEGVIDRCTHIRVGSTKV 534
SERCA_2_Xeno_t       KQLMKKEFTLEFSRDRKSMSVYCTPNKPSRTSMS-KMFVKGAPEGLIDRCTHIRVGSIKV 521
SERCA_2a_Danio.r     KQLMKKEFTLEFSRDRKSMSVYCSPNK-AKSSSS-KMFVKGAPEGVIDRCAYVRVGGSKV 533
SERCA_2b_Danio.r     KQLMKKEFTLEFSRDRKSMSVYCTPNK-ARSSMG-KMFVKGAPEGVIDRCTHIRVGGNKV 527
SERCA_1a_Homo.s      RQLMKKEFTLEFSRDRKSMSVYCSPAKSSRAAVGNKMFVKGAPEGVIDRCNYVRVGTTRV 535
SERCA_1b_Homo.s      RQLMKKEFTLEFSRDRKSMSVYCSPAKSSRAAVGNKMFVKGAPEGVIDRCNYVRVGTTRV 535
SERCA_1_Mus.m        RQLMKKEFTLEFSRDRKSMSVYCSPAKSSRAAVGNKMFVKGAPEGVIDRCNYVRVGTTRV 535
SERCA_1_Xeno_t       KQLMKKEFTLEFSRDRKSMSVYCTPAKASRAAVGNKMFVKGAPEGVIDRCNYVRVGTTRV 535
SERCA_1_Danio.r      KQLMKKDFTLEFSRDRKSMSVYCSPAKASKAPVGNKMFVKGAPEGVIDRCAYVRVGTTRV 535
SERCA_b_Dros.m       ETKWKKEFTLEFSRDRKSMSSYCTPLKASRLGTGPKLFVKGAPEGVLERCTHARVGTTKV 535
SERCA_a_Dros.m       ETKWKKEFTLEFSRDRKSMSSYCTPLKASRLGTGPKLFVKGAPEGVLERCTHARVGTTKV 535
SERCA_Caen.e         QQKWKKEFTLEFSRDRKSMSAYCFPASG---GSGAKMFVKGAPEGVLGRCTHVRVNGQKV 536
                     .   :*. ************ ** .          *:*******.:: **   **.

SERCA_3e_Homo.s      PLTPTSREQILAKIRDWGSGSDTLRCLALATRDAPPRKEDMELDDCSKFVQYETDLTFVG 595
SERCA_3c_Homo.s      PLTPTSREQILAKIRDWGSGSDTLRCLALATRDAPPRKEDMELDDCSKFVQYETDLTFVG 595
SERCA_3f_Homo.s      PLTPTSREQILAKIRDWGSGSDTLRCLALATRDAPPRKEDMELDDCSKFVQYETDLTFVG 595
SERCA_2d_Homo.s      PLTPTSREQILAKIRDWGSGSDTLRCLALATRDAPPRKEDMELDDCSKFVQYETDLTFVG 595
SERCA_3b_Homo.s      PLTPTSREQILAKIRDWGSGSDTLRCLALATRDAPPRKEDMELDDCSKFVQYETDLTFVG 595
SERCA_3a_Homo.s      PLTPTSREQILAKIRDWGSGSDTLRCLALATRDAPPRKEDMELDDCSKFVQYETDLTFVG 595
SERCA_3c_Mus.m       PLSTTSREHILAKIRDWGSGSDTLRCLALATRDTPPRKEDMHLDDCSRFVQYETDLTFVG 595
SERCA_3b_Mus.m       PLSTTSREHILAKIRDWGSGSDTLRCLALATRDTPPRKEDMHLDDCSRFVQYETDLTFVG 595
SERCA_3a_Mus.m       PLSTTSREHILAKIRDWGSGSDTLRCLALATRDTPPRKEDMHLDDCSRFVQYETDLTFVG 595
SERCA_3_Xeno_t       PLTPSAREKIMSKIRDWGTGMDTLRCLALATRDVPPKLEDMQLDDSTKFINYETNLTFVG 595
SERCA_3_Danio.r      PLTMAVKEELMSTIRDWGTGRDTLRCLALATRDSPPAVDKMDLENAGKFAEYESSLTFVG 592
SERCA_2b_Homo.s      PMTSGVKQKIMSVIREWGSGSDTLRCLALATHDNPLRREEMHLEDSANFIKYETNLTFVG 594
SERCA_2a_Mus.m       PMTPGVKQKIMSVIREWGSGSDTLRCLALATHDNPLKREEMHLEDSANFIKYETNLTFVG 594
SERCA_2b_Mus.m       PMTPGVKQKIMSVIREWGSGSDTLRCLALATHDNPLKREEMHLEDSANFIKYETNLTFVG 594
SERCA_2a_Homo.s      PMTSGVKQKIMSVIREWGSGSDTLRCLALATHDNPLRREEMHLEDSANFIKYETNLTFVG 594
SERCA_2_Xeno_t       PLTAGIKQKIMSVIREWGTGRDTLRCLALATHDNPPRKEDMNLEDSTNFINYETNLTFVG 581
SERCA_2a_Danio.r     PLTQGIKDKIMSVIREYGTGRDTLRCLALATRDNPLKKEEMVLSDTARFADYESDLTFVG 593
SERCA_2b_Danio.r     PMTPGIKEKIMSVIREYGTGRDTLRCLALATRDNPLSKESLVLEDSTRFVEYETDLTFVG 587
SERCA_1a_Homo.s      PLTGPVKEKIMAVIKEWGTGRDTLRCLALATRDTPPKREEMVLDDSARFLEYETDLTFVG 595
SERCA_1b_Homo.s      PLTGPVKEKIMAVIKEWGTGRDTLRCLALATRDTPPKREEMVLDDSARFLEYETDLTFVG 595
SERCA_1_Mus.m        PLTGPVKEKIMSVIKEWGTGRDTLRCLALATRDTPPKREEMVLDDSAKFMEYEMDLTFVG 595
SERCA_1_Xeno_t       PLTPAIKDKILTVIKEWGTGRDTLRCLALATRDTPPKREEMVLDDATKFVDYETDLTFVG 595
SERCA_1_Danio.r      PLTGPVKDKIMAVIKEWGTGRDTLRCLALATRDNPLRPEEMNLEDSTKFAEYETDLTFVG 595
SERCA_b_Dros.m       PLTSALKAKILALTGQYGTGRDTLRCLALAVADSPMKPDEMDLGDSTKFYQYEVNLTFVG 595
SERCA_a_Dros.m       PLTSALKAKILALTGQYGTGRDTLRCLALAVADSPMKPDEMDLGDSTKFYQYEVNLTFVG 595
SERCA_Caen.e         PLTSAMTQKIVDQCVQYGTGRDTLRCLALGTIDTPVSVSNMNLEDSTQFVKYEQDITFVG 596
                     *::     .::    ::*:* ********.. * *   ..: * :  .* .** .:****

SERCA_3e_Homo.s      CVGMLDPPRPEVAACITRCYQAGIRVVMITGDNKGTAVAICRRLGIFGDTEDVAGKAYTG 655
SERCA_3c_Homo.s      CVGMLDPPRPEVAACITRCYQAGIRVVMITGDNKGTAVAICRRLGIFGDTEDVAGKAYTG 655
SERCA_3f_Homo.s      CVGMLDPPRPEVAACITRCYQAGIRVVMITGDNKGTAVAICRRLGIFGDTEDVAGKAYTG 655
SERCA_2d_Homo.s      CVGMLDPPRPEVAACITRCYQAGIRVVMITGDNKGTAVAICRRLGIFGDTEDVAGKAYTG 655
SERCA_3b_Homo.s      CVGMLDPPRPEVAACITRCYQAGIRVVMITGDNKGTAVAICRRLGIFGDTEDVAGKAYTG 655
SERCA_3a_Homo.s      CVGMLDPPRPEVAACITRCYQAGIRVVMITGDNKGTAVAICRRLGIFGDTEDVAGKAYTG 655
SERCA_3c_Mus.m       CVGMLDPPRPEVAACITRCSRAGIRVVMITGDNKGTAVAICRRLGIFGDTEDVLGKAYTG 655
SERCA_3b_Mus.m       CVGMLDPPRPEVAACITRCSRAGIRVVMITGDNKGTAVAICRRLGIFGDTEDVLGKAYTG 655
SERCA_3a_Mus.m       CVGMLDPPRPEVAACITRCSRAGIRVVMITGDNKGTAVAICRRLGIFGDTEDVLGKAYTG 655
SERCA_3_Xeno_t       CVGMLDPPRKEVSISIELCKRAGIKVIMITGDNKGTAVAICRKIGIFSDYEDITDKAYTG 655
SERCA_3_Danio.r      CVGMLDPPRKEVIGSIKLCNKAGIRVIMITGDNKGTAVAICRRIGIFSENEDVEGRAYTG 652
SERCA_2b_Homo.s      CVGMLDPPRIEVASSVKLCRQAGIRVIMITGDNKGTAVAICRRIGIFGQDEDVTSKAFTG 654
SERCA_2a_Mus.m       CVGMLDPPRIEVASSVKLCRQAGIRVIMITGDNKGTAVAICRRIGIFGQDEDVTSKAFTG 654
SERCA_2b_Mus.m       CVGMLDPPRIEVASSVKLCRQAGIRVIMITGDNKGTAVAICRRIGIFGQDEDVTSKAFTG 654
SERCA_2a_Homo.s      CVGMLDPPRIEVASSVKLCRQAGIRVIMITGDNKGTAVAICRRIGIFGQDEDVTSKAFTG 654
SERCA_2_Xeno_t       CVGMLDPPRTEVAASVKMCRQAGIRVIMITGDNKGTAVAICRRVGIFREDEDVSERAFTG 641
```

```
SERCA_2a_Danio.r      CVGMLDPPRTEVAASIKLCRHAGIRVIMITGDNKGTAVAICRRIGIFSDDDDVHRMAFTG 653
SERCA_2b_Danio.r      CVGMLDPPRAEVAASIKLCRQAGIRVIMITGDNKGTAVAICRRIGIFGENDDVSRMAYTG 647
SERCA_1a_Homo.s       VVGMLDPPRKEVTGSIQLCRDAGIRVIMITGDNKGTAIAICRRIGIFGENEEVADRAYTG 655
SERCA_1b_Homo.s       VVGMLDPPRKEVTGSIQLCRDAGIRVIMITGDNKGTAIAICRRIGIFGENEEVADRAYTG 655
SERCA_1_Mus.m         VVGMLDPPRKEVTGSIQLCRDAGIRVIMITGDNKGTAIAICRRIGIFSENEEVTDRAYTG 655
SERCA_1_Xeno_t        CVGMLDPPRKEVMGSIKLCREAGIRVIMITGDNKGTAIAICRRIGIFGEDDDVSRCAFTG 655
SERCA_1_Danio.r       CVGMLDPPRKEVVGSIELCRAAGIRVIMITGDNKGTAVAICRRIGIFSDDEDVTGRAFTG 655
SERCA_b_Dros.m        VVGMLDPPRKEVFDSIVRCRAAGIRVIVITGDNKATAEAICRRIGVFAEDEDTTGKSYSG 655
SERCA_a_Dros.m        VVGMLDPPRKEVFDSIVRCRAAGIRVIVITGDNKATAEAICRRIGVFAEDEDTTGKSYSG 655
SERCA_Caen.e          VVGMLDPPRTEVSDSIKACNHAGIRVIMITGDNKNTAEAIGRRIGLFGENEDTTGKAYTG 656
                       ******** **  .:  *  ***:*::****** ** ** *::*:* : ::    ::::*

SERCA_3e_Homo.s       REFDDLSPEQQRQACRTARCFARVEPAHKSRIVENLQSFNEITAMTGDGVNDAPALKKAE 715
SERCA_3c_Homo.s       REFDDLSPEQQRQACRTARCFARVEPAHKSRIVENLQSFNEITAMTGDGVNDAPALKKAE 715
SERCA_3f_Homo.s       REFDDLSPEQQRQACRTARCFARVEPAHKSRIVENLQSFNEITAMTGDGVNDAPALKKAE 715
SERCA_2d_Homo.s       REFDDLSPEQQRQACRTARCFARVEPAHKSRIVENLQSFNEITAMTGDGVNDAPALKKAE 715
SERCA_3b_Homo.s       REFDDLSPEQQRQACRTARCFARVEPAHKSRIVENLQSFNEITAMTGDGVNDAPALKKAE 715
SERCA_3a_Homo.s       REFDDLSPEQQRQACRTARCFARVEPAHKSRIVENLQSFNEITAMTGDGVNDAPALKKAE 715
SERCA_3c_Mus.m        REFDDLSPEQQRQACRTARCFARVEPAHKSRIVENLQSFNEITAMTGDGVNDAPALKKAE 715
SERCA_3b_Mus.m        REFDDLSPEQQRQACRTARCFARVEPAHKSRIVENLQSFNEITAMTGDGVNDAPALKKAE 715
SERCA_3a_Mus.m        REFDDLSPEQQRQACRTARCFARVEPAHKSRIVENLQSFNEITAMTGDGVNDAPALKKAE 715
SERCA_3_Xeno_t        REFDDLPPERQREACRSARCFARVEPAHKSKIVEYLQSYSEITAMTGDGVNDAPALKKAE 715
SERCA_3_Danio.r       REFDDLAPEAQREAVKRARCFARVEPAHKSKIVAYLQSFDEITAMTGDGVNDAPALKKAE 712
SERCA_2b_Homo.s       REFDELNPSAQRDACLNARCFARVEPSHKSKIVEFLQSFDEITAMTGDGVNDAPALKKAE 714
SERCA_2a_Mus.m        REFDELSPSAQRDACLNARCFARVEPSHKSKIVEFLQSFDEITAMTGDGVNDAPALKKSE 714
SERCA_2b_Mus.m        REFDELSPSAQRDACLNARCFARVEPSHKSKIVEFLQSFDEITAMTGDGVNDAPALKKSE 714
SERCA_2a_Homo.s       REFDELNPSAQRDACLNARCFARVEPSHKSKIVEFLQSFDEITAMTGDGVNDAPALKKAE 714
SERCA_2_Xeno_t        REFDELSPAAQRDACLNARCFARVEPSHKSKIVEFLQSFDEITAMTGDGVNDAPALKKAE 701
SERCA_2a_Danio.r      REFDDLSPHAQREAVTVARCFARVEPSHKSKIVEFLQGFDEITAMTGDGVNDAPALKKAE 713
SERCA_2b_Danio.r      REFDDLSAAAQREAVLTARCFARVEPSHKSKIVEFLQSYDEITAMTGDGVNDAPALKKAE 707
SERCA_1a_Homo.s       REFDDLPLAEQREACRRACCFARVEPSHKSKIVEYLQSYDEITAMTGDGVNDAPALKKAE 715
SERCA_1b_Homo.s       REFDDLPLAEQREACRRACCFARVEPSHKSKIVEYLQSYDEITAMTGDGVNDAPALKKAE 715
SERCA_1_Mus.m         REFDDLPLAEQREACRRACCFARVEPSHKSKIVEYLQSYDEITAMTGDGVNDAPALKKAE 715
SERCA_1_Xeno_t        REFDDLPPTEQREACKRASCFARVEPTHKSKIVEFLQSFDEITAMTGDGVNDAPALKKAE 715
SERCA_1_Danio.r       REFDDLPLPQQREAVRKACCYARVEPSHKSKIVEFLQGFDEITAMTGDGVNDAPALKKAE 715
SERCA_b_Dros.m        REFDDLSPTEQKAAVARSRLFSRVEPQHKSKIVEFLQSMNEISAMTGDGVNDAPALKKAE 715
SERCA_a_Dros.m        REFDDLSPTEQKAAVARSRLFSRVEPQHKSKIVEFLQSMNEISAMTGDGVNDAPALKKAE 715
SERCA_Caen.e          REFDDLPPEQQSEACRRAKLFARVEPSHKSKIVDILQSQGEITAMTGDGVNDAPALKKAE 716
                      ****:*    *  *   :  ::***** ***:**  **. .**:****************:*

SERCA_3e_Homo.s       IGIAMGSGTAVAKSAAEMVLSDDNFASIVAAVEEGRAIYSNMKQFIRYLISSNVGEVVCI 775
SERCA_3c_Homo.s       IGIAMGSGTAVAKSAAEMVLSDDNFASIVAAVEEGRAIYSNMKQFIRYLISSNVGEVVCI 775
SERCA_3f_Homo.s       IGIAMGSGTAVAKSAAEMVLSDDNFASIVAAVEEGRAIYSNMKQFIRYLISSNVGEVVCI 775
SERCA_2d_Homo.s       IGIAMGSGTAVAKSAAEMVLSDDNFASIVAAVEEGRAIYSNMKQFIRYLISSNVGEVVCI 775
SERCA_3b_Homo.s       IGIAMGSGTAVAKSAAEMVLSDDNFASIVAAVEEGRAIYSNMKQFIRYLISSNVGEVVCI 775
SERCA_3a_Homo.s       IGIAMGSGTAVAKSAAEMVLSDDNFASIVAAVEEGRAIYSNMKQFIRYLISSNVGEVVCI 775
SERCA_3c_Mus.m        IGIAMGSGTAVAKSAAEMVLSDDNFASIVAAVEEGRAIYNNMKQFIRYLISSNVGEVVCI 775
SERCA_3b_Mus.m        IGIAMGSGTAVAKSAAEMVLSDDNFASIVAAVEEGRAIYNNMKQFIRYLISSNVGEVVCI 775
SERCA_3a_Mus.m        IGIAMGSGTAVAKSAAEMVLSDDNFASIVAAVEEGRAIYNNMKQFIRYLISSNVGEVVCI 775
SERCA_3_Xeno_t        IGIAMGSGTAVAKSAAEMVLADDNFSSIVSAVEEGRAIYNNMKQFIRYLISSNVGEVVCI 775
SERCA_3_Danio.r       IGIAMGSGTAVAKSASEMVLSDDNFSTIVAAVEEGRAIYNNMKQFIRYLISSNVGEVVCI 772
SERCA_2b_Homo.s       IGIAMGSGTAVAKTASEMVLADDNFSTIVAAVEEGRAIYNNMKQFIRYLISSNVGEVVCI 774
SERCA_2a_Mus.m        IGIAMGSGTAVAKTASEMVLADDNFSTIVAAVEEGRAIYNNMKQFIRYLISSNVGEVVCI 774
SERCA_2b_Mus.m        IGIAMGSGTAVAKTASEMVLADDNFSTIVAAVEEGRAIYNNMKQFIRYLISSNVGEVVCI 774
SERCA_2a_Homo.s       IGIAMGSGTAVAKTASEMVLADDNFSTIVAAVEEGRAIYNNMKQFIRYLISSNVGEVVCI 774
SERCA_2_Xeno_t        IGIAMGSGTAVAKTASEMVLADDNFSTIVAAVEEGRAIYNNMKQFIRYLISSNVGEVVCI 761
SERCA_2a_Danio.r      IGIAMGSGTAVAKTASEMVLADDNFSTIVAAVEEGRAIYNNMKQFIRYLISSNVGEVVCI 773
SERCA_2b_Danio.r      IGIAMGSGTAVAKTASEMVLADDNFSTIVAAVEEGRAIYNNMKQFIRYLISSNVGEVVCI 767
SERCA_1a_Homo.s       IGIAMGSGTAVAKTASEMVLADDNFSTIVAAVEEGRAIYNNMKQFIRYLISSNVGEVVCI 775
SERCA_1b_Homo.s       IGIAMGSGTAVAKTASEMVLADDNFSTIVAAVEEGRAIYNNMKQFIRYLISSNVGEVVCI 775
SERCA_1_Mus.m         IGIAMGSGTAVAKTASEMVLADDNFSTIVAAVEEGRAIYNNMKQFIRYLISSNVGEVVCI 775
SERCA_1_Xeno_t        IGIAMGSGTAVAKTASEMVLADDNFSTIVAAVEEGRAIYNNMKQFIRYLISSNVGEVVCI 775
SERCA_1_Danio.r       IGIAMGSGTAVAKSASEMVLADDNFSSIVAAVEEGRAIYNNMKQFIRYLISSNVGEVVCI 775
SERCA_b_Dros.m        IGIAMGSGTAVAKSAAEMVLADDNFSSIVSAVEEGRAIYNNMKQFIRYLISSNIGEVVSI 775
SERCA_a_Dros.m        IGIAMGSGTAVAKSAAEMVLADDNFSSIVSAVEEGRAIYNNMKQFIRYLISSNIGEVVSI 775
SERCA_Caen.e          IGISMGSGTAVAKSASEMVLADDNFASIVSAVEEGRAIYNNMKQFIRYLISSNVGEVVSI 776
                      ***:*********:*:****:****::**:*********.*************:****.*

SERCA_3e_Homo.s       FLTAILGLPEALIPVQLLWVNLVTDGLPATALGFNPPDLDIMEKLPRSPREALISGWLFF 835
SERCA_3c_Homo.s       FLTAILGLPEALIPVQLLWVNLVTDGLPATALGFNPPDLDIMEKLPRSPREALISGWLFF 835
SERCA_3f_Homo.s       FLTAILGLPEALIPVQLLWVNLVTDGLPATALGFNPPDLDIMEKLPRSPREALISGWLFF 835
SERCA_2d_Homo.s       FLTAILGLPEALIPVQLLWVNLVTDGLPATALGFNPPDLDIMEKLPRSPREALISGWLFF 835
SERCA_3b_Homo.s       FLTAILGLPEALIPVQLLWVNLVTDGLPATALGFNPPDLDIMEKLPRSPREALISGWLFF 835
SERCA_3a_Homo.s       FLTAILGLPEALIPVQLLWVNLVTDGLPATALGFNPPDLDIMEKLPRSPREALISGWLFF 835
SERCA_3c_Mus.m        FLTAILGLPEALIPVQLLWVNLVTDGLPATALGFNPPDLDIMEKPPRNPREALISGWLFF 835
SERCA_3b_Mus.m        FLTAILGLPEALIPVQLLWVNLVTDGLPATALGFNPPDLDIMEKPPRNPREALISGWLFF 835
SERCA_3a_Mus.m        FLTAILGLPEALIPVQLLWVNLVTDGLPATALGFNPPDLDIMEKPPRNPREALISGWLFF 835
SERCA_3_Xeno_t        FLTAILGLPEALIPVQLLWVNLVTDGLPATALGFNPPDLDIMEKLPRNPREPLISGWLFF 835
```

```
SERCA_3_Danio.r      FLTAILGLPEALIPVQLLWVNLVTDGLPATALGFNPPDLDIMDKPPRNPKEPLISGWLFF 832
SERCA_2b_Homo.s      FLTAALGFPEALIPVQLLWVNLVTDGLPATALGFNPPDLDIMNKPPRNPKEPLISGWLFF 834
SERCA_2a_Mus.m       FLTAALGFPEALIPVQLLWVNLVTDGLPATALGFNPPDLDIMNKPPRNPKEPLISGWLFF 834
SERCA_2b_Mus.m       FLTAALGFPEALIPVQLLWVNLVTDGLPATALGFNPPDLDIMNKPPRNPKEPLISGWLFF 834
SERCA_2a_Homo.s      FLTAALGFPEALIPVQLLWVNLVTDGLPATALGFNPPDLDIMNKPPRNPKEPLISGWLFF 834
SERCA_2_Xeno_t       FLTAALGFPEALIPVQLLWVNLVTDGLPATALGFNPPDLDIMNKPPRNPKEPLISGWLFF 821
SERCA_2a_Danio.r     FLTAALGFPEALIPVQLLWVNLVTDGLPATALGFNPPDLDIMNKPPRSAKEPLISGWLFF 833
SERCA_2b_Danio.r     FLTAALGFPEALIPVQLLWVNLVTDGLPATALGFNPPDLDIMSKPPRNAREPLISGWLFF 827
SERCA_1a_Homo.s      FLTAALGLPEALIPVQLLWVNLVTDGLPATALGFNPPDLDIMDRPPRSPKEPLISGWLFF 835
SERCA_1b_Homo.s      FLTAALGLPEALIPVQLLWVNLVTDGLPATALGFNPPDLDIMDRPPRSPKEPLISGWLFF 835
SERCA_1_Mus.m        FLTAALGLPEALIPVQLLWVNLVTDGLPATALGFNPPDLDIMDRPPRSPKEPLISGWLFF 835
SERCA_1_Xeno_t       FLTAALGLPEALIPVQLLWVNLVTDGLPATALGFNPPDLDIMDRPPRSPKEPLISGWLFF 835
SERCA_1_Danio.r      FLTAALGLPEALIPVQLLWVNLVTDGLPATALGFNPPDLDIMGKAPRSPKEPLISGWLFF 835
SERCA_b_Dros.m       FLTAALGLPEALIPVQLLWVNLVTDGLPATALGFNPPDLDIMEKPPRKADEGLISGWLFF 835
SERCA_a_Dros.m       FLTAALGLPEALIPVQLLWVNLVTDGLPATALGFNPPDLDIMEKPPRKADEGLISGWLFF 835
SERCA_Caen.e         FMVAALGIPEALIPVQLLWVNLVTDGLPATALGFNPPDLDIMDRHPRSANDGLISGWLFF 836
                     *:.* **:*********************************** : **.. : ********

SERCA_3e_Homo.s      RYLAIGVYVGLATVAAATWWFVYDAEGPHINFYQLRNFLKCSEDNPLFAGIDCEVFESRF 895
SERCA_3c_Homo.s      RYLAIGVYVGLATVAAATWWFVYDAEGPHINFYQLRNFLKCSEDNPLFAGIDCEVFESRF 895
SERCA_3f_Homo.s      RYLAIGVYVGLATVAAATWWFVYDAEGPHINFYQLRNFLKCSEDNPLFAGIDCEVFESRF 895
SERCA_2d_Homo.s      RYLAIGVYVGLATVAAATWWFVYDAEGPHINFYQLRNFLKCSEDNPLFAGIDCEVFESRF 895
SERCA_3b_Homo.s      RYLAIGVYVGLATVAAATWWFVYDAEGPHINFYQLRNFLKCSEDNPLFAGIDCEVFESRF 895
SERCA_3a_Homo.s      RYLAIGVYVGLATVAAATWWFVYDAEGPHINFYQLRNFLKCSEDNPLFAGIDCEVFESRF 895
SERCA_3c_Mus.m       RYLAIGVYVGLATVAAATWWFLYDTEGPQVTFYQLRNFLKCSEDNPLFAGIDCKVFESRF 895
SERCA_3b_Mus.m       RYLAIGVYVGLATVAAATWWFLYDTEGPQVTFYQLRNFLKCSEDNPLFAGIDCKVFESRF 895
SERCA_3a_Mus.m       RYLAIGVYVGLATVAAATWWFLYDTEGPQVTFYQLRNFLKCSEDNPLFAGIDCKVFESRF 895
SERCA_3_Xeno_t       RYLAIGVYVGLATVGAATWWFLYDEDGPQVTFYQLRHFMKCTSDNPLFSGIDCDVFESRY 895
SERCA_3_Danio.r      RYLAIGGYVGLGTVSAATWWYLFDEDGPQVSFYQLRHFMQCTEENPMFEGINCEVFESRY 892
SERCA_2b_Homo.s      RYLAIGCYVGAATVGAAAWWFIAADGGPRVSFYQLSHFLQCKEDNPDFEGVDCAIFESPY 894
SERCA_2a_Mus.m       RYLAIGCYVGAATVGAAAWWFIAADGGPRVSFYQLSHFLQCKEDNPDFDGVDCAIFESPY 894
SERCA_2b_Mus.m       RYLAIGCYVGAATVGAAAWWFIAADGGPRVSFYQLSHFLQCKEDNPDFDGVDCAIFESPY 894
SERCA_2a_Homo.s      RYLAIGCYVGAATVGAAAWWFIAADGGPRVSFYQLSHFLQCKEDNPDFEGVDCAIFESPY 894
SERCA_2_Xeno_t       RYLAIGCYVGAATVGAAAWWFIAAEDGPRITFYQLSHFLQCREENPDFDGVECEIFESPY 881
SERCA_2a_Danio.r     RYLAIGCYVGAATVGAAAWWFIVADDGPMITLYQLSHFLQCSPDNPDFQDLECHVFESPY 893
SERCA_2b_Danio.r     RYLAIGCYVGAATVGAAAWWFIAAEDGPRVTFYQLSHFLQCAPDNPEFEGLQCEIFGSPY 887
SERCA_1a_Homo.s      RYMAIGGYVGAATVGAAAWWFLYAEDGPHVNYSQLTHFMQCTEDNTHFEGIDCEVFEAPE 895
SERCA_1b_Homo.s      RYMAIGGYVGAATVGAAAWWFLYAEDGPHVNYSQLTHFMQCTEDNTHFEGIDCEVFEAPE 895
SERCA_1_Mus.m        RYMAIGGYVGAATVGAAAWWFLYAEDGPHVSYHQLTHFMQCTEHNPEFDGLDCEVFEAPE 895
SERCA_1_Xeno_t       RYLAIGGYVGAATVGAAAWWFMYADDGPEVTFYQLSHFMQCTEENADFEGLECEIFESPV 895
SERCA_1_Danio.r      RYLAIGGYVGAATVAAAGWWFLYCDEGPMVSFYQLSHFMQCTADNEDFAGIECEVFEAAP 895
SERCA_b_Dros.m       RYMAIGFYVGAATVGAAAWWFVFSDEGPKLSYWQLTHHLSCLGGGDEFKGVDCKIFSDPH 895
SERCA_a_Dros.m       RYMAIGFYVGAATVGAAAWWFVFSDEGPKLSYWQLTHHLSCLGGGDEFKGVDCKIFSDPH 895
SERCA_Caen.e         RYLAVGTYVGVATVGASMWWFLLYEEGPQITYYQLTHWMRCEIEPDNFADLDCAVFEDNH 896
                     **:*:* *** .**.*: **::    ** :.  ** : : *      * .::* :*

SERCA_3e_Homo.s      PTTMALSVLVTIEMCNALNSVSENQSLLRMPPWMNPWLLVAVAMSMALHFLILLVPPLPL 955
SERCA_3c_Homo.s      PTTMALSVLVTIEMCNALNSVSENQSLLRMPPWMNPWLLVAVAMSMALHFLILLVPPLPL 955
SERCA_3f_Homo.s      PTTMALSVLVTIEMCNALNSVSENQSLLRMPPWMNPWLLVAVAMSMALHFLILLVPPLPL 955
SERCA_2d_Homo.s      PTTMALSVLVTIEMCNALNSVSENQSLLRMPPWMNPWLLVAVAMSMALHFLILLVPPLPL 955
SERCA_3b_Homo.s      PTTMALSVLVTIEMCNALNSVSENQSLLRMPPWMNPWLLVAVAMSMALHFLILLVPPLPL 955
SERCA_3a_Homo.s      PTTMALSVLVTIEMCNALNSVSENQSLLRMPPWMNPWLLVAVAMSMALHFLILLVPPLPL 955
SERCA_3c_Mus.m       PTTMALSVLVTIEMCNALNSVSENQSLLRMPPWLNPWLLGAVVMSMALHFLILLVPPLPL 955
SERCA_3b_Mus.m       PTTMALSVLVTIEMCNALNSVSENQSLLRMPPWLNPWLLGAVVMSMALHFLILLVPPLPL 955
SERCA_3a_Mus.m       PTTMALSVLVTIEMCNALNSVSENQSLLRMPPWLNPWLLGAVVMSMALHFLILLVPPLPL 955
SERCA_3_Xeno_t       PTTMALSVLVTIEMCNALNSLSENQSLLRMPPWLNIWLLGAIIMSMALHFLILYIKPMPL 955
SERCA_3_Danio.r      PTTMALSVLVTIEMFNALNSLSENQSLLRMPPWVNIWLLGAIILSLSLHFLILHVEPLPL 952
SERCA_2b_Homo.s      PMTMALSVLVTIEMCNALNSLSENQSLLRMPPWENIWLVGSICLSMSLHFLILYVEPLPL 954
SERCA_2a_Mus.m       PMTMALSVLVTIEMCNALNSLSENQSLLRMPPWENIWLVGSICLSMSLHFLILYVEPLPL 954
SERCA_2b_Mus.m       PMTMALSVLVTIEMCNALNSLSENQSLLRMPPWENIWLVGSICLSMSLHFLILYVEPLPL 954
SERCA_2a_Homo.s      PMTMALSVLVTIEMCNALNSLSENQSLLRMPPWENIWLVGSICLSMSLHFLILYVEPLPL 954
SERCA_2_Xeno_t       PMTMALSVLVTIEMCNALNSLSENQSLLRMPPWENVWLLGSICLSMSLHFLILYVEPLPL 941
SERCA_2a_Danio.r     PMTMALSVLVTIEMCNALNSLSENQSLVRMPPWENIWLLGAICLSMSLHFLILYVEPLPV 953
SERCA_2b_Danio.r     PMTMALSVLVTIEMCNALNSVSENQSLLHMPPWENVWLLGAICLSMSLHFLILYVEPLPM 947
SERCA_1a_Homo.s      PMTMALSVLVTIEMCNALNSLSENQSLLRMPPWVNIWLLGSICLSMSLHFLILYVDPLPM 955
SERCA_1b_Homo.s      PMTMALSVLVTIEMCNALNSLSENQSLLRMPPWVNIWLLGSICLSMSLHFLILYVDPLPM 955
SERCA_1_Mus.m        PMTMALSVLVTIEMCNALNSLSENQSLLRMPPWVNIWLLGSICLSMSLHFLILYVDPLPM 955
SERCA_1_Xeno_t       PMTMALSVLVTIEMCNALNSLSENQSLVRMPPWVNIWLLGSICLSMSLHFLILYVEPLPM 955
SERCA_1_Danio.r      PMTMALSVLVTIEMCNALNSLSENQSLLRMPPWSNLWLAGAMTLSMSLHFMIIYVDPLPM 955
SERCA_b_Dros.m       AMTMALSVLVTIEMLNAMNSLSENQSLITMPPWCNLWLIGSMALSFTLHFVILYVDVLST 955
SERCA_a_Dros.m       AMTMALSVLVTIEMLNAMNSLSENQSLITMPPWCNLWLIGSMALSFTLHFVILYVDVLST 955
SERCA_Caen.e         PNAMALSVLVTIEMLNAINSLSENQSLLVMPPWKNIWLMAAISLSMSLHFVILYVDIMAT 956
                     . :*********** **:**:******: **** * **  :: :*::***:*: :  :.

SERCA_3e_Homo.s      IFQVTPLSGRQWVVVLQISLPVILLDEALKYLSRNHMHACLYPGLLRTVSQAWSRQPLTT 1015
SERCA_3c_Homo.s      IFQVTPLSGRQWVVVLQISLPVILLDEALKYLSRNHMHACLYPGLLRTVSQAWSRQPLTT 1015
SERCA_3f_Homo.s      IFQVTPLSGRQWVVVLQISLPVILLDEALKYLSRNHMHEMSQK----------------- 998
SERCA_2d_Homo.s      IFQVTPLSGRQWVVVLQISLPVILLDEALKYLSRNHMHACLYPGLLRTVSQAWSRQPLTT 1015
```

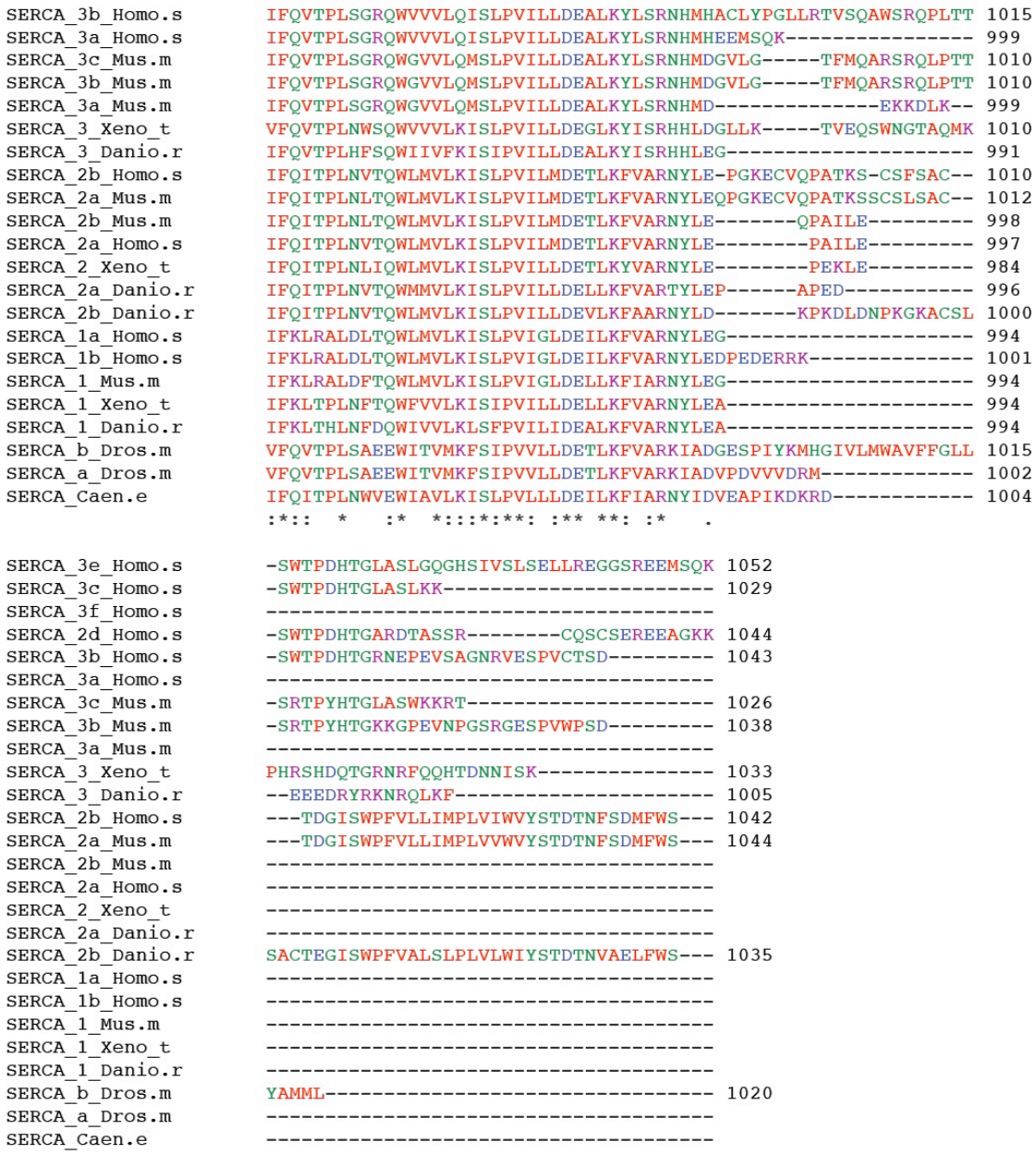

Alignment of predicted protein sequences for SERCA in a number of model organisms and humans

Multiple protein sequence alignments were undertaken between various paralogues and splice variants of SERCA, using ClustalW2 at the European Bioinformatics Institute (available at http://www.ebi.ac.uk/Tools/msa/clustalw2/), after retrieving predicted protein sequences from the National Center for Biotechnology (NCBI, available at http://www.ncbi.nlm.nih.gov) and Flybase (available at http://flybase.org/) databases. Key: Homo.s = *Homo sapiens* (Human); Mus.m = *Mus musculus* (Mouse); Xeno_t = *Xenopus tropicalis* (Western claw frog); Dros.m = *Drosophila melanogaster* (Fruitfly) Danio.r = *Danio rerio* (Zebrafish); Caen.e = *Caenorhabditis elegans* (Roundworm).

Appendix 2

Assessment of potential off-target effects of SERCA RNAi

mis=0	mis=1	mis=2	Name of off-target candidate sequences
267	0	0	gi|24762452|ref|NM_166637.1| Drosophila melanogaster CG3725-PF, isoform F (Ca-P60A) mRNA, complete cds
267	0	0	gi|24762456|ref|NM_166639.1| Drosophila melanogaster CG3725-PH, isoform H (Ca-P60A) mRNA, complete cds
267	0	0	gi|19549426|ref|NM_057484.2| Drosophila melanogaster CG3725-PA, isoform A (Ca-P60A) mRNA, complete cds
267	0	0	gi|24762450|ref|NM_166636.1| Drosophila melanogaster CG3725-PE, isoform E (Ca-P60A) mRNA, complete cds
267	0	0	gi|24762454|ref|NM_166638.1| Drosophila melanogaster CG3725-PG, isoform G (Ca-P60A) mRNA, complete cds
267	0	0	gi|24762448|ref|NM_166635.1| Drosophila melanogaster CG3725-PD, isoform D (Ca-P60A) mRNA, complete cds
267	0	0	gi|24762444|ref|NM_166633.1| Drosophila melanogaster CG3725-PB, isoform B (Ca-P60A) mRNA, complete cds
267	0	0	gi|24762446|ref|NM_166634.1| Drosophila melanogaster CG3725-PC, isoform C (Ca-P60A) mRNA, complete cds
0	3	2	gi|24658458|ref|NM_139717.1| Drosophila melanogaster CG5146-PA (CG5146) mRNA, complete cds
0	2	3	gi|24650785|ref|NM_143354.1| Drosophila melanogaster CG4787-PA (CG4787) mRNA, complete cds
0	1	7	gi|28572112|ref|NM_079733.3| Drosophila melanogaster CG4677-PA, isoform A (lmd) mRNA, complete cds
0	1	7	gi|28572113|ref|NM_170044.2| Drosophila melanogaster CG4677-PB, isoform B (lmd) mRNA, complete cds
0	1	4	gi|28574868|ref|NM_168732.2| Drosophila melanogaster CG32174-PB (CG32174) mRNA, complete cds
0	1	4	gi|24654189|ref|NM_137292.2| Drosophila melanogaster CG8332-PA, isoform A (RpS15) mRNA, complete cds
0	1	4	gi|24654190|ref|NM_166183.1| Drosophila melanogaster CG8332-PB, isoform B (RpS15) mRNA, complete cds
0	1	4	gi|24639717|ref|NM_131950.2| Drosophila melanogaster CG3024-PA (torp4a) mRNA, complete cds
0	1	3	gi|24639284|ref|NM_166931.1| Drosophila melanogaster CG3707-PB, isoform B (wapl) mRNA, complete cds
0	1	3	gi|24639282|ref|NM_080303.2| Drosophila melanogaster CG3707-PA, isoform A (wapl) mRNA, complete cds
0	1	2	gi|45552278|ref|NM_205940.1| Drosophila melanogaster CG10595-PB, isoform B (d) mRNA, complete cds
0	1	2	gi|28574076|ref|NM_175991.1| Drosophila melanogaster CG10595-PA, isoform A (d) mRNA, complete cds
0	1	2	gi|45552276|ref|NM_205939.1| Drosophila melanogaster CG10595-PC, isoform C (d) mRNA, complete cds
0	0	6	gi|24585505|ref|NM_165344.1| Drosophila melanogaster CG9328-PB, isoform B (CG9328) mRNA, complete cds
0	0	4	gi|24653932|ref|NM_137212.2| Drosophila melanogaster CG30089-PA (CG30089) mRNA, complete cds
0	0	4	gi|28574935|ref|NM_176315.1| Drosophila melanogaster CG6527-PA (CG6527) mRNA, complete cds
0	0	4	gi|24654392|ref|NM_166223.1| Drosophila melanogaster CG6556-PA (cnk) mRNA, complete cds
0	0	4	gi|24646340|ref|NM_169475.1| Drosophila melanogaster CG17369-PA, isoform A (Vha55) mRNA, complete cds
0	0	4	gi|28573290|ref|NM_176100.1| Drosophila melanogaster CG30492-PC, isoform C (CG30492) mRNA, complete cds
0	0	4	gi|28573292|ref|NM_176101.1| Drosophila melanogaster CG30492-PE, isoform E (CG30492) mRNA, complete cds
0	0	4	gi|24646342|ref|NM_057560.3| Drosophila melanogaster CG17369-PB, isoform B (Vha55) mRNA, complete cds
0	0	4	gi|28573286|ref|NM_170614.2| Drosophila melanogaster CG30492-PB, isoform B (CG30492) mRNA, complete cds

RNAi 4474 (VDRC Transformant ID 4474; Construct ID GD436)

mis=0	mis=1	mis=2	Name of off-target candidate sequences
700	0	0	gi|24762452|ref|NM_166637.1| Drosophila melanogaster CG3725-PF, isoform F (Ca-P60A) mRNA, complete cds
700	0	0	gi|24762456|ref|NM_166639.1| Drosophila melanogaster CG3725-PH, isoform H (Ca-P60A) mRNA, complete cds
700	0	0	gi|19549426|ref|NM_057484.2| Drosophila melanogaster CG3725-PA, isoform A (Ca-P60A) mRNA, complete cds
700	0	0	gi|24762450|ref|NM_166636.1| Drosophila melanogaster CG3725-PE, isoform E (Ca-P60A) mRNA, complete cds
700	0	0	gi|24762454|ref|NM_166638.1| Drosophila melanogaster CG3725-PG, isoform G (Ca-P60A) mRNA, complete cds
700	0	0	gi|24762446|ref|NM_166634.1| Drosophila melanogaster CG3725-PC, isoform C (Ca-P60A) mRNA, complete cds
700	0	0	gi|24762444|ref|NM_166633.1| Drosophila melanogaster CG3725-PB, isoform B (Ca-P60A) mRNA, complete cds
700	0	0	gi|24762448|ref|NM_166635.1| Drosophila melanogaster CG3725-PD, isoform D (Ca-P60A) mRNA, complete cds
2	6	8	gi|24668707|ref|NM_168963.1| Drosophila melanogaster CG32451-PA, isoform A (CG32451) mRNA, complete cds
2	6	8	gi|24668703|ref|NM_168962.1| Drosophila melanogaster CG32451-PC, isoform C (CG32451) mRNA, complete cds
2	6	8	gi|45551824|ref|NM_168961.2| Drosophila melanogaster CG32451-PB, isoform B (CG32451) mRNA, complete cds
0	9	13	gi|45553436|ref|NM_206526.1| Drosophila melanogaster CG5670-PG, isoform G (Atpalpha) mRNA, complete cds
0	9	13	gi|45553434|ref|NM_206525.1| Drosophila melanogaster CG5670-PH, isoform H (Atpalpha) mRNA, complete cds
0	9	13	gi|45553440|ref|NM_206528.1| Drosophila melanogaster CG5670-PE, isoform E (Atpalpha) mRNA, complete cds
0	9	13	gi|45553438|ref|NM_206527.1| Drosophila melanogaster CG5670-PF, isoform F (Atpalpha) mRNA, complete cds
0	9	13	gi|24648581|ref|NM_169939.1| Drosophila melanogaster CG5670-PD, isoform D (Atpalpha) mRNA, complete cds
0	9	13	gi|24648575|ref|NM_169936.1| Drosophila melanogaster CG5670-PA, isoform A (Atpalpha) mRNA, complete cds
0	9	13	gi|24648577|ref|NM_169937.1| Drosophila melanogaster CG5670-PB, isoform B (Atpalpha) mRNA, complete cds
0	9	13	gi|24648579|ref|NM_169938.1| Drosophila melanogaster CG5670-PC, isoform C (Atpalpha) mRNA, complete cds
0	5	11	gi|45551178|ref|NM_166755.2| Drosophila melanogaster CG2165-PB, isoform B (CG2165) mRNA, complete cds
0	5	11	gi|45551176|ref|NM_166754.2| Drosophila melanogaster CG2165-PA, isoform A (CG2165) mRNA, complete cds
0	5	2	gi|24647708|ref|NM_142377.1| Drosophila melanogaster CG18139-PA (CG18139) mRNA, complete cds
0	3	3	gi|24581872|ref|NM_080185.2| Drosophila melanogaster CG18251-PB, isoform B (Msp-300) mRNA, complete cds
0	3	3	gi|45552220|ref|NM_205911.1| Drosophila melanogaster CG18251-PC, isoform C (Msp-300) mRNA, complete cds
0	3	2	gi|24664426|ref|NM_140483.2| Drosophila melanogaster CG13463-PA (CG13463) mRNA, complete cds
0	2	5	gi|24581666|ref|NM_057665.3| Drosophila melanogaster CG15444-PA, isoform A (ine) mRNA, complete cds
0	2	5	gi|28574700|ref|NM_057664.4| Drosophila melanogaster CG15444-PB, isoform B (ine) mRNA, complete cds
0	2	5	gi|28574701|ref|NM_175958.1| Drosophila melanogaster CG15444-PC, isoform C (ine) mRNA, complete cds
0	2	5	gi|28574703|ref|NM_175959.1| Drosophila melanogaster CG15444-PD, isoform D (ine) mRNA, complete cds
0	2	3	gi|24656425|ref|NM_137663.1| Drosophila melanogaster CG13437-PA (CG13437) mRNA, complete cds

RNAi 107446 (VDRC Transformant ID 107446; Construct ID KK107371)

RNAi constructs used were checked for predicted off-target effects by inputting their DNA sequence into dsCheck (available at http://dscheck.rnai.jp/). This software predicts genes that the RNAi could potentially interfere with, other than the gene intended for knockdown. It 'dices' the input sequence into 19 nucleotide lengths of small interfering RNA (siRNA) and performs exhaustive scans for each 'diced siRNA' to find off-target gene candidates, simulating the biochemical process of dsRNA-mediated RNAi in vivo. The software then provides the number of hits with a complete match (mis=0 column), one mismatch (mis=1) and two mismatches (mis=2) for every off-target gene candidate individually.

References

Abell E, Ahrends R, Bandara S, Park BO, & Teruel MN. (2011). Parallel adaptive feedback enhances reliability of the Ca2+ signaling system. Proc Natl Acad Sci U S A, 108(35), 14485-14490.

Ackerman KG, Herron BJ, Vargas SO, Huang HL, Tevosian SG, Kochilas L, et al. (2005). Fog2 is required for normal diaphragm and lung development in mice and humans. Plos Genetics, 1(1), 58-65.

Adzick NS, Harrison MR, Glick PL, Villa RL, & Finkbeiner W. (1984). Experimental pulmonary hypoplasia and oligohydramnios: Relative contributions of lung fluid and fetal breathing movements. Journal of Pediatric Surgery, 19(6), 658-665.

Affolter M, Montagne J, Walldorf U, Groppe J, Kloter U, LaRosa M, et al. (1994). The Drosophila SRF homolog is expressed in a subset of tracheal cells and maps within a genomic region required for tracheal development. Development, 120(4), 743-753.

Agilent Technologies. (2009). MxPro QPCR Software Instruction Manual For Mx3000P and Mx3005P QPCR Systems Software version 4.10. Retrieved 18th November, 2011, from http://www.genomics.agilent.com/files/Manual/MxPro_Manual.pdf

Akimoto A, Wada H, & Hayashi S. (2005). Enhancer trapping with a red fluorescent protein reporter in Drosophila. Dev Dyn, 233(3), 993-997.

Alarid ET, Rubin JS, Young P, Chedid M, Ron D, Aaronson SA, et al. (1994). Keratinocyte growth factor functions in epithelial induction during seminal vesicle development. Proc Natl Acad Sci U S A, 91(3), 1074-1078.

Aldaz S, Escudero LM, & Freeman M. (2010). Live imaging of Drosophila imaginal disc development. Proc Natl Acad Sci U S A, 107(32), 14217-14222.

Alescio T, & Cassini A. (1962). Induction in vitro of tracheal buds by pulmonary mesenchyme grafted on tracheal epithelium. The Journal of experimental zoology, 150, 83-94.

Allen RS, Millgate AG, Chitty JA, Thisleton J, Miller JA, Fist AJ, et al. (2004). RNAi-mediated replacement of morphine with the nonnarcotic alkaloid reticuline in opium poppy. Nat Biotechnol, 22(12), 1559-1566.

Andersen DH. (1941). Incidence of congenital diaphragmatic hernia in the young of rats bred on a diet deficient in Vitamin A. American Journal of Diseases of Children, 62, 888–889.

Anger M, Samuel JL, Marotte F, Wuytack F, Rappaport L, & Lompre AM. (1993). The sarco(endo)plasmic reticulum Ca(2+)-ATPase mRNA isoform, SERCA 3, is expressed in endothelial and epithelial cells in various organs. FEBS Lett, 334(1), 45-48.

Applied Biosystems. (1997, 2001). User Bulletin #2: ABI Prism 7700 Sequence Detection System. Retrieved 18th November, 2011, from http://www3.appliedbiosystems.com/cms/groups/mcb_support/documents/generaldocuments/cms_040980.pdf

Arai M, Alpert NR, Maclennan DH, Barton P, & Periasamy M. (1993). Alterations in sarcoplasmic-reticulum gene-expression in human heart-failure - a possible mechanism for alterations in systolic and diastolic properties of the failing myocardium. Circulation Research, 72(2), 463-469.

Arredouani A, Guiot Y, Jonas JC, Liu LH, Nenquin M, Pertusa JA, et al. (2002). SERCA3 ablation does not impair insulin secretion but suggests distinct roles of different sarcoendoplasmic reticulum Ca2+ pumps for Ca2+ homeostasis in pancreatic ßcells. Diabetes, 51(11), 3245-3253.

Artavanis-Tsakonas S, Rand MD, & Lake RJ. (1999). Notch Signaling: Cell Fate Control and Signal Integration in Development. Science, 284(5415), 770-776.

Askenazi SS, & Perlman M. (1979). Pulmonary hypoplasia: lung weight and radial alveolar count as criteria of diagnosis. Archives of Disease in Childhood, 54(8), 614-618.

Avery ME, & Mead J. (1959). Surface properties in relation to atelectasis and hyaline membrane disease. Ama Journal of Diseases of Children, 97(5), 517-523.

Ba'ath ME, Jesudason EC, & Losty PD. (2007). How useful is the lung-to-head ratio in predicting outcome in the fetus with congenital diaphragmatic hernia? A systematic review and meta-analysis. Ultrasound Obstet Gynecol, 30(6), 897-906.

Bai J, Sepp KJ, & Perrimon N. (2009). Culture of Drosophila primary cells dissociated from gastrula embryos and their use in RNAi screening. Nat Protoc, 4(10), 1502-1512.

Baird GS, Zacharias DA, & Tsien RY. (1999). Circular permutation and receptor insertion within green fluorescent proteins. Proceedings of the National Academy of Sciences of the United States of America, 96(20), 11241-11246.

Baldwin L, & Roche WR. (2002). Does remodelling of the airway wall precede asthma? Paediatr Respir Rev, 3(4), 315-320.

Baraldi E, & Filippone M. (2007). Chronic lung disease after premature birth. N Engl J Med, 357(19), 1946-1955.

Barbiero G, Munaron L, Antoniotti S, Baccino PM, Bonelli G, & Lovisolo D. (1995). Role of mitogen-induced calcium influx in the control of the cell cycle in Balb-c 3T3 fibroblasts. Cell Calcium, 18(6), 542-556.

Bate M. (1990). The embryonic development of larval muscles in Drosophila. Development, 110(3), 791-804.

Baum JA, Bogaert T, Clinton W, Heck GR, Feldmann P, Ilagan O, et al. (2007). Control of coleopteran insect pests through RNA interference. Nature Biotechnology, 25(11), 1322-1326.

Behr M, Wingen C, Wolf C, Schuh R, & Hoch M. (2007). Wurst is essential for airway clearance and respiratory-tube size control. Nat Cell Biol, 9(7), 847-853.

Beitel GJ, & Krasnow MA. (2000). Genetic control of epithelial tube size in the Drosophila tracheal system. Development, 127(15), 3271-3282.

Bellusci S, Furuta Y, Rush MG, Henderson R, Winnier G, & Hogan BL. (1997). Involvement of Sonic hedgehog (Shh) in mouse embryonic lung growth and morphogenesis. Development, 124(1), 53-63.

Bellusci S, Grindley J, Emoto H, Itoh N, & Hogan BLM. (1997). Fibroblast Growth Factor 10(FGF10) and branching morphogenesis in the embryonic mouse lung. Development, 124(23), 4867-4878.

Berger AL, Randak CO, Ostedgaard LS, Karp PH, Vermeer DW, & Welsh MJ. (2005). Curcumin stimulates cystic fibrosis transmembrane conductance regulator Cl- channel activity. Journal of Biological Chemistry, 280(7), 5221-5226.

Berney C, & Danuser G. (2003). FRET or No FRET: A Quantitative Comparison. Biophysical Journal, 84(6), 3992-4010.

Bernstein E, Caudy AA, Hammond SM, & Hannon GJ. (2001). Role for a bidentate ribonuclease in the initiation step of RNA interference. Nature, 409(6818), 363-366.

Berridge MJ, Lipp P, & Bootman MD. (2000). The versatility and universality of calcium signalling. Nat Rev Mol Cell Biol, 1(1), 11-21.

Bisgaard H, Hermansen MN, Loland L, Halkjaer LB, & Buchvald F. (2006). Intermittent inhaled corticosteroids in infants with episodic wheezing. N Engl J Med, 354(19), 1998-2005.

Bisgaard H, Jensen SM, & Bonnelykke K. (2012). Interaction between asthma and lung function growth in early life. Am J Respir Crit Care Med, 185(11), 1183-1189.

Bitgood MJ, & McMahon AP. (1995). Hedgehog and Bmp genes are coexpressed at many diverse sites of cell-cell interaction in the mouse embryo. Dev Biol, 172(1), 126-138.

Blochlinger K, Bodmer R, Jan LY, & Jan YN. (1990). Patterns of expression of cut, a protein required for external sensory organ development in wild-type and cut mutant Drosophila embryos. Genes & Development, 4(8), 1322-1331.

Bobe R, Hadri L, Lopez JJ, Sassi Y, Atassi F, Karakikes I, et al. (2011). SERCA2a controls the mode of agonist-induced intracellular Ca2+ signal, transcription factor NFAT and proliferation in human vascular smooth muscle cells. Journal of Molecular and Cellular Cardiology, 50(4), 621-633.

Bochdalek VA. (1848). Einige Betrachtungen die Entstehung des angeborenen Zwerchfellbruches. Als Beitrag zur pathologischen Anatomie der Hernien. Vierteljahrschrift fur die praktische Heilkunde, 19, 89–97.

Bousquet J, Chanez P, Lacoste JY, White R, Vic P, Godard P, et al. (1992). Asthma: A disease remodeling the airways. Allergy: European Journal of Allergy and Clinical Immunology, 47(1), 3-11.

Bousquet J, Yssel H, & Vignola AM. (2000). Is allergic asthma associated with delayed fetal maturation or the persistence of conserved fetal genes? Allergy, 55(12), 1194-1197.

Boutros M, Kiger AA, Armknecht S, Kerr K, Hild M, Koch B, et al. (2004). Genome-Wide RNAi Analysis of Growth and Viability in Drosophila Cells. Science, 303(5659), 832-835.

Bownes M. (1975). A photographic study of development in the living embryo of Drosophila melanogaster. J Embryol Exp Morphol, 33(3), 789-801.

Brand AH, & Perrimon N. (1993). Targeted gene expression as a means of altering cell fates and generating dominant phenotypes. Development, 118(2), 401-415.

Brandl CJ, Green NM, Korczak B, & MacLennan DH. (1986). Two Ca2+ ATPase genes: homologies and mechanistic implications of deduced amino acid sequences. Cell, 44(4), 597-607.

British Thoracic Society and others. (1997). BTS guidelines for the management of chronic obstructive pulmonary disease. The COPD Guidelines Group of the Standards of Care Committee of the BTS. Thorax, 52 Suppl 5, S1-28.

Brody IA. (1969). Muscle contracture induced by exercise. A syndrome attributable to decreased relaxing factor. New England Journal of Medicine, 281(4), 187-192.

Brundage RA, Fogarty KE, Tuft RA, & Fay FS. (1991). Calcium gradients underlying polarization and chemotaxis of eosinophils. Science, 254(5032), 703-706.

Brunner D, Ducker K, Oellers N, Hafen E, Scholz H, & Klambt C. (1994). The ETS domain protein pointed-P2 is a target of MAP kinase in the sevenless signal transduction pathway. Nature, 370(6488), 386-389.

Cabernard C, & Affolter M. (2005). Distinct roles for two receptor tyrosine kinases in epithelial branching morphogenesis in Drosophila. Dev Cell, 9(6), 831-842.

Camacho P, & Lechleiter JD. (1993). Increased frequency of calcium waves in Xenopus laevis oocytes that express a calcium-ATPase. Science, 260(5105), 226-229.

Campbell RE, Tour O, Palmer AE, Steinbach PA, Baird GS, Zacharias DA, et al. (2002). A monomeric red fluorescent protein. Proceedings of the National Academy of Sciences of the United States of America, 99(12), 7877-7882.

Campos-Ortega JA, & Hartenstein V. (1985). The Embryonic development of Drosophila melanogaster. Berlin: Springer-Verlag.

Caplen NJ, Fleenor J, Fire A, & Morgan RA. (2000). dsRNA-mediated gene silencing in cultured Drosophila cells: A tissue culture model for the analysis of RNA interference. Gene, 252(1-2), 95-105.

Cardoso WV, & Lu J. (2006). Regulation of early lung morphogenesis: questions, facts and controversies. Development, 133(9), 1611-1624.

Cardoso WV, Williams MC, Mitsialis SA, Joyce-Brady M, Rishi AK, & Brody JS. (1995). Retinoic acid induces changes in the pattern of airway branching and alters epithelial cell differentiation in the developing lung in vitro. Am J Respir Cell Mol Biol, 12(5), 464-476.

Cartiera MS, Ferreira EC, Caputo C, Egan ME, Caplan MJ, & Saltzman WM. (2009). Partial Correction of Cystic Fibrosis Defects with PLGA Nanoparticles Encapsulating Curcumin. Molecular Pharmaceutics, 7(1), 86-93.

Caspersen C, Pedersen P, & Treiman M. (2000). The Sarco-Endoplasmic Reticulum Calcium ATPase 2b is an endoplasmic reticulum stress-inducible protein. J. Biol. Chem., 275, 22363 - 22372.

Cassel TN, & Nord M. (2003). C/EBP transcription factors in the lung epithelium. Am J Physiol Lung Cell Mol Physiol, 285(4), L773-781.

Celli G, LaRochelle WJ, Mackem S, Sharp R, & Merlino G. (1998). Soluble dominant-negative receptor uncovers essential roles for fibroblast growth factors in multi-organ induction and patterning. EMBO J, 17(6), 1642-1655.

Chanut-Delalande H, Jung AC, Lin L, Baer MM, Bilstein A, Cabernard C, et al. (2007). A genetic mosaic analysis with a repressible cell marker screen to identify genes involved in tracheal cell migration during Drosophila air sac morphogenesis. Genetics, 176(4), 2177-2187.

Charlesworth A, & Rozengurt E. (1994). Thapsigargin and di-tert-butylhydroquinone induce synergistic stimulation of DNA synthesis with phorbol ester and bombesin in Swiss 3T3 cells. Journal of Biological Chemistry, 269(51), 32528-32535.

Chen CK, Kuhnlein RP, Eulenberg KG, Vincent S, Affolter M, & Schuh R. (1998). The transcription factors KNIRPS and KNIRPS RELATED control cell migration and branch morphogenesis during Drosophila tracheal development. Development, 125(24), 4959-4968.

Chen H, Sun J, Buckley S, Chen C, Warburton D, Wang XF, et al. (2005). Abnormal mouse lung alveolarization caused by Smad3 deficiency is a developmental antecedent of centrilobular emphysema. American Journal of Physiology - Lung Cellular and Molecular Physiology, 288(4 32-4), L683-L691.

Cheng G, Liu B-F, Yu Y, Diglio C, & Kuo TH. (1996). The Exit from G0into the Cell Cycle Requires and Is Controlled by Sarco(endo)plasmic Reticulum Ca2+Pump. Archives of Biochemistry and Biophysics, 329(1), 65-72.

Cheng SH, Gregory RJ, Marshall J, Paul S, Souza DW, White GA, et al. (1990). Defective intracellular-transport and processing of cftr is the molecular-basis of most cystic-fibrosis. Cell, 63(4), 827-834.

Chihara T, & Hayashi S. (2000). Control of tracheal tubulogenesis by Wingless signaling. Development, 127(20), 4433-4442.

Cho JH, Bandyopadhyay J, Lee J, Park CS, & Ahnn J. (2000). Two isoforms of sarco/endoplasmic reticulum calcium ATPase (SERCA) are essential in Caenorhabditis elegans. Gene, 261(2), 211-219.

Clark TJ, Martin WL, Divakaran TG, Whittle MJ, Kilby MD, & Khan KS. (2003). Prenatal bladder drainage in the management of fetal lower urinary tract obstruction: A systematic review and meta-analysis. Obstetrics and Gynecology, 102(2), 367-382.

Clements JA. (1957). Surface tension of lung extracts. Proc Soc Exp Biol Med, 95(1), 170-172.

Colvin J, Bower C, Dickinson JE, & Sokol J. (2005). Outcomes of congenital diaphragmatic hernia: A population-based study in western Australia. Pediatrics, 116(3), E356-E363.

Colvin JS, Feldman B, Nadeau JH, Goldfarb M, & Ornitz DM. (1999). Genomic organization and embryonic expression of the mouse fibroblast growth factor 9 gene. Dev Dyn, 216(1), 72-88.

Colvin JS, White AC, Pratt SJ, & Ornitz DM. (2001). Lung hypoplasia and neonatal death in Fgf9-null mice identify this gene as an essential regulator of lung mesenchyme. Development, 128(11), 2095-2106.

Costa RH, Kalinichenko VV, & Lim L. (2001). Transcription factors in mouse lung development and function. American Journal of Physiology - Lung Cellular and Molecular Physiology, 280(5 25-5), L823-L838.

Cox PG, Miller J, Mitzner W, & Leff AR. (2004). Radiofrequency ablation of airway smooth muscle for sustained treatment of asthma: Preliminary investigations. European Respiratory Journal, 24(4), 659-663.

Crepin A, Bidaux G, Vanden-Abeele F, Dewailly E, Goffin V, Prevarskaya N, et al. (2007). Prolactin stimulates prostate cell proliferation by increasing endoplasmic reticulum content due to SERCA 2b over-expression. Biochemical Journal, 401(1), 49-55.

Cronin SJF, Nehme NT, Limmer S, Liegeois S, Pospisilik JA, Schramek D, et al. (2009). Genome-Wide RNAi Screen Identifies Genes Involved in Intestinal Pathogenic Bacterial Infection. Science, 325(5938), 340-343.

Cullen JM, Wilson M, Hagler WM, Jr., Ort JF, & Cole RJ. (1988). Histologic lesions in broiler chicks given cyclopiazonic acid orally. Am J Vet Res, 49(5), 728-731.

Dalemans W, Barbry P, Champigny G, Jallat S, Dott K, Dreyer D, et al. (1991). Altered chloride-ion channel kinetics associated with the delta-f508 cystic-fibrosis mutation. Nature, 354(6354), 526-528.

de Carvalho F, Gheysen G, Kushnir S, Van Montagu M, Inze D, & Castresana C. (1992). Suppression of beta-1,3-glucanase transgene expression in homozygous plants. EMBO J, 11(7), 2595-2602.

De Moerlooze L, Spencer-Dene B, Revest JM, Hajihosseini M, Rosewell I, & Dickson C. (2000). An important role for the IIIb isoform of fibroblast growth factor receptor 2 (FGFR2) in mesenchymal-epithelial signalling during mouse organogenesis. Development, 127(3), 483-492.

del Monte F, Harding SE, Schmidt U, Matsui T, Kang ZB, Dec W, et al. (1999). Restoration of contractile function in isolated cardiomyocytes from failing human hearts by gene transfer of SERCA2a. Circulation, 100(23), 2308-2311.

del Monte F, Williams E, Lebeche D, Schmidt U, Rosenzweig A, Gwathmey JK, et al. (2001). Improvement in survival and cardiac metabolism after gene transfer of sarcoplasmic reticulum Ca2+-ATPase in a rat model of heart failure. Circulation, 104(12), 1424-1429.

Denmeade SR, Jakobsen CM, Janssen S, Khan SR, Garrett ES, Lilja H, et al. (2003). Prostate-specific antigen-activated thapsigargin prodrug as targeted therapy for prostate cancer. J Natl Cancer Inst, 95(13), 990-1000.

Deprest J, Gratacos E, & Nicolaides KH. (2004). Fetoscopic tracheal occlusion (FETO) for severe congenital diaphragmatic hernia: Evolution of a technique and preliminary results. Ultrasound in Obstetrics and Gynecology, 24(2), 121-126.

DeVincenzo J, Cehelsky JE, Alvarez R, Elbashir S, Harborth J, Toudjarska I, et al. (2008). Evaluation of the safety, tolerability and pharmacokinetics of ALN-RSV01, a novel RNAi antiviral therapeutic directed against respiratory syncytial virus (RSV). Antiviral Research, 77(3), 225-231.

DeVincenzo J, Lambkin-Williams R, Wilkinson T, Cehelsky J, Nochur S, Walsh E, et al. (2010). A randomized, double-blind, placebo-controlled study of an RNAi-based therapy directed against respiratory syncytial virus. Proceedings of the National Academy of Sciences of the United States of America, 107(19), 8800-8805.

Dickman ED, Thaller C, & Smith SM. (1997). Temporally-regulated retinoic acid depletion produces specific neural crest, ocular and nervous system defects. Development, 124(16), 3111-3121.

Didon L, Qvarfordt I, Andersson O, Nord M, & Riise GC. (2005). Decreased CCAAT/enhancer binding protein transcription factor activity in chronic bronchitis and COPD. Chest, 127(4), 1341-1346.

Didon L, Roos AB, Elmberger GP, Gonzalez FJ, & Nord M. (2010). Lung-specific inactivation of CCAAT/enhancer binding protein alpha causes a pathological pattern characteristic of COPD. Eur Respir J, 35(1), 186-197.

Diegelmann S, Fiala A, Leibold C, Spall T, & Buchner E. (2002). Transgenic flies expressing the fluorescence calcium sensor Cameleon 2.1 under UAS control. Genesis, 34(1-2), 95-98.

Dietzl G, Chen D, Schnorrer F, Su KC, Barinova Y, Fellner M, et al. (2007). A genome-wide transgenic RNAi library for conditional gene inactivation in Drosophila. Nature, 448(7150), 151-156.

DiFiore JW, Fauza DO, Slavin R, Peters CA, Fackler JC, & Wilson JM. (1994). Experimental fetal tracheal ligation reverses the structural and physiological effects of pulmonary hypoplasia in congenital diaphragmatic hernia. Journal of Pediatric Surgery, 29(2), 248-257.

Dixon RE, Britton FC, Baker SA, Hennig GW, Rollings CM, Sanders KM, et al. (2011). Electrical slow waves in the mouse oviduct are dependent upon extracellular and intracellular calcium sources. American Journal of Physiology - Cell Physiology.

Dizier MH, Besse-Schmittler C, Guilloud-Bataille M, Annesi-Maesano I, Boussaha M, Bousquet J, et al. (2000). Genome screen for asthma and related phenotypes in the French EGEA study. Am J Respir Crit Care Med, 162(5), 1812-1818.

Dolmetsch RE, Lewis RS, Goodnow CC, & Healy JI. (1997). Differential activation of transcription factors induced by Ca2+ response amplitude and duration. Nature, 386(6627), 855-858.

Douglas G, Higgins B, Barnes N, Boyter A, Burge S, Cates C, et al. (2008). British guideline on the management of asthma: A national clinical guideline. Thorax, 63(SUPPL. 4), iv1-iv121.

Dragomir A, Bjʃðrstad J, Hjelte L, & Roomans GM. (2004). Curcumin does not stimulate cAMP-mediated chloride transport in cystic fibrosis airway epithelial cells. Biochemical and Biophysical Research Communications, 322(2), 447-451.

Duffy JB. (2002). GAL4 system in Drosophila: a fly geneticist's Swiss army knife. Genesis, 34(1-2), 1-15.

Duffy JB, Harrison DA, & Perrimon N. (1998). Identifying loci required for follicular patterning using directed mosaics. Development, 125(12), 2263-2271.

Dura JM. (1981). Stage dependent synthesis of heat shock induced proteins in early embryos of Drosophila melanogaster. Mol Gen Genet, 184(3), 381-385.

Eberlein S, & Mitchell HK. (1987). Protein synthesis patterns following stage-specific heat shock in early Drosophila embryos. Mol Gen Genet, 210(3), 407-412.

Eckstein-Ludwig U, Webb RJ, Van Goethem ID, East JM, Lee AG, Kimura M, et al. (2003). Artemisinins target the SERCA of Plasmodium falciparum. Nature, 424(6951), 957-961.

Egan ME, Glöckner-Pagel J, Ambrose CA, Cahill PA, Pappoe L, Balamuth N, et al. (2002). Calcium-pump inhibitors induce functional surface expression of ΔF508-CFTR protein in cystic fibrosis epithelial cells. Nature medicine, 8(5), 485-492.

Egan ME, Pearson M, Weiner SA, Rajendran V, Rubin D, Glʃðckner-Pagel J, et al. (2004). Curcumin, a Major Constituent of Turmeric, Corrects Cystic Fibrosis Defects. Science, 304(5670), 600-602.

Elbashir SM, Harborth J, Lendeckel W, Yalcin A, Weber K, & Tuschl T. (2001). Duplexes of 21-nucleotide RNAs mediate RNA interference in cultured mammalian cells. Nature, 411(6836), 494-498.

Ellgaard L, Molinari M, & Helenius A. (1999). Setting the Standards: Quality Control in the Secretory Pathway. Science, 286(5446), 1882-1888.

Enhorning G, & Robertson B. (1972). Lung expansion in the premature rabbit fetus after tracheal deposition of surfactant. Pediatrics, 50(1), 58-66.

Everest NJ, Jacobs SE, Davis PG, Begg L, & Rogerson S. (2008). Outcomes following prolonged preterm premature rupture of the membranes. Archives of Disease in Childhood - Fetal and Neonatal Edition, 93(3), F207-F211.

Farkas L, Farkas D, Warburton D, Gauldie J, Shi W, Stampfli MR, et al. (2011). Cigarette smoke exposure aggravates air space enlargement and alveolar cell apoptosis in Smad3 knockout mice. American Journal of Physiology - Lung Cellular and Molecular Physiology, 301(4), L391-L401.

Featherstone N, Connell M, Fernig D, Wray S, Burdyga T, Losty P, et al. (2006). Sarcoplasmic calcium reuptake is essential for lung branching morphogenesis and required for development and peristalsis of prenatal airway smooth muscle, 19th international symposium of pediatric surgical research. Florence, Italy.

Featherstone N, Jesudason E, Connell M, Fernig D, Wray S, Losty P, et al. (2005). Sarcoplasmic reticulum regulates calcium transients, airway peristalsis and branching morphogenesis of lung explants in vitro. Paper presented at the American Thoracic Society International Conference, San Diego.

Featherstone NC, Connell MG, Fernig DG, Wray S, Burdyga TV, Losty PD, et al. (2006). Airway smooth muscle dysfunction precedes teratogenic congenital diaphragmatic hernia and may contribute to hypoplastic lung morphogenesis. Am J Respir Cell Mol Biol, 35(5), 571-578.

Featherstone NC, Jesudason EC, Connell MG, Fernig DG, Wray S, Losty PD, et al. (2005). Spontaneous propagating calcium waves underpin airway peristalsis in embryonic rat lung. Am J Respir Cell Mol Biol, 33(2), 153-160.

Felix JF, van Dooren MF, Klaassens M, Hop WC, Torfs CP, & Tibboel D. (2008). Environmental factors in the etiology of esophageal atresia and congenital

diaphragmatic hernia: results of a case-control study. Birth Defects Res A Clin Mol Teratol, 82(2), 98-105.

Fernandes-Alnemri T, Litwack G, & Alnemri ES. (1994). CPP32, a novel human apoptotic protein with homology to Caenorhabditis elegans cell death protein Ced-3 and mammalian interleukin-1 beta-converting enzyme. J Biol Chem, 269(49), 30761-30764.

Fewell JE, Hislop AA, Kitterman JA, & Johnson P. (1983). Effect of tracheostomy on lung development in fetal lambs. Journal of Applied Physiology, 55(4), 1103-1108.

Fiala A, Spall T, Diegelmann S, Eisermann B, Sachse S, Devaud JM, et al. (2002). Genetically expressed cameleon in Drosophila melanogaster is used to visualize olfactory information in projection neurons. Current Biology, 12(21), 1877-1884.

Fire A, Xu SQ, Montgomery MK, Kostas SA, Driver SE, & Mello CC. (1998). Potent and specific genetic interference by double-stranded RNA in Caenorhabditis elegans. Nature, 391(6669), 806-811.

Fleige S, & Pfaffl MW. RNA integrity and the effect on the real-time qRT-PCR performance. Molecular Aspects of Medicine, 27(2-3), 126-139.

Folkman J, & Klagsbrun M. (1987). Angiogenic factors. Science, 235(4787), 442-447.

Förster T. (1965). Delocalized excitation and excitation transfer. In O. Sinanoglu (Ed.), Modern Quantum Chemistry (Vol. 3, pp. 93-137). New York: Academic Press Inc.

Fraser AG, Kamath RS, Zipperlen P, Martinez-Campos M, Sohrmann M, & Ahringer J. (2000). Functional genomic analysis of C. elegans chromosome I by systematic RNA interference. Nature, 408(6810), 325-330.

Fujiwara T, Chida S, Watabe Y, Maeta H, Morita T, & Abe T. (1980). Artificial surfactant therapy in hyaline-membrane disease. The Lancet, 315(8159), 55-59.

Furuya Y, Lundmo P, Short AD, Gill DL, & Isaacs JT. (1994). The role of calcium, pH, and cell proliferation in the programmed (apoptotic) death of androgen-independent prostatic cancer cells induced by thapsigargin. Cancer Res, 54(23), 6167-6175.

Fuse N, Hirose S, & Hayashi S. (1994). Diploidy of Drosophila imaginal cells is maintained by a transcriptional repressor encoded by escargot. Genes Dev, 8(19), 2270-2281.

Gabay L, Seger R, & Shilo BZ. (1997). In situ activation pattern of Drosophila EGF receptor pathway during development. Science, 277(5329), 1103-1106.

Gallot D, Boda C, Ughetto S, Perthus I, Robert-Gnansia E, Francannet C, et al. (2007). Prenatal detection and outcome of congenital diaphragmatic hernia: a French registry-based study. Ultrasound in Obstetrics & Gynecology, 29(3), 276-283.

Ghantous A, Gali-Muhtasib H, Vuorela H, Saliba NA, & Darwiche N. (2010). What made sesquiterpene lactones reach cancer clinical trials? Drug Discovery Today, 15(15,Äì16), 668-678.

Ginzinger DG. (2002). Gene quantification using real-time quantitative PCR: an emerging technology hits the mainstream. Exp Hematol, 30(6), 503-512.

Glazer L, & Shilo BZ. (1991). The Drosophila FGF-R homolog is expressed in the embryonic tracheal system and appears to be required for directed tracheal cell extension. Genes & Development, 5(4), 697-705.

Gluckman PD, Hanson MA, Cooper C, & Thornburg KL. (2008). Effect of in utero and early-life conditions on adult health and disease. New England Journal of Medicine, 359(1), 61-73+66.

Gordon GW, Berry G, Liang XH, Levine B, & Herman B. (1998). Quantitative Fluorescence Resonance Energy Transfer Measurements Using Fluorescence Microscopy. Biophysical Journal, 74(5), 2702-2713.

Goto A, Kadowaki T, & Kitagawa Y. (2003). Drosophila hemolectin gene is expressed in embryonic and larval hemocytes and its knock down causes bleeding defects. Developmental Biology, 264(2), 582-591.

Graveley BR, Brooks AN, Carlson JW, Duff MO, Landolin JM, Yang L, et al. (2011). The developmental transcriptome of Drosophila melanogaster. Nature, 471(7339), 473-479.

Graziosi G, de Cristini F, di Marcotullio A, Marzari R, Micali F, & Savoini A. (1983). Morphological and molecular modifications induced by heat shock in Drosophila melanogaster embryos. J Embryol Exp Morphol, 77, 167-182.

Graziosi G, Micali F, Marzari R, de Cristini F, & Savoini A. (1980). Variability of response of early Drosophila embryos to heat shock. Journal of Experimental Zoology, 214, 141-145.

Greenberg JM, Thompson FY, Brooks SK, Shannon JM, McCormick-Shannon K, Cameron JE, et al. (2002). Mesenchymal expression of vascular endothelial growth factors D and A defines vascular patterning in developing lung. Dev Dyn, 224(2), 144-153.

Grieder NC, Caussinus E, Parker DS, Cadigan K, Affolter M, & Luschnig S. (2008). gammaCOP is required for apical protein secretion and epithelial morphogenesis in Drosophila melanogaster. PLoS One, 3(9), e3241.

Grubb BR, Gabriel SE, Mengos A, Gentzsch M, Randell SH, Van Heeckeren AM, et al. (2006). SERCA pump inhibitors do not correct biosynthetic arrest of ΔF508 CFTR in cystic fibrosis. American Journal of Respiratory Cell and Molecular Biology, 34(3), 355-363.

Guha A, Lin L, & Kornberg TB. (2008). Organ renewal and cell divisions by differentiated cells in Drosophila. Proceedings of the National Academy of Sciences of the United States of America, 105(31), 10832-10836.

Guilbert TW, Morgan WJ, Zeiger RS, Mauger DT, Boehmer SJ, Szefler SJ, et al. (2006). Long-term inhaled corticosteroids in preschool children at high risk for asthma. N Engl J Med, 354(19), 1985-1997.

Guillemin K, Groppe J, Ducker K, Treisman R, Hafen E, Affolter M, et al. (1996). The pruned gene encodes the Drosophila serum response factor and regulates cytoplasmic outgrowth during terminal branching of the tracheal system. Development, 122(5), 1353-1362.

Ha T, Enderle T, Ogletree DF, Chemla DS, Selvin PR, & Weiss S. (1996). Probing the interaction between two single molecules: fluorescence resonance energy transfer between a single donor and a single acceptor. Proc Natl Acad Sci U S A, 93(13), 6264-6268.

Hacohen N, Kramer S, Sutherland D, Hiromi Y, & Krasnow MA. (1998). Sprouty encodes a novel antagonist of FGF signaling that patterns apical branching of the Drosophila airways. Cell, 92(2), 253-263.

Hales CN, & Barker DJP. (1992). Type 2 (non-insulin-dependent) diabetes mellitus: The thrifty phenotype hypothesis. Diabetologia, 35(7), 595-601.

Hamilton AJ, & Baulcombe DC. (1999). A species of small antisense RNA in posttranscriptional gene silencing in plants. Science, 286(5441), 950-952.

Hammond SM, Bernstein E, Beach D, & Hannon GJ. (2000). An RNA-directed nuclease mediates post-transcriptional gene silencing in Drosophila cells. Nature, 404(6775), 293-296.

Hansen JC, Tse C, & Wolffe AP. (1998). Structure and Function of the Core Histone N-Termini: More Than Meets the Eye. Biochemistry, 37(51), 17637-17641.

Harbecke R, Meise M, Holz A, Klapper R, Naffin E, Nordhoff V, et al. (1996). Larval and imaginal pathways in early development of Drosophila. Int J Dev Biol, 40(1), 197-204.

Harborth J, Elbashir SM, Bechert K, Tuschl T, & Weber K. (2001). Identification of essential genes in cultured mammalian cells using small interfering RNAs. Journal of Cell Science, 114(24), 4557-4565.

Harding R, & Hooper SB. (1996). Regulation of lung expansion and lung growth before birth. J Appl Physiol, 81(1), 209-224.

Harrison MR, Golbus MS, & Filly RA. (1982). Management of the fetus with congenital hydronephrosis. Journal of Pediatric Surgery, 17(6), 728-742.

Harrison MR, Keller RL, Hawgood SB, Kitterman JA, Sandberg PL, Farmer DL, et al. (2003). A randomized trial of fetal endoscopic tracheal occlusion for severe fetal congenital diaphragmatic hernia. N Engl J Med, 349(20), 1916-1924.

Harrison MR, Mychaliska GB, Albanese CT, Jennings RW, Farrell JA, Hawgood S, et al. (1998). Correction of congenital diaphragmatic hernia in utero IX: Fetuses with poor prognosis (liver herniation and low lung-to-head ratio) can be saved fetoscopic temporary tracheal occlusion. Journal of Pediatric Surgery, 33(7), 1017-1023.

Harrison MR, Nakayama DK, Noall R, & De Lorimier AA. (1982). Correction of congenital hydronephrosis in utero. II. Decompression reverses the effects of obstruction on the fetal lung and urinary tract. Journal of Pediatric Surgery, 17(6), 965-974.

Hasan MT, Friedrich RW, Euler T, Larkum ME, Giese G, Both M, et al. (2004). Functional fluorescent Ca2+ indicator proteins in transgenic mice under TET control. PLoS Biology, 2(6).

Hasenfuss G, Reinecke H, Studer R, Meyer M, Pieske B, Holtz J, et al. (1994). Relation between myocardial-function and expression of sarcoplasmic-reticulum Ca2+-ATPase in failing and nonfailing human myocardium. Circulation Research, 75(3), 434-442.

Hedrick MH, Estes JM, Sullivan KM, Bealer JF, Kitterman JA, Flake AW, et al. (1994). Plug the lung until it grows (PLUG): A new method to treat congenital diaphragmatic hernia in utero. Journal of Pediatric Surgery, 29(5), 612-617.

Heid CA, Stevens J, Livak KJ, & Williams PM. (1996). Real time quantitative PCR. Genome Res, 6(10), 986-994.

Heitzler P, & Simpson P. (1991). The choice of cell fate in the epidermis of Drosophila. Cell, 64(6), 1083-1092.

Hendzel MJ, Wei Y, Mancini MA, Van Hooser A, Ranalli T, Brinkley BR, et al. (1997). Mitosis-specific phosphorylation of histone H3 initiates primarily within pericentromeric heterochromatin during G2 and spreads in an ordered fashion coincident with mitotic chromosome condensation. Chromosoma, 106(6), 348-360.

Hersh CP, DeMeo DL, Lazarus R, Celed√≥n JC, Raby BA, Benditt JO, et al. (2006). Genetic association analysis of functional impairment in chronic obstructive pulmonary disease. American Journal of Respiratory and Critical Care Medicine, 173(9), 977-984.

Hilfer SR. (1996). Morphogenesis of the lung: control of embryonic and fetal branching. Annu Rev Physiol, 58, 93-113.

Hirota S, Helli P, & Janssen LJ. (2007). Ionic mechanisms and Ca2+ handling in airway smooth muscle. European Respiratory Journal, 30(1), 114-133.

Hochheim K. (1903). Über einige Befunde in den Lungen von Neugeborenen und die Bezie- hung derselben zur Aspiration von Frucht- wasser. Centralbl Pathol 14, 537–538.

Hojmann Larsen A, Frandsen A, & Treiman M. (2001). Upregulation of the SERCA-type Ca2+ pump activity in response to endoplasmic reticulum stress in PC12 cells. BMC Biochemistry, 2(1), 4.

Holgate ST. (2008). Pathogenesis of Asthma. Clinical & Experimental Allergy, 38(6), 872-897.

Holgate ST, Lackie PM, Howarth PH, Roche WR, Puddicombe SM, Richter A, et al. (2001). Invited lecture: activation of the epithelial mesenchymal trophic unit in the pathogenesis of asthma. Int Arch Allergy Immunol, 124(1-3), 253-258.

Hoppe HC, van Schalkwyk DA, Wiehart UIM, Meredith SA, Egan J, & Weber BW. (2004). Antimalarial Quinolines and Artemisinin Inhibit Endocytosis in Plasmodium falciparum. Antimicrobial Agents and Chemotherapy, 48(7), 2370-2378.

Hori K, Fostier M, Ito M, Fuwa TJ, Go MJ, Okano H, et al. (2004). Drosophila Deltex mediates Suppressor of Hairless-independent and late-endosomal activation of Notch signaling. Development, 131(22), 5527-5537.

Humez S, Legrand G, Vanden-Abeele F, Monet M, Marchetti P, Lepage G, et al. (2004). Role of endoplasmic reticulum calcium content in prostate cancer cell growth regulation by IGF and TNFalpha. Journal of Cellular Physiology, 201(2), 201-213.

Husain M, Jiang L, See V, Bein K, Simons M, Alper SL, et al. (1997). Regulation of vascular smooth muscle cell proliferation by plasma membrane Ca2+-ATPase. American Journal of Physiology - Cell Physiology, 272(6 41-6), C1947-C1959.

Huttenlocher A, Palecek SP, Lu Q, Zhang W, Mellgren RL, Lauffenburger DA, et al. (1997). Regulation of cell migration by the calcium-dependent protease calpain. Journal of Biological Chemistry, 272(52), 32719-32722.

Hyatt BA, Shangguan X, & Shannon JM. (2002). BMP4 modulates fibroblast growth factor-mediated induction of proximal and distal lung differentiation in mouse embryonic tracheal epithelium in mesenchyme-free culture. Dev Dyn, 225(2), 153-165.

Ikeya T, & Hayashi S. (1999). Interplay of Notch and FGF signaling restricts cell fate and MAPK activation in the Drosophila trachea. Development, 126(20), 4455-4463.

Imam F, Sutherland D, Huang W, & Krasnow MA. (1999). stumps, a Drosophila gene required for fibroblast growth factor (FGF)- directed migrations of tracheal and mesodermal cells. Genetics, 152(1), 307-318.

Ingram JL, & Bonner JC. (2006). EGF and PDGF receptor tyrosine kinases as therapeutic targets for chronic lung diseases. Curr Mol Med, 6(4), 409-421.

Jackson AL, Bartz SR, Schelter J, Kobayashi SV, Burchard J, Mao M, et al. (2003). Expression profiling reveals off-target gene regulation by RNAi. Nature Biotechnology, 21(6), 635-637.

Jackson AL, & Linsley PS. (2004). Noise amidst the silence: off-target effects of siRNAs? Trends in genetics : TIG, 20(11), 521-524.

Jackson D, Bresnick J, Rosewell I, Crafton T, Poulsom R, Stamp G, et al. (1997). Fibroblast growth factor receptor signalling has a role in lobuloalveolar development of the mammary gland. J Cell Sci, 110 (Pt 11), 1261-1268.

Jain L, & Eaton DC. (2006). Physiology of fetal lung fluid clearance and the effect of labor. Seminars in Perinatology, 30(1), 34-43.

Jani J, Gratac√≥s E, Greenough A, Pier√≥ JL, Benachi A, Harrison M, et al. (2005). Percutaneous fetal endoscopic tracheal occlusion (FETO) for severe left-sided congenital diaphragmatic hernia. Clinical Obstetrics and Gynecology, 48(4), 910-922.

Jaski BE, Jessup ML, Mancini DM, Cappola TP, Pauly DF, Greenberg B, et al. (2009). Calcium upregulation by percutaneous administration of gene therapy in cardiac disease (CUPID Trial), a first-in-human phase 1/2 clinical trial. J Card Fail, 15(3), 171-181.

Jayaram SA, Senti KA, Tiklova K, Tsarouhas V, Hemphala J, & Samakovlis C. (2008). COPI vesicle transport is a common requirement for tube expansion in Drosophila. PLoS One, 3(4), e1964.

Jessup M, Greenberg B, Mancini D, Cappola T, Pauly DF, Jaski B, et al. (2011). Calcium Upregulation by Percutaneous Administration of Gene Therapy in Cardiac Disease (CUPID). Circulation.

Jesudason EC. (2009). Airway smooth muscle: an architect of the lung? Thorax, 64(6), 541-545.

Jesudason EC, Connell MG, Fernig DG, Lloyd DA, & Losty PD. (2000). Early lung malformations in congenital diaphragmatic hernia. J Pediatr Surg, 35(1), 124-127; discussion 128.

Jesudason EC, Smith NP, Connell MG, Spiller DG, White MR, Fernig DG, et al. (2005). Developing rat lung has a sided pacemaker region for morphogenesis-related airway peristalsis. Am J Respir Cell Mol Biol, 32(2), 118-127.

Ji J, Loukianov E, Loukianova T, Jones LR, & Periasamy M. (1999). SERCA1a can functionally substitute for SERCA2a in the heart. American Journal of Physiology - Heart and Circulatory Physiology, 276(1 45-1), H89-H97.

Joos L, He JQ, Shepherdson MB, Connett JE, Anthonisen NR, Pare PD, et al. (2002). The role of matrix metalloproteinase polymorphisms in the rate of decline in lung function. Hum Mol Genet, 11(5), 569-576.

Jostarndt-Fogen K, Djonov V, & Draeger A. (1998). Expression of smooth muscle markers in the developing murine lung: potential contractile properties and lineal descent. Histochem Cell Biol, 110(3), 273-284.

Kajstura J, Rota M, Hall SR, Hosoda T, D'Amario D, Sanada F, et al. (2011). Evidence for Human Lung Stem Cells. New England Journal of Medicine, 364(19), 1795-1806.

Kaliss N. (1939). The Effect on Development of a Lethal Deficiency in Drosophila Melanogaster: With a Description of the Normal Embryo at the Time of Hatching. Genetics, 24(2), 244-270.

Kaneko Y, & Tsukamoto A. (1994). Thapsigargin-induced persistent intracellular calcium pool depletion and apoptosis in human hepatoma cells. Cancer Lett, 79(2), 147-155.

Karim FD, & Rubin GM. (1998). Ectopic expression of activated Ras1 induces hyperplastic growth and increased cell death in Drosophila imaginal tissues. Development, 125(1), 1-9.

Karpova TS, Baumann CT, He L, Wu X, Grammer A, Lipsky P, et al. (2003). Fluorescence resonance energy transfer from cyan to yellow fluorescent protein detected by acceptor photobleaching using confocal microscopy and a single laser. J Microsc, 209(Pt 1), 56-70.

Kasahara Y, Tuder RM, Taraseviciene-Stewart L, Le Cras TD, Abman S, Hirth PK, et al. (2000). Inhibition of VEGF receptors causes lung cell apoptosis and emphysema. J Clin Invest, 106(11), 1311-1319.

Kasper M, & Fehrenbach H. (2000). Immunohistochemical evidence for the occurrence of similar epithelial phenotypes during lung development and radiation-induced fibrogenesis. Int J Radiat Biol, 76(4), 493-501.

Kaufman RJ. (1999). Stress signaling from the lumen of the endoplasmic reticulum: coordination of gene transcriptional and translational controls. Genes & Development, 13(10), 1211-1233.

Keijzer R, Liu J, Deimling J, Tibboel D, & Post M. (2000). Dual-hit hypothesis explains pulmonary hypoplasia in the nitrofen model of congenital diaphragmatic hernia. Am J Pathol, 156(4), 1299-1306.

Kemper M, & Mueller-Wiefel D. (2007). Prognosis of antenatally diagnosed oligohydramnios of renal origin. European Journal of Pediatrics, 166(5), 393-398.

Kennerdell JR, & Carthew RW. (1998). Use of dsRNA-mediated genetic interference to demonstrate that frizzled and frizzled 2 act in the wingless pathway. Cell, 95(7), 1017-1026.

Kerr R, Lev-Ram V, Baird G, Vincent P, Tsien RY, & Schafer WR. (2000). Optical imaging of calcium transients in neurons and pharyngeal muscle of C. elegans. Neuron, 26(3), 583-594.

Ketting RF, Fischer SE, Bernstein E, Sijen T, Hannon GJ, & Plasterk RH. (2001). Dicer functions in RNA interference and in synthesis of small RNA involved in developmental timing in C. elegans. Genes Dev, 15(20), 2654-2659.

Kiehart DP, & Feghali R. (1986). Cytoplasmic myosin from Drosophila melanogaster. The Journal of Cell Biology, 103(4), 1517-1525.

Kimura C, Oike M, Koyama T, & Ito Y. (2001). Alterations of Ca2+ mobilizing properties in migrating endothelial cells. American Journal of Physiology - Heart and Circulatory Physiology, 281(2), H745-H754.

Kircher MF, Gambhir SS, & Grimm J. (2011). Noninvasive cell-tracking methods. Nature Reviews Clinical Oncology, 8(11), 677-688.

Kitagawa M, Hislop A, Boyden EA, & Reid L. (1971). Lung hypoplasia in congenital diaphragmatic hernia. A quantitative study of airway, artery, and alveolar development. Br J Surg, 58(5), 342-346.

Klambt C, Glazer L, & Shilo BZ. (1992). breathless, a Drosophila FGF receptor homolog, is essential for migration of tracheal and specific midline glial cells. Genes Dev, 6(9), 1668-1678.

Kohn EC, Alessandro R, Spoonster J, Wersto RP, & Liotta LA. (1995). Angiogenesis: role of calcium-mediated signal transduction. Proceedings of the National Academy of Sciences, 92(5), 1307-1311.

Korosec B, Glavaç D, Rott T, & Ravnik-Glavaç M. (2006). Alterations in the ATP2A2 gene in correlation with colon and lung cancer. Cancer Genetics and Cytogenetics, 171(2), 105-111.

Kotton DN. (2012). Next-generation regeneration: The hope and hype of lung stem cell research. American Journal of Respiratory and Critical Care Medicine, 185(12), 1255-1260.

Kotturi MF, Carlow DA, Lee JC, Ziltener HJ, & Jefferies WA. (2003). Identification and Functional Characterization of Voltage-dependent Calcium Channels in T Lymphocytes. Journal of Biological Chemistry, 278(47), 46949-46960.

Kulesa PM, Bailey CM, Cooper C, & Fraser SE. (2010). In Ovo Live Imaging of Avian Embryos. Cold Spring Harbor Protocols, 2010(6), pdb.prot5446.

Kuromi H, & Kidokoro Y. (2002). Selective replenishment of two vesicle pools depends on the source of Ca2+ at the Drosophila synapse. Neuron, 35(2), 333-343.

Kylsten P, & Saint R. (1997). Imaginal tissues of Drosophila melanogaster exhibit different modes of cell proliferation control. Dev Biol, 192(2), 509-522.

Lama VN, Smith L, Badri L, Flint A, Andrei AC, Murray S, et al. (2007). Evidence for tissue-resident mesenchymal stem cells in human adult lung from studies of transplanted allografts. Journal of Clinical Investigation, 117(4), 989-996.

Lansdale N, Alam S, Losty PD, & Jesudason EC. (2010). Neonatal endosurgical congenital diaphragmatic hernia repair: a systematic review and meta-analysis. Ann Surg, 252(1), 20-26.

Lansdale N, Connell MG, Featherstone NC, Midgley A, & Jesudason EC. (2010). Cyclopiazonic Acid (CPA) Inhibition Of Sarco-Endoplasmic Reticulum Ca2+-ATPase (SERCA) Reduces, With Similar Dose-dependency, Prenatal Airway Branching, Peristalsis And Cell Proliferation And Modulates Gene Expression Required For

Lung Development. American Journal of Respiratory and Critical Care Medicine, 181(1_MeetingAbstracts), A4140-.

Larrivee B, & Karsan A. (2000). Signaling pathways induced by vascular endothelial growth factor (review). Int J Mol Med, 5(5), 447-456.

Lasko P. (2002). Diabetic flies? Using Drosophila melanogaster to understand the causes of monogenic and genetically complex diseases. Clinical Genetics, 62(5), 358-367.

Lawson MA, & Maxfield FR. (1995). Ca2+- and calcineurin-dependent recycling of an integrin to the front of migrating neutrophils. Nature, 377(6544), 75-79.

Lebeche D, Malpel S, & Cardoso WV. (1999). Fibroblast growth factor interactions in the developing lung. Mech Dev, 86(1-2), 125-136.

Lee A, Kratochwil A, St√°mpften I, Deutinger J, & Bernaschek G. (1996). Fetal lung volume determination by three-dimensional ultrasonography. American Journal of Obstetrics and Gynecology, 175(3 PART I), 588-592.

Lee RC, Feinbaum RL, & Ambros V. (1993). The C. elegans heterochronic gene lin-4 encodes small RNAs with antisense complementarity to lin-14. Cell, 75(5), 843-854.

Lee T, & Luo L. (1999). Mosaic analysis with a repressible cell marker for studies of gene function in neuronal morphogenesis. Neuron, 22(3), 451-461.

Lee T, & Luo L. (2001). Mosaic analysis with a repressible cell marker (MARCM) for Drosophila neural development. Trends Neurosci, 24(5), 251-254.

Legrand G, Humez S, Slomianny C, Dewailly E, Abeele FV, Mariot P, et al. (2001). Ca2+ Pools and Cell Growth: Evidence for sarcoendoplasmic Ca2+-ATPases 2B involvement in human prostate cancer cell growth control Journal of Biological Chemistry, 276(50), 47608-47614.

Lemons JA, Bauer CR, Oh W, Korones SB, Papile LA, Stoll BJ, et al. (2001). Very low birth weight outcomes of the National Institute of Child health and human

development neonatal research network, January 1995 through December 1996. NICHD Neonatal Research Network. Pediatrics, 107(1).

Levy J, Zhu Z, & Dunbar JC. (1998). The effect of glucose and calcium on Ca2+-adenosine triphosphatase in pancreatic islets isolated from a normal and a non-insulin-dependent diabetes mellitus rat model. Metabolism: Clinical and Experimental, 47(2), 185-189.

Lin X, Buff EM, Perrimon N, & Michelson AM. (1999). Heparan sulfate proteoglycans are essential for FGF receptor signaling during Drosophila embryonic development. Development, 126(17), 3715-3723.

Lindsley DL, & Zimm GG. (1992). The genome of Drosophila melanogaster (Illustrated ed.): Academic Press.

Lippincott-Schwartz J, & Patterson GH. (2003). Development and use of fluorescent protein markers in living cells. Science, 300(5616), 87-91.

Lipskaia L, Hulot JS, & Lompr√© AM. (2009). Role of sarco/endoplasmic reticulum calcium content and calcium ATPase activity in the control of cell growth and proliferation. Pflugers Archiv European Journal of Physiology, 457(3), 673-685.

Lipskaia L, & Lompr√© AM. (2004). Alteration in temporal kinetics of Ca2+ signaling and control of growth and proliferation. Biology of the Cell, 96(1), 55-68.

Lissandron V, Rossetto MG, Erbguth K, Fiala A, Daga A, & Zaccolo M. (2007). Transgenic fruit-flies expressing a FRET-based sensor for in vivo imaging of cAMP dynamics. Cellular Signalling, 19(11), 2296-2303.

Liu JD, Carmell MA, Rivas FV, Marsden CG, Thomson JM, Song JJ, et al. (2004). Argonaute2 is the catalytic engine of mammalian RNAi. Science, 305(5689), 1437-1441.

Liu L, Yermolaieva O, Johnson WA, Abboud FM, & Welsh MJ. (2003). Identification and function of thermosensory neurons in Drosophila larvae. Nature Neuroscience, 6(3), 267-273.

Liu LH, Boivin GP, Prasad V, Periasamy M, & Shull GE. (2001). Squamous Cell Tumors in Mice Heterozygous for a Null Allele of Atp2a2, Encoding the Sarco(endo)plasmic Reticulum Ca2+-ATPase Isoform 2 Ca2+ Pump. Journal of Biological Chemistry, 276(29), 26737-26740.

Liu LH, Paul RJ, Sutliff RL, Miller ML, Lorenz JN, Pun RYK, et al. (1997). Defective Endothelium-dependent Relaxation of Vascular Smooth Muscle and Endothelial Cell Ca2+ Signaling in Mice Lacking Sarco(endo)plasmic Reticulum Ca2+-ATPase Isoform 3. Journal of Biological Chemistry, 272(48), 30538-30545.

Llimargas M. (1999). The Notch pathway helps to pattern the tips of the Drosophila tracheal branches by selecting cell fates. Development, 126(11), 2355-2364.

Llimargas M. (2000). Wingless and its signalling pathway have common and separable functions during tracheal development. Development, 127(20), 4407-4417.

Llimargas M, & Casanova J. (1999). EGF signalling regulates cell invagination as well as cell migration during formation of tracheal system in Drosophila. Dev Genes Evol, 209(3), 174-179.

Lomax LG, Cole RJ, & Dorner JW. (1984). The Toxicity of Cyclopiazonic Acid in Weaned Pigs. Veterinary Pathology Online, 21(4), 418-424.

Loo TW, Bartlett MC, & Clarke DM. (2004). Thapsigargin or curcumin does not promote maturation of processing mutants of the ABC transporters, CFTR, and P-glycoprotein. Biochemical and Biophysical Research Communications, 325(2), 580-585.

Lwebuga-Mukasa JS. (1991). Matrix-driven pneumocyte differentiation. Am Rev Respir Dis, 144(2), 452-457.

Lytton J, & MacLennan DH. (1988). Molecular cloning of cDNAs from human kidney coding for two alternatively spliced products of the cardiac Ca2+-ATPase gene. J Biol Chem, 263(29), 15024-15031.

Lytton J, Westlin M, Burk SE, Shull GE, & MacLennan DH. (1992). Functional comparisons between isoforms of the sarcoplasmic or endoplasmic reticulum family of calcium pumps. Journal of Biological Chemistry, 267(20), 14483-14489.

Ma TS, Mann DL, Lee JH, & Gallinghouse GJ. (1999). SR compartment calcium and cell apoptosis in SERCA overexpression. Cell Calcium, 26(1-2), 25-36.

Macchiarini P, Jungebluth P, Go T, Asnaghi MA, Rees LE, Cogan TA, et al. (2008). Clinical transplantation of a tissue-engineered airway. Lancet, 372(9655), 2023-2030.

MacDonald ML, Lamerdin J, Owens S, Keon BH, Bilter GK, Shang Z, et al. (2006). Identifying off-target effects and hidden phenotypes of drugs in human cells. Nat Chem Biol, 2(6), 329-337.

Macklin C. (1954). The pulmonary alveolar mucoid film and the pneumonocytes. The Lancet, 263(6822), 1099-1104.

MacLennan DH, Brandl CJ, Korczak B, & Green NM. (1985). Amino-acid sequence of a Ca2+ + Mg2+-dependent ATPase from rabbit muscle sarcoplasmic reticulum, deduced from its complementary DNA sequence. Nature, 316(6030), 696-700.

Magnier C, Papp B, Corvazier E, Bredoux R, Wuytack F, Eggermont J, et al. (1992). Regulation of sarco-endoplasmic reticulum Ca2+-ATPases during platelet-derived growth factor-induced smooth muscle cell proliferation. Journal of Biological Chemistry, 267(22), 15808-15815.

Magyar A, Bakos E, & Varadi A. (1995). Structure and tissue-specific expression of the Drosophila melanogaster organellar-type Ca(2+)-ATPase gene. Biochem J, 310 (Pt 3), 757-763.

Mahn K, Hirst SJ, Ying S, Holt MR, Lavender P, Ojo OO, et al. (2009). Diminished sarco/endoplasmic reticulum Ca2+ ATPase (SERCA) expression contributes to airway remodelling in bronchial asthma. Proc Natl Acad Sci U S A, 106(26), 10775-10780.

Mailleux AA, Kelly R, Veltmaat JM, De Langhe SP, Zaffran S, Thiery JP, et al. (2005). Fgf10 expression identifies parabronchial smooth muscle cell progenitors and is required for their entry into the smooth muscle cell lineage. Development, 132(9), 2157-2166.

Mailleux AA, Tefft D, Ndiaye D, Itoh N, Thiery JP, Warburton D, et al. (2001). Evidence that SPROUTY2 functions as an inhibitor of mouse embryonic lung growth and morphogenesis. Mech Dev, 102(1-2), 81-94.

Mank M, Reiff DF, Heim N, Friedrich MW, Borst A, & Griesbeck O. (2006). A FRET-based calcium biosensor with fast signal kinetics and high fluorescence change. Biophysical Journal, 90(5), 1790-1796.

Manning G, & Krasnow MA. (1993). Development of the Drosophila tracheal system. In M. A. A. Bate (Ed.), The Development of Drosophila melanogaster (pp. 609–686): Cold Spring Harbor Laboratory Press.

Marks PW, Hendey B, & Maxfield FR. (1991). Attachment to fibronectin or vitronectin makes human neutrophil migration sensitive to alterations in cytosolic free calcium concentration. The Journal of Cell Biology, 112(1), 149-158.

Martis PC, Whitsett JA, Xu Y, Perl AK, Wan H, & Ikegami M. (2006). C/EBPalpha is required for lung maturation at birth. Development, 133(6), 1155-1164.

Maruyama R, & Andrew DJ. (2012). Drosophila as a model for epithelial tube formation. Developmental Dynamics, 241(1), 119-135.

Masoli M, Fabian D, Holt S, & Beasley R. (2004). The global burden of asthma: executive summary of the GINA Dissemination Committee report. Allergy, 59(5), 469-478.

Matsuno K, Diederich RJ, Go MJ, Blaumueller CM, & Artavanis-Tsakonas S. (1995). Deltex acts as a positive regulator of Notch signaling through interactions with the Notch ankyrin repeats. Development, 121(8), 2633-2644.

Matsuno T. (1990). Metamorphosis of Tracheae in the Pupal Abdomen of a Fruit Fly, Drosophila melanogaster MEIGEN. Japanese journal of applied entomology and zoology , 34(2), 167-169.

Mavrakis M, Rikhy R, Lilly M, & Lippincott-Schwartz J. (2008). Fluorescence imaging techniques for studying Drosophila embryo development. Curr Protoc Cell Biol, Chapter 4, Unit 4 18.

McGowan S, Jackson SK, Jenkins-Moore M, Dai HH, Chambon P, & Snyder JM. (2000). Mice bearing deletions of retinoic acid receptors demonstrate reduced lung elastin and alveolar numbers. Am J Respir Cell Mol Biol, 23(2), 162-167.

McGuire SE, Le PT, Osborn AJ, Matsumoto K, & Davis RL. (2003). Spatiotemporal rescue of memory dysfunction in Drosophila. Science, 302(5651), 1765-1768.

McGuire SE, Mao Z, & Davis RL. (2004). Spatiotemporal gene expression targeting with the TARGET and gene-switch systems in Drosophila. Sci STKE, 2004(220), pl6.

McGuire SE, Roman G, & Davis RL. (2004). Gene expression systems in Drosophila: a synthesis of time and space. Trends in Genetics, 20(8), 384-391.

Mehler K, Beck BB, Kaul I, Rahimi G, Hoppe B, & Kribs A. (2011). Respiratory and general outcome in neonates with renal oligohydramnios - A single-centre experience. Nephrology Dialysis Transplantation, 26(11), 3514-3522.

Meister G, Landthaler M, Patkaniowska A, Dorsett Y, Teng G, & Tuschl T. (2004). Human Argonaute2 mediates RNA cleavage targeted by miRNAs and siRNAs. Molecular Cell, 15(2), 185-197.

Mercadier JJ, Lompr√© AM, Duc P, Boheler KR, Fraysse JB, Wisnewsky C, et al. (1990). Altered sarcoplasmic reticulum Ca2(+)-ATPase gene expression in the

human ventricle during end-stage heart failure. The Journal of Clinical Investigation, 85(1), 305-309.

Metzger RJ, Klein OD, Martin GR, & Krasnow MA. (2008). The branching programme of mouse lung development. Nature, 453(7196), 745-750.

Metzger RJ, & Krasnow MA. (1999). Genetic control of branching morphogenesis. Science, 284(5420), 1635-1639.

Milan M, Campuzano S, & Garcia-Bellido A. (1997). Developmental parameters of cell death in the wing disc of,ÄâDrosophila. Proceedings of the National Academy of Sciences, 94(11), 5691-5696.

Miller AA, Hooper SB, & Harding R. (1993). Role of fetal breathing movements in control of fetal lung distension. J Appl Physiol, 75(6), 2711-2717.

Min H, Danilenko DM, Scully SA, Bolon B, Ring BD, Tarpley JE, et al. (1998). Fgf-10 is required for both limb and lung development and exhibits striking functional similarity to Drosophila branchless. Genes Dev, 12(20), 3156-3161.

Misquitta L, & Paterson BM. (1999). Targeted disruption of gene function in Drosophila by RNA interference (RNA-i): A role for nautilus in embryonic somatic muscle formation. Proceedings of the National Academy of Sciences, 96(4), 1451-1456.

Miyamoto MI, del Monte F, Schmidt U, DiSalvo TS, Kang ZB, Matsui T, et al. (2000). Adenoviral gene transfer of SERCA2a improves left-ventricular function in aortic-banded rats in transition to heart failure. Proceedings of the National Academy of Sciences of the United States of America, 97(2), 793-798.

Miyawaki A, Griesbeck O, Heim R, & Tsien RY. (1999). Dynamic and quantitative Ca2+ measurements using improved cameleons. Proceedings of the National Academy of Sciences of the United States of America, 96(5), 2135-2140.

Miyawaki A, Llopis J, Heim R, Michael McCaffery J, Adams JA, Ikura M, et al. (1997). Fluorescent indicators for Ca2+ based on green fluorescent proteins and calmodulin. Nature, 388(6645), 882-887.

Miyoshi K, Tsukumo H, Nagami T, Siomi H, & Siomi MC. (2005). Slicer function of Drosophila Argonautes and its involvement in RISC formation. Genes & Development, 19(23), 2837-2848.

Moccia F, Berra-Romani R, Tritto S, Signorelli S, Taglietti V, & Tanzi F. (2003). Epidermal growth factor induces intracellular Ca2+ oscillations in microvascular endothelial cells. Journal of Cellular Physiology, 194(2), 139-150.

Moessinger AC, Harding R, Adamson TM, Singh M, & Kiu GT. (1990). Role of lung fluid volume in growth and maturation of the fetal sheep lung. The Journal of Clinical Investigation, 86(4), 1270-1277.

Mummery-Widmer JL, Yamazaki M, Stoeger T, Novatchkova M, Bhalerao S, Chen D, et al. (2009). Genome-wide analysis of Notch signalling in Drosophila by transgenic RNAi. Nature, 458(7241), 987-U959.

Muratore CS, Kharasch V, Lund DP, Sheils C, Friedman S, Brown C, et al. (2001). Pulmonary morbidity in 100 survivors of congenital diaphragmatic hernia monitored in a multidisciplinary clinic. Journal of Pediatric Surgery, 36(1), 133-140.

Murray CS, Woodcock A, Langley SJ, Morris J, & Custovic A. (2006). Secondary prevention of asthma by the use of Inhaled Fluticasone propionate in Wheezy INfants (IFWIN): double-blind, randomised, controlled study. Lancet, 368(9537), 754-762.

Nagai T, Sawano A, Eun Sun P, & Miyawaki A. (2001). Circularly permuted green fluorescent proteins engineered to sense Ca2+. Proceedings of the National Academy of Sciences of the United States of America, 98(6), 3197-3202.

Naito Y, Yamada T, Matsumiya T, Ui-Tei K, Saigo K, & Morishita S. (2005). dsCheck: highly sensitive off-target search software for double-stranded RNA-

mediated RNA interference. Nucleic acids research, 33(Web Server issue), W589-591.

Nakai J, Ohkura M, & Imoto K. (2001). A high signal-to-noise ca2+ probe composed of a single green fluorescent protein. Nature Biotechnology, 19(2), 137-141.

Nakao A. (2001). Is TGF-beta1 the key to suppression of human asthma? Trends Immunol, 22(3), 115-118.

Nepveu A. (2001). Role of the multifunctional CDP/Cut/Cux homeodomain transcription factor in regulating differentiation, cell growth and development. Gene, 270(1-2), 1-15.

Ng YS, Rohan R, Sunday ME, Demello DE, & D'Amore PA. (2001). Differential expression of VEGF isoforms in mouse during development and in the adult. Dev Dyn, 220(2), 112-121.

Ni JQ, Markstein M, Binari R, Pfeiffer B, Liu LP, Villalta C, et al. (2008). Vector and parameters for targeted transgenic RNA interference in Drosophila melanogaster. Nat Methods, 5(1), 49-51.

NIG-Fly. Fly Stocks at the National Institute of Genetics. Retrieved 2nd December, 2011, from http://www.shigen.nig.ac.jp/fly/nigfly/index.jsp

Norez C, Antigny F, Becq F, & Vandebrouck C. (2006). Maintaining low Ca2+ level in the endoplasmic reticulum restores abnormal endogenous F508del-CFTR trafficking in airway epithelial cells. Traffic, 7(5), 562-573.

Northway Jr WH, Rosan RC, & Porter DY. (1967). Pulmonary disease following respirator therapy of hyaline-membrane disease. Bronchopulmonary dysplasia. New England Journal of Medicine, 276(7), 357-368.

O'Neill EM, Rebay I, Tjian R, & Rubin GM. (1994). The activities of two Ets-related transcription factors required for Drosophila eye development are modulated by the Ras/MAPK pathway. Cell, 78(1), 137-147.

Odermatt A, Taschner PEM, Khanna VK, Busch HFM, Karpati G, Jablecki CK, et al. (1996). Mutations in the gene-encoding SERCA1, the fast-twitch skeletal muscle sarcoplasmic reticulum Ca2+ ATPase, are associated with Brody disease. Nature Genetics, 14(2), 191-194.

Olivier V. (2001). RNA silencing as a plant immune system against viruses. Trends in Genetics, 17(8), 449-459.

Olver RE, & Strang LB. (1974). Ion fluxes across the pulmonary epithelium and the secretion of lung liquid in the foetal lamb. J Physiol, 241(2), 327-357.

Ornitz DM, & Itoh N. (2001). Fibroblast growth factors. Genome Biol, 2(3), REVIEWS3005.

Ott HC, Clippinger B, Conrad C, Schuetz C, Pomerantseva I, Ikonomou L, et al. (2010). Regeneration and orthotopic transplantation of a bioartificial lung. Nature medicine, 16(8), 927-933.

Paddison PJ, Silva JM, Conklin DS, Schlabach M, Li M, Aruleba S, et al. (2004). A resource for large-scale RNA-interference-based screens in mammals. Nature, 428(6981), 427-431.

Page DV, & Stocker JT. (1982). Anomalies associated with pulmonary hypoplasia. Am Rev Respir Dis, 125(2), 216-221.

Pal-Bhadra M, Bhadra U, & Birchler JA. (1997). Cosuppression in Drosophila: gene silencing of Alcohol dehydrogenase by white-Adh transgenes is Polycomb dependent. Cell, 90(3), 479-490.

Pallister PD, Meisner LF, Elejalde BR, Francke U, Herrmann J, Spranger J, et al. (1977). The pallister mosaic syndrome. Birth Defects Orig Artic Ser, 13, 103-110.

Palmer AE, Giacomello M, Kortemme T, Hires SA, Lev-Ram V, Baker D, et al. (2006). Ca2+ indicators based on computationally redesigned calmodulin-peptide pairs. Chem Biol, 13(5), 521-530.

Palmer AE, & Tsien RY. (2006). Measuring calcium signaling using genetically targetable fluorescent indicators. Nat Protoc, 1(3), 1057-1065.

Pan Y, Zvaritch E, Tupling AR, Rice WJ, de Leon S, Rudnicki M, et al. (2003). Targeted Disruption of the ATP2A1 Gene Encoding the Sarco(endo)plasmic Reticulum Ca2+ ATPase Isoform 1 (SERCA1) Impairs Diaphragm Function and Is Lethal in Neonatal Mice. Journal of Biological Chemistry, 278(15), 13367-13375.

Parameswaran K, Janssen LJ, & O'Byrne PM. (2002). Airway hyperresponsiveness and calcium handling by smooth muscle: A "Deeper Look". Chest, 121(2), 621-624.

Park WY, Miranda B, Lebeche D, Hashimoto G, & Cardoso WV. (1998). FGF-10 is a chemotactic factor for distal epithelial buds during lung development. Dev Biol, 201(2), 125-134.

Pattle RE. (1955). Properties, function and origin of the alveolar lining layer. Nature, 175(4469), 1125-1126.

Pepicelli CV, Lewis PM, & McMahon AP. (1998). Sonic hedgehog regulates branching morphogenesis in the mammalian lung. Curr Biol, 8(19), 1083-1086.

Periasamy M, Reed TD, Liu LH, Ji Y, Loukianov E, Paul RJ, et al. (1999). Impaired Cardiac Performance in Heterozygous Mice with a Null Mutation in the Sarco(endo)plasmic Reticulum Ca2+-ATPase Isoform 2 (SERCA2) Gene. Journal of Biological Chemistry, 274(4), 2556-2562.

Periz G, & Fortini ME. (1999). Ca(2+)-ATPase function is required for intracellular trafficking of the Notch receptor in Drosophila. EMBO J, 18(21), 5983-5993.

Petersen TH, Calle EA, Zhao L, Lee EJ, Gui L, Raredon MB, et al. (2010). Tissue-engineered lungs for in vivo implantation. Science, 329(5991), 538-541.

Piccin A, Salameh A, Benna C, Sandrelli F, Mazzotta G, Zordan M, et al. (2001). Efficient and heritable functional knock-out of an adult phenotype in Drosophila

using a GAL4-driven hairpin RNA incorporating a heterologous spacer. Nucleic acids research, 29(12), E55-55.

Pitsouli C, & Perrimon N. (2010). Embryonic multipotent progenitors remodel the Drosophila airways during metamorphosis. Development, 137(21), 3615-3624.

Potter EL. (1946). Bilateral renal agenesis. The Journal of Pediatrics, 29(1), 68-76.

Prober DA, & Edgar BA. (2002). Interactions between Ras1, dMyc, and dPI3K signaling in the developing Drosophila wing. Genes & Development, 16(17), 2286-2299.

Puddicombe SM, Polosa R, Richter A, Krishna MT, Howarth PH, Holgate ST, et al. (2000). Involvement of the epidermal growth factor receptor in epithelial repair in asthma. FASEB J, 14(10), 1362-1374.

Purchase IF. (1971). The acute toxicity of the mycotoxin cyclopiazonic acid to rats. Toxicol Appl Pharmacol, 18(1), 114-123.

Ramaswami M, Rao S, van der Bliek A, Kelly RB, & Krishnan KS. (1993). Genetic studies on dynamin function in Drosophila. J Neurogenet, 9(2), 73-87.

Rana TM. (2007). Illuminating the silence: Understanding the structure and function of small RNAs. Nature Reviews Molecular Cell Biology, 8(1), 23-36.

Rao RV, Hermel E, Castro-Obregon S, del Rio G, Ellerby LM, Ellerby HM, et al. (2001). Coupling Endoplasmic Reticulum Stress to the Cell Death Program. Journal of Biological Chemistry, 276(36), 33869-33874.

Rao S, Lang C, Levitan ES, & Deitcher DL. (2001). Visualization of neuropeptide expression, transport, and exocytosis in Drosophila melanogaster. J Neurobiol, 49(3), 159-172.

Rasmussen U, Broogger Christensen S, & Sandberg F. (1978). Thapsigargine and thapsigargicine, two new histamine liberators from Thapsia garganica L. Acta Pharm Suec, 15(2), 133-140.

Rawlins EL, & Hogan BLM. (2006). Epithelial stem cells of the lung: Privileged few or opportunities for many? Development, 133(13), 2455-2465.

Raymond-Delpech V, Towers PR, & Sattelle DB. (2004). Gene silencing of selected calcium-signalling molecules in a Drosophila cell line using double-stranded RNA interference. Cell Calcium, 35(2), 131-139.

Reale FR, & Esterly JR. (1973). Pulmonary hypoplasia: a morphometric study of the lungs of infants with diaphragmatic hernia, anencephaly, and renal malformations. Pediatrics, 51(1), 91-96.

Reiff DF, Ihring A, Guerrero G, Isacoff EY, Joesch M, Nakai J, et al. (2005). In vivo performance of genetically encoded indicators of neural activity in flies. Journal of Neuroscience, 25(19), 4766-4778.

Reiff DF, Thiel PR, & Schuster CM. (2002). Differential regulation of active zone density during long-term strengthening of Drosophila neuromuscular junctions. Journal of Neuroscience, 22(21), 9399-9409.

Ribeiro C, Ebner A, & Affolter M. (2002). In Vivo Imaging Reveals Different Cellular Functions for FGF and Dpp Signaling in Tracheal Branching Morphogenesis. Developmental Cell, 2(5), 677-683.

Ribeiro C, Neumann M, & Affolter M. (2004). Genetic Control of Cell Intercalation during Tracheal Morphogenesis in Drosophila. Current biology : CB, 14(24), 2197-2207.

Robertson PA, Sniderman SH, Laros RK, Jr., Cowan R, Heilbron D, Goldenberg RL, et al. (1992). Neonatal morbidity according to gestational age and birth weight from five tertiary care centers in the United States, 1983 through 1986. Am J Obstet Gynecol, 166(6 Pt 1), 1629-1641; discussion 1641-1625.

Rodriguez RJ, Martin RJ, & Fanaroff AA. (2002). Respiratory distress syndrome and its management. In A. A. Fanaroff & R. J. Martin (Eds.), Fanaroff and Martin's Neonatal-Perinatal Medicine: Diseases of the Fetus and Infant (7 ed., pp. 1001–1011). St. Louis: Mosby.

Romoser VA, Hinkle PM, & Persechini A. (1997). Detection in living cells of Ca2+-dependent changes in the fluorescence emission of an indicator composed of two green fluorescent protein variants linked by a calmodulin-binding sequence. A new class of fluorescent indicators. J Biol Chem, 272(20), 13270-13274.

Roos J, DiGregorio PJ, Yeromin AV, Ohlsen K, Lioudyno M, Zhang S, et al. (2005). STIM1, an essential and conserved component of store-operated Ca 2+ channel function. Journal of Cell Biology, 169(3), 435-445.

Roy S, Hsiung F, & Kornberg TB. (2011). Specificity of Drosophila Cytonemes for Distinct Signaling Pathways. Science, 332(6027), 354-358.

Ruano R, Yoshisaki CT, da Silva MM, Ceccon MEJ, Grasi MS, Tannuri U, et al. (2011). A randomized controlled trial of fetal endoscopic tracheal occlusion versus postnatal management of severe isolated congenital diaphragmatic hernia. Ultrasound in Obstetrics and Gynecology, In press.

Rubenstein RC, Egan ME, & Zeitlin PL. (1997). In vitro pharmacologic restoration of CFTR-mediated chloride transport with sodium 4-phenylbutyrate in cystic fibrosis epithelial cells containing Delta F508-CFTR. Journal of Clinical Investigation, 100(10), 2457-2465.

Rudolf R, Mongillo M, Rizzuto R, & Pozzan T. (2003). Looking forward to seeing calcium. Nat Rev Mol Cell Biol, 4(7), 579-586.

Rutkowski DT, & Kaufman RJ. (2004). A trip to the ER: coping with stress. Trends Cell Biol, 14(1), 20-28.

Sagara Y, & Inesi G. (1991). Inhibition of the sarcoplasmic reticulum Ca2+ transport ATPase by thapsigargin at subnanomolar concentrations. J Biol Chem, 266(21), 13503-13506.

Sakuntabhai A, Ruiz-Perez V, Carter S, Jacobsen N, Burge S, Monk S, et al. (1999). Mutations in ATP2A2, encoding a Ca2+ pump, cause Darier disease. Nature Genetics, 21(3), 271-277.

Samakovlis C. (2010). A Genome-Wide Analysis of Airway Maturation in Drosophila. Paper presented at the Keystone Symposia on Molecular and Cellular Biology: Lung Development and Repair (B5), Santa Fe, New Mexico.

Samakovlis C, Hacohen N, Manning G, Sutherland DC, Guillemin K, & Krasnow MA. (1996). Development of the Drosophila tracheal system occurs by a series of morphologically distinct but genetically coupled branching events. Development, 122(5), 1395-1407.

Samakovlis C, Manning G, Steneberg P, Hacohen N, Cantera R, & Krasnow MA. (1996). Genetic control of epithelial tube fusion during Drosophila tracheal development. Development, 122(11), 3531-3536.

Santamaria P. (1979). Heat shock induced phenocopies of dominant mutants of the bithorax complex in Drosophila melanogaster. Molecular and General Genetics MGG, 172(2), 161-163.

Sanyal S, Consoulas C, Kuromi H, Basole A, Mukai L, Kidokoro Y, et al. (2005). Analysis of conditional paralytic mutants in Drosophila sarco-endoplasmic reticulum calcium ATPase reveals novel mechanisms for regulating membrane excitability. Genetics, 169(2), 737-750.

Sanyal S, Jennings T, Dowse H, & Ramaswami M. (2006). Conditional mutations in SERCA, the Sarco-endoplasmic reticulum Ca2+-ATPase, alter heart rate and rhythmicity in Drosophila. J Comp Physiol B, 176(3), 253-263.

Sathish V, Thompson MA, Bailey JP, Pabelick CM, Prakash YS, & Sieck GC. (2009). Effect of proinflammatory cytokines on regulation of sarcoplasmic reticulum Ca2+ reuptake in human airway smooth muscle. American Journal of Physiology - Lung Cellular and Molecular Physiology, 297(1), L26-L34.

Sato M, Kitada Y, & Tabata T. (2008). Larval cells become imaginal cells under the control of homothorax prior to metamorphosis in the Drosophila tracheal system. Developmental Biology, 318(2), 247-257.

Sato M, & Kornberg TB. (2002). FGF is an essential mitogen and chemoattractant for the air sacs of the drosophila tracheal system. Dev Cell, 3(2), 195-207.

Sauer B, & Henderson N. (1988). Site-specific DNA recombination in mammalian cells by the Cre recombinase of bacteriophage P1. Proceedings of the National Academy of Sciences of the United States of America, 85(14), 5166-5170.

Saumon G. (2000). Chloride fluxes during cAMP stimulation of liquid absorption across the native rat alveolar epithelium. Exp Lung Res, 26(4), 219-227.

Schittny JC, Miserocchi G, & Sparrow MP. (2000). Spontaneous peristaltic airway contractions propel lung liquid through the bronchial tree of intact and fetal lung explants. Am J Respir Cell Mol Biol, 23(1), 11-18.

Schmittgen TD, Zakrajsek BA, Mills AG, Gorn V, Singer MJ, & Reed MW. (2000). Quantitative reverse transcription-polymerase chain reaction to study mRNA decay: comparison of endpoint and real-time methods. Anal Biochem, 285(2), 194-204.

Scholz H, Deatrick J, Klaes A, & Klambt C. (1993). Genetic dissection of pointed, a Drosophila gene encoding two ETS-related proteins. Genetics, 135(2), 455-468.

Seidler NW, Jona I, Vegh M, & Martonosi A. (1989). Cyclopiazonic acid is a specific inhibitor of the Ca2+-ATPase of sarcoplasmic reticulum. J Biol Chem, 264(30), 17816-17823.

Sekine K, Ohuchi H, Fujiwara M, Yamasaki M, Yoshizawa T, Sato T, et al. (1999). Fgf10 is essential for limb and lung formation. Nature Genetics, 21(1), 138-141.

Seng Y, Sonawane ND, Salinas D, Qian L, Pedemonte N, Galietta LJV, et al. (2004). Evidence against the rescue of defective ΔF508-CFTR cellular processing by curcumin in cell culture and mouse models. Journal of Biological Chemistry, 279(39), 40629-40633.

Sethi JM, & Rochester CL. (2000). Smoking and chronic obstructive pulmonary disease. Clinics in Chest Medicine, 21(1), 67-86.

Shannon JM, & Hyatt BA. (2004). Epithelial-mesenchymal interactions in the developing lung. Annu Rev Physiol, 66, 625-645.

Simon VR, & Moran MF. (2001). SERCA activity is required for timely progression through G1/S. Cell Proliferation, 34(1), 15-30.

Singerman L. (2009). Combination therapy using the small interfering RNA bevasiranib. Retina, 29(6 Suppl), S49-50.

Skou JC. (1957). The influence of some cations on an adenosine triphosphatase from peripheral nerves. BBA - Biochimica et Biophysica Acta, 23(C), 394-401.

Snider GL. (1989). Chronic obstructive pulmonary disease: Risk factors, pathophysiology and pathogenesis. Annual Review of Medicine, 40, 411-429.

Soll RF. (2000a). Prophylactic natural surfactant extract for preventing morbidity and mortality in preterm infants. Cochrane database of systematic reviews (Online : Update Software)(2).

Soll RF. (2000b). Prophylactic synthetic surfactant for preventing morbidity and mortality in preterm infants. Cochrane database of systematic reviews (Online : Update Software)(2).

Sparrow MP, Warwick SP, & Everett AW. (1995). Innervation and function of the distal airways in the developing bronchial tree of fetal pig lung. Am J Respir Cell Mol Biol, 13(5), 518-525.

Starrett RW, & de Lorimier AA. (1975). Congenital diaphragmatic hernia in lambs: hemodynamic and ventilatory changes with breathing. J Pediatr Surg, 10(5), 575-582.

Stege G, Fenton A, & Jaffray B. (2003). Nihilism in the 1990s: The true mortality of congenital diaphragmatic hernia. Pediatrics, 112(3), 532-535.

Steneberg P, Hemphala J, & Samakovlis C. (1999). Dpp and Notch specify the fusion cell fate in the dorsal branches of the Drosophila trachea. Mech Dev, 87(1-2), 153-163.

Stern CD. (2005). The chick: A great model system becomes even greater. Developmental Cell, 8(1), 9-17.

Stirling PC, Lundin VF, & Leroux MR. (2003). Getting a grip on non-native proteins. EMBO Reports, 4(6), 565-570.

Stocum DL. (2008). Developmental mechanisms of regeneration. In A. Atala (Ed.), Principles of regenerative medicine (pp. 100-124): Academic Press.

Stripp B, Hogan BL, & Thannickal VJ. (2011). Lung stem cells: looking beyond the hype. Nature medicine, 17(7), 788-789.

Struhl G, & Basler K. (1993). Organizing activity of wingless protein in Drosophila. Cell, 72(4), 527-540.

Sutherland D, Samakovlis C, & Krasnow MA. (1996). branchless encodes a Drosophila FGF homolog that controls tracheal cell migration and the pattern of branching. Cell, 87(6), 1091-1101.

Swischuk LE, Richardson CJ, Nichols MM, & Ingman MJ. (1979). Primary pulmonary hypoplasia in the neonate. J Pediatr, 95(4), 573-577.

Syed SH, Larin KV, Dickinson ME, & Larina IV. (2011). Optical coherence tomography for high-resolution imaging of mouse development in utero. Journal of Biomedical Optics, 16(4).

Tabara H, Sarkissian M, Kelly WG, Fleenor J, Grishok A, Timmons L, et al. (1999). The rde-1 gene, RNA interference, and transposon silencing in C. elegans. Cell, 99(2), 123-132.

Tanaka-Matakatsu M, Uemura T, Oda H, Takeichi M, & Hayashi S. (1996). Cadherin-mediated cell adhesion and cell motility in Drosophila trachea regulated by the transcription factor Escargot. Development, 122(12), 3697-3705.

Tavadia S, Tait RC, McDonagh TA, & Munro CS. (2001). Platelet and cardiac function in Darier's disease. Clin Exp Dermatol, 26(8), 696-699.

Tefft D, Lee M, Smith S, Crowe DL, Bellusci S, & Warburton D. (2002). mSprouty2 inhibits FGF10-activated MAP kinase by differentially binding to upstream target proteins. Am J Physiol Lung Cell Mol Physiol, 283(4), L700-706.

Thastrup O, Cullen PJ, Drobak BK, Hanley MR, & Dawson AP. (1990). Thapsigargin, a tumor promoter, discharges intracellular Ca2+ stores by specific inhibition of the endoplasmic reticulum Ca2(+)-ATPase. Proc Natl Acad Sci U S A, 87(7), 2466-2470.

Thomas IT, & Smith DW. (1974). Oligohydramnios, cause of the nonrenal features of Potter's syndrome, including pulmonary hypoplasia. The Journal of Pediatrics, 84(6), 811-814.

Thomas KR, & Capecchi MR. (1987). Site-directed mutagenesis by gene targeting in mouse embryo-derived stem cells. Cell, 51(3), 503-512.

Tian L, Hires SA, Mao T, Huber D, Chiappe ME, Chalasani SH, et al. (2009). Imaging neural activity in worms, flies and mice with improved GCaMP calcium indicators. Nat Methods, 6(12), 875-881.

Tollet J, Everett AW, & Sparrow MP. (2001). Spatial and temporal distribution of nerves, ganglia, and smooth muscle during the early pseudoglandular stage of fetal mouse lung development. Dev Dyn, 221(1), 48-60.

Torralba S, & Heath IB. (2001). Cytoskeletal and Ca2+ regulation of hyphal tip growth and initiation. Current topics in developmental biology, 51, 135-187.

Toyoshima C, Nakasako M, Nomura H, & Ogawa H. (2000). Crystal structure of the calcium pump of sarcoplasmic reticulum at 2.6 A resolution. Nature, 405(6787), 647-655.

Toyoshima C, & Nomura H. (2002). Structural changes in the calcium pump accompanying the dissociation of calcium. Nature, 418(6898), 605-611.

Trewavas A, & Knight M. (1994). Mechanical signalling, calcium and plant form. Plant Mol Biol, 26(5), 1329-1341.

Triggle DJ. (1983). Calcium, the control of smooth muscle function and bronchial hyperreactivity. Allergy: European Journal of Allergy and Clinical Immunology, 38(1), 1-9.

TRiP. Drosophila Transgenic RNAi Project at Harvard Medical School (NIH/NIGMS R01-GM084947). Retrieved 2nd December, 2011, from http://www.flyrnai.org/TRiP-HOME.html

Tsarouhas V, Senti KA, Jayaram SA, Tiklova K, Hemphala J, Adler J, et al. (2007). Sequential pulses of apical epithelial secretion and endocytosis drive airway maturation in Drosophila. Dev Cell, 13(2), 214-225.

Tsien RY. (1980). New calcium indicators and buffers with high selectivity against magnesium and protons: design, synthesis, and properties of prototype structures. Biochemistry, 19(11), 2396-2404.

Tsien RY. (1981). A non-disruptive technique for loading calcium buffers and indicators into cells. Nature, 290(5806), 527-528.

Turnbull DH, Bloomfield TS, Baldwin HS, Foster FS, & Joyner AL. (1995). Ultrasound backscatter microscope analysis of early mouse embryonic brain development. Proceedings of the National Academy of Sciences of the United States of America, 92(6), 2239-2243.

Tweedie S, Ashburner M, Falls K, Leyland P, McQuilton P, Marygold S, et al. (2009). FlyBase: enhancing Drosophila Gene Ontology annotations. Nucleic Acids Res, 37(Database issue), D555-559.

Unbekandt M, del Moral PM, Sala FG, Bellusci S, Warburton D, & Fleury V. (2008). Tracheal occlusion increases the rate of epithelial branching of embryonic mouse lung via the FGF10-FGFR2b-Sprouty2 pathway. Mech Dev, 125(3-4), 314-324.

Urnov FD, Rebar EJ, Holmes MC, Zhang HS, & Gregory PD. (2010). Genome editing with engineered zinc finger nucleases. Nature Reviews Genetics, 11(9), 636-646.

Uv A, Cantera R, & Samakovlis C. (2003). Drosophila tracheal morphogenesis: intricate cellular solutions to basic plumbing problems. Trends Cell Biol, 13(6), 301-309.

Uv A, Tang E, & Cavoshi TM. (2009). Balancing forces shape the Drosophila tracheal lumen. Paper presented at the 2nd International Congress of Respiratory Science, Bad Honnef, Germany.

v. Neergaard K. (1929). Neue Auffassungen über einen Grundbegriff der Atemmechanik. Research in Experimental Medicine, 66(1), 373-394.

Vaessin H, Brand M, Jan LY, & Jan YN. (1994). daughterless is essential for neuronal precursor differentiation but not for initiation of neuronal precursor formation in Drosophila embryo. Development, 120(4), 935-945.

van der Krol AR, Mur LA, Beld M, Mol J, & Stuitje AR. (1990). Flavonoid Genes in Petunia: Addition of a Limited Number of Gene Copies May Lead to a Suppression of Gene Expression. The Plant Cell Online, 2(4), 291-299.

van Tuyl M, & Post M. (2000). From fruitflies to mammals: mechanisms of signalling via the Sonic hedgehog pathway in lung development. Respir Res, 1(1), 30-35.

Vanario-Alonso CE, O'Hara E, McGinnis W, & Pick L. (1995). Targeted ribozymes reveal a conserved function of the Drosophila paired gene in sensory organ development. Mech Dev, 53(3), 323-328.

Varadi A, Lebel L, Hashim Y, Mehta Z, Ashcroft SJH, & Turner R. (1999). Sequence variants of the sarco(endo)plasmic reticulum Ca2+-transport ATPase 3 gene (SERCA3) in Caucasian Type II diabetic patients (UK Prospective Diabetes Study 48). Diabetologia, 42(10), 1240-1243.

Varsha Wesley S, Helliwell CA, Smith NA, Wang M, Rouse DT, Liu Q, et al. (2001). Construct design for efficient, effective and high-throughput gene silencing in plants. Plant Journal, 27(6), 581-590.

Vazquez-Martinez O, Canedo-Merino R, Diaz-Munoz M, & Riesgo-Escovar JR. (2003). Biochemical characterization, distribution and phylogenetic analysis of Drosophila melanogaster ryanodine and IP3 receptors, and thapsigargin-sensitive Ca2+ ATPase. Journal of Cell Science, 116(12), 2483-2494.

Vincent S, Wilson R, Coelho C, Affolter M, & Leptin M. (1998). The Drosophila protein Dof is specifically required for FGF signaling. Molecular Cell, 2(4), 515-525.

Waldron RT, Short AD, Meadows JJ, Ghosh TK, & Gill DL. (1994). Endoplasmic reticulum calcium pump expression and control of cell growth. Journal of Biological Chemistry, 269(16), 11927-11933.

Walter MF, Biessmann H, & Petersen NS. (1990). Heat shock causes the collapse of the intermediate filament cytoskeleton in Drosophila embryos. Developmental Genetics, 11(4), 270-279.

Wang JW, Wong AM, Flores J, Vosshall LB, & Axel R. (2003). Two-photon calcium imaging reveals an odor-evoked map of activity in the fly brain. Cell, 112(2), 271-282.

Wang Q, Uhlirova M, & Bohmann D. (2010). Spatial restriction of FGF signaling by a matrix metalloprotease controls branching morphogenesis. Dev Cell, 18(1), 157-164.

Wappner P, Gabay L, & Shilo BZ. (1997). Interactions between the EGF receptor and DPP pathways establish distinct cell fates in the tracheal placodes. Development, 124(22), 4707-4716.

Warburton D, El-Hashash A, Carraro G, Tiozzo C, Sala F, Rogers O, et al. (2010). Lung organogenesis. Curr Top Dev Biol, 90, 73-158.

Warner JO, Marguet C, Rao R, Roche WR, & Pohunek P. (1998). Inflammatory mechanisms in childhood asthma. Clin Exp Allergy, 28 Suppl 5, 71-75; discussion 90-71.

Weaver M, Dunn NR, & Hogan BL. (2000). Bmp4 and Fgf10 play opposing roles during lung bud morphogenesis. Development, 127(12), 2695-2704.

Weaver M, & Krasnow MA. (2008). Dual origin of tissue-specific progenitor cells in Drosophila tracheal remodeling. Science, 321(5895), 1496-1499.

Weiss DJ, Bertoncello I, Borok Z, Kim C, Panoskaltsis-Mortari A, Reynolds S, et al. (2011). Stem cells and cell therapies in lung biology and lung diseases. Proceedings of the American Thoracic Society, 8(3), 223-272.

White AC, Xu J, Yin Y, Smith C, Schmid G, & Ornitz DM. (2006). FGF9 and SHH signaling coordinate lung growth and development through regulation of distinct mesenchymal domains. Development, 133(8), 1507-1517.

Whitten J. (1980). The tracheal system. In M. Ashburner & T. R. F. Wright (Eds.), The Genetics and Biology of Drosophila (pp. 499-540). New York: Academic Press.

Wieschaus E, Nüsslein-Volhard C, & Jürgens G. (1984). Mutations affecting the pattern of the larval cuticle in Drosophila melanogaster. Development Genes and Evolution, 193(5), 296-307.

Wigglesworth JS, Desai R, & Guerrini P. (1981). Fetal lung hypoplasia: biochemical and structural variations and their possible significance. Arch Dis Child, 56(8), 606-615.

Wightman B, Ha I, & Ruvkun G. (1993). Posttranscriptional regulation of the heterochronic gene lin-14 by lin-4 mediates temporal pattern formation in C. elegans. Cell, 75(5), 855-862.

Wilson JM, Difiore JW, & Peters CA. (1993). Experimental fetal tracheal ligation prevents the pulmonary hypoplasia associated with fetal nephrectomy - possible application for congenital diaphragmatic-hernia. Journal of Pediatric Surgery, 28(11), 1433-1440.

Wittwer CT, Herrmann MG, Moss AA, & Rasmussen RP. (1997). Continuous fluorescence monitoring of rapid cycle DNA amplification. Biotechniques, 22(1), 130-131, 134-138.

World Health Organization. (2008). The global burden of disease: 2004 update. Geneva: WHO Press.

Worrell JW, & Levine RB. (2008). Characterization of voltage-dependent Ca2+ currents in identified drosophila motoneurons in situ. Journal of Neurophysiology, 100(2), 868-878.

Wu JS, & Luo L. (2006). A protocol for mosaic analysis with a repressible cell marker (MARCM) in Drosophila. Nat Protoc, 1(6), 2583-2589.

Wung JT, Sahni R, Moffitt ST, Lipsitz E, & Stolar CJ. (1995). Congenital diaphragmatic hernia: survival treated with very delayed surgery, spontaneous respiration, and no chest tube. J Pediatr Surg, 30(3), 406-409.

Wuytack F, Raeymaekers L, & Missiaen L. (2002). Molecular physiology of the SERCA and SPCA pumps. Cell Calcium, 32(5-6), 279-305.

Xiang Y, Yuan Q, Vogt N, Looger LL, Jan LY, & Jan YN. (2010). Light-avoidance-mediating photoreceptors tile the Drosophila larval body wall. Nature, 468(7326), 921-926.

Xu T, & Artavanis-Tsakonas S. (1990). deltex, a locus interacting with the neurogenic genes, Notch, Delta and mastermind in Drosophila melanogaster. Genetics, 126(3), 665-677.

Yagodin S, Pivovarova NB, Andrews SB, & Sattelle DB. (1999). Functional characterization of thapsigargin and agonist-insensitive acidic Ca2+ stores in Drosophila melanogaster S2 cell lines. Cell Calcium, 25(6), 429-438.

Yang Y, Beqaj S, Kemp P, Ariel I, & Schuger L. (2000). Stretch-induced alternative splicing of serum response factor promotes bronchial myogenesis and is defective in lung hypoplasia. J Clin Invest, 106(11), 1321-1330.

Yeromin AV, Roos J, Stauderman KA, & Cahalan MD. (2004). A store-operated calcium channel in Drosophila S2 cells. J Gen Physiol, 123(2), 167-182.

You LR, Takamoto N, Yu CT, Tanaka T, Kodama T, Demayo FJ, et al. (2005). Mouse lacking COUP-TFII as an animal model of Bochdalek-type congenital diaphragmatic hernia. Proceedings of the National Academy of Sciences of the United States of America, 102(45), 16351-16356.

Yung Y, Dolginov Y, Yao Z, Rubinfeld H, Michael D, Hanoch T, et al. (1997). Detection of ERK activation by a novel monoclonal antibody. FEBS Letters, 408(3), 292-296.

Yusa K, Rashid ST, Strick-Marchand H, Varela I, Liu PQ, Paschon DE, et al. (2011). Targeted gene correction of a1-antitrypsin deficiency in induced pluripotent stem cells. Nature, 478(7369), 391-394.

Zamore PD, Tuschl T, Sharp PA, & Bartel DP. (2000). RNAi: Double-Stranded RNA Directs the ATP-Dependent Cleavage of mRNA at 21 to 23 Nucleotide Intervals. Cell, 101(1), 25-33.

Zeng Y, Yi R, & Cullen BR. (2003). MicroRNAs and small interfering RNAs can inhibit mRNA expression by similar mechanisms. Proc Natl Acad Sci U S A, 100(17), 9779-9784.

Zhang SL, Yeromin AV, Zhang XHF, Yu Y, Safrina O, Penna A, et al. (2006). Genome-wide RNAi screen of Ca2+ influx identifies genes that regulate Ca2+ release-activated Ca2+ channel activity. Proceedings of the National Academy of Sciences of the United States of America, 103(24), 9357-9362.

Zhao XS, Shin DM, Liu LH, Shull GE, & Muallem S. (2001). Plasticity and adaptation of Ca2+ signaling and Ca2+-dependent exocytosis in SERCA2+/- mice. EMBO Journal, 20(11), 2680-2689.